ASSESSMENT OF THE BEHAVIOR OF GEMINI SURFACTANT NANOPARTICLES WITHIN BIOLOGICAL SYSTEMS USING MASS SPECTROMETRY

A Thesis Submitted to
the College of Graduate and Postdoctoral Studies
in Partial Fulfillment of the Requirements
for the Degree of Doctor of Philosophy
in the College of Pharmacy and Nutrition
University of Saskatchewan
Saskatoon, Saskatchewan

By

Wei Jin

PERMISSION TO USE

In presenting this thesis in partial fulfillment of the requirements for a postgraduate degree from the University of Saskatchewan, I agree that the libraries of this university may make it freely available for inspection. I further agree that permission for copying of this thesis in any manner, in whole or in part, for scholarly purposes may be granted by the professor who supervised my thesis work or, in their absence, by the head of the department or the dean of the college in which my thesis work was done. It is understood that any copying or publication or use of this thesis or parts thereof for financial gain shall not be allowed without my written permission. It is also understood that due recognition shall be given to me and to the University of Saskatchewan in any scholarly use which may be made of any material in my thesis. Requests for permission to copy or to make other uses of materials in this thesis in whole or part should be addressed to:

Dean of the College of Pharmacy and Nutrition

University of Saskatchewan

Saskatoon, Saskatchewan, Canada, S7N 4L3.

OR

Dean of the College of Graduate and Postdoctoral Studies

University of Saskatchewan

Saskatoon, Saskatchewan, Canada, S7N 5C9.

ABSTRACT

Gemini surfactants are a class of lipid molecules that have been successfully used *in vitro* and *in vivo* as non-viral gene delivery vectors. However, the biological behavior of gemini surfactant nanoparticles has not been well understood and little is known about their cellular uptake, distribution, and metabolism after entering a biological system. Such knowledge is of great importance as it could explain their varying efficiencies and toxicities, and ultimately contribute to the development of novel gemini surfactants with enhanced efficiency and reduced toxicity. Therefore, my Ph.D. research investigated the biological behavior of gemini surfactant nanoparticles using mass spectrometry with a focus on their quantitative determination in the cellular matrix and identification of their potential metabolites.

To determine the cellular uptake and distribution of gemini surfactants, a simple flow injection analysis-tandem mass spectrometry (FIA-MS/MS) method was developed and validated for the quantification of three model gemini surfactants, unsubstituted (16-3-16), with pyridinium head groups (16(Py)-S-2-S-16(Py)), and substituted with a glycyl-lysine di-peptide (16-7N(GK)-16), in the cellular matrix. To our knowledge, this is the first FIA-MS/MS method that was developed for the determination of three gemini surfactants belonging to different structural families. The method is superior to previous liquid chromatography-tandem mass spectrometry (LC-MS/MS) methods, developed in our laboratory, with respect to sensitivity and time of analysis. The application of the method allowed for a time-course monitoring of the cellular uptake and subcellular distribution of gemini surfactants.

Differential cellular uptake and distribution were observed among three gemini surfactants, which explained their varying efficiencies and toxicities. In general, high cellular uptake of gemini

surfactant corresponds to high transfection efficiency, while non-preferential accumulation in the nucleus may have contributed to the observed toxicity. The gemini surfactant 16-7N(GK)-16 displayed the highest cellular uptake among three compounds, consistent with its high efficiency in gene transfection; whereas 16(Py)-S-2-S-16(Py) showed the highest distribution in the nucleus, corresponding to its high toxicity. In addition, the DNA binding capability and the shape of aggregates of the gemini surfactants explained their different behaviors in biological systems. The gemini surfactant 16-7N(GK)-16 has a balanced DNA binding property and tends to form aggregates with flexible bilayer structures, resulting in its high efficiency and low toxicity. At the same time, 16(Py)-S-2-S-16(Py) and 16-3-16 display relatively strong DNA binding properties and have cylindrical micelle aggregates, leading to their low efficiency and high toxicity.

Different metabolic pathways for the three gemini surfactants were also determined for the first time. The gemini surfactant 16-3-16 was not metabolized in PAM 212 cells, which suggests it most likely remains intact during cellular detoxification and elimination. On the other hand, 16(Py)-S-2-S-16(Py) was metabolized primarily *via* phase I biotransformations, including oxidation and dealkylation. Finally, the gemini surfactant 16-7N(GK)-16 was metabolized mainly *via* phase II biotransformations, such as methylation, acetylation, and conjugations (glucose, palmitoyl and stearyl conjugations). The metabolism studies of gemini surfactants provide insight for future directions in the design and development of novel compounds with low toxicity for gene delivery.

Together, the work accomplished in this Ph.D. study lays the foundation for investigating the behavior of gemini surfactant nanoparticles in biological systems and feeds into the rationale for designing novel gene delivery systems. Ultimately, the results would contribute to the development of more effective and less toxic novel gene delivery systems.

ACKNOWLEDGEMENTS

First and foremost, I would like to express my sincere thanks and appreciation to my supervisor, Dr. Anas El-Aneed, for his professional supervision, guidance, and support during my study in the program. I have learned from him in various different aspects, such as solid knowledge, fruitful experience and great vision. He provided great inspiration in my research and tremendous revisions to my published paper and this thesis.

I would also like to thank my advisory committee members, Drs. Ildiko Badea, Randy Purves, and George Katselis. Their careful reviews, valuable discussion, and great advices on my progress reports significantly contributed to the success of my overall research and experience. I also like to thank the committee chairs: Drs. Kate Dadachova and David Blackburn, for their great help with my meetings.

I thank Dr. Mays Al-Dulaymi for her help and discussion in my research, which greatly contributed to the completion of my research. I also like to thank Dr. Scot C. Leary for his help in the isolation and identification of subcellular fractions and Dr. Ed Krol for his useful suggestion and discussion for the determination of the metabolic pathways of gemini surfactants.

In the meantime, I thank Dr. Waleed Mohammed-Saeid for the training in cell transfection and the purification of plasmid DNA, Dr. David Schneberger for the initial training in western blotting assay, and Ms. Deborah Michel for her technical assistance on the operation of quadrupole-linear ion trap (Q-Trap 4000) instrument. I also like to acknowledge Ms. Jeveria Rehman for collecting the data to determine molecular packing parameters and Mr. Ken Thomas for obtaining the data on quadrupole-time of flight (Q-TOF) mass spectrometer. In addition, Drs. Jackson M. Chitanda and

McDonald Donkuru are acknowledged for the synthesis of gemini surfactants and their labelled counterparts used in my research.

Sincere appreciation is also extended to all my colleagues, Dr. Mona Hamada, Ms. Fatma Elzahraa Elessawy, Ms. Asmita Poudel, Dr. George Gachumi, Mr. Kang Jiang, Mr. Raj Rai, and Ms. Saniya Alwani, at the Drug Discovery & Development Research Group for great friendship, technical assistance, and other supports during my study in the program.

In addition, the following institutions are acknowledged for their great supports during my research. A postgraduate scholarship was provided by the Natural Sciences and Engineering Research Council of Canada (NSERC), and this research was supported by a NSERC Discovery Grant. The College of Pharmacy and Nutrition in the University of Saskatchewan provided research equipment, workspace, and reputable mentorship. The International Student and Study Abroad Center of University of Saskatchewan and the Canadian Society of Mass Spectrometry (CSMS) provided funding for my travel to attend and present my research results at conferences. The research equipment and supplies were funded by NSERC, the Canadian Foundation for Innovation, and the College of Pharmacy and Nutrition. The Saskatchewan Structural Science Centre and the Centre for Veterinary Drug Residues, Canadian Food Inspection Agency also provided the use of their instrumental research facilities.

Finally, I like to express ultimate acknowledgements to my family and all my extended families for their continued love, support, and encouragement throughout my academic pursuits. All the motivation, persistence, and determination I have had for this journey came from my family.

Wei Jin

Saskatoon, SK, Canada

DEDICATION

To my wife, Ying Zhang, who is my forever lover and has been a great source of inspiration, motivation, and encouragement; and to my son, Miles Jin, who is my bright future.

CONTENTS

LIST OF ABBREVIATIONS

16-3-16	N, N-bis(dimethylhexadecyl)-1,3-propane-diammonium dibromide
16(Py)-S-2-S-(Py)16	1,1'-[ethane-1,2-diylbis(sulfanediylhexadecane-1,2-diyl)]dipyridinium dibromide
5DMyr	1-(1,3-dimyristoyloxyprop-2-yl)-2,4,6-trimethylpyridinium
a_o	The head group area of a molecule
ANOVA	One-way analysis of variance
APCI	Atmospheric pressure chemical ionization
BGSC	3P3[4N-(QN,8N-diguanidino spermidine)-carbamoyl] cholesterol
BGTC	3/3[N', N'-diguanidinoethyl-aminoethane) carbamoyl] cholesterol
DC	Direct current
CE	Collision energy
CFTR	Cystic fibrosis transmembrane conductance regulator
CID	Collision-induced dissociation
CMC	Critical micelle concentration
COS-7	Kidney cells of the African green monkey
C-trap	Curved linear trap
CV	Coefficient of variation
CXP	Collision exit potential
DESI	Desorption electrospray ionization
diC$_{14}$-amidine	*N*-t-butyl-*N*'-tetradecyl-3-tetradecylaminopropionamidine
DNA	Deoxyribonucleic acid
DOGS	Dioctadecylamido-glycylspermine
DOPE	1, 2-di-(9Z-octadecenoyl)-*sn*-glycero-3-phosphoethanolamine

DORI	1, 2-dioleoyloxypropyl-3-dimethylhydroxyethyl ammonium chloride
DORIE	1, 2-dioleoyl-3-dimethyl-hydroxyethyl ammonium bromide
DOTAP	1, 2-dioleoyloxy-3-[trimethylammonio]-propane
DOTMA	N-(1-(2, 3-dioleyloxy) propyl)-N,N,Ntrimethylammonium chloride)
DP	Decluster potential
DMRIE	1, 2-dimyristyloxypropyl-3-dimethylhydroxyethylammonium bromide
DMSO	Dimethyl sulfoxide
DPRIE	1,2-dipalmityloxy propyl-3-dimethyl-hydroxyethyl ammonium bromide
DSRIE	1,2-disteryloxypropyl-3-dimethyl-hydroxyethyl ammonium bromide
ELISA	Enzyme-linked immunosorbent assay
ESI	Electrospray ionization
FA	Formic acid
EP	Entrance potential
FC	Fast chromatography
FIA	Flow injection analysis
GFP	Green fluorescent protein
HCD	High energy collisional dissociation
HILIC	Hydrophilic interaction liquid chromatography
HPLC	High-performance liquid chromatography
HQC	High quality control
IFN-γ	Interferon gamma
l	The length of hydrocarbon tails
LIT	Linear ion trap
LOD	Limit of detection

LLOQ	Lower limit of quantification
LMV	Large multilamellar vesicles
LQC	Low quality control
MALDI	Matrix assisted laser desorption ionization
MQC	Middle quality control
MEM	Modified eagle's medium
MRM	Multiple reaction monitoring
MS	Mass spectrometry
MS/MS	Tandem mass spectrometry
m/z	Mass to charge ratio
MTT	3-(4, 5-Dimethylthiazol-2-yl)-2, 5-diphenyltetrazolium bromide
NCE	Normalized collision energy
NMR	Nuclear magnetic resonance
N/P	Nitrogen to phosphate charge ratio
NSERC	Natural Sciences and Engineering Research Council of Canada
P	Molecular packing parameter
PAM 212	Mouse keratinocytes cells
PBS	Phosphate buffered saline
PEG	Polyethylene glycol
PEI	Polyethylenimine
P/G/L	p-DNA/gemini surfactant/lipid
p-DNA	Plasmid DNA
ppm	Parts per million
Q-Exactive	Quadrupole-Orbitrap mass spectrometry

QhQ-MS	Quadrupole-hexapole-quadrupole mass spectrometry
QqQ	Triple quadrupole
QqQ-LIT	Triple quadrupole-linear ion trap
Q-TOF	Quadrupole-time of flight
RD-4	Human rhabdomyosarcoma cells
RF	Radio frequency
r^2	Coefficient of determination
RSD	Relative standard deviation
S/N	Signal to noise ratio
SUV	Small unilamellar vesicles
ULOQ	Upper limit of quantification
USFDA	United States of America Food and Drug Administration
v	The volume of hydrophobic tails

LIST OF FIGURES

LIST OF TABLES

1 Chapter 1 - Literature Review and Proposed Research

1.1 Introduction

The first successful gene transfer in humans was performed in 1989 [1]. Since then, gene therapy has attracted a great interest over the past few decades [2-4]. To date, over 2,600 gene therapy clinical trials have been conducted worldwide, in which more than half are in the field of cancer gene therapy [5]. The tools used to achieve gene delivery are called vectors, which are key for an efficient and safe gene delivery. There are two types of gene delivery methods: viral and non-viral vectors [6]. Viral vectors use the viruses' natural infection capability to introduce the target gene into cells [7, 8]. Viral vectors are known for high efficiency in transfection, but with potential genotoxicity and severe immune response; they also have limitations in the packing capacity for genetic materials that can be delivered [9, 10]. In contrast, non-viral vectors provide a non-immunogenic and safer method for gene delivery, which are not limited to the size of genes that can be encapsulated and can be easily produced at low cost; however, they suffer from lower gene transfer abilities, especially *in vivo*, in comparison with viral vectors [11]. As such, numerous efforts have been focused on the development of novel non-viral vectors that provide high efficiency and low toxicity in gene transfection.

Among numerous non-viral vectors, cationic lipids have been prominent gene delivery systems in recent years. In particular, cationic gemini surfactants are the most promising molecules as gene delivery agents due to their unique chemical structures that possess dual positively charged hydrophilic head groups, a spacer region, and two hydrophobic tail regions [12]. Such structures enable gemini surfactants to bind and compact DNA to form nano-sized particles, and subsequently

facilitate their cellular uptake for gene transfection [13, 14]. To date, a variety of gemini surfactants with different head groups, spacer regions, and tails have been used to successfully deliver nucleic acids into cells for efficient transfection [13, 15, 16]. For example, the gemini surfactant 14-2-14 and serine-derived gemini surfactants $(nSer)_2N5$ (n=14 and 16) showed the ability to efficiently deliver plasmid DNA into mitochondria in HeLa cells and promote gene expression [17]. To increase efficiency and reduce toxicity, numerous efforts have been made to design and develop novel gemini surfactants, such as varying the length of hydrophobic carbon tails, introduction of pyridinium head groups, and substitution with a di-peptide moiety in the spacer region [18-22]. In addition, the formulation methods of gemini surfactant-based lipoplexes and their cellular uptake mechanism have been well studied with the aim of enhancing efficiency while reducing toxicity [23-26]. Collectively, these researches have resulted in the development of numerous novel gemini surfactants with significantly improved efficiency and reduced toxicity.

Despite the substantial improvement of efficiency and toxicity profiles, gemini surfactants are still not able to achieve the required efficiency in gene transfection *in vivo* so that they can fulfill clinical application for gene therapy. In addition, there are no unequivocal explanations for the varying toxicities among different gemini surfactant structures. Therefore, a better understanding of the mechanism of transfection and toxicity will aid in the development of more efficient and less toxic gemini surfactants for gene delivery. One factor that is possibly related to the efficiency and toxicity of gemini surfactant is their biological fate post transfection (i.e., their subcellular and tissue distribution, and metabolism). However, as of yet, the biological fate of gemini surfactants as gene delivery agents is still poorly understood and little is known about their cellular uptake, distribution, and metabolite formation within cells. Such knowledge may explain the reasons of

observed efficiencies and toxicities of various gemini surfactant structures, which will contribute to the design and development of more effective gemini surfactants.

My Ph.D. research focused on the assessment of the behavior of gemini surfactant nanoparticles within biological systems using analytical mass spectrometry. In particular, I investigated the cellular uptake, distribution, and metabolism of three gemini surfactants, symmetrical *m*-*s*-*m* gemini surfactant 16-3-16, pyridinium gemini surfactant 16(Py)-S-2-S-16(Py), and di-peptide substituted gemini surfactant 16-7N(GK)-16, which have demonstrated great efficiency in the delivery of DNA into cells with low toxicities [13, 19, 27]. My research findings assisted in the understanding of the unknown behavior of gemini surfactant nanoparticles within biological systems and correlated their cellular uptake, distribution, and metabolite formation with their efficiencies and toxicities. The long-term goal is to develop novel gemini surfactants as gene delivery agents with high efficiency and low toxicity.

1.2 Lipid-Based Gene Delivery Systems

Cationic lipids have been widely used as non-viral gene delivery agents for decades. Cationic lipids are amphiphilic molecules that have a general structure with a cationic head group, a linker, and a hydrophobic tail [28]. The positively charged head groups can interact with the negatively charged phosphate groups in nucleic acids, allowing for the formation of compacted structures called lipoplexes [29], which are able to protect DNA from cellular nuclease degradation, interact with cell membrane for cellular uptake, and facilitate the release of DNA from intracellular vesicles for gene transfection. Typically, transfection efficiency of cationic lipids relies on a number of factors, such as the shape of the structure, the number of charges carried per molecule, the nature of the lipid tails, and the type of the linker [30]. To date, numerous cationic lipids with different structures

have been developed and synthesized as non-viral gene delivery agents, which were used for both *in vitro* and *in vivo* gene delivery. Due to the structural versatility, cationic lipids can often be categorized into different groups according to their specific characteristics of the structures. Typically, cationic lipids used for gene delivery can be classified into four main categories based on their different head groups, as outlined below.

1.2.1 Quaternary ammonium lipids

Quaternary ammonium lipids are a class of cationic compounds that have been well studied for gene delivery. Generally, quaternary ammonium lipid compounds contain positively charged quaternary ammonium groups that can interact with and compact negatively charged DNA to form nanosized particles and achieve gene delivery. Among numerous quaternary ammonium lipids, compound 2,3-dioleyloxypropyl-1-trimethylammonium bromide (DOTMA) (Figure 1.1) was the first one that displayed gene transfection capability. DOTMA has a structure with a quaternary amine connected to two unsaturated aliphatic hydrocarbon chains via ether groups, showing efficient DNA transfection in several cell lines [11].

To improve transfection efficiency, a wide range of quaternary ammonium lipids were developed with various head groups, including 1,2-dioleoyl-3-dimethyl-hydroxyethyl ammonium bromide (DORIE) and 1,2-dioleoyloxypropyl-3-dimethyl-hydroxyethyl ammonium chloride (DORI) (Figure 1.1) [31, 32]. In general, these compounds showed great efficiency and toxicity profiles. Both DORIE and DORI are the quaternary ammonium compounds that have a hydroxyethyl group instead of a methyl group in their structures compared to DOTMA [32]. They showed a 2-3 fold increased transfection activity compared with their original structures [32]. The improved transfection efficiency was attributed to the hydroxyl moiety in the structure that may aid in the

interaction between DNA-lipid complexes and cell membranes, resulting in a greater transfection activity [32].

Furthermore, modifications to the tails of the structure were also conducted to increase transfection efficiency, which resulted in the development of a number of additional quaternary ammonium lipid compounds, such as 1,2-disteryloxypropyl-3-dimethyl-hydroxyethyl ammonium bromide (DSRIE), 1,2-dipalmityloxy propyl-3-dimethyl-hydroxyethyl ammonium bromide (DPRIE), and 1,2-dimyristyloxypropyl-3-dimethyl-hydroxy ethyl ammonium bromide (DMRIE) (Figure 1.1) [32]. These compounds have the tails with varying lengths in the structure, displaying diverse transfection efficiencies. In particular, DSRIE and DPRIE are the quaternary ammonium lipids with saturated 18-carbon and 16-carbon tails, respectively, showing similar transfection activities compared with DORIE [32]. However, DMRIE is another quaternary ammonium lipid with saturated 14-carbon tails that displayed two times greater transfection activity than DORIE [32]. More importantly, DMRIE allowed DNA to be delivered *in viv*o at an increased concentration in the formulation, resulting in greater efficiency in gene transfection [33]. As such, different lengths of the tails showed a great influence on the transfection activity of quaternary ammonium lipids. Since DMRIE exhibited a significantly improved efficiency and toxicity profile compared with other quaternary ammonium lipid compounds, a number of gene therapy clinical trials have been conducted based on the DMRIE-mediated gene delivery systems and great therapeutic results were reported [34-36]. Collectively, these results demonstrated that quaternary ammonium lipids are effective non-viral gene delivery agents.

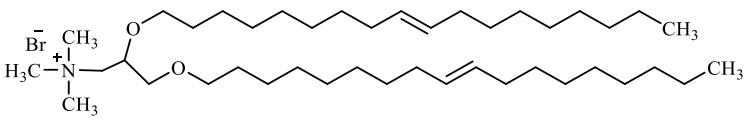

DOTMA

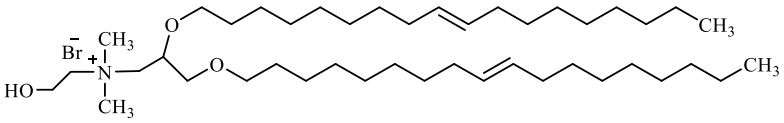

DORIE

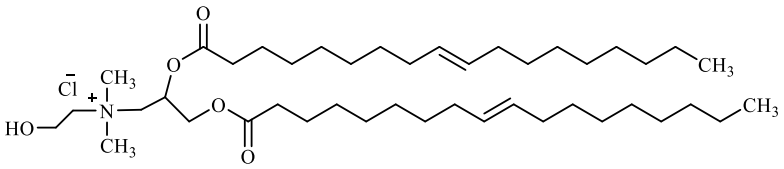

DORI

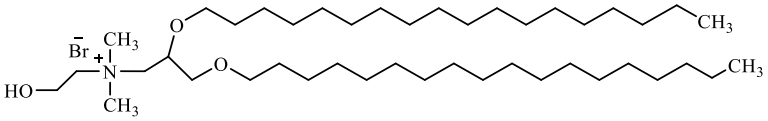

DSRIE

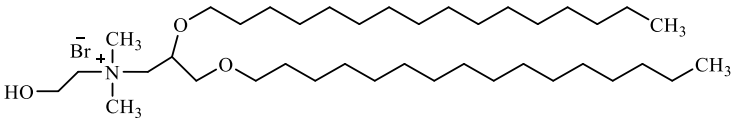

DPRIE

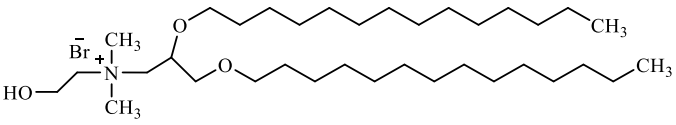

DMRIE

Figure 1.1. Chemical structures of quaternary ammonium lipids

In addition, various approaches have also been implemented to improve transfection efficiency of quaternary ammonium lipids. One strategy was to promote the internalization of the lipid/DNA complexes through receptor-mediated cellular uptake. For instance, Cheng et al. [37] attached transferrin to the DOTMA/DNA complexes in an attempt to target the cell surface transferrin receptors, a significantly enhanced transfection activity with transferrin-DOTMA/NDA complexes was achieved compared with the complexes alone. Another approach was to facilitate the cytoplasmic release of DNA from the endosomes using endosomal disrupting agents. For example, a fusogenic peptide, Glu-Ala-Leu-Ala, was used along with the complexes to destabilize the endosomal membrane that facilitated the release of DNA into the cytoplasm, thus resulting in a significant increase in transfection efficiency [38].

Physicochemical characterization indicated that quaternary ammonium lipids typically form lamellar bilayer vesicle complexes, which can facilitate the fusion of the DNA-containing complexes with cell membrane, resulting in their cellular uptake [11, 39]. A lamellar bilayer vesicle has a closed bilayer structure, which consists of two layers of lipid molecules with the hydrophobic tails pointing toward the center of the bilayer [39]. The DNA is typically encapsulated and protected in the center of the vesicle complexes. In general, large multilamellar vesicles (LMV) are more efficient in gene transfection than small unilamellar vesicles (SUV), this is because LMVs have the ability to interact with more DNA molecules due to their large molecular weight [32] and possibly have an enhanced sedimentation on the cells compared with SUVs, leading to more efficient cellular uptake [40]. Typically, quaternary ammonium lipids require additive lipids to achieve a high level of gene transfection activity. Such additive lipids generally can be 1,2-di-(9Z-octadecenoyl)-*sn*-glycero-3-phosphoethanol amine (DOPE) or cholesterol, which increase the stability of formed lipoplexes and promote endosomal escape of DNA to enhance gene transfection

efficiency. In addition, the charge ratio of quaternary ammonium lipid/DNA is also of great importance to achieve a transfection activity, as it has a direct impact on the physicochemical properties of formed complexes, and an excess of positive surface charge of the complexes is imperative to obtain high transfection efficiency.

However, quaternary ammonium lipids are still limited for their application in gene delivery due to relatively low transfection efficiency, especially *in vivo*, and high toxicity. As endogenous negatively charged substances interact and neutralize the positive charges of the lipids and the complexes, the electrostatic interaction between the complexes and cells is dramatically diminished, thereby resulting in reduced cellular uptake and subsequent low transfection activity. On the other hand, the toxicity of quaternary ammonium lipids is mainly determined by the structures of cationic groups and quaternary ammonium lipids are often more toxic than their tertiary amine counterparts. A 10-fold higher toxicity was observed in quaternary ammonium compounds compared with the corresponding ones with tertiary amines [41]. In addition, the toxicity is also dependent on the surface charge of the complexes and complexes with high charges are generally more toxic than those with low charges. Xu et al. [42] reported that the purified DOTAP/DNA complexes with low charges at 1:2.2 (lipid/DNA) were less toxic than the mixture with high charges at 3.5:1 (lipid/DNA), resulting in a 16-fold increase in transfection efficiency.

1.2.2 Polyamine lipids

Polyamine lipids are a class of compounds containing a large number of amine groups in the structure, which are protonated at physiological pH. They are efficient in compacting DNA to form nanosized particles with a typical size of 200 nm [43]. Polyamine lipid compounds have the ability to not only buffer the endosomal compartment to prevent DNA degradation but also drive nuclear

accumulation of the lipoplexes through the interaction with chromatin, resulting in enhanced gene transfection [43]. Due to this special property, polyamine lipids have been widely used as non-viral gene delivery agents. Dioctadecylamidoglycyl spermine (DOGS) (Figure 1.2) was the first polyamine lipid compound used for gene delivery, which contains a spermine attached to the hydrophobic tails via a glycyl spacer [44]. Spermine is a naturally nucleus-occurring polyamine that plays an important role in DNA compaction during cell division [45]. An *in vitro* transfection study indicated that DOGS was 2-fold more effective and 6-fold less toxic compared with quaternary ammonium lipid dimethyldioctadecylammonium chloride [44].

In addition to DOGS, a wide range of polyamine lipids were also developed and synthesized to improve transfection efficiency by varying the shape of the structure, the type of the linker, and the length of the tails [46]. These compounds showed a variety of transfection efficiency and toxicity profiles. Although all these compounds demonstrated great transfection activities, compounds RPR-12650, RPR-126097 and RPR-120535 (Figure 1.2) displayed the highest transfection efficiency in multiple cell lines, equivalent to that of commercially available Transfectam and Lipofectamine [46]. Structurally, these three compounds have a linear geometry of polyamine group, which demonstrated a 4-fold higher transfection activity compared with those with a branched, T-shape, or globular geometry of polyamine group [46], indicating the linear polyamine shape is essential to achieve a high level of gene transfection. In addition, the substitution on the amino acid linker also significantly improved the transfection activity of these polyamine lipid compounds [46]. Such an increase in transfection efficiency was attributed to the substitution group that can facilitate the cellular entry of lipid/DNA complexes [46]. In addition, physicochemical characterization of the DNA/PPR-120535 complexes indicated that plasmid DNA was in compacted state in the complexes, which protects DNA against degradation [46].

Aside from long alkyl chain, a cholesterol moiety has also been used as the lipid anchor in the structures of polyamine lipids [47]. As cholesterol is a naturally occurring molecule in cell membrane that can facilitate the cellular uptake of lipid/DNA complexes, these cholesterol derivative compounds typically display enhanced transfection activity. For example, the lipid #67 (Figure 1.2) is a cholesterol derivative compound that has a spermine head group attached to cholesterol moiety via a spacer[48]. This compound was able to efficiently transfer a cystic fibrosis transmembrane conductance regulator (CFTR) cDNA to cells for the treatment of cystic fibrosis, which was significantly more active than other cationic lipids used previously for CFTR gene expression in BALB/c mice, exhibiting equivalent activity to virally-mediated transfection [48]. In addition, an aerosol formulation of lipid #67 with dimyristoyl phosphatidyl ethanolamine was developed with a significant increase in the concentration of DNA, which has the ability to protect DNA from degradation and thus maintained its biological activity [49, 50]. As a result, the lipid #67 formulation with plasmid DNA encoding for CFTR has been used in clinical trials for treating patients suffering from cystic fibrosis and promising results were reported with low toxicity [51].

Similar to quaternary ammonium lipids, polyamine lipids are also able to form multilamellar bilayer complexes with DNA that favor efficient gene delivery, and typically large complexes are more potent in gene transfection than small ones [52, 53]. Daniel et al. [54] demonstrated that gene transfer was more efficient with large RPR120535 particles due to the formation of large intracellular vesicles that could be more easily disrupted to release DNA into the cytoplasm for gene transfection. However, there is limited information regarding the intracellular trafficking of lipid/DNA particles. One *in vitro* study using fluorescently labeled plasmid DNA indicated that lipid/DNA complexes were able to rapidly localize in the cellular cytoplasm of the transfected NIH 3T3 and CV-1 cells, mostly in the perinuclear region [54].

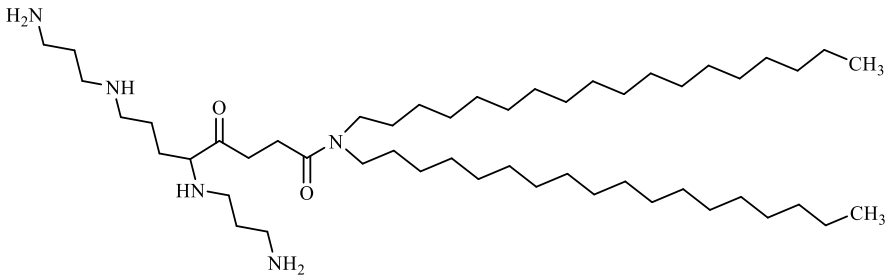

DOGS

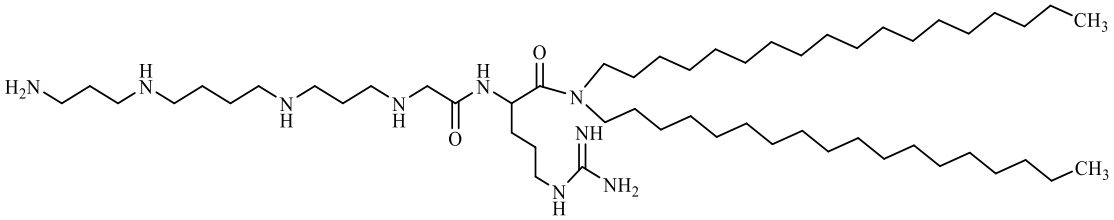

RPR-12650

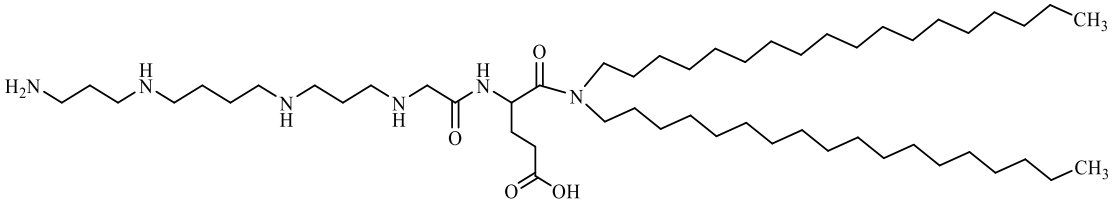

RPR-126097

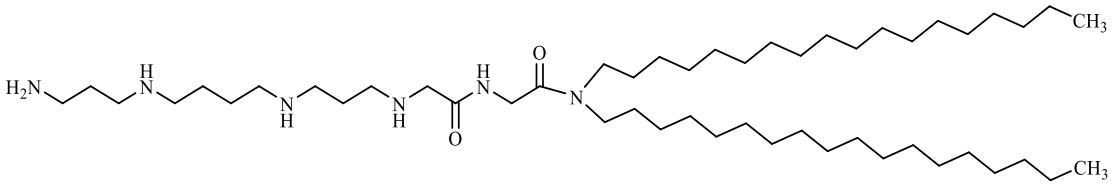

RPR-120535

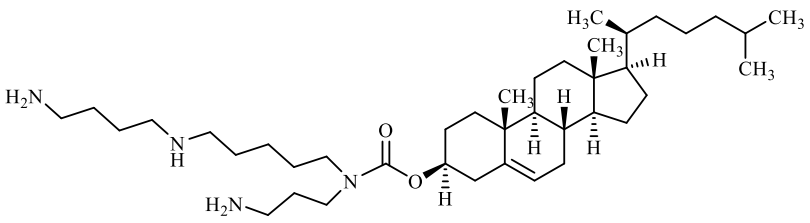

Lipid #67

Figure 1.2. Chemical structures of polyamine lipids

1.2.3 Amidinium, guanidinium and pyridinium lipids

Amidinium and guanidinum lipids are versatile cationic compounds used for gene delivery. Generally, amidinium and guanidinum compounds have relatively high pKa, which allows them to be protonated in physiological conditions [55]. Once these compounds are positively charged, they can interact with the negatively charged DNA phosphate groups and compact the DNA. In addition, they also can interact with DNA through the formation of hydrogen bonds with the phosphate groups in DNA [56]. To date, a number of amidinium lipid compounds have been developed for non-viral gene delivery. Among them, *N*-t-butyl-*N*'-tetradecyl-3-tetradecylamino propionamidine (diC_{14}-amidine) (Figure 1.3) is the first amidinium lipid used as a gene delivery agent [57, 58]. DiC_{14}-amidine is a pH-sensitive cationic lipid with two titratable groups, an amine and an amidine, in the structure, which can possess two positive charges at low pH [59]. Its bilayer structure is highly sensitive to the pH of a medium. At high pH, diC_{14}-amidine presents an organized bilayer structure, whereas it typically displays a rather non-organized bilayer phase at low pH due to the strong electrostatic repulsion of head groups [55]. An *in vitro* study demonstrated that diC_{14}-amidine-containing liposomes were efficient in mediating transfection of both adherent and suspension cell lines [57]. In addition, low toxicity was observed with a 95% cell viability in treated cells compared with controls (non-treated cells) [57]. Other amidinium cationic lipids, such as ADPDE and ADODE (Figure 1.3), have also been developed. Their formulations with cholesterol and DNA were administered intravenously to mice, and great transgene activity was observed in lung, liver and heart, indicating a promise as gene delivery agents [60].

Similar to amidinium lipids, guanidinum cationic lipids are also used as effective gene delivery agents since they can be protonated in a wide range of pH. For example, compounds 3/3[N',N'-diguanidinoethyl-aminoethane) carbamoyl] cholesterol (BGTC) and 3P3[4N-(QN,8N-diguanidino

spermidine)-carbamoyl] cholesterol (BGSC) (Figure 1.3) are the first two guanidinum lipids used as gene delivery agents, which were synthesized by attaching a bisguanidinium group to a cholesterol [56]. An *in vitro* study showed that both BGTC and BGSC have an up to two-fold higher gene transfection activity than Lipofectin in a number of mammalian cell lines [56]. The rationale of the development of such cationic lipids was to take advantage of the membrane-compatible feature of a cholesterol moiety and the highly favorable DNA binding feature of a guanidinium to facilitate DNA delivery [56, 61]. Structural characterization of guanidinium-cholesterol cationic lipid/DNA complex indicated that highly ordered multilamellar domains were formed with DNA condensation, and the DNA molecules were intercalated among the lipid bilayers [62]. It was proposed that the multilamellar complexes may have high endosomal membrane fusion/destabilization properties that contributed to their high transfection efficiency [62]. In addition, BGTC was sufficiently stable to permit effective gene delivery by the aerosol route to pulmonary sites, indicating a promise for clinical application of aerosol gene delivery [63]. Together, the results indicated that cationic lipids containing guanidinium head groups can be efficient non-viral gene delivery agents.

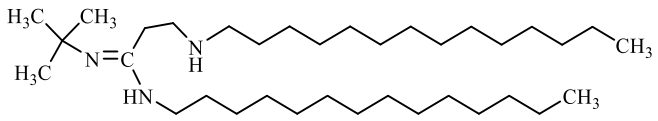

diC$_{14}$-amidine

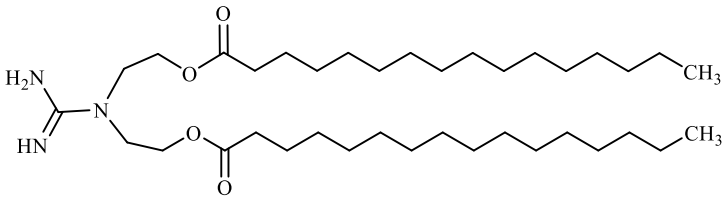

ADPDE

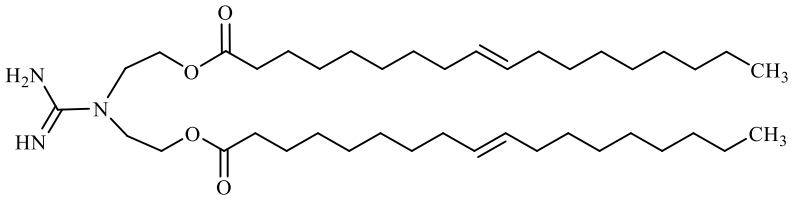

ADODE

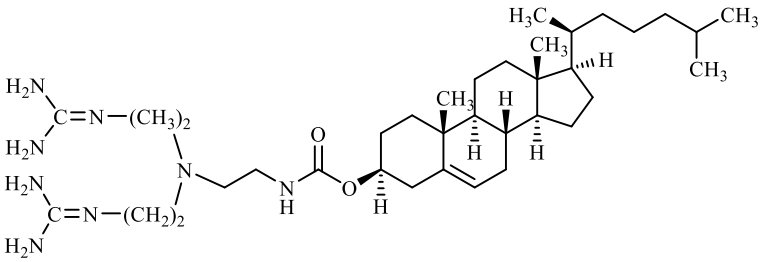

BGTC

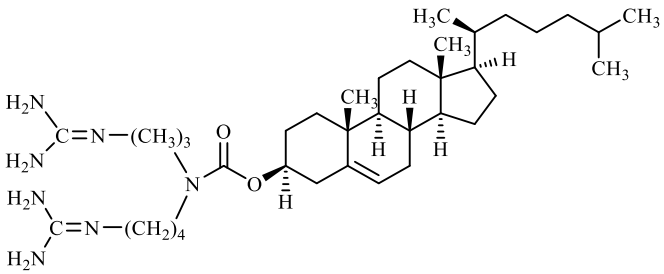

BGSC

Figure 1.3. Chemical structures of amidinium and guanidinum lipids

In addition to the polar head groups of amidine and guanidine, nitrogen-containing heterocycles have also been introduced in the structures of cationic lipids for gene delivery. Typically, heterocyclic cationic lipid compounds display relatively higher transfection efficiency and lower toxicity compared to the classical transfection systems, this is mainly due to the delocalization of the positive charge on the aromatic ring that might the ability to improve the interaction and compaction of DNA and facilitate their endosomal escape [19, 64]. Although a variety of heterocyclic compounds, such as pyridine, piperazine, and imidazoline, have been used as the head groups [20, 65, 66], pyridinium head groups are the most commonly used heterocyclic moieties in the design and development of novel cationic lipids used as gene delivery vectors. Their transfection efficiency has been reported to reach or surpass that of commercial transfection agents, while maintaining a low cytotoxicity profile [20, 67, 68].

Pyridinium cationic lipids were first introduced by Hoekstra et al. [20], who developed a series of double-chained pyridinium compounds named SAINT for transfection study. SAINT-1 (Figure 1.4) was the first pyridinium compound showing a transfection activity, which was comparable with the commercial agent lipofectin, but with less toxicity [20]. However, SAINT-2 (Figure 1.4) demonstrated 10 times more transfection efficiency than SAINT-1 in multiple cell lines [20], and most importantly without a concomitant increase in toxicity. In addition, SAINT-2 was able to not only transfect a relatively large number of cells per cell population (up to 45%) but also deliver a high number of DNA per cell (around 45%) compared with lipofectin (23% cell population and 30% DNA), resulting in their high transfection efficiency [20].

To increase transfection efficiency of pyridinium cationic lipids, Balaban et al. [69] synthesized a series of pyridinium cationic lipids with different linkers and hydrophobic tails to determine the structural elements that produced high transfection efficiency. The results revealed that an aliphatic

linker is superior to an aromatic one, as the former provided better fluidity of the formed cationic liposomes than the latter [69]. In addition, pyridinium cationic lipids with myristoyl fatty acid chains have higher efficiency in transfection than compounds bearing other fatty acid tails [69], however, the reason for this was not articulated in this study. As a result, the highest transfection efficiency was obtained with 1-(1,3-dimyristoyloxyprop-2-yl)-2,4,6-trimethylpyridinium chloride (5DMyr) (Figure 1.4), which was able to transfect NCI-H23 lung carcinoma more effectively than DOTAP and with low cytotoxicity [69]. On the other hand, the structure-toxicity relationship of pyridinium cationic lipids was also studied. Recently, Singh et al. [70] developed a series of glycerol-based pyridinium cationic compounds and found that their toxicities have a direct relationship with the alky chain length of the compounds, with increasing the chain length resulting in an increase in toxicity.

The other class of pyridinium cationic lipids are gemini pyridinium surfactants that contain two pyridines in the head group. Typically, gemini pyridinium surfactants provide strong binding and compaction of DNA due to double positive charges in the structure, resulting in enhanced efficiency in gene transfections. As such, gemini pyridinium surfactants have been a focus of pyridinium lipids used for gene delivery in recent years. Fisicaro et al. [15] developed a series of gemini pyridinium surfactants with different lengths of alkyl spacer (P16-n, n=3, 4, 8 and 12, Figure 1.4) for transfection study. The gene transfection capability of these compounds was found to be highly dependent on the spacer length [15]. Compound P16-4 (Figure 1.4) with a four-carbon atoms spacer showed the highest transfection activity on human rhabdomyosarcoma cell line RD-4 comparable to that of the commercial agent [15]. The similar structure-activity relationship was also observed with highly fluorinated gemini pyridinium surfactants (FGPn, n=3, 4, 8 and 12, Figure 1.4) [16]. Compound FGP8 (Figure 1.4) that has a spacer formed by eight-carbon atoms

displayed the best gene delivery capability among tested compounds on RD-4 cells equivalent to that of commercial agent [16].

Similar to amidinium and guanidinum compounds, pyridinium cationic lipids also tend to form lamellar bilayer structures in combination with DNA, facilitating its gene delivery [67]. Typically, the morphology of the DNA-containing complexes poses a significant influence on their transfection activity. The molecular shapes of pyridinium cationic compounds affect the stability of the structures of the complexes and thus impact the efficiency of gene delivery. For example, SIANT-2 has a low ratio of polar head group to hydrophobic tail, which forms unstable bilayers in the media and tends to be converted into the hexagonal structures to promote the endosomal release of DNA, improving transfection efficiency [71]. In addition, the overall charge of the complexes is important to achieve a high transfection efficiency, as a net positive charge is needed for the complexes to interact with the negatively charged cell membrane, facilitating their cellular uptake and gene transfection.

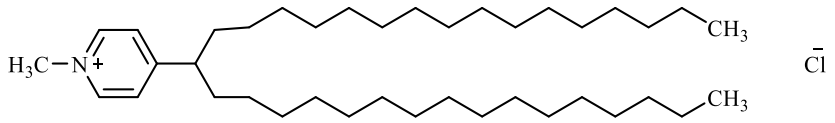

SAINT-1

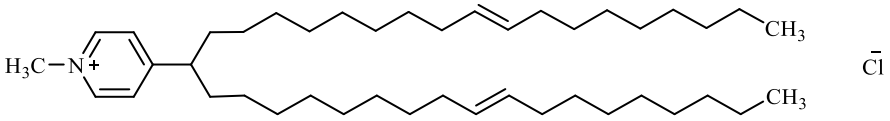

SAINT-2

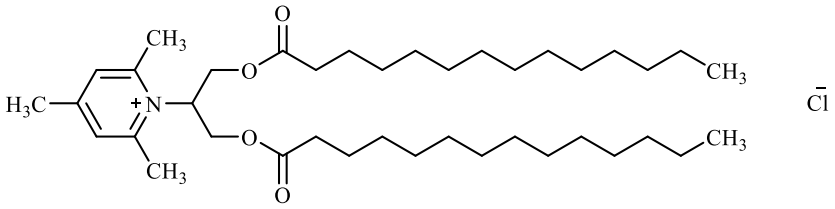

5DMyr

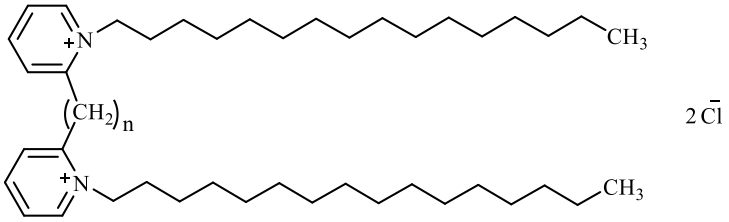

P16-n, n=3, 4, 8 and 12

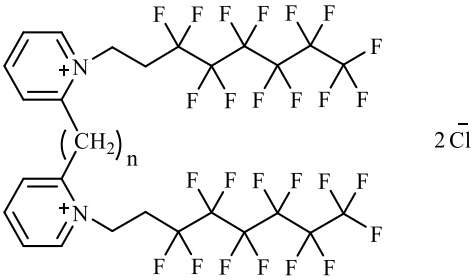

FGPn, n=3, 4, 8 and 12

Figure 1.4. Chemical structures of pyridinium lipids

1.2.4 Cationic gemini surfactants

1.2.4.1 Gemini surfactants

Gemini surfactants are a class of surfactant molecules that are comprised of two conventional monomeric surfactants covalently linked by a spacer (Figure 1.5A). Unlike conventional surfactants, gemini surfactants typically possess two hydrophilic head groups and two hydrophobic tail chains that are inter-connected through a spacer region [72]. Their structures are very versatile as the head groups can be positive, negative, or neutral moieties [73-76]; the spacer region can be a hydrocarbon chain at various lengths [77]; and the tails may consist of two hydrophobic alkyl chains with different degrees of unsaturation [78]. Typically, halide anions, such as chloride and bromide, are present as the counter ions to maintain the neutral charge of the molecules.

Although gemini surfactants can have differential head groups or tails in their structures, the most common gemini surfactants have symmetrical structures with two identical head groups and tails. Typically, a gemini surfactant with two C_m (m is the number of carbon atoms) tails and a C_s (s is the number of carbon atoms) spacer is denoted as *m-s-m* (Figure 1.5B), which is the most conventional type of gemini surfactants. By varying the head group, the length of hydrophobic tails, and the type of the spacer group, a wide range of gemini surfactant compounds can be designed and developed for their intended applications. The physicochemical property of gemini surfactants can often be predicted based on their structures. In general, increasing hydrophilicity of the head group increases its solubility in water, whereas increasing hydrophobicity of the tail chain makes the molecule less soluble in aqueous media. In addition, the addition of hydrophilic functional groups in the spacer region will also increase water solubility [79].

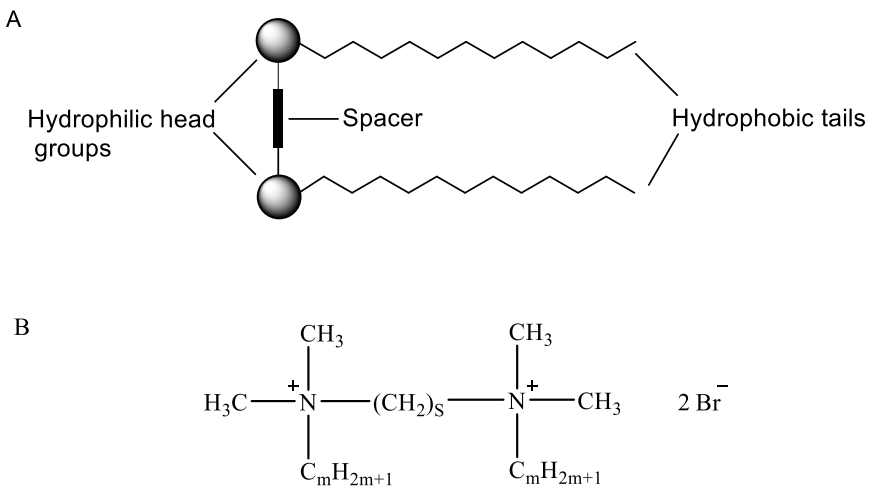

Figure 1.5. Structures of gemini surfactants, A) general structure of gemini surfactant, B) chemical structure of *m-s-m* gemini surfactant.

Due to their unique structures, gemini surfactants possess a number of superior properties compared with conventional monomeric surfactants, such as: 1) lower critical micellar concentration (CMC), a concentration above which gemini surfactant molecules spontaneously aggregate to form micelles; 2) lower Krafft temperature, the minimum temperature at which ionic gemini surfactants form micelles; 3) three orders of magnitude or more surface activity; 4) greater solubilization power; and 5) a wide variety of aggregate arrangements depending on the surfactant structure, concentration, temperature, and type of solvent [72]. These properties have allowed gemini surfactants to be used in a variety of industrial applications, such as detergents, cosmetics, and solubilizing agents [80], as well as in the pharmaceutical sphere as gene and drug delivery agents [13, 23].

1.2.4.2 Cationic gemini surfactants as gene delivery agents

Cationic gemini surfactants are promising non-viral gene delivery agents, which have been used for decades as they have the capability to compact and encapsulate large size of genetic materials

with low toxicity, and they are produced with relatively low cost [13, 81]. To date, a wide range of cationic gemini surfactants have been developed and successfully used for the delivery of DNA to cells [13, 82, 83].

In general, cationic gemini surfactants have several essential structural characteristics that make them suitable as gene delivery agents. Firstly, they have two positively charged head groups that can bind with the negatively charged phosphate groups of DNA, compacting and encapsulating DNA to form nanosized complexes, which allow for their cellular uptake *via* endocytosis [84]. Furthermore, cationic gemini surfactants have the capability of protecting DNA from enzymatic degradation during intracellular trafficking as DNA is condensed and encapsulated in lipoplexes [84]. Secondly, cationic gemini surfactants are able to fuse with cell membrane due to the fusogenic properties of their hydrophobic tails and thus facilitate the internalization of DNA into the cell [84]. Finally, cationic gemini surfactants are able to maintain an overall positive surface charge on the lipoplexes through appropriate formulation, which enables electrostatic interactions with the negative cell surface and subsequently enhances their cellular uptake [85]. For example, cationic gemini surfactants with C_3-C_{12} alkyl spacers are able to compact DNA and form particles with sizes at 100-200 nm, which enable their interaction with the cell membrane allowing for endocytosis [86]. Typically, a helper lipid, such as 1,2-di-(9Z-octadecenoyl)-*sn*-glycero-3-phosphoethanol amine (DOPE), is added to the gemini surfactant/DNA complexes to increase transfection efficiency as it has the ability to stabilize the lipoplexes and destabilize the endosomal membrane to facilitate intracellular release of DNA, leading to enhanced transgene expression [87, 88].

To improve the transfection efficiency of cationic gemini surfactants, extensive research has been conducted to study their structure-activity relationship. Badea et al. [13] reported that the length of

the tails and type of spacer region played a significant role in determining transfection efficiency, with a 3-carbon spacer being the most efficient for the *m*-*s*-*m* gemini surfactant structural family. For instance, the gemini surfactants 12-3-12 and 16-3-16 (Figure 1.6) showed the highest transfection efficiency among the same category of gemini surfactants [86]. This is because the distance between the cationic head groups in their structures is similar to that between two phosphate groups in a DNA molecule, resulting in stronger interaction and complexation of DNA [86]. However, increasing the length of the spacer group up to 8 carbon atoms decreased the transfection efficiency, after which the efficiency began to increase [86]. It was proposed that as the length of the spacer increases, the spacer tends to bend into a U-shape conformation, especially for the spacer length greater than 12 carbons, which results in a decrease in the distance between the two cationic head groups, thus enhancing the compaction of DNA [86]. Therefore, the length of the spacer of gemini surfactants also plays an important role in their transfection activity.

Furthermore, substitution of the alkyl spacer with pH-sensitive imino groups also increases the transfection efficiency of cationic gemini surfactants [8]. For example, the gemini surfactant 12-7NH-12 (Figure 1.6) was able to transfect monkey kidney fibroblast cells (COS-7) at a 9-fold higher level than an unsubstituted alkyl spacer derivative (12-7-12) (Figure 1.6) and a 3-fold increase compared with the corresponding aza-substituted compound (12-7N-12) (Figure 1.6) [89]. Such results were attributed to the enhanced pH activity due to the incorporation of a protonable imino group in the structures, which contributed to the efficient escape of the complexes from the endosomes and subsequent intracellular release of DNA, thereby resulting in high gene transfection efficiency [89].

Recently, amino acid-substituted gemini surfactants have been introduced with the aim of making the delivery system more bio-compatible, thus enhancing transfection efficiency [26, 83, 90]. For

example, the amino acids-substituted gemini surfactants 12-7N(Gly)-12 and 12-7N(Gly-Lys)-12 (Figure 1.6) exhibited significantly higher gene transfection efficiency compared with the imino substituted compound 12-7NH-12 in three different epithelial cell lines [83]. Such results indicated that the presence of amino acid group in the structure improved the interaction of the gemini surfactant/DNA complexes with the cell membrane *via* the formation of hydrogen bonds and, more importantly, aided in the endosomal escape of the complexes, thus facilitating the DNA release for transgene expression [83]. Collectively, structural modifications have greatly contributed to the development of novel gemini surfactants with enhanced efficiency and reduced toxicity.

Physicochemical properties of gemini surfactant nanoparticles, such as size and *zeta* potential, have also been evaluated to explore their relations with transfection efficiency and toxicity. In general, the particle size decreases with the increase in the charge ratio of gemini surfactants/DNA, as increasing the charge ratio results in enhanced electrostatic interaction between gemini surfactants and DNA, thus resulting in a better DNA compaction [90]. In addition, the size of nanoparticles has a great impact on their cellular entry, cytotoxicity, and intracellular fate. Typically, small nanoparticles display a higher efficiency in gene transfection compared to large-sized nanoparticles. For example, the 16-7N(GK)-16/DNA nanoparticles with sizes of 81 ± 3 nm had a significantly higher transfection efficiency than the 18:1-7N(GK)-18:1/DNA nanoparticles in sizes of 206 ± 6 nm [90]. Similarly, *zeta* potential is also a key parameter that influences the performance of the delivery systems both *in vitro* and *in vivo.* A high charge density can cause cell membrane to rupture, thus resulting in increased toxicity; whereas a low charge density is insufficient to enable nanoparticles to interact with the cell membrane, thereby leading to reduced transfection efficiency. As such, an optimal surface charge is generally needed to achieve high transfection efficiency of

nanoparticle-based gene delivery systems. Typically, gemini surfactant nanoparticles show a positive *zeta* potential of 10-30 mV at their optimal transfection efficiency [90].

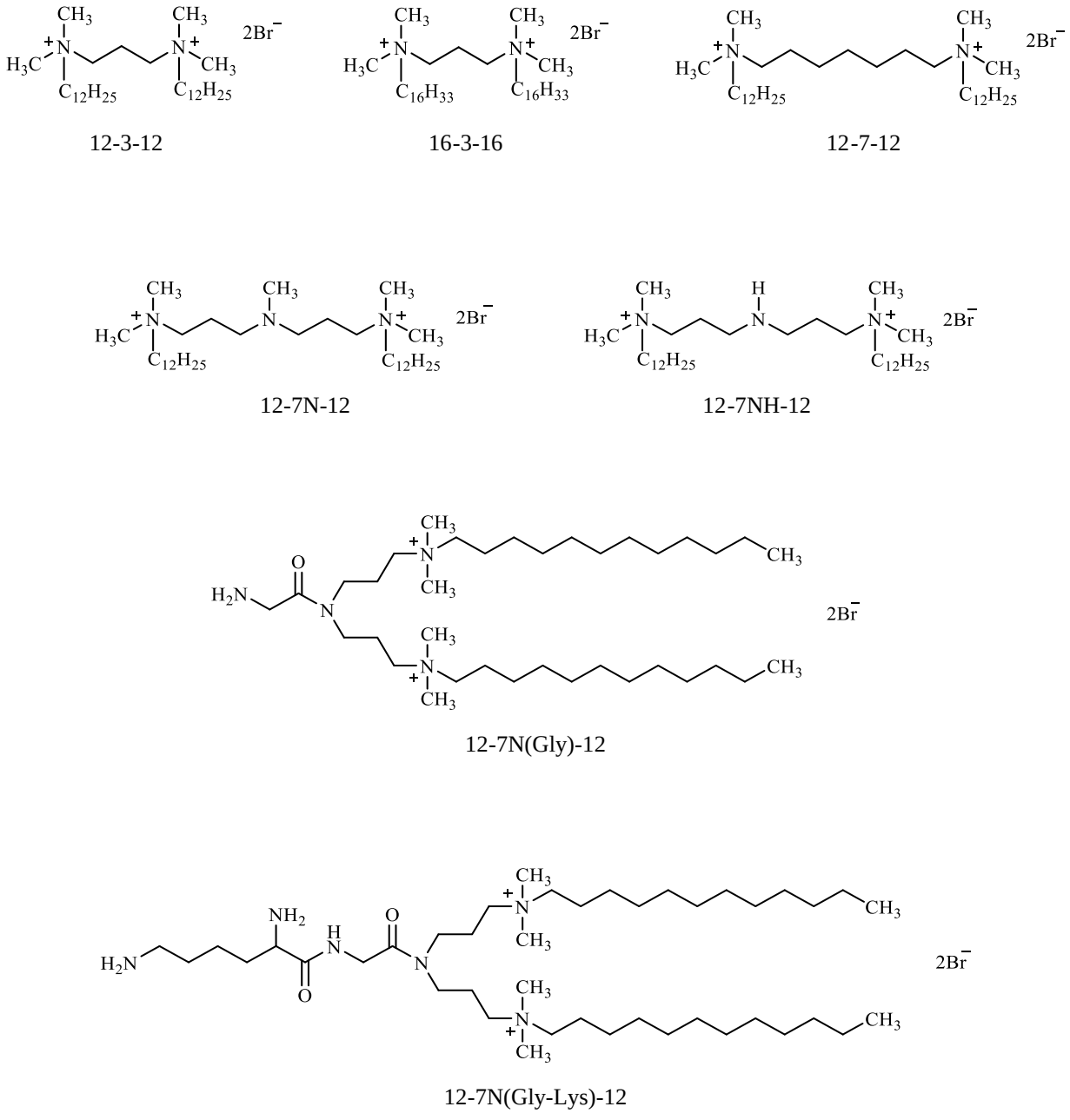

Figure 1.6. Chemical structures of cationic gemini surfactants

Despite the significant improvement in transfection efficiency and toxicity profiles, gemini surfactants are still limited in gene transfection efficacy for therapeutic applications. Furthermore, there are no clear explanations for the varying toxicities among different gemini surfactant structures. Therefore, a better understanding of the mechanism of transfection and toxicity will aid in the development of more efficient and less toxic gemini surfactants. One factor that could be investigated is their biological fate upon transfection, as gemini surfactant nanoparticles could deposit and be potentially metabolized in various cellular compartments during their intracellular trafficking that may affect their transfection efficiencies and toxicities. However, as of yet, little attention has been paid to study the biological fate of gemini surfactant nanoparticles. Understanding the behavior of these gemini surfactants nanoparticles within biological systems will gain insight on their cellular uptake, biodistribution, and metabolism, which will provide knowledge to comprehensively understand the role of gemini surfactants nanoparticles as non-viral gene delivery agents.

The gemini surfactants being investigated in my research belong to three main categories: 1) *m-s-m* gemini surfactant (16-3-16), 2) pyridinium gemini surfactant (16(Py)-S-2-S-16(Py)), and 3) peptide-substituted gemimi surfactant (16-7N(GK)-16) (Figure 1.7), which have been reported with high efficiencies and low toxicities in gene delivery [13, 90]. Structurally, 16-3-16 is a conventional gemini surfactant with two quaternary amines linked by a 3-carbon spacer region, 16(Py)-S-2-S-(Py)16 contains two pyridinium head groups instead of quaternary amines, and 16-7N(GK)-16 has a biocompatible glycyl-lysine di-peptide in the space region. However, these gemini surfactants vary amongst each other in terms of their gene transfection efficiency and toxicity profiles, this could theoretically be attributable to their different biological fate upon transfection, such as variable cellular uptake, subcellular biodistribution, and metabolism. Such

knowledge may provide a mechanistic explanation for the observed differences among these gemini surfactants in terms of efficiency and toxicity. In addition, the three gemini surfactants contain a variety of chemical structures, which allow them to be used for investigating the impact of different structures on their intracellular fate. Ultimately, these results will aid in the development of novel gemini surfactants with high efficiency and low toxicity in the long term.

Although various analytical techniques are available for the detection, characterization, and analysis of gemini surfactant nanoparticles [91-93], mass spectrometry (MS) has the advantages of high sensitivity and selectivity, capability to provide accurate mass measurement, and a large dynamic range for detection, which allow for the identification and quantification of a variety of molecules in biological systems [94]. Since gemini surfactants lack chromophores or fluorophores in the structure, the fluorescent/UV-detection is not suitable for their analysis. However, they have two positively charged quaternary ammonium groups and thus MS is an ideal analytical technique for their detection and analysis [95, 96]. Therefore, I employed MS to study the behavior of gemini surfactant nanoparticles within biological systems.

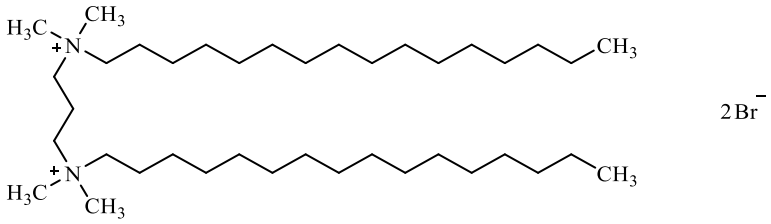

16-3-16

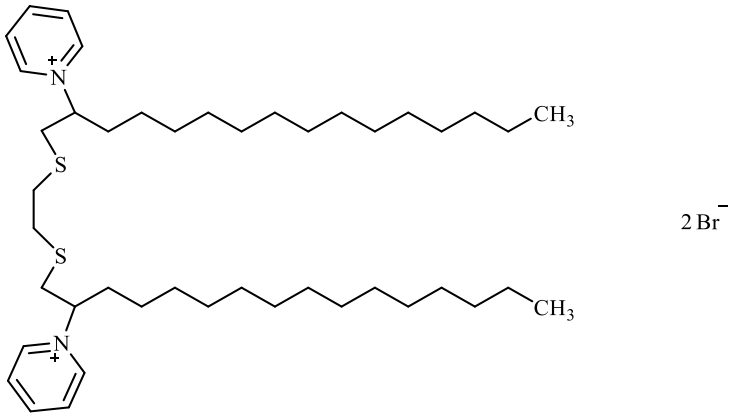

16(Py)-S-2-S-16(Py). Py=Pyridine, S=Sulfur

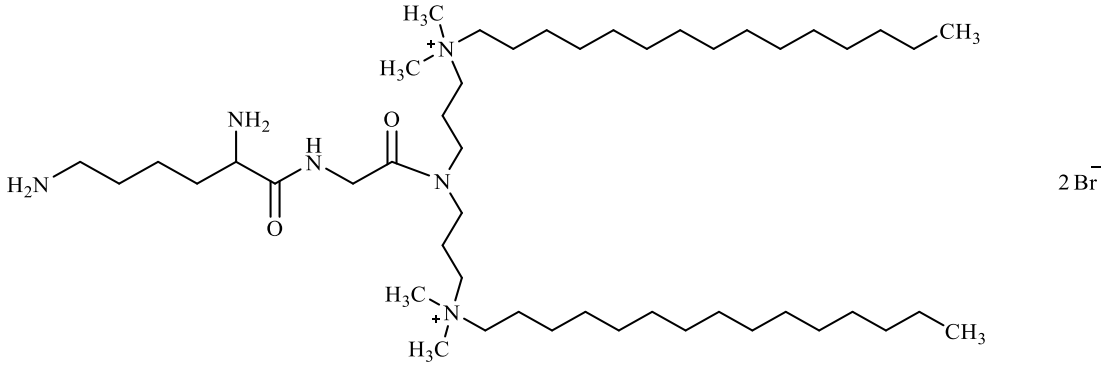

16-7N(GK)-16. GK=Glycyl-lysine

Figure 1.7. Chemical structures of gemini surfactants evaluated in this study

1.3 Mass Spectrometric Analysis of Gemini Surfactant Nanoparticles

Mass spectrometry (MS) is a powerful analytical technique that has been used for both qualitative and quantitative applications in a variety of fields, such as food science, environmental science, forensic science, and life sciences [97-101]. Recently, MS has progressed rapidly in terms of sensitivity, accuracy, and high throughput capability, which allows it to be widely applied in pharmaceutical research and industry. For instance, MS has been used for the identification and quantification of a variety of drug molecules and their metabolites [102], for the determination of isotopic composition of elements [103], and for the structural elucidation of chemical compounds [104]. To date, MS has become an indispensable tool for the analysis of a wide range of analytes from small molecules to large biomolecules, such as peptides and proteins.

1.3.1 Analytical mass spectrometry

MS has dramatically evolved and improved in terms of function and performance over the past few decades, which allows it to be used for the detection, identification, and quantification of molecules in complex biological matrices [105]. Fundamentally, however, the principle concept of MS operation remains the same, which is to generate charged gas phase ions and then separate them based on their mass-to-charge ratios (*m/z*) under vacuum conditions, followed by the detection and recording of the relative abundance of each ion [94]. Typically, a MS instrument consists of three major components: 1) Ion source - for generating gaseous analyte ions, 2) Analyzer - for separating the ions based on their *m/z* values, and 3) Detector - for detecting the ions and recording their relative abundances [94] (Figure 1.8). Single-stage MS instruments contain one analyzer, whereas multiple-stage MS instruments have more than one analyzer in their configuration. Tandem MS, also known as MS/MS, involves two stages of MS selection, with fragmentation occurring in

between the stages. There are two types of tandem MS: tandem in space and tandem in time [94]. Tandem in space usually has two mass analyzers sequentially connected and one reaction region (i.e., collision cell) in between. On the other hand, tandem in time involves the use of an ion trap where the ion separation is accomplished in the same space over time [94]. In addition, a sample input system is necessary to introduce sample to the ion source and a data system is required to operate the instrument, acquire and generate mass spectra (Figure 1.8).

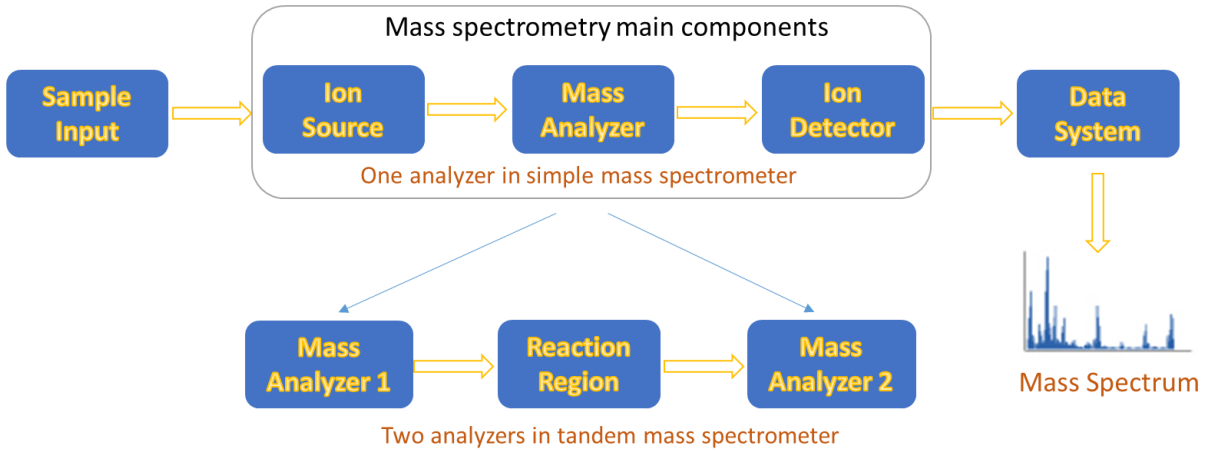

Figure 1.8. Schematic representation of single-stage and tandem in space mass spectrometry

As analyte molecules have to be ionized in order to be separated and detected in MS, various ionization techniques, such as electrospray ionization (ESI), atmospheric pressure chemical ionization (APCI), and matrix-assisted laser desorption ionization (MALDI), have been developed [94]. Each ionization technique has its own advantages and shortcomings and the use of a particular ionization method is mainly dependent on the physiochemical properties of the analytes and the type of the sample matrix [94]. For example, APCI is an ionization technique that uses the gas-phase ion-molecule reactions at atmospheric pressure and is mainly applied to analyze relatively non-polar compounds with molecular weight below 1500 Da [106]. Conversely, ESI involves the

formation of highly charged droplets formed in a high electric field, which is ideal for the analysis of relatively polar compounds with a broad range of molecular weights, including large biomolecules, such as peptides, proteins, and polymers [107, 108]. In addition, as a soft ionization technique, ESI allows the formation of protonated or deprotonated ions with high abundance that can then be subjected to MS/MS analysis allowing for the identification and characterization of chemical compounds [108].

Similar to the wide variety of ionization sources, different types of mass analyzers and their combinations in hybrid instruments are available, such as triple quadrupole (QqQ), triple quadrupole-linear ion trap (QqQ-LIT), quadrupole-time of flight (Q-TOF), and hybrid quadrupole-Orbitrap (Q-Exactive®) [94, 109]. Due to the difference in the structures and functions of various analyzers, each instrument has its own advantages and disadvantages that should be considered for a given application. In general, the use of a particular instrument is largely dependent on the type of the application. For example, QqQ and QqQ-LIT instruments are well known for high selectivity and sensitivity in the multiple reaction monitoring (MRM) mode and have been primarily used for the quantification of small molecules in complex biological matrices. On the other hand, Q-TOF and Q-Exactive instruments are often used for the characterization and identification of chemical compounds due to their capability of providing accurate mass measurements for parent molecules and their product ions [94, 109].

In my study, I utilized the QqQ-LIT (4000 QTRAP®) to quantify gemini surfactants for the assessment of their subcellular uptake and biodistribution at various time points post transfection. Both free gemini surfactant compounds and any remaining gemini surfactant liposomes in treated cells are quantified as gemini surfactant molecules will be extracted in organic solvents from both forms and analyzed by MS. In addition, I used the Q-TOF (QSTAR XL®) and Q-Exactive

instruments to detect and identify the potential metabolites of these gemini surfactants within transfected cells. Positive ESI ionization was used for the analysis of these gemini surfactants, since they are amphiphilic compounds with two positively charged quaternary ammonium head groups, making them ideal for ESI in the positive ionization mode. Furthermore, the soft ionization of gemini surfactants in ESI allows for the formation of intact ions with limited in-source fragmentation, which can be used for identification and quantification of gemini surfactant compounds.

1.3.2 Triple quadrupole-linear ion trap for quantitative analysis

QqQ-LIT is a unit-resolution tandem mass spectrometer that has the ability to simultaneously measure and characterize target analytes [110]. QqQ-LIT is a hybrid system in which a quadrupole is sequentially connected with a linear ion trap (LIT) separated by a collision cell [94]. A quadrupole consists of four parallel rods, with opposite rod pairs being connected electrically. By applying an alternating radio-frequency (RF) potential and a positive direct current (DC) potential to one electrode pair while applying a negative potential to the other pair, accelerated ions entering the quadrupole will possess an oscillatory movement. As such, ions with particular *m/z* values will have a stable trajectory going through the quadrupole, whereas the rest of ions will have unstable trajectories and collide with the rods [94]. Functionally, the first quadrupole of a triple quadrupole system typically works as a mass filter that selects only ions with specific *m/z* values to enter the second quadrupole. The second quadrupole is a collision cell, in which the ions collide with a neutral gas (typically N_2 or Ar) and fragment through a process known as collision activated dissociation (CAD) to generate product ions. The resulting product ions are transmitted to the LIT operating as a quadrupole, where only the product ions with specific *m/z* values are allowed to pass and reach the detector. In addition, the LIT can also be operated in the linear ion trapping mode

that can trap ions and subject them for further fragmentation (i.e., MS^3) to generate more detailed structural information.

QqQ-LIT combines the features of a triple quadrupole with that of a linear ion trap that allows the system to operate in various modes, such as product ion scan, precursor ion scan, neutral loss scan, MRM scan and MS^3, for a wide range of applications. In particular, MRM scan is the most commonly used technique for the quantitative analysis of small molecules [94]. The MRM scan in QqQ-LIT combines the selectivity of the first quadrupole and that of the linear ion trap operated as a quadrupole, which, even without chromatographic separation, enables high selectivity and sensitivity for quantitative analysis [111-113]. Therefore, analytical methods based on MRM in QqQ-LIT have been predominately used for quantitative applications in the pharmaceutical industry and research, including measurement of dosed drugs and their metabolites [102, 114], as well as studying lipid metabolites in biological systems [110].

In our group, we studied the mass spectrometric fragmentation behaviors of various families of gemini surfactants used as non-viral gene delivery agents and established the universal tandem mass spectrometric fragmentation patterns for each family [115-118]. Identification of these product ions allows for the development of tandem mass spectrometry MRM-based methods for the quantitative analysis of gemini surfactants. Initially, a high performance liquid chromatography (HPLC)-MS/MS method employing a cyano column for the quantification of *m-s-m* gemini surfactants in epidermal keratinocytes PAM 212 was developed and validated [95]. Subsequently, a quantitative hydrophilic interaction liquid chromatography (HILIC)-MS/MS method was established for the analysis of gemini surfactants 16-3-16 and 16(Py)-S-2-S-16(Py) within two different families. The latter method achieved a lower limit of quantification (LLOQ) at 50 ng/mL for compound 16-3-16, as compared with 300 ng/mL obtained in the former method [95, 96]. Both

compounds were observed to rapidly accumulate in PAM 212 cells during the course of treatment and subsequently depleted in a similar trend post transfection [96]. These results demonstrated the feasibility of LC-MS/MS method for the detection and quantification of gemini surfactants in a complex biological matrix.

In addition, various high-throughput MS-based methods for the quantification of the gemimi surfactant 16-3-16 in cell lysates were also developed and compared [119]. These methods include fast chromatography (FC)-QTRAP-MS/MS, FC-ORBITRAP-MS, matrix-assisted laser desorption ionization (MALDI)-TOF/TOF-MS, and desorption electrospray ionization (DESI)-MS/MS [119]. FC-QTRAP-MS/MS and MALDI-TOF/TOF-MS were shown to be superior to the previous LC-MS/MS method in terms of the linearity range and sample analysis time for the quantification of gemini surfactant 16-3-16 [119]. Furthermore, the LLOQ was 10-fold lower in the FC-QTRAP-MS/MS method compared with the LC-MS/MS method [95, 119]. As such, high-throughput MS methods based on direct analysis, such as flow injection analysis, could be also utilized for the quantitative analysis of gemini surfactants in biological matrices.

Flow injection analysis-tandem mass spectrometry (FIA-MS/MS) is an analytical technique that can be used for rapid quantitative analysis of a variety of compounds. In this approach, both separation and detection of the analyte occur within the MS instrument as no column is used [112]. Without prior column separation, the FIA-MS/MS method mainly relies on the mass spectrometer's separation capability in multiple reaction monitoring (MRM) mode, as the MRM in the QqQ-LIT system has the capability of selectively monitoring and accurately quantifying the analytes of interest in complex matrices [120]. In addition, the removal of the analytical column can significantly reduce the complexity of the method, shorten the time of method development, and decrease the time of sample analysis. Although matrix effect and interference could be a

potential challenge in the FIA-MS/MS analysis, finding suitable sample extraction techniques can be used to avoid this issue. In fact, a wide range of molecules have been detected and quantified in biological samples using FIA-MS/MS methods [121-123].

In my research, I developed a FIA-MS/MS method using a QqQ-LIT (4000 QTRAP®) instrument to quantify the three gemini surfactants belonging to different families for the assessment of their subcellular uptake and distribution in treated cells at various time points after treatment. The rationale for the use of FIA-MS/MS is to achieve a simple and reliable analysis that can accurately determine the tested compounds while reducing sample analysis time.

1.3.3 Quadrupole-time of flight for qualitative analysis

Q-TOF is a high-resolution tandem mass spectrometer that offers simultaneously high speed data acquisition, accurate mass measurement, and full scan spectral sensitivity [101]. In this hybrid system, the first quadrupole (Q) and second quadrupole (collision cell) are coupled with time of flight (TOF) in such a way that acceleration of the ions in the TOF occurs perpendicular to the initial trajectory of the ions [124]. Structurally, a Q-TOF instrument is similar to a QqQ-LIT, whereas the LIT is replaced by a TOF analyzer, which contains an ion acceleration region and a field free region (flight tube). The TOF analyzer measures the time for ions to travel through the flight tube; ions with small *m/z* values need a shorter time to reach the detector than those with large *m/z* values. The mass can be determined based on the time taken to travel the distance [124]. Thus, the resolution of a TOF analyzer is highly dependent on the length of the field-free region. Given the specific structure, a Q-TOF instrument typically can provide a high detection sensitivity in the atto-mole range, a high resolution of 20,000 or more, and a high mass accuracy of less than 5 ppm [124, 125], which has enabled it to be used in a wide scope of applications.

Depending on the type of application, a Q-TOF is typically operated in two modes: TOF-MS and TOF-MS/MS. In TOF-MS mode, the first and second quadrupoles are used as ion guides operated in RF-only mode that allow all ions to enter the fight tube travelling to the detector. Therefore, accurate mass measurement can be achieved, providing the confirmation and possible elemental composition of target analytes [126]. In TOF-MS/MS mode, the first quadrupole is used as an ion filter that selects specific ions for fragmentation *via* CAD in the collision cell. The product ions are then transmitted into the flight tube for differentiation and subsequent detection. Thus, both precursor and product ions can be detected with accurate mass information that can be used to characterize and identify unknown compounds. Based on these advantages, Q-TOF has been extensively used for the characterization and identification of drug molecules and their metabolites [94, 127].

Similarly, Q-TOF can also be used to study the metabolism of gemini surfactants in biological systems. Upon transfection, gemini surfactant nanoparticles enter cells and travel through different cellular compartments prior to releasing the genetic materials for gene expression. During this process, nanoparticles will potentially be metabolized by various cytoplasmic enzymes. The metabolites can possibly be related to the toxicity and efficiency of nanoparticles. Thus, understanding the metabolism of gemini surfactants can contribute to the design and development of more effective gemini surfactants for gene delivery. Therefore, it is of great importance to understand the metabolism and metabolite formation of gemini surfactants in cells. To achieve this goal, a Q-TOF instrument would be suitable as it can detect and characterize the metabolites of gemini surfactant nanoparticles in biological systems. Characterization and structural elucidation of gemini surfactants using Q-TOF has been extensively conducted in our group. For example, the MS/MS fingerprints of 10 novel di-quaternary ammonium gemini surfactants were illustrated using

an ESI-Q-TOF-MS/MS [117]. Similarly, 29 novel di-quaternary ammonium gemini surfactants were analyzed using a Q-TOF-MS and a quadrupole-hexapole-quadrupole mass spectrometer (QhQ-MS) for their structural elucidation and characterization [116]. Most recently, the analysis of a series of novel amino acid/dipeptide-modified gemini surfactants were accomplished by an ESI-Q-TOF-MS to obtain accurate mass measurements for the confirmation of their structures [118].

In my work, I used a non-targeted metabolic profiling approach to study the metabolites of the three gemini surfactants 16-3-16, 16(Py)-S-2-S-16(Py), and 16-7N(GK)-16 in PAM 212 cells. Despite the potential change with matrix effects and interferences, flow injection analysis-high resolution MS methods were used for establishing the metabolic profiles of treated cells as they offer simple and fast analysis along with accurate mass measurements suitable for the putative identification and characterization of metabolites. Specifically, FIA-TOF-MS methods in both positive and negative ESI modes were initially developed on a Q-TOF (QSTAR XL®) instrument. The extracts of treated and untreated (control) cells were then analyzed by the FIA-TOF-MS methods to establish their metabolic profiles in each mode, in which accurate mass measurements for potential metabolites were achieved to assist in their identification. Furthermore, potential metabolites were analyzed in FIA-TOF-MS/MS mode to obtain its product ions that offers additional confirmation for structural elucidation. However, after a preliminary evaluation of the potential metabolites of these gemini surfactants on a Q-TOF instrument, their metabolisms were further investigated using a hybrid quadruple-Qrbitrap (Q-Exactive) mass spectrometer due to its higher sensitivity and superior resolution, providing high confidence for the putative identification and characterization of the metabolites.

1.3.4 Hybrid quadrupole-Orbitrap for qualitative analysis

A Q-Exactive is also a high-resolution tandem mass spectrometer that provides high sensitivity, accurate mass measurement, and a wide dynamic range [128]. In this system, a quadrupole mass filter is connected to a high energy collisional dissociation (HCD) cell *via* an intermediate curved linear trap (C-trap) that is coupled with an Orbitrap mass analyzer [109]. Samples are introduced into the ion source and the ions are transmitted to the quadrupole which works as an ion guide and can filter the ions based on their *m/z* values. The ions are then transferred into the C-Trap and injected into the Orbitrap for analysis. In the Orbitrap analyzer, ions are trapped by rotating around a central spindle electrode with harmonic oscillations [129]. As the frequency of harmonic oscillation depends on the ion's *m/z* value, a time-domain image current transient is generated based on the frequency of harmonic ion oscillation, which is used to produce the high-resolution mass spectra *via* Fourier transformation [129]. In addition, ions can be passed through the C-Trap into the HCD cell to conduct fragmentation experiments and then the fragment ions can be moved back into the C-Trap and ejected into the Orbitrap for detection. Given the specific structure, Q-Exactive can achieve a resolution of 140,000 at *m/z* 200 and a mass accuracy of less than 2 ppm [128, 130]. Such an advantage enables the Q-Exactive to be used for a wide range of applications, including characterization, identification, and quantification of small molecules, peptides, and intact proteins [131-133].

Typically, a Q-Exactive instrument can be operated in two modes: MS scan and MS/MS scan. In MS mode, the quadrupole is used as an ion guide that allows all ions to pass into the C-trap for injection and analysis in the Orbitrap analyzer at high resolution. As such, accurate mass measurements can be achieved to provide possible elemental compositions of molecules. In MS/MS mode, the quadrupole is operated as an ion filter to select desired ions with specific *m/z*

values to pass through the C trap and enter the HCD cell for fragmentation. The product ions are then transmitted back into the C trap and ejected into the Orbitrap analyzer for high resolution mass detection. In this mode, both precursor and product ions are measured with accurate masses that contribute to the identification and characterization of unknown molecules. Therefore, Q-Exactive can be used to identify and characterize the metabolites of gemini surfactants in biological systems.

In my project, the metabolism of the three gemini surfactants in PAM 212 cells were mainly investigated on a Q-Exactive instrument. All metabolites were structurally proposed and characterized based on accurate mass measurements and characteristic product ions. As such, the metabolic pathways of gemini surfactants were elaborated.

1.4 Biological Fate of Gemini Surfactant Nanoparticles

In biomedicine, drug molecules must reach their target sites to exert therapeutic effects. However, the target sites can be in various locations, such as the organs, issues, and cells, in the body depending on the type of drug molecules. For nucleic acids used in gene therapy, the target sites are either in the cytoplasm or in the nucleus of a cell. Thus, it is imperative that these molecules travel through the plasma membrane to reach their target sites in cells for transgene expression. However, due to the unique structure of cell membrane that is dynamic and relatively lipophilic in nature, it restricts the entry of large and hydrophilic molecules, such as DNA and RNA. Therefore, an appropriate delivery system is required for nucleic acids to enter the cells and achieve gene transfection.

Nanoparticle-based medicine has the ability to deliver drugs and genetic materials to specific locations, such as specific regions in the body, specific cells, and even specific sites within cells, to achieve therapeutic effect [134]. In general, the behavior of nanoparticles can be summarized as

follows: 1) nanoparticles can be administrated *via* various routes, such as intravenous, subcutaneous, intraperitoneal, dermal, inhalation, and oral [135]; 2) they are absorbed once they begin to interact with biological components; 3) they circulate and distribute to various organs in the body and may remain structurally intact or be metabolized during this process [136]; 4) they enter the cells of target organ to release therapeutic contents; and 5) finally they are excreted or metabolized by various cellular enzymes. As such, the biological fate of nanoparticles varies largely depending on the characteristics of nanoparticles, the route of entry, and the biological conditions. Specifically, a series of events, including cellular uptake, trafficking, biodistribution, and metabolism, as well as systemic absorption, distribution, and clearance, can take place after administration that could dictate the biological fate of gemini surfactant nanoparticles.

1.4.1 Cellular uptake

Cellular uptake is one of the most important processes for gene delivery, as it determines the cellular internalization of therapeutic genes available for gene expression. The mechanism of internalization of gene-encapsulated nanoparticles in cells has been widely studied [26, 137]. Endocytosis has been established to be the main approach for the internalization of polycation/DNA complex into the cells, as the use of endocytosis inhibitors significantly reduced gene expression and the interference of endocytic pathway with lysosomotropic reagents substantially enhanced gene expression [138-140]. Endocytosis is a cellular uptake process that involves a controlled invagination of the cell membrane, allowing macromolecules, such as liposome/DNA complexes, to be enveloped by cell membrane; and subsequently the membrane buds off to form new vesicles inside the cell, which eventually fuses with the lysosome where the liposome/DNA complexes are degraded [84].

To date, a variety of mechanisms for endocytosis have been identified (Figure 1.9) [141, 142]. Among them, clathrin-mediated endocytosis, caveolae-mediated endocytosis, and macropinocytosis are the most common uptake pathways used by mammalian cells to internalize macromolecules [143]. However, these endocytic pathways differ in the composition of coat, the size of detached vesicles, and the fate of internalized particles. Clathrin-mediated endocytosis is a process that involves the formation of ligand-receptor complexes in coated pit on the cell membrane and subsequent generation of clathrin-coated vesicles in the cytoplasm; the intracellular vesicles then form endosomes and fuse with lysosomes where the particles are degraded in low pH environment [144]. It is the major endocytic pathway for the uptake of essential nutrients, antigens, and pathogens [144]. Caveolae-mediated endocytosis is another important uptake pathway that typically involves the use of small hydrophobic membrane microdomains (caveolae) to achieve an entry to cells [145]. Compared with clathrin-mediated uptake, caveolar-mediated uptake is a non-acidic and nondigestive route for internalization of particles, which avoids normal lysosomal degradation due to the drop in pH [146]. Macropinocytosis is an actin-driven invagination of the plasma membrane that generates the large endocytic vesicles with irregular sizes and shapes [147]. It is an efficient route for the non-selective endocytosis of macromolecules and large volumes of extracellular medium, which has no formation of the coat and is also not receptor-dependent. For a given delivery agent, the specific mechanism of endocytosis is typically dependent on many factors, such as the properties of the carriers, the ligands attached to the complexes, and the surface characteristics of the cells.

Numerous studies have indicated that gene-encapsulated nanoparticles interact with cells to achieve cellular uptake *via* the above endocytic processes. For example, the cellular uptake of lipoplexes formed with the cationic lipid DOTAP and DNA has been observed to occur solely by

clathrin-mediated endocytosis and internalized particles were eventually degraded in the lysosomes [148]. Similarly, it was observed that SAINT-2/DNA lipoplexes-mediated transfection occurred through the cholesterol-dependent clathrin-mediated endocytosis and cholesterol depletion decreased the transfection activity [140]. Recently, an *in vitro* study showed that the internalization of gemini surfactant nanoparticles of P/L/12-7NH-12 and amino acid-substituted gemini surfactant nanoparticles of P/L/12-7N(GK)-12 was via both clathrin-mediated and caveolae-mediated uptake pathways [26]. Collectively, these results suggested that receptor-mediated endocytosis is an essential uptake pathway for gene-encapsulated nanoparticles.

In addition to the endocytic uptake pathway, non-endocytic pathways are also able to achieve the intracellular delivery of genes using various techniques, such as, microinjection, permeablization, and electroporation [149]. Microinjection is a technique that uses a glass capillary pipette to inject genes into the cytosol or the nucleus to achieve rapid delivery of genes [149]. Permeabilization is another technique for non-endocytic delivery, in which a pore-forming agent is used to induce transmembrane channels in cell membrane, allowing for the entry of large molecules [150]. Similarly, electroporation involves the use of an electric field to open pores in cell membrane to facilitate the entry of DNA [151]. Although these techniques have the ability to rapidly deliver genes to target sites in cell, they are not typically used for *in vivo* gene delivery due to their highly invasive nature [152]. In addition, the gene delivery efficiency of non-endocytic pathway is still limited, preventing their clinical applications. Therefore, the use of non-invasive endocytic cellular uptake is anticipated in the area of gene therapy.

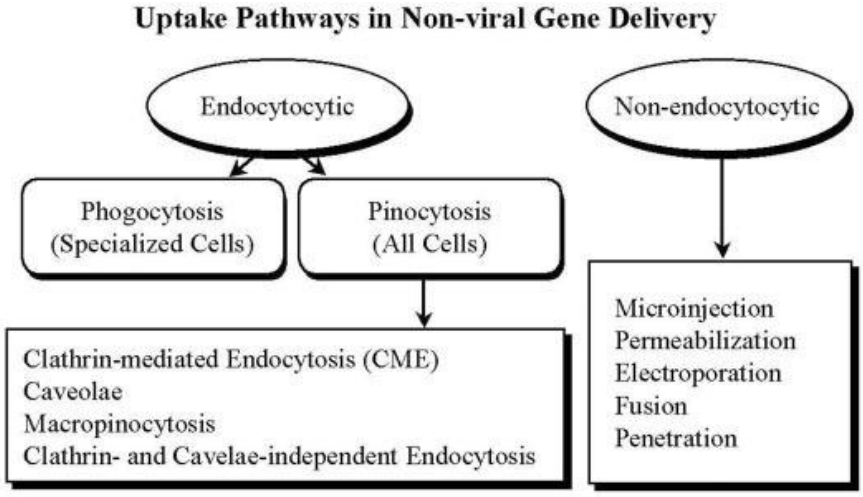

Figure 1.9. Different cellular uptake pathways in non-viral gene delivery [137]

As the quantity of nanoparticles internalized in cells can directly correlate with transfection efficiency and/or toxicity, it is of great importance to measure the level of cellular uptake of nanoparticles. This can be achieved by the quantitative determination of nanoparticles in cells using MS-based methods. In our lab, the cellular uptake of the gemini surfactants 16-3-16 and 16(Py)-S-2-S-(Py)16 was previously determined in PAM 212 cells using a quantitative LC-MS/MS method [96]. The results showed a rapid increase in the cellular concentration of both gemini surfactants during the course of 5 h treatment, followed by a gradual depletion post transfection [96]. However, the similar trend was not able to explain the difference in the efficiency and toxicity of the two compounds as gene delivery agents. Thus, we anticipate there is a difference within the cellular uptake and biodistribution of the two gemini surfactants nanoparticles, which could provide an insight on their different efficiency and toxicity profiles. The subcellular level of each gemini surfactant nanoparticle upon transfection can be determined by an FIA-MS/MS method.

1.4.2 Cellular trafficking and biodistribution

After internalization, the nanoparticles reside in the endosomes, which further develop and fuse with lysosomes where the nanoparticles can be degraded in the reduced pH condition. To achieve a successful gene transfection, a fraction of nanoparticles has to escape from the endosomes into the cytoplasm prior to their fusion with the lysosomes, which then goes through the intracellular trafficking and translocation process to reach various subcellular compartments. During this process, DNA within the complexes is protected from nuclease actions, but will inevitably be degraded unless it enters the nucleus. Currently, the most established mechanism for internalization, cellular trafficking and translocation, and gene release and expression of lipid-based nanoparticles is described below (Figure 1.10).

a) **Binding of the lipoplex to cell membrane** - The first step for internalization of DNA-encapsulated gemini surfactant nanoparticles is to bind with the cell membrane [153]. Both non-specific and specific bindings can trigger the internalization of the lipoplex into the cell [154]. Non-specific binding is primarily driven by electrostatic interaction between positive charge of the complexes and negative charge of the cell membrane surface, whereas specific binding is typically initiated by a specific targeting ligand that is specifically recognized by a cell surface receptor.

b) **Internalization into the endosome -** It is an internalization process primarily *via* endocytosis [84, 140], in which the complexes are surrounded by an area of plasma membrane and then buds off inside the cell to form a vesicle containing the ingested materials in the cytoplasm. Such vesicles can combine to form the endosomes, which develop powerful hydrolytic capabilities as the internal pH falls sharply. Eventually, the endosomes merge with the lysosomes where the lipoplexes are degraded [84].

c) **Endosomal escape of the lipoplexes** - The escape of lipoplexes from the endosome into cytoplasm is to prevent from degradation in the late endosome and lysosome due to the decreased pH. The pH decrease in the late endosome can induce the formation of an inverted hexagonal phase of the lipid/DNA complex, resulting in the fusion with endosomal membrane. Such an integration destabilizes the membrane and allows the escape of lipoplex from the endosome, facilitating the subsequent cellular trafficking and release of DNA into cytoplasm [84, 155]. In addition, DNA escape from the endosome can be facilitated by pH-sensitive cationic lipids, which possess a buffering capacity to promote the influx of protons in the late endosome/lysosome, resulting in an osmotic effect. This is called “proton sponge” effect that can aid in the disruption of endosomal membrane, enhancing the availability of DNA for nuclear transport and gene expression [156].

d) **Translocation into the nucleus** - In the cytoplasm, free DNAs or DNA-encapsulated nanoparticles can translocate to the nucleus through intracellular trafficking, which represents a significant barrier for gene expression [155, 157]. In the translocation process, the passage through the nuclear membrane competes with the rapid degradation of DNA by cytoplasmic nucleases [84]. Only a fraction of DNAs is able to enter the nucleus and the rest are destroyed in the cytoplasm. To increase the nuclear localization of DNA, nuclear localization ligands have been used to promote an efficient nuclear import of DNA, thus resulting in higher gene expression [158].

e) **Transcription of the therapeutic gene in the nucleus** - Once inside the nucleus, the therapeutic gene is transcribed to mRNA, followed by its translation in the cytoplasm and expression of therapeutic protein [155].

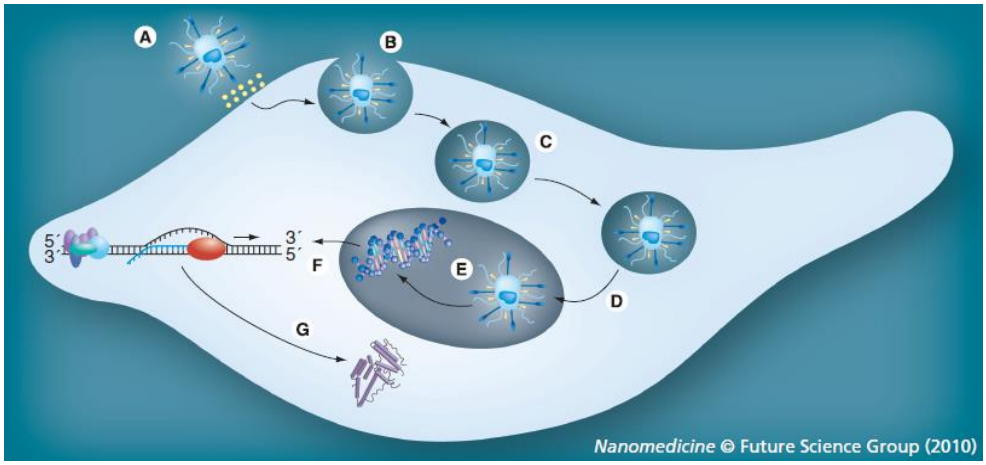

Figure 1.10. Cellular uptake, trafficking, and distribution of lipid/DNA nanoparticle. The process starts with a binding of the lipoplex to the cell membrane (A), followed by internalization into the endosome (B). Endosomal escape of the lipoplex (C) occurs for the subsequent intracellular trafficking and translocation into the nucleus (D). Transcription of the therapeutic gene takes place in the nucleus (E), followed by its translation in the cytoplasm and expression of therapeutic protein [155].

As shown in Figure 1.10, the internalization, cellular trafficking, and biodistribution of gemini surfactant nanoparticles involves a series of events taking place in various intracellular compartments. During this process, the nanoparticles travel through different cellular compartments and remain for a certain period of time at each compartment. Furthermore, the biodistribution of gemini surfactant nanoparticles within subcellular compartments also changes as the nanoparticles might migrate from one compartment to another and also undergo degradation by cytoplasmic nucleases [159]. As such, a time-course determination of the concentration of gemini surfactant nanoparticles in subcellular compartment is essential to assess their biodistribution. This can be achieved by a quantitative measurement of gemini surfactant nanoparticles in the isolated intact subcellular compartments of treated cells.

By using differential centrifugation, the subcellular compartments, such as the nucleus, mitochondria, plasma membrane, and cytosol, can be isolated intact from treated cells [160, 161].

These are the major compartments that gemini surfactant nanoparticles most likely accumulate during their intracellular trafficking process. Differential centrifugation is an isolation and purification technique that uses different centrifugal forces to pull on the subcellular components for precipitation based on their distinct densities, sizes, and shapes [161]. Once the subcellular compartments containing gemini surfactant nanoparticles are obtained, the gemini surfactant nanoparticles can be extracted from biological matrix using various extraction methods [95, 162]. In this process, free gemini surfactant molecules will also be extracted along with gemini surfactant nanoparticles from cellular compartments. Together, the quantity of gemini surfactants in each compartment can then be determined by a FIA-MS/MS method to assess their subcellular distributions.

1.4.3 Metabolite formation

Understanding the metabolism of gemini surfactants nanoparticles in biological systems provides information on how gemini surfactants interact with biological components and how the metabolites can possibly affect biological systems. Such information will aid in the design and optimization of gemini surfactant structures to improve efficiency and decrease toxicity. Currently, extensive research have been conducted to achieve the most efficient delivery systems by means of optimization of formulation strategy, facilitation of cellular uptake, and promoting efficient endosomal escape [163, 164]. For instance, various formulation conditions have been investigated with a number of gemini surfactant compounds to obtain the delivery system with high efficiency and low toxicity [164]. Although such investigations obtained the knowledge pertaining to the formulation methods of lipoplexes, other important factors, such as metabolite formation, were not explored, which might have great impact on their efficiency and toxicity. In addition, the

metabolites of the nanoparticles might also play important biological roles in host body, which need to be further investigated.

To obtain optimal transfection and minimal toxicity, drug-loaded nanoparticles should deliver and release their therapeutic contents at the target sites, followed by their biodegradation and excretion. However, the therapeutic agents might be practically released at any time during the delivery process depending on the characteristics of nanoparticles and their interactions with biological components, leading to reduced efficiency and increased toxicity. Furthermore, nanoparticles typically possess high toxicity when genetic materials are not incorporated as a result of the carried excessive positive charges [21]. Also, the metabolites of nanoparticles might pose potential harm to host cells, contributing to the overall toxicity of the delivery system. To date, the detailed mechanism of degradation and excretion processes for nanoparticles has not been well understood, and there is no report describing the metabolite formation of nanoparticles, including gemini surfactant nanoparticles, as gene delivery agents.

Generally, the internalized nanoparticles in the endosomes will be either degraded in the lysosomes or recycled back to the cell surface *via* exocytosis if they are not able to escape from the endosomes [84]. Therefore, an efficient escape of the nanoparticles from the endosomes into cytoplasm is essential to achieve effective transfection as it dictates the amount of genetic materials that can reach the nucleus for gene expression. After escape from the endosome, the nanoparticles can either release DNA in the cytoplasm, which further migrates to the nucleus for expression [165, 166]; or as a whole enters the nucleus, followed by the release of therapeutic materials [167]. During this process, the nanoparticles can possibly be metabolized by various cytoplasmic enzymes depending on their structures and characteristics.

Phase I and II biotransformations are common pathways for drugs and other foreign substances to be detoxified and eliminated [168-170]. Typically, phase I biotransformations contain oxidation, hydroxylation, reduction, and hydrolysis, which involve the modification of a substrate molecule with polar functional groups, such as hydroxyl (-OH), carboxyl (-COOH), sulfhydryl (-SH), and amino ($-NH_2$) group [169]. Such reactions often result in a modest increase in the parent drug's water solubility, which usually makes the drug ready to undergo subsequent phase II conjugation reactions. On the other hand, phase II biotransformations generally involve the addition of endogenous polar functional moieties, such as glucuronic acid, glycine, and amino acids, to make the drugs more hydrophilic so that they can be easily excreted [169]. These reactions often include a variety of conjugation reactions, such as glucuronic acid, sulfate, amino acids, and glutathione conjugations [171].

A variety of xenobiotics, including drugs and delivery agents, have been reported to undergo phase I and phase II biotransformations to achieve cellular detoxification and elimination [172]. It is well known that liver is the principal organ of drug metabolism with a large number of enzymes, however, other tissues, such as the lungs, the skin, and the kidneys, also exhibit substantial enzymatic activities [173-175]. Therefore, the metabolism of the gemini surfactants nanoparticles in the keratinocyte PAM 212 cells was also investigated in my research to understand their metabolite formation as the main therapeutic use of these gemini surfactants are for topical applications. Since the potential metabolites of these gemini surfactants might have close structural relationship with their original compounds, their masses can be accurately determined by high-resolution MS to assist in structural identification. Thus, by using high-resolution mass spectrometry, the metabolites of the gemini surfactant nanoparticles in cells can possibly be identified and characterized.

1.4.4 *In vivo* fate

The *in vivo* biological fate of lipid-based nanoparticles is closely related to the absorption, distribution, and excretion in host body, which might also have a profound impact on their efficiency and toxicity. Typically, nanoparticle-based medicines are introduced into the body *via* a variety of routes, including oral administration, injection, inhalation, and topical application, depending on their physiochemical properties [135]. Once the nanoparticles are in the host body, they enter blood circulation by two main approaches, active diffusion and passive diffusion, followed by systemic circulation and distribution in various organs, such as the liver, the heart, the spleen, the lungs, the brain, and the lymphatics [176, 177]. During the distribution process, the nanoparticles will interact with the blood components and travel through the blood stream to reach the organs, followed by absorption and distribution in the tissues and cells. The net positive charge of the particles is a crucial factor that determines the circulation time and tissue distribution, as it can interact with the negative charge of blood constituents, such as erythrocytes and proteins. Such an interaction will reduce the net positive charge of the nanoparticles that changes their physicochemical property. As a result, the circulation time and distribution preference will be changed, resulting in reduced efficiency of the nanoparticles. In addition, particle size is another critical factor that affects the circulation and distribution in the body. Typically, small particles with sizes less than 40 nm diffuse fast in the inner layers of tissues and extracellular matrix, whereas large particles in sizes greater than 100 nm circulate and diffuse relatively slow due to the steric hindrance [178].

The clearance of nanoparticles from systemic circulation is inevitable after distribution, primarily conducted by macrophages in the liver and spleen [179]. Clearance and opsonization are the natural processes in biological systems to remove foreign particles by innate immune systems [180]. This

process can also occur under certain conditions for nanoparticles depending upon their sizes and surface characteristics [179, 181]. However, several strategies can be taken to reduce the rapid clearance of lipid-based nanoparticles, For example, the attachment of hydrophilic polymers polyethylene glycol (PEG) to the surface of nanoparticles can sterically enhance its stability and avoid rapid clearance by the phagocyte systems, which significantly increases its circulation time [182]. Similarly, coating hydrophilic polymers to hydrophobic particles can prevent their adsorption of opsonins, thereby reducing the uptake by the phagocyte systems and prolonging the circulation half-life of encapsulated genetic materials [182]. In addition, the route of administration has a great impact on the elimination process of nanoparticles in the host body. Typically, inhaled nanoparticles are cleared in the alveolar region *via* phagocytosis, which was facilitated by chemotactic attraction of alveolar macrophages to the deposition sites [182]. On the other hand, orally administrated nanoparticles are often removed from the host body by urinary excretion and they can also be eliminated by passing through the gastrointestinal tract in feces [183]. Intravenously injected nanoparticles are normally eliminated from circulation by the reticuloendothelial system in a process that is facilitated by the surface deposition of opsonic factors and complement proteins on the nanoparticles [184, 185]. In general, large particles are eliminated more rapidly than small nanoparticles as they can activate the complement systems more efficiently [179, 186].

1.5 Proposed Research

1.5.1 Research hypotheses

1) Gemini surfactant nanoparticles 16-3-16, 16(Py)-S-2-S-16(Py), and 16-7N(GK)-16 will show different cellular uptake and distribution profiles that can explain their varying transfection efficiencies and toxicities.

2) Upon transfection, the gemini surfactant nanoparticles 16-3-16, 16(Py)-S-2-S-16(Py), and 16-7N(GK)-16 will be degraded/metabolized by enzymes in cells. The metabolites can be detected and possbily identified using high-resolution mass spectrometry, which will help explain their various transfection efficiencies and toxicities.

1.5.2 Research objectives

1) Assessment of the cellular uptake and distribution of the three gemini surfactants nanoparticles 16-3-16, 16(Py)-S-2-S-16(Py), and 16-7N(GK)-16 using mass spectrometry to explore their relationship with the varying efficiencies and toxicities in gene transfection.

    a. *In vitro* evaluation of gene transfection efficiencies and toxicities of the gemini surfactants nanoparticles 16-3-16 and 16(Py)-S-2-S-16(Py) within PAM 212 cells.

    b. Development and validation of a flow injection analysis-tandem mass spectrometric (FIA-MS/MS) method for the quantification of the three gemini surfactant nanoparticles in cellular matrix.

    c. Determination of the three gemini surfactant nanoparticles in the subcellular compartments at various time points after treatment using the validated FIA-MS/MS method.

2) Evaluation of DNA binding capabilities and molecular packing parameters of the three gemini surfactants to understand their behaviors in subcellular compartments.

   a. Evaluation of DNA binding capabilities of the three gemini surfactants using ethidium bromide dye exclusion assay.

   b. Determination of molecular packing parameters of the three gemini surfactants using Langmuir studies.

3) Investigation of the metabolite formation of the gemini surfactants nanoparticles 16-3-16, 16(Py)-S-2-S-16(Py), and 16-7N(GK)-16 using high-resolution mass spectrometry.

   a. Development of FIA-MS and FIA-MS/MS methods on high-resolution mass spectrometry instruments for the analysis of gemini surfactant metabolites.

   b. Establishment of the metabolic profiles of cells treated with gemini surfactant nanoparticles using a non-targeted metabolic profiling approach.

   c. Putative identification and characterization of the metabolites of the three gemini surfactants and understanding their metabolic pathways.

1.6 References

1. Rosenberg, S.A., et al., *Gene transfer into humans--immunotherapy of patients with advanced melanoma, using tumor-infiltrating lymphocytes modified by retroviral gene transduction.* N Engl J Med, 1990. **323**(9): p. 570-578.
2. Boye, S.E., et al., *A comprehensive review of retinal gene therapy.* Molecular therapy, 2013. **21**(3): p. 509-519.
3. Branski, L.K., et al., *A review of gene and stem cell therapy in cutaneous wound healing.* Burns, 2009. **35**(2): p. 171-180.
4. Gaudet, D., et al., *Review of the clinical development of alipogene tiparvovec gene therapy for lipoprotein lipase deficiency.* Atherosclerosis Supplements, 2010. **11**(1): p. 55-60.
5. Ginn SL, A.A., Alexander IE, Edelstein M, Abedi MR, *Gene therapy clinical trials worldwide to 2017: An update.* J Gene Med., 2018 Mar 25.
6. Nayerossadat, N., T. Maedeh, and P.A. Ali, *Viral and nonviral delivery systems for gene delivery.* Advanced biomedical research, 2012. **1**: p. 27-27.
7. Howarth, J.L., Y.B. Lee, and J.B. Uney, *Using viral vectors as gene transfer tools (Cell Biology and Toxicology Special Issue: ETCS-UK 1 day meeting on genetic manipulation of cells).* Cell biology and toxicology, 2010. **26**(1): p. 1-20.
8. Walter, W. and U. Stein, *Viral vectors for gene transfer a review of their use in the treatment of human disease.* Drugs, 2000. **60**: p. 249-271.
9. Hacein-Bey-Abina, S., et al., *A serious adverse event after successful gene therapy for X-linked severe combined immunodeficiency.* N Engl J Med, 2003. **348**(3): p. 255-256.
10. Thomas, C.E., A. Ehrhardt, and M.A. Kay, *Progress and problems with the use of viral vectors for gene therapy.* Nat Rev Genet, 2003. **4**(5): p. 346-358.
11. Felgner, P.L., et al., *Lipofection: a highly efficient, lipid-mediated DNA-transfection procedure.* Proceedings of the National Academy of Sciences, 1987. **84**(21): p. 7413-7417.
12. Foldvari, M., *Nanopharmaceutics: Structural Design of Cationic Gemini Surfactant-Phospholipid-DNA Nanoparticles for Gene Delivery.* Horizons in Clinical Nanomedicine, 2014: p. 129-145.
13. Badea, I., et al., *In vivo cutaneous interferon-gamma gene delivery using novel dicationic (gemini) surfactant-plasmid complexes.* J Gene Med, 2005. **7**(9): p. 1200-1214.

14. Grueso, E., et al., *DNA conformational changes induced by cationic gemini surfactants: the key to switching DNA compact structures into elongated forms.* RSC Advances, 2015. **5**(37): p. 29433-29446.
15. Fisicaro, E., et al., *Nonviral gene delivery: gemini bispyridinium surfactant-based DNA nanoparticles.* The Journal of Physical Chemistry B, 2014. **118**(46): p. 13183-13191.
16. Fisicaro, E., et al., *Nonviral gene-delivery by highly fluorinated gemini bispyridinium surfactant-based DNA nanoparticles.* J Colloid Interface Sci, 2017. **487**: p. 182-191.
17. Cardoso, A.M., et al., *Gemini surfactants mediate efficient mitochondrial gene delivery and expression.* Molecular pharmaceutics, 2015. **12**(3): p. 716-730.
18. Singh, J., et al., *Amino acid-substituted gemini surfactant-based nanoparticles as safe and versatile gene delivery agents.* Curr Drug Deliv, 2011. **8**(3): p. 299-306.
19. Bhadani, A. and S. Singh, *Novel gemini pyridinium surfactants: synthesis and study of their surface activity, DNA binding, and cytotoxicity.* Langmuir, 2009. **25**(19): p. 11703-11712.
20. Van Der Woude, I., et al., *Novel pyridinium surfactants for efficient, nontoxic in vitro gene delivery.* Proceedings of the National Academy of Sciences, 1997. **94**(4): p. 1160-1165.
21. Singh, J., et al., *Amino acid-substituted gemini surfactant-based nanoparticles as safe and versatile gene delivery agents.* Current drug delivery, 2011. **8**(3): p. 299-306.
22. Donkuru, M., et al., *Designing pH-sensitive gemini nanoparticles for non-viral gene delivery into keratinocytes.* Journal of Materials Chemistry, 2012. **22**(13): p. 6232-6244.
23. Mohammed-Saeid, W., et al., *Development of lyophilized gemini surfactant-based gene delivery systems: influence of lyophilization on the structure, activity and stability of the lipoplexes.* Journal of Pharmacy & Pharmaceutical Sciences, 2012. **15**(4): p. 548-567.
24. Foldvari, M., et al., *Structural characterization of novel gemini non-viral DNA delivery systems for cutaneous gene therapy.* Journal of Experimental Nanoscience, 2006. **1**(2): p. 165-176.
25. Wang, C., et al., *Investigation of complexes formed by interaction of cationic gemini surfactants with deoxyribonucleic acid.* Physical Chemistry Chemical Physics, 2007. **9**(13): p. 1616-1628.
26. Singh, J., et al., *Evaluation of cellular uptake and intracellular trafficking as determining factors of gene expression for amino acid-substituted gemini surfactant-based DNA nanoparticles.* J Nanobiotechnology, 2012. **10**(7): p. 1-14.

27. Badea, I., et al., *Topical non-invasive gene delivery using gemini nanoparticles in interferon-gamma-deficient mice.* Eur J Pharm Biopharm, 2007. **65**(3): p. 414-422.
28. Felgner, P.L., et al., *Cationic lipids for intracellular delivery of biologically active molecules*. 1993, Google Patents.
29. Gascón, A.R. and J.L. Pedraz, *Cationic lipids as gene transfer agents: a patent review.* Expert Opinion on Therapeutic Patents, 2008. **18**(5): p. 515-524.
30. Ramamoorth, M. and A. Narvekar, *Non viral vectors in gene therapy-an overview.* Journal of clinical and diagnostic research, 2015. **9**(1): p. GE01-06.
31. Leventis, R. and J.R. Silvius, *Interactions of mammalian cells with lipid dispersions containing novel metabolizable cationic amphiphiles.* Biochimica et Biophysica Acta (BBA)-Biomembranes, 1990. **1023**(1): p. 124-132.
32. Felgner, J.H., et al., *Enhanced gene delivery and mechanism studies with a novel series of cationic lipid formulations.* Journal of Biological Chemistry, 1994. **269**(4): p. 2550-2561.
33. San, H., et al., *Safety and short-term toxicity of a novel cationic lipid formulation for human gene therapy.* Human gene therapy, 1993. **4**(6): p. 781-788.
34. Hottiger, M., et al., *Liposome-mediated gene transfer into human basal cell carcinoma.* Gene therapy, 1999. **6**(12): p. 1929-1935.
35. Bergen, M., R. Chen, and R. Gonzalez, *Efficacy and safety of HLA-B7/β-2 microglobulin plasmid DNA/lipid complex (Allovectin-7®) in patients with metastatic melanoma.* Expert opinion on biological therapy, 2003. **3**(2): p. 377-384.
36. Belldegrun, A., et al., *Interleukin 2 gene therapy for prostate cancer: phase I clinical trial and basic biology.* Human gene therapy, 2001. **12**(8): p. 883-892.
37. Cheng, P.-W., *Receptor ligand-facilitated gene transfer: enhancement of liposome-mediated gene transfer and expression by transferrin.* Human gene therapy, 1996. **7**(3): p. 275-282.
38. Parente, R., S. Nir, and F. Szoka, *pH-dependent fusion of phosphatidylcholine small vesicles. Induction by a synthetic amphipathic peptide.* Journal of Biological Chemistry, 1988. **263**(10): p. 4724-4730.
39. Zuidam, N.J. and Y. Barenholz, *Electrostatic and structural properties of complexes involving plasmid DNA and cationic lipids commonly used for gene delivery.* Biochimica et Biophysica Acta (BBA)-Biomembranes, 1998. **1368**(1): p. 115-128.

40. Ross, P. and S. Hui, *Lipoplex size is a major determinant of in vitro lipofection efficiency.* Gene therapy, 1999. **6**(4): p. 651-659.
41. Bottega, R. and R.M. Epand, *Inhibition of protein kinase C by cationic amphiphiles.* Biochemistry, 1992. **31**(37): p. 9025-9030.
42. Xu, Y., et al., *Physicochemical characterization and purification of cationic lipoplexes.* Biophysical Journal, 1999. **77**(1): p. 341-353.
43. Remy, J.-S., et al., *Gene transfer with a series of lipophilic DNA-binding molecules.* Bioconjugate chemistry, 1994. **5**(6): p. 647-654.
44. Behr, J.-P., et al., *Efficient gene transfer into mammalian primary endocrine cells with lipopolyamine-coated DNA.* Proceedings of the National Academy of Sciences, 1989. **86**(18): p. 6982-6986.
45. Byk, G. and D. Scherman, *Novel cationic lipids for gene delivery and gene therapy.* Expert Opinion on Therapeutic Patents, 1998. **8**(9): p. 1125-1141.
46. Byk, G., et al., *Synthesis, activity, and structure-activity relationship studies of novel cationic lipids for DNA transfer.* Journal of medicinal chemistry, 1998. **41**(2): p. 224-235.
47. Gao, X. and L. Huang, *A novel cationic liposome reagent for efficient transfection of mammalian cells.* Biochemical and biophysical research communications, 1991. **179**(1): p. 280-285.
48. Lee, E.R., et al., *Detailed analysis of structures and formulations of cationic lipids for efficient gene transfer to the lung.* Human gene therapy, 1996. **7**(14): p. 1701-1717.
49. Eastman, S.J., et al., *Aerosolization of cationic lipid: pDNA complexes-in vitro optimization of nebulizer parameters for human clinical studies.* Human gene therapy, 1998. **9**(1): p. 43-52.
50. Eastman, S.J., et al., *A concentrated and stable aerosol formulation of cationic lipid: DNA complexes giving high-level gene expression in mouse lung.* Human gene therapy, 1997. **8**(6): p. 765-773.
51. Alton, E., et al., *Cationic lipid-mediated CFTR gene transfer to the lungs and nose of patients with cystic fibrosis: a double-blind placebo-controlled trial.* The Lancet, 1999. **353**(9157): p. 947-954.
52. Boukhnikachvili, T., et al., *Structure of in-serum transfecting DNA–cationic lipid complexes.* FEBS letters, 1997. **409**(2): p. 188-194.

53. Pitard, B., et al., *Virus-sized self-assembling lamellar complexes between plasmid DNA and cationic micelles promote gene transfer.* Proceedings of the National Academy of Sciences, 1997. **94**(26): p. 14412-14417.
54. Escriou, V., et al., *Cationic lipid-mediated gene transfer: effect of serum on cellular uptake and intracellular fate of lipopolyamine/DNA complexes.* Biochimica et Biophysica Acta (BBA)-Biomembranes, 1998. **1368**(2): p. 276-288.
55. Benatti, C.R., J.-M. Ruysschaert, and M.T. Lamy, *Structural characterization of diC14-amidine, a pH-sensitive cationic lipid used for transfection.* Chemistry and physics of lipids, 2004. **131**(2): p. 197-204.
56. Vigneron, J.-P., et al., *Guanidinium-cholesterol cationic lipids: efficient vectors for the transfection of eukaryotic cells.* Proceedings of the National Academy of Sciences, 1996. **93**(18): p. 9682-9686.
57. Ruysschaert, J.-M., et al., *A novel cationic amphiphile for transfection of mammalian cells.* Biochemical and biophysical research communications, 1994. **203**(3): p. 1622-1628.
58. El Ouahabi, A., et al., *Double long-chain amidine liposome-mediated self replicating DNA transfection.* FEBS letters, 1996. **380**(1-2): p. 108-112.
59. Pector, V., et al., *Physico-chemical characterization of a double long-chain cationic amphiphile (Vectamidine) by microelectrophoresis.* Biochimica et Biophysica Acta (BBA)-Biomembranes, 1998. **1372**(2): p. 339-346.
60. CORP., M., *The present invention describes the first gene delivery system based on amidinium lipids*. 1995.
61. Oudrhiri, N., et al., *Guanidinium-cholesterol cationic lipids: novel reagents for gene transfection and perspectives for gene therapy.* Biogenic amines, 1998. **14**(5): p. 537-552.
62. Pitard, B., et al., *Structural characteristics of supramolecular assemblies formed by guanidinium-cholesterol reagents for gene transfection.* Proceedings of the National Academy of Sciences, 1999. **96**(6): p. 2621-2626.
63. Densmore, C.L., et al., *Gene transfer by guanidinium-cholesterol: dioleoylphosphatidyl-ethanolamine liposome-DNA complexes in aerosol.* The journal of gene medicine, 1999. **1**(4): p. 251-264.
64. Ilies, M.A., et al., *Pyridinium-Based Cationic Lipids as Gene-Transfer Agents.* European Journal of Organic Chemistry, 2003. **2003**(14): p. 2645-2655.

65. Islam, R.U., et al., *Efficient nucleic acid transduction with lipoplexes containing novel piperazine-and polyamine-conjugated cholesterol derivatives.* Bioorganic & medicinal chemistry letters, 2009. **19**(1): p. 100-103.
66. Solodin, I., et al., *A novel series of amphiphilic imidazolinium compounds for in vitro and in vivo gene delivery.* Biochemistry, 1995. **34**(41): p. 13537-13544.
67. Meekel, A.A., et al., *Synthesis of pyridinium amphiphiles used for transfection and some characteristics of amphiphile/DNA complex formation.* European Journal of Organic Chemistry, 2000. **2000**(4): p. 665-673.
68. Roosjen, A., et al., *Synthesis and characteristics of biodegradable pyridinium amphiphiles used for in vitro DNA delivery.* European Journal of Organic Chemistry, 2002. **2002**(7): p. 1271-1277.
69. Ilies, M.A., et al., *Pyridinium cationic lipids in gene delivery: a structure-activity correlation study.* Journal of medicinal chemistry, 2004. **47**(15): p. 3744-3754.
70. Singh, S., et al., *Synthesis of glycerol-based pyridinium surfactants and appraisal of their properties.* Industrial & Engineering Chemistry Research, 2009. **48**(3): p. 1673-1677.
71. Smisterová, J., et al., *Molecular shape of the cationic lipid controls the structure of cationic lipid/dioleylphosphatidylethanolamine-DNA complexes and the efficiency of gene delivery.* Journal of Biological Chemistry, 2001. **276**(50): p. 47615-47622.
72. Hait, S. and S. Moulik, *Gemini surfactants: a distinct class of self-assembling molecules.* CURRENT SCIENCE-BANGALORE-, 2002. **82**(9): p. 1101-1111.
73. Wang, X., et al., *Micellization of a series of dissymmetric gemini surfactants in aqueous solution.* The Journal of Physical Chemistry B, 2003. **107**(41): p. 11428-11432.
74. Dix, L.R. and R. Gilblas, *Lyotropic and interfacial behaviour of an anionic gemini surfactant.* Journal of colloid and interface science, 2006. **296**(2): p. 762-765.
75. Yang, J., et al., *Surface, interfacial and aggregation properties of sulfonic acid-containing gemini surfactants with different spacer lengths.* Langmuir, 2009. **25**(11): p. 6100-6105.
76. Wang, Y., et al., *Aggregation behaviors of a series of anionic sulfonate gemini surfactants and their corresponding monomeric surfactant.* Journal of colloid and interface science, 2008. **319**(2): p. 534-541.

77. Liu, X.-P., et al., *Synthesis and properties of a novel class of anionic gemini surfactants with polyoxyethylene spacers.* Colloids and Surfaces A: Physicochemical and Engineering Aspects, 2010. **362**(1): p. 39-46.
78. Ikeda, I., *Synthesis of gemini (dimeric) and related surfactants.* Surfactant science series, 2004: p. 9-36.
79. Rosen, M.J., *Surfactants and Interfacial Phenomena*. 1989, New York: Wiley, 2nd Edition.
80. Kumar, N. and R. Tyagi, *Industrial applications of dimeric surfactants: a review.* Journal of Dispersion Science and Technology, 2014. **35**(2): p. 205-214.
81. Wettig, S.D., R.E. Verrall, and M. Foldvari, *Gemini surfactants: a new family of building blocks for non-viral gene delivery systems.* Current gene therapy, 2008. **8**(1): p. 9-23.
82. Fisicaro, E., et al., *Nonviral gene delivery: gemini bispyridinium surfactant-based DNA nanoparticles.* J Phys Chem B, 2014. **118**(46): p. 13183-13191.
83. Yang, P., et al., *Enhanced gene expression in epithelial cells transfected with amino acid-substituted gemini nanoparticles.* European Journal of Pharmaceutics and Biopharmaceutics, 2010. **75**(3): p. 311-320.
84. Kirby, A.J., et al., *Gemini surfactants: new synthetic vectors for gene transfection.* Angewandte Chemie International Edition, 2003. **42**(13): p. 1448-1457.
85. Foldvari, M., et al. *Dicationic gemini surfactant gene delivery complexes contain cubic-lamellar mixed polymorphic phase*. in *NSTI-Nanotech*. 2006.
86. Badea, I., et al., *In vivo cutaneous interferon-gamma gene delivery using novel dicationic (gemini) surfactant-plasmid complexes.* J Gene Med, 2005. **7**(9): p. 1200-14.
87. Dass, C.R., *Biochemical and biophysical characteristics of lipoplexes pertinent to solid tumour gene therapy.* International journal of pharmaceutics, 2002. **241**(1): p. 1-25.
88. Chesnoy, S. and L. Huang, *Structure and function of lipid-DNA complexes for gene delivery.* Annual review of biophysics and biomolecular structure, 2000. **29**(1): p. 27-47.
89. Wettig, S.D., et al., *Structural and transfection properties of amine-substituted gemini surfactant-based nanoparticles.* The journal of gene medicine, 2007. **9**(8): p. 649-658.
90. Al-Dulaymi, M.A., et al., *Di-Peptide-Modified Gemini Surfactants as Gene Delivery Vectors: Exploring the Role of the Alkyl Tail in Their Physicochemical Behavior and Biological Activity.* The AAPS journal, 2016. **18**(5): p. 1168-1181.
91. Schnablegger, H. and Y. Singh, *A practical guide to SAXS.* Anton Paar, Graz, Austria, 2006.

92. Bendjeriou-Sedjerari, A., et al., *Contribution of 1H NMR to the investigation of the adsorption of cationic Gemini surfactants with oligooxyethylene spacer group onto silica.* Journal of colloid and interface science, 2009. **331**(2): p. 281-287.
93. Huc, I. and R. Oda, *Gemini surfactants: studying micellisation by 1H and 19F NMR spectroscopy.* Chemical Communications, 1999(20): p. 2025-2026.
94. De Hoffmann, E. and V. Stroobant, *Mass spectrometry: principles and applications*. Third Edition ed. 2007, The Atrium, Southern Gate, Chichester, West Susses PO 19 8SQ, England: John Wiley & Sons, Ltd.
95. Buse, J., et al., *A general liquid chromatography tandem mass spectrometry method for the quantitative determination of diquaternary ammonium gemini surfactant drug delivery agents in mouse keratinocytes' cellular lysate.* Journal of Chromatography A, 2013. **1294**: p. 98-105.
96. Donkuru, M., et al., *Hydrophilic interaction liquid chromatography-tandem mass spectrometry quantitative method for the cellular analysis of varying structures of gemini surfactants designed as nanomaterial drug carriers.* Journal of Chromatography A, 2016. **1446**: p. 114-124.
97. Gros, M., M. Petrović, and D. Barceló, *Development of a multi-residue analytical methodology based on liquid chromatography-tandem mass spectrometry (LC-MS/MS) for screening and trace level determination of pharmaceuticals in surface and wastewaters.* Talanta, 2006. **70**(4): p. 678-690.
98. Lee, M.S. and E.H. Kerns, *LC/MS applications in drug development.* Mass Spectrometry Reviews, 1999. **18**(3-4): p. 187-279.
99. Wang, X., et al., *Determination of ginsenosides in plant extracts from Panax ginseng and Panax quinquefolius L. by LC/MS/MS.* Analytical chemistry, 1999. **71**(8): p. 1579-1584.
100. Chèze, M., M. Villain, and G. Pépin, *Determination of bromazepam, clonazepam and metabolites after a single intake in urine and hair by LC-MS/MS: Application to forensic cases of drug facilitated crimes.* Forensic Science International, 2004. **145**(2-3): p. 123-130.
101. Lacorte, S. and A.R. Fernandez-Alba, *Time of flight mass spectrometry applied to the liquid chromatographic analysis of pesticides in water and food.* Mass spectrometry reviews, 2006. **25**(6): p. 866-880.

102. Maurer, H.H., *Advances in analytical toxicology: the current role of liquid chromatography-mass spectrometry in drug quantification in blood and oral fluid.* Analytical and bioanalytical chemistry, 2005. **381**(1): p. 110-118.
103. Park, K.H., et al., *Simultaneous molecular formula determinations of natural compounds in a plant extract using 15 T Fourier transform ion cyclotron resonance mass spectrometry.* Plant methods, 2013. **9**(15): p. 1-12.
104. Kujawinski, E.B., et al., *The application of electrospray ionization mass spectrometry (ESI MS) to the structural characterization of natural organic matter.* Organic Geochemistry, 2002. **33**(3): p. 171-180.
105. Wood, M., et al., *Development of a rapid and sensitive method for the quantitation of amphetamines in human plasma and oral fluid by LC-MS-MS.* Journal of analytical toxicology, 2003. **27**(2): p. 78-87.
106. Andrade, F.J., et al., *Atmospheric pressure chemical ionization source. 1. Ionization of compounds in the gas phase.* Analytical chemistry, 2008. **80**(8): p. 2646-2653.
107. Fenn, J.B., et al., *Electrospray ionization–principles and practice.* Mass Spectrometry Reviews, 1990. **9**(1): p. 37-70.
108. Fenn, J.B., et al., *Electrospray ionization for mass spectrometry of large biomolecules.* Science, 1989. **246**(4926): p. 64-71.
109. Michalski, A., et al., *Mass spectrometry-based proteomics using Q Exactive, a high-performance benchtop quadrupole Orbitrap mass spectrometer.* Molecular & Cellular Proteomics, 2011. **10**(9): p. 1-10.
110. Ni, J. and J. Rowe, *Microdosing Assessment to Evaluate Pharmacokinetics and Drug Metabolism Using Liquid Chromatography-Tandem Mass Spectrometry Technology*. Topics on Drug Metabolism. 2012, 32 London Bridge Street, London, Se19SG, United Kingdom: InterchOpen Limited.
111. Chainulu, S.C., S. Shukla, and P. Sarma, *Highly Sensitive and Specific Tandem Mass Spectrometric Flow Injection method for the Identification of Pyrethroids.* J Flow Injection Anal, 2008. **25**(1): p. 20-23.
112. Boscaro, F., et al., *Rapid quantitation of globotriaosylceramide in human plasma and urine: a potential application for monitoring enzyme replacement therapy in Anderson-Fabry disease.* Rapid communications in mass spectrometry, 2002. **16**(16): p. 1507-1514.

113. Weinmann, W. and M. Svoboda, *Fast screening for drugs of abuse by solid-phase extraction combined with flow-injection ionspray-tandem mass spectrometry*. Journal of analytical toxicology, 1998. **22**(4): p. 319-328.
114. King, R. and C. Fernandez-Metzler, *The use of Qtrap technology in drug metabolism.* Current drug metabolism, 2006. **7**(5): p. 541-545.
115. Donkuru, M., et al., *Multi-stage tandem mass spectrometric analysis of novel β-cyclodextrin-substituted and novel bis-pyridinium gemini surfactants designed as nanomedical drug delivery agents.* Rapid Communications in Mass Spectrometry, 2014. **28**(7): p. 757-772.
116. Buse, J., et al., *Tandem mass spectrometric analysis of novel diquaternary ammonium gemini surfactants and their bromide adducts in electrospray-positive ion mode ionization.* Journal of Mass Spectrometry, 2011. **46**(10): p. 1060-1070.
117. Buse, J., et al., *Tandem mass spectrometric analysis of the novel gemini surfactant nanoparticle families G12-s and G18: 1-s.* Spectroscopy Letters, 2010. **43**(6): p. 447-457.
118. Mohammed-Saeid, W., et al., *Mass spectrometric analysis of amino acid/di-peptide modified gemini surfactants used as gene delivery agents: Establishment of a universal mass spectrometric fingerprint.* International Journal of Mass Spectrometry, 2012. **309**: p. 182-191.
119. Buse, J., et al., *The development and assessment of high-throughput mass spectrometry-based methods for the quantification of a nanoparticle drug delivery agent in cellular lysate.* J Mass Spectrom, 2014. **49**(11): p. 1171-80.
120. Floegel, A., et al., *Identification of serum metabolites associated with risk of type 2 diabetes using a targeted metabolomic approach.* Diabetes, 2013. **62**: p. 639-648.
121. Dankers, J., et al., *Determination of nifedipine in human plasma by flow-injection tandem mass spectrometry.* Journal of Chromatography B: Biomedical Sciences and Applications, 1998. **710**(1-2): p. 115-120.
122. Al-Dulaymi, M., et al., *The development of simple flow injection analysis tandem mass spectrometric methods for the cutaneous determination of peptide-modified cationic gemini surfactants used as gene delivery vectors.* Journal of pharmaceutical and biomedical analysis, 2018. **159**: p. 536-547.

123. Michel, D., et al., *Development and validation of fast and simple flow injection analysis–tandem mass spectrometry (FIA–MS/MS) for the determination of metformin in dog serum.* Journal of pharmaceutical and biomedical analysis, 2015. **107**: p. 229-235.
124. Chernushevich, I.V., A.V. Loboda, and B.A. Thomson, *An introduction to quadrupole-time-of-flight mass spectrometry.* Journal of Mass Spectrometry, 2001. **36**(8): p. 849-865.
125. Ferrer, I., E.M. Thurman, and A.R. Fernández-Alba, *Quantitation and accurate mass analysis of pesticides in vegetables by LC/TOF-MS.* Analytical Chemistry, 2005. **77**(9): p. 2818-2825.
126. Maizels, M. and W.L. Budde, *Exact mass measurements for confirmation of pesticides and herbicides determined by liquid chromatography/time-of-flight mass spectrometry.* Analytical chemistry, 2001. **73**(22): p. 5436-5440.
127. Eckers, C., N. Haskins, and J. Langridge, *The use of liquid chromatography combined with a quadrupole time-of-flight analyser for the identification of trace impurities in drug substance.* Rapid communications in mass spectrometry, 1997. **11**(17): p. 1916-1922.
128. Michalski, A., et al., *Mass spectrometry-based proteomics using Q Exactive, a high-performance benchtop quadrupole Orbitrap mass spectrometer.* Molecular & Cellular Proteomics, 2011. **10**(9): p. M111. 011015.
129. Hu, Q., et al., *The Orbitrap: a new mass spectrometer.* Journal of mass spectrometry, 2005. **40**(4): p. 430-443.
130. Jiwan, J.-L.H., P. Wallemacq, and M.-F. Hérent, *HPLC-high resolution mass spectrometry in clinical laboratory?* Clinical biochemistry, 2011. **44**(1): p. 136-147.
131. Rose, R.J., et al., *High-sensitivity Orbitrap mass analysis of intact macromolecular assemblies.* Nature methods, 2012. **9**(11): p. 1084-1086.
132. Kumar, P., et al., *Targeted analysis with benchtop quadrupole-orbitrap hybrid mass spectrometer: Application to determination of synthetic hormones in animal urine.* Analytica chimica acta, 2013. **780**: p. 65-73.
133. Solliec, M., A. Roy-Lachapelle, and S. Sauvé, *Quantitative performance of liquid chromatography coupled to Q-Exactive high resolution mass spectrometry (HRMS) for the analysis of tetracyclines in a complex matrix.* Analytica chimica acta, 2015. **853**: p. 415-424.

134. Kipen, H.M. and D.L. Laskin, *Smaller is not always better: nanotechnology yields nanotoxicology.* American Journal of Physiology-Lung Cellular and Molecular Physiology, 2005. **289**(5): p. 696-697.
135. Rayman-Rasmussen, J., J. Riviere, and N. Monteiro-Riviere, *Variables infleuncing interactions of uncharged quantum dot nanoparticles with skin cells and identification of biochemical modulators.* Nano Letters, 2007. **7**(5): p. 1344-1348.
136. Borm, P., et al., *Research strategies for safety evaluation of nanomaterials, part V: role of dissolution in biological fate and effects of nanoscale particles.* Toxicological Sciences, 2006. **90**(1): p. 23-32.
137. Khalil, I.A., et al., *Uptake pathways and subsequent intracellular trafficking in nonviral gene delivery.* Pharmacological reviews, 2006. **58**(1): p. 32-45.
138. Friend, D.S., D. Papahadjopoulos, and R.J. Debs, *Endocytosis and intracellular processing accompanying transfection mediated by cationic liposomes.* Biochimica et Biophysica Acta (BBA)-Biomembranes, 1996. **1278**(1): p. 41-50.
139. Labat-Moleur, F., et al., *An electron microscopy study into the mechanism of gene transfer with lipopolyamines.* Gene therapy, 1996. **3**(11): p. 1010-1017.
140. Zuhorn, I.S., R. Kalicharan, and D. Hoekstra, *Lipoplex-mediated transfection of mammalian cells occurs through the cholesterol-dependent clathrin-mediated pathway of endocytosis.* Journal of Biological Chemistry, 2002. **277**(20): p. 18021-18028.
141. Conner, S.D. and S.L. Schmid, *Regulated portals of entry into the cell.* Nature, 2003. **422**: p. 37-44.
142. Lamaze, C. and S.L. Schmid, *The emergence of clathrin-independent pinocytic pathways.* Current opinion in cell biology, 1995. **7**(4): p. 573-580.
143. Conner, S.D. and S.L. Schmid, *Regulated portals of entry into the cell.* Nature, 2003. **422**(6927): p. 37-44.
144. Takei, K. and V. Haucke, *Clathrin-mediated endocytosis: membrane factors pull the trigger.* Trends in cell biology, 2001. **11**(9): p. 385-391.
145. Pelkmans, L., J. Kartenbeck, and A. Helenius, *Caveolar endocytosis of simian virus 40 reveals a new two-step vesicular-transport pathway to the ER.* Nature cell biology, 2001. **3**(5): p. 473-483.

146. Ferrari, A., et al., *Caveolae-mediated internalization of extracellular HIV-1 tat fusion proteins visualized in real time.* Molecular therapy, 2003. **8**(2): p. 284-294.
147. Amyere, M., et al., *Origin, originality, functions, subversions and molecular signalling of macropinocytosis.* International journal of medical microbiology, 2001. **291**(6-7): p. 487-494.
148. Rejman, J., A. Bragonzi, and M. Conese, *Role of clathrin-and caveolae-mediated endocytosis in gene transfer mediated by lipo-and polyplexes.* Molecular Therapy, 2005. **12**(3): p. 468-474.
149. Leonetti, J.P., et al., *Intracellular distribution of microinjected antisense oligonucleotides.* Proceedings of the National Academy of Sciences, 1991. **88**(7): p. 2702-2706.
150. Barry, E., F. Gesek, and P.J.B. Friedman, *Introduction of antisense oligonucleotides into cells by permeabilization with streptolysin O.* BioTechniques, 1993. **15**(6): p. 1016-1020.
151. Mahvi, D.M., M.J. Sheehy, and N.-S. Yang, *DNA cancer vaccines: a gene gun approach.* Immunology and cell biology, 1997. **75**(5): p. 456-460.
152. Mellott, A.J., M.L. Forrest, and M.S. Detamore, *Physical non-viral gene delivery methods for tissue engineering.* Annals of biomedical engineering, 2013. **41**(3): p. 446-468.
153. Niculescu-Duvaz, D., J. Heyes, and C.J. Springer, *Structure-activity relationship in cationic lipid mediated gene transfection.* Current medicinal chemistry, 2003. **10**(14): p. 1233-1261.
154. Elouahabi, A. and J.-M. Ruysschaert, *Formation and intracellular trafficking of lipoplexes and polyplexes.* Molecular therapy, 2005. **11**(3): p. 336-347.
155. Donkuru, M., et al., *Advancing nonviral gene delivery: lipid-and surfactant-based nanoparticle design strategies.* Nanomedicine, 2010. **5**(7): p. 1103-1127.
156. Boussif, O., et al., *A versatile vector for gene and oligonucleotide transfer into cells in culture and in vivo: polyethylenimine.* Proceedings of the National Academy of Sciences, 1995. **92**(16): p. 7297-7301.
157. Moore, N.M., C.L. Sheppard, and S.E. Sakiyama-Elbert, *Characterization of a multifunctional PEG-based gene delivery system containing nuclear localization signals and endosomal escape peptides.* Acta biomaterialia, 2009. **5**(3): p. 854-864.
158. Vaysse, L., et al., *Development of a self-assembling nuclear targeting vector system based on the tetracycline repressor protein.* Journal of Biological Chemistry, 2004. **279**(7): p. 5555-5564.

159. Oberdörster, G., E. Oberdörster, and J. Oberdörster, *Nanotoxicology: an emerging discipline evolving from studies of ultrafine particles.* Environmental health perspectives, 2005. **113**(7): p. 823-839.
160. Guillemin, I., et al., *A subcellular prefractionation protocol for minute amounts of mammalian cell cultures and tissue.* Proteomics, 2005. **5**(1): p. 35-45.
161. Graham, J.M. and D. Rickwood, *Subcellular fractionation: a practical approach*. Vol. 173. 1997, New York, United States: Oxford University Press Inc.
162. Bligh, E.G. and W.J. Dyer, *A rapid method of total lipid extraction and purification.* Canadian journal of biochemistry and physiology, 1959. **37**(8): p. 911-917.
163. Huth, U.S., R. Schubert, and R. Peschka-Süss, *Investigating the uptake and intracellular fate of pH-sensitive liposomes by flow cytometry and spectral bio-imaging.* Journal of controlled release, 2006. **110**(3): p. 490-504.
164. Singh, J., et al., *Evaluation of cellular uptake and intracellular trafficking as determining factors of gene expression for amino acid-substituted gemini surfactant-based DNA nanoparticles.* J Nanobiotechnology, 2012. **10**: p. 7.
165. Zanta, M.A., P. Belguise-Valladier, and J.-P. Behr, *Gene delivery: a single nuclear localization signal peptide is sufficient to carry DNA to the cell nucleus.* Proceedings of the National Academy of Sciences, 1999. **96**(1): p. 91-96.
166. Brandén, L.J., A.J. Mohamed, and C.E. Smith, *A peptide nucleic acid-nuclear localization signal fusion that mediates nuclear transport of DNA.* Nature biotechnology, 1999. **17**(8): p. 784-787.
167. Xia, T., et al., *Comparison of the abilities of ambient and manufactured nanoparticles to induce cellular toxicity according to an oxidative stress paradigm.* Nano letters, 2006. **6**(8): p. 1794-1807.
168. Brodie, B.B., J.R. Gillette, and B.N. La Du, *Enzymatic metabolism of drugs and other foreign compounds.* Annual review of biochemistry, 1958. **27**(1): p. 427-454.
169. Foye, W.O., *Foye's principles of medicinal chemistry*. Sixth Edition ed. 2008, Baltimore, MD, United States: Lippincott Williams & Wilkins.
170. Wilson, C.O., et al., *Wilson and Gisvold's textbook of organic medicinal and pharmaceutical chemistry*. Eleventh ed. 2004, Baltimore, MD, United States.: Lippincott Williams & Wilkins.

171. Wilson, C.O., et al., *Wilson and Gisvold's textbook of organic medicinal and pharmaceutical chemistry/edited by John H. Block, John M. Beale Jr*. 2004: Philadelphia: Lippincott Williams & Wilkins.
172. Omiecinski, C.J., et al., *Xenobiotic metabolism, disposition, and regulation by receptors: from biochemical phenomenon to predictors of major toxicities.* Toxicological Sciences, 2010. **120**(suppl_1): p. S49-S75.
173. Gonzalez, F.J. and R.H. Tukey, *Drug metabolism.* Goodman & Gilman's. The Pharmacological Basis of Therapeutics. 11th ed. New York: McGraw-Hill, 2006: p. 71-91.
174. Pannatier, A., et al., *The skin as a drug-metabolizing organ.* Drug metabolism reviews, 1978. **8**(2): p. 319-343.
175. Lohr, J.W., G.R. Willsky, and M.A. Acara, *Renal drug metabolism.* Pharmacological reviews, 1998. **50**(1): p. 107-142.
176. Fabian, E., et al., *Tissue distribution and toxicity of intravenously administered titanium dioxide nanoparticles in rats.* Archives of toxicology, 2008. **82**(3): p. 151-157.
177. Huang, X.-L., et al., *In vivo toxic studies and biodistribution of near infrared sensitive Au–Au 2 S nanoparticles as potential drug delivery carriers.* Journal of Materials Science: Materials in Medicine, 2008. **19**(7): p. 2581-2588.
178. Ng, C.P. and S.H. Pun, *A perfusable 3D cell–matrix tissue culture chamber for in situ evaluation of nanoparticle vehicle penetration and transport.* Biotechnology and bioengineering, 2008. **99**(6): p. 1490-1501.
179. Moghimi, S.M., A.C. Hunter, and J.C. Murray, *Nanomedicine: current status and future prospects.* The FASEB journal, 2005. **19**(3): p. 311-330.
180. Owens III, D.E. and N.A. Peppas, *Opsonization, biodistribution, and pharmacokinetics of polymeric nanoparticles.* International journal of pharmaceutics, 2006. **307**(1): p. 93-102.
181. Curtis, J., et al., *Nanotechnology and nanotoxicology.* Toxicological reviews, 2006. **25**(4): p. 245-260.
182. Garnett, M.C. and P. Kallinteri, *Nanomedicines and nanotoxicology: some physiological principles.* Occupational Medicine, 2006. **56**(5): p. 307-311.
183. Hagens, W.I., et al., *What do we (need to) know about the kinetic properties of nanoparticles in the body?* Regulatory toxicology and pharmacology, 2007. **49**(3): p. 217-229.

184. Singh, R., et al., *Tissue biodistribution and blood clearance rates of intravenously administered carbon nanotube radiotracers.* Proceedings of the National Academy of Sciences of the United States of America, 2006. **103**(9): p. 3357-3362.
185. Cherukuri, P., et al., *Near-infrared fluorescence microscopy of single-walled carbon nanotubes in phagocytic cells.* Journal of the American Chemical Society, 2004. **126**(48): p. 15638-15639.
186. Emerich, D.F. and C.G. Thanos, *Targeted nanoparticle-based drug delivery and diagnosis.* Journal of drug targeting, 2007. **15**(3): p. 163-183.

2 Chapter 2 - The Determination of Gemini Surfactants Used as Gene Delivery Agents in Cellular Matrix Using a Validated Tandem Mass Spectrometric Method

This chapter has been published as a research article, cited from "*Journal of Pharmaceutical and Biomedical Analysis 164 (2019) 164-172".*

The Determination of Gemini Surfactants Used as Gene Delivery Agents in Cellular Matrix Using a Validated Tandem Mass Spectrometric Method

Wei Jin[1], Ildiko Badea[1], Scot C. Leary[2], Anas El-Aneed[1]*

[1] Drug Design & Discovery Group, College of Pharmacy and Nutrition, University of Saskatchewan, 107 Wiggins Road, Saskatoon, SK S7N 5E5, Canada.

[2] Department of Biochemistry, University of Saskatchewan, 107 Wiggins Road, Saskatoon, SK S7N 5E5, Canada.

*Corresponding author. E-mail address: anas.el-aneed@usask.ca (A. El-Aneed).

Authors' contribution: Wei Jin contributed to the experimental design, conducted the experimental work, analyzed the data, and drafted the manuscript. Dr. Badea helped with the nanoparticle formulation. Dr. Leary helped with the isoaltion of cellular organelles using differential centrifugation. Dr. El-Aneed is the PI; he conceptualized the idea, obtained funding, supervised the work and revised the manuscript.

Transitioning Rationale:

To determine cellular uptake and subcellular distribution, a flow injection analysis-tandem mass spectrometry (FIA-MS/MS) method was developed and validated for the quantification of three gemini surfactants 16-3-16, 16(Py)-S-2-S-(Py)16, and 16-7N(GK)-16 in the cellular matrix. In additon, an application of this method was demonstrated to quantitatively determine the gemini surfactants in the nuclear fraction of PAM 212 cells.

2.1 Abstract

A simple, reliable flow injection analysis-tandem mass spectrometric (FIA-MS/MS) method was developed for the determination of gemini surfactants, designated as 16-3-16, 16(Py)-S-2-S-(Py)16, and 16-7N(GK)-16, as gene delivery agents in the cellular matrix. Compound 16-3-16 is a conventional gemini surfactant bearing two quaternary amines, linked by a 3-carbon spacer region, compound 16(Py)-S-2-S-(Py)16 contains two pyridinium head groups, while 16-7N(GK)-16 bears a glycyl-lysine di-peptide in the space region. The method was fully validated according to the USFDA guidelines. It is the first FIA-MS/MS method that was developed for the quantification of three gemini surfactants belonging to different structural families. The method was superior to the existing liquid chromatographic (LC)-MS/MS methods in terms of sensitivity and time of analysis. Positive electrospray ionization (ESI) in multiple reaction monitoring (MRM) mode was used on a triple quadrupole-linear ion trap (4000 QTRAP®) instrument. Deuterated internal standards were used to correct for matrix effects and variations in ionization within the ESI source. Isotope dilution standard curves were established in the cellular matrix, with a linear range of 10 nM-1000 nM for 16-3-16 and 16(Py)-S-2-S-(Py)16, and 20 nM-2000 nM for 16-7N(GK)-16. The precision, accuracy, recovery, and stability were all within the acceptable ranges as per the USFDA guidelines. The method was successfully applied for the quantification of target gemini surfactants in the nuclear fraction of PAM 212 cells treated with nanoparticles, which varied significantly and may explain differences in the observed efficiency and toxicity of these gemini surfactants in gene delivery.

Keywords: FIA-MS/MS, Quantification, Gemini surfactants, Lipid-based gene delivery agents, Cellular matrix.

2.2 Introduction

Gene therapy is a promising approach to treat or improve the health condition of patients by introducing therapeutic genetic materials into the patient's cells [1-4]. To date, almost 2,600 gene therapy clinical trials have been conducted worldwide, with more than half of them being in the field of cancer gene therapy [5]. The most difficult challenge in gene therapy is the issue of gene delivery. Typically, there are two main types of gene delivery methods; viral and non-viral vectors [6]. Viral vectors utilize the viruses' natural infection capability to introduce a target gene into cells [7, 8]. While viruses are efficient vectors for transfection, a limited capacity of genetic material can be delivered and they present challenges with respect to potential genotoxicity and induction of a severe immune response [9, 10]. On the other hand, non-viral vectors have relatively low toxicity profiles, are not limited to the size of genes they can encapsulate, and can be easily produced at low cost [4, 11, 12]. However, the major disadvantage of non-viral vectors is their low gene delivery efficiency compared to viral vectors [13]. Thus, major efforts have been made to discover and develop novel non-viral vectors that offer both high transfection efficiency and low toxicity.

A family of lipid cationic molecules, called gemini surfactants, has been investigated as gene delivery vehicles [14, 15]. They are comprised of two surfactant monomers that are chemically linked by a rigid spacer group [16]. Gemini surfactants possess dual positively charged hydrophilic head groups and hydrophobic tail regions [17] (Figure 2.1A). This structure enables gemini surfactants to bind and compact DNA, and subsequently facilitate its cellular entry [18, 19]. For example, the conventional bis-quaternary gemini surfactant 14-2-14 and the serine-derived bis-quaternary gemini surfactants $(nSer)_2N5$ (n=12 and 14) were shown to efficiently deliver plasmid DNA into mitochondria in HeLa cells in combination with the helper lipids 1,2-di-(9Z-

octadecenoyl)-*sn*-glycero-3-phosphoethanolamine (DOPE) and cholesterol [20]. A transfection of up to 40% of the cells was achieved, which is almost twice of that obtained with the commercial transfection agent, Lipofectamine 2000.

A

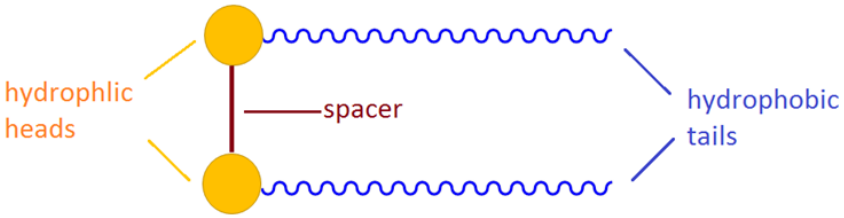

B 16-3-16

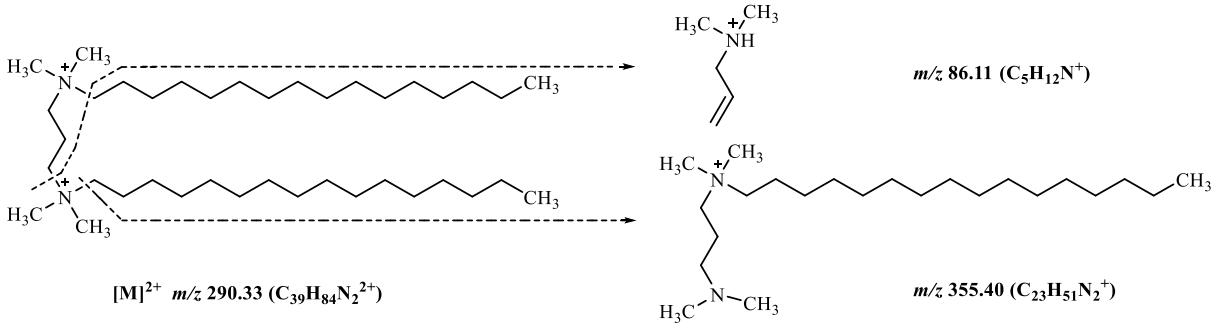

C 16(Py)-S-2-S-(Py)16

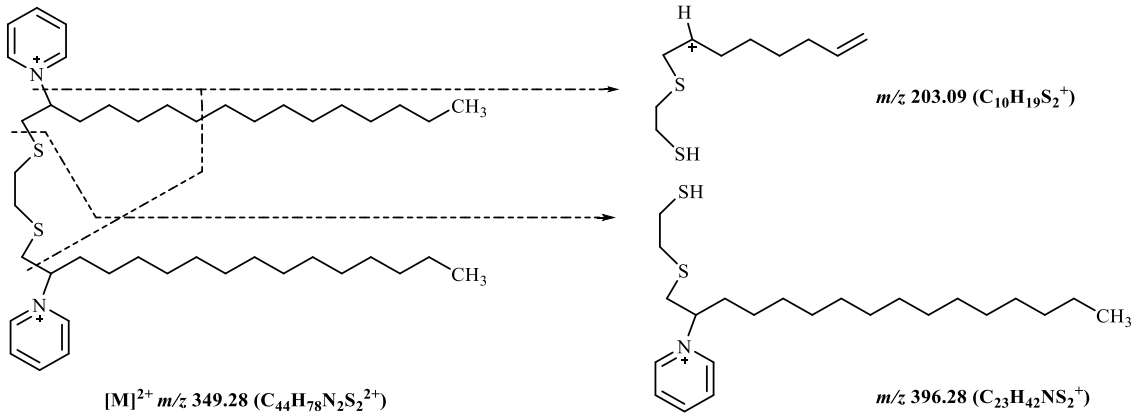

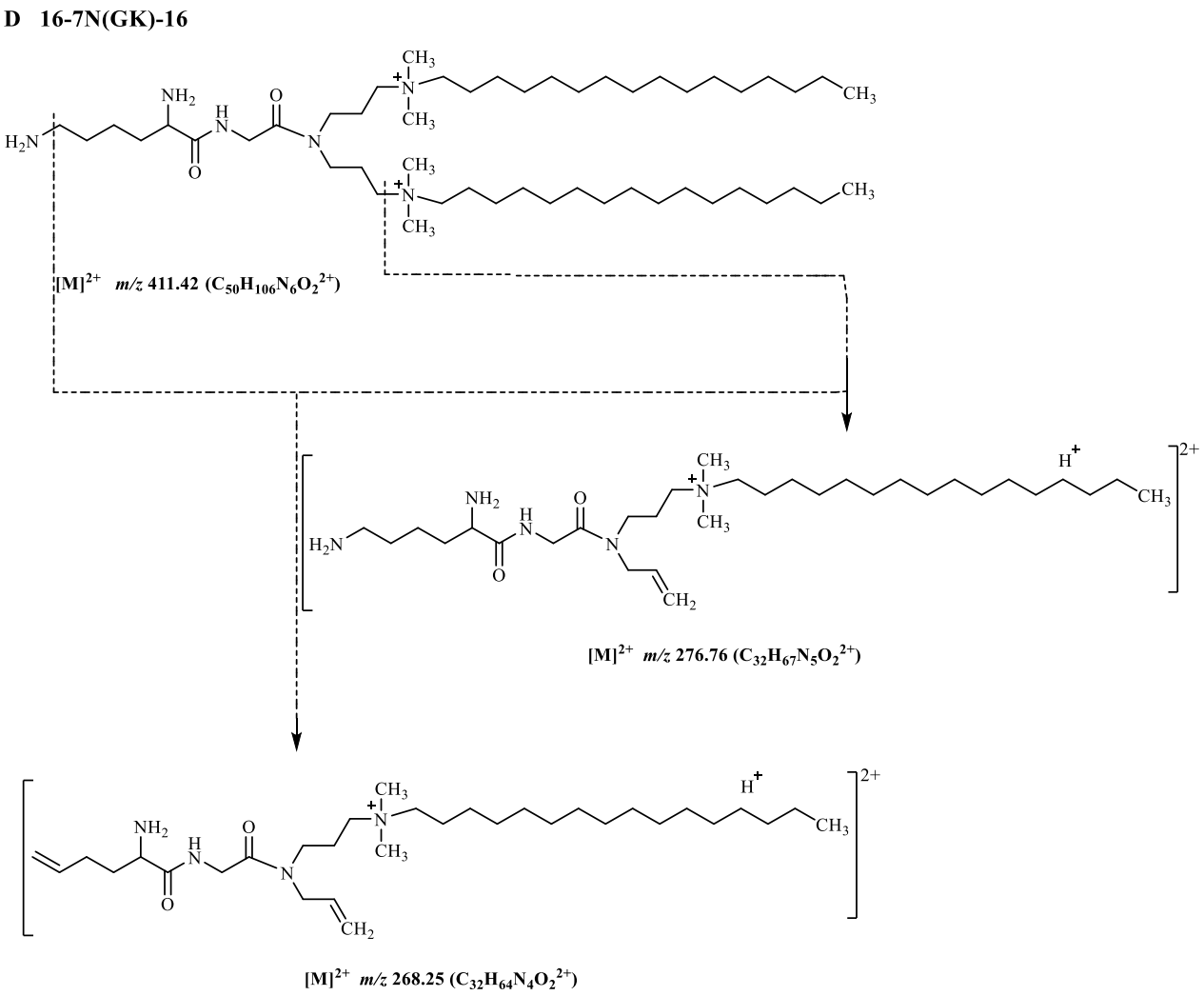

Figure 2.1. (A) Schematic representation of the general structure of gemini surfactant, (B) structures of 16-3-16 and the monitored product ions, (C) structures of 16(Py)-S-2-S-16(Py), and the monitored product ions, and (D) structures of 16-7N(GK)-16 and the monitored product ions.

By varying the head group, the length of hydrophobic tails and the spacer region, a wide range of gemini surfactant compounds can be designed and synthesized. The aim is to increase efficacy while reducing toxicity. N, N-bis(dimethylhexadecyl)-1,3-propanediammonium (denoted 16-3-16, Figure 2.1B) is a representative of the traditional non-substituted *m*-*s*-*m* gemini surfactants, where *m* is the number of carbon atoms in the tail chain and *s* is the number of carbon atoms in the spacer region [17]. Other classes of gemini surfactants with variations in the head group have also been

studied, such as 1,1'-[ethane-1,2-diylbis(sulfanediylhexadecane-1,2-diyl)]dipyridinium bromide (denoted 16(Py)-S-2-S-16(Py), Figure 2.1C) [21], which displayed effective DNA binding capability and low cytotoxicity [21]. Most recently, bio-compatible moieties, such as amino acids, have been incorporated within gemini surfactant structure to enhance the biocompatibility of the delivery agent [22]. One compound, in particular, substituted with a di-peptide glycyl-lysine (denoted 16-7N(GK)-16, Figure 2.1D) showed higher transfection efficiency with lower toxicity in gene delivery compared with earlier generations of gemini surfactants [23].

However, these gemini surfactants nonetheless vary amongst each other in terms of their gene transfection efficiency and toxicity profiles. This could theoretically be attributable to their different biological fate upon transfection, such as variable cellular uptake, subcellular biodistribution and metabolism. Garnering such knowledge is important and may provide a mechanistic explanation for the observed differences among these gemini surfactants in their efficiency and toxicity. However, there is a need for sensitive analytical methods that can detect, differentiate, and quantify these gemini surfactants in biological matrices to determine their post-transfection fate.

Since gemini surfactants lack a chromophore or fluorophore and contain permanent positive charges, mass spectrometry (MS) is ideal for their qualitative and quantitative analysis [24-26]. Tandem mass spectrometry (MS/MS) using multiple reaction monitoring (MRM) allows for the detection and quantification of gemini surfactants using specific precursor ion-to-product ion transitions, which provides high specificity to target gemini surfactants in complex biological matrices. Our group has established the collision-induced dissociation (CID)-MS/MS fragmentation patterns of over 50 gemini surfactant structures belonging to various structural families and identified their characteristic product ions [27-31]. In addition, we developed liquid

chromatography electrospray ionization (LC-ESI)-MS/MS methods employing cyano and hydrophilic interaction liquid chromatography (HILIC) columns for the quantification of gemini surfactants within cells [25, 26]. However, these methods suffered from some drawbacks, such as ion suppression due to the addition of an ion pairing reagent, relatively long run time, and the use of an analytical column and gradient elution. Therefore, we aim herein to develop a simple and reliable method that can quantify the gemini surfactants in the cellular matrix.

Flow injection analysis (FIA)-MS/MS is an analytical approach for rapid quantitative analysis, in which no analytical column is used and both separation and detection occur within the MS instrument [32]. The removal of the analytical column can dramatically reduce the time for method development and sample analysis. Furthermore, the FIA-MS/MS can offer high-throughput quantitative analysis without compromising the sensitivity, precision, and accuracy [33]. Many studies have demonstrated the feasibility of FIA-MS/MS for the quantification of small molecules in biological samples [34-36]. For example, FIA-MS/MS has been used to quantify nifedipine in human plasma samples, with high sensitivity, selectivity, and a short run time [37]. Similarly, the drug metformin was quantified in dog plasma using a validated FIA-MS/MS method that was superior to all existing methods in terms of speed of analysis without compromising sensitivity [38]. Most recently, a simple FIA-MS/MS method has been developed for the cutaneous determination of peptide-modified cationic gemini surfactants used as gene delivery vectors [39].

In this work, we report for the first time the development and validation of a fast and simple FIA-MS/MS quantification method that was applied for the quantification of structurally different gemini surfactants at the subcellular level.

2.3 Materials and Methods

2.3.1 Materials

All gemini surfactants and the deuterated internal standards were previously synthesized using established protocols [21, 23]. Their structures are listed in Figures 2.1 and 2.S1 in supporting information. For analyte 16-3-16, the internal standard (16-3-16-D_{66}) contains 66 deuterium atoms in the alkyl tails. Analyte 16(Py)-S-2-S-16(Py) has an internal standard (16(Py)-S-2-S-16(Py)-D_{10}) with deuterated pyridinium head groups (10 deuterium atoms), whereas the internal standard (16-7N(GK)-16-D_4) for analyte 16-7N(GK)-16 possesses 4 deuterium atoms on the peptide group (Figure 2.S1 in supporting information).

PAM 212 keratinocyte cells were kindly provided by Dr. S. Yuspa, National Cancer Institute, Bethesda, MD, USA. The neutral lipid, 1, 2-dioleoyl-sn-glycero-3-phosphoethanolamine (DOPE), was purchased from Avanti Polar Lipids Inc. (Alabaster, AL, USA). Formic acid, chloroform, methanol, and acetonitrile were purchased from Fisher Scientific (Ottawa, ON, Canada). Minimum essential media (MEM), fetal bovine serum albumin (FBS), and antibiotic-antimycotic solution were obtained from Sigma-Aldrich (Oakville, ON, Canada). Tissue culture flasks (150 cm^2) and petri dishes (150 cm^2) were purchased from Fisher Scientific (Ottawa, ON, Canada). The motorized tissue-grinder/pellet homogenizer (#12-141-361, 12-141-368) was purchased from Fisher Scientific (Toronto, ON, Canada).

2.3.2 Instrumentation

A quadrupole-linear ion trap (4000 QTRAP®) mass spectrometer (AB Sciex, Concord, ON, Canada) was coupled with an Agilent 1200 series HPLC, comprised of a quaternary pump, degasser and auto sampler (Agilent Technologies, Mississauga, ON, Canada), to perform the FIA-MS/MS

analysis. 3 µL of sample at 6 ℃ was loop-injected into the turbo ion source with an isocratic mobile phase consisting of acetonitrile-water (98:2, v/v) with 0.1% formic acid at a flow rate of 0.5 mL/min. The data acquisition time was 2 min. No sample carryover was observed and to eliminate any chance of carryover, the injection of the highest calibration curve sample was followed by one blank sample injection during sample analysis.

The source was set at 600 ℃ at the interface, with ion spray voltage (ISV) at 5500 V, curtain gas (CUR) at 30, nebulizer gas (GS1) at 55, and heater gas (GS2) at 50. Nitrogen was used for all gas consumption. Multiple reaction monitoring (MRM) in positive electrospray ionization (ESI) mode with unit resolution was employed to monitor all analytes and internal standards. Two MRM transitions were monitored for each analyte, with one as a quantifier ion and the other as a qualifier ion (Figure 2.1); one MRM transition was used for each internal standard (Figure 2.S1 in supporting information). Dwell times for all transitions were set at 150 ms. The monitored MRM transitions and compound-dependent parameters for analytes and internal standards are listed in Table 2.1. Data acquisition and analysis was performed with Applied Biosystems/MDS Sciex Analyst software (v. 1.6.0).

Table 2.1. MRM transitions and compound-dependent parameters for analytes and internal standards

Gemini surfactants	Molecular Formula	MRM Transition (*m/z*)	DP	EP	CE	CX
16-3-16	$C_{39}H_{84}N_2^{2+}$	290.3/355.4 (quantifier)	70	10	22	10
		290.3/86.1 (qualifier)	70	10	35	10
16-3-16-D_{66}	$C_{39}H_{18}D_{66}N_2^{2+}$	323.5/388.6	70	10	22	10
16(Py)-S-2-S-16(Py)	$C_{44}H_{78}N_2S_2^{2+}$	349.3/396.3 (quantifier)	50	10	22	10
		349.3/203.1 (qualifier)	50	10	22	10
16(Py)-S-2-S-16(Py)-D_{10}	$C_{44}H_{68}$ $D_{10}N_2S_2^{2+}$	354.3/401.3	50	10	22	10
16-7N(GK)-16	$C_{50}H_{106}N_6O_2^{2+}$	411.4/276.8 (quantifier)	100	12	28	10
		411.4/268.3 (qualifier)	100	12	31	10
16-7N(GK)-16-D_4	$C_{50}H_{102}$ $D_4N_6O_2^{2+}$	413.4/278.8	100	12	28	10

DP- declustering potential, EP-entrance potential, CE-collision energy, and CXP-collision exit potential.

2.3.3 Standard preparation

All gemini surfactants and internal standards were prepared as aqueous stock solutions at a concentration of 3 mM and stored at -80 ℃ under darkness. Working solutions for each analyte were prepared by a serial dilution of the stock solution to achieve a concentration range of 50 nM-5,000 nM for 16-3-16 and 16(Py)-S-2-S-16(Py), and 100 nM-1,0000 nM for 16-7N(GK)-16. Working solutions for each internal standard were prepared at a concentration of 1,000 nM. For the preparation of standard curves and quality control samples, 50 µL of analyte and internal standard working solutions were added to 900 µL of blank cell lysate (untreated cell lysate), the mixture then was processed in the same sample extraction process as described below. After extraction, 150 µL of organic solution was transferred into an HPLC vial for FIA-MS/MS analysis.

DOPE vesicles were prepared freshly at 1 mM in isotonic sucrose solution (9.25% w/v, pH=9) as per established protocol [14]. Plasmid DNA (pGT·IFN-GFP) solution at 200 µg/mL was prepared

in ultra-pure water and stored at -80 ℃. The DOPE vesicles and plasmid DNA solutions were used without further dilutions.

2.3.4 Cell treatment and sample collection

The plasmid DNA, gemini surfactant, and lipid DOPE (P/G/L) nano-lipoplex was formulated as previously described [14]. Briefly, a gemini surfactant solution (190 µL) was added to the plasmid DNA (190 µL) and mixed, followed by a 15 min incubation at room temperature; the DOPE solution (4620 µL) was then added to the binary mixture, which was incubated at room temperature for 15 min to yield 5,000 µL of the ternary P/G/L system (nanoparticles).

PAM 212 cells were cultured inside a humidified incubator at 37 ℃ in an atmosphere of 5% CO_2. The MEM cell culture medium was supplemented with 10% (v/v) FBS and 1 % (v/v) antibiotic-antimycotic solution. Upon reaching 80% confluence in the 150 cm^2 flasks, cells were washed with phosphate buffered saline (PBS, 25 ml), dissociated with a 5 min incubation in a versene (5ml) and trypsin (0.5 mL) mixture, and collected by centrifugation (250 *x g*, 5 min, 4 ℃). The cells were then seeded at 8×10^6 cells per dish (150 cm^2) 24 h prior to treatments. At 1 h prior to transfection, cells were switched to a serum-free media. Nanoparticle formulations (500 µL) were added to each dish in a dropwise manner and incubated for 5 h, after which the cells were returned to the supplemented media for all subsequent incubation steps. During the incubation period, triplicates of treated cell samples were trypsinized and collected along with one control (untreated cells) at 2 h, 5 h, and 8 h. The collected cells were pelleted (250 *x g*, 5 min, 4 ℃), rinsed with PBS, reconstituted in 500 µL ice-cold hypotonic homogenization buffer (10 mM NaCl, 1.5 mM $MgCl_2$, 10 mM Tris-HCL (pH=7.5), cOmplete™ protease inhibitor cocktail) and incubated on ice for 10 min.

The ice-cooled 500 µL treated cell samples were gently homogenized using a motorized tissue-grinder/pellet homogenizer to release the subcellular components and diluted in ice-cold hypertonic homogenization buffer (420 mM mannitol, 140 mM sucrose, 10 mM Tris-HCL (pH=7.5), and 2 mM EDTA (pH=7.5)) to a total volume of 1,000 µL. Cell homogenates were then fractionated by differential centrifugation as described [40] to obtain the nuclear, mitochondrial, plasma membrane, and cytosolic fractions. It should be mentioned that the reported differential centrifugation procedure was slightly modified using 100,000 *x g*, instead of 80,000 *x g*, to separate the plasma membrane and cytosolic fractions. Finally, all fractions were suspended in an equal volume of 950 µL PBS and stored at -80 ℃ prior to sample preparation.

2.3.5 Sample preparation

The 950 µL subcellular fractions were thawed and lysed by undergoing six freeze/thaw cycles plus 1 h sonication at 25 kHz on a water bath at room temperature. After that, each sample was spiked with 50 µL of internal standard bringing the volume for subsequent extraction to 1 mL. Liquid-liquid extraction of the analytes and internal standards from cellular matrix was carried out using the Bligh/Dyer method [41]. Briefly, each 1mL of sample was mixed with 3.75 mL of methanol-chloroform (2:1, v/v), followed by mixing with 1.25 mL of chloroform and finally 1.25 mL of water. At each step, samples were vortexed for at least 10 s to ensure that a thorough mixing was achieved. The final combined mixture was centrifuged at 2,800 *x g* for 10 min at room temperature to separate the aqueous and organic phases. The bottom organic phase (80% portion) was retrieved and dried under a nitrogen gas stream, followed by reconstitution in 200 µL of methanol. Methanol solution (150 µL) was transferred into an HPLC vial for FIA-MS/MS analysis.

2.3.6 Method validation

Method validation for all gemini surfactants was conducted in accordance with the USFDA guidelines [42], which include matrix effects, selectivity, linearity, precision, accuracy, recovery, and stability.

Matrix effects were assessed by comparing the instrument response of analytes added to the extracted cell samples to that of analytes in a methanol solution at low, mid, and high concentration. Selectivity was evaluated to ensure no interference from other components of the sample matrix through the analysis of six different blank cell samples.

Linearity was explored over a wide range of analyte concentrations in the sample extract, from 10 nM to 1,000 nM for both 16-3-16 and 16(Py)-2-S-2-16(Py), and from 20 nM to 2,000 nM for 16-7N(GK)-16. Standard curves were constructed by plotting the ratio of peak areas of analytes to peak areas of internal standards versus the analyte concentrations using the least-square regression with a weighting factor of *1/x*. Each standard curve was established with the slope, intercept and coefficient of determination (r^2). The curve was accepted if the ± 15% deviation of the nominal value for each standard point other than LLOQ, which can be ± 20%, is achieved. The limit of detection (LOD) was set as the lowest detectable concentration with a signal-to-noise ratio (S/N) ≥3, while the lower limit of quantification (LLOQ) was set as the lowest concentration with S/N ≥5, with a precision of ± 20% coefficient of variation (CV) and a accuracy of ± 20% deviation from the nominal value as per the USFDA guidelines [42].

Precision and accuracy of the method were determined by the analysis of six replicates of quality control samples at four different concentrations (LLOQ, low quality control (LQC), middle quality control (MQC), and high quality control (HQC)). The LQC was within 3-fold of the LLOQ, the

MQC was at the middle part of the standard curve range, and the HQC was within 80% of the upper limit of quantitation (ULOQ). One run per day was conducted across three consecutive days to assess the intra- and inter-day precision and accuracy. Precision was accepted if the CV is ± 15% for concentrations other than the LLOQ, which can be ± 20%; while accuracy was accepted if they were ± 20% deviation of the nominal value for the LLOQ and ± 15% deviation of nominal values for other concentrations.

Recovery experiments were conducted by preparing one set of samples with analyte pre-spiked prior to extraction and the other set with analyte post-spiked after extraction and comparing the peak areas of analytes obtained from each set. For each analyte, three different concentrations at LQC, MQC, and HQC levels in each set were used to determine the recovery.

Freeze-thaw stability, bench-top stability, auto-sampler stability, and long-term stability were carried out using samples with the concentrations at LQC, MQC, and HQC levels. Six replicates of samples at each concentration were prepared for the stability evaluation. Freeze/thaw stability was tested after all samples had gone through six freeze-thaw cycles, with one cycle involving taking out samples stored at -80 ℃ for at least 24 h and allowing them to thaw completely at room temperature prior to refreezing. Bench top stability was evaluated after the samples were placed on the bench at room temperature for 8h and then extracted and analyzed. For the auto-sampler stability, a set of samples was prepared and placed in the auto-sampler at 6 ℃ for 20 h prior to injection for analysis. Long-term stability was tested for samples that were stored at -80 ℃ for 90 days. All samples were analyzed along with freshly prepared standard curves. Samples were considered stable when the USFDA criteria for precision and accuracy were met [42].

2.4 Results and Discussion

2.4.1 Method development

In this work, we aimed at developing a simple and reliable method that can quantify the three target gemini surfactants in biological matrix for the assessment of their cellular uptake and biodistribution. Although gemini surfactants have been previously separated and determined using LC-MS/MS methods with various analytical columns, such as cyano [25] and HILIC columns [26], all of these methods require relatively long run time for the separation and the prior optimization of LC method for the analysis. Therefore, we chose to develop an FIA-MS/MS method that relies on the mass spectrometer's separation capability, as the MRM mode in the quadrupole-linear ion trap system has the capability of selectively monitoring and accurately quantifying the analytes of interest in complex matrices.

Optimization of the FIA-MS/MS condition was the main focus in the process of method development. All source-dependent parameters, such as nebulizer gas and heater gas, and compound-dependent parameters (i.e., DP, EP, and CE) were properly optimized so that a high sensitivity of the MRM transitions for each analyte and internal standard can be achieved. Two MRM transitions were selected for each analyte in this method; the qualifier transition was used to confirm the presence of the analyte peak, whereas the quantifier transition was used for the calculation of the concentration of analyte. Matrix effects have been identified as a challenge in the ESI-MS/MS analysis as it can result in the inconsistency in ion current response [43]. To correct for such variations, we used deuterium-labeled gemini surfactants as internal standards that have similar physicochemical properties and MS behavior to the analytes. The deuterated gemini surfactants possess various numbers (n=4, 10, and 66) of deuterium atoms (Figure 2.S1 in supporting information), which resulted in large mass differences between the analytes and their

respective internal standards and thus eliminated the potential for cross-talk. In addition, we did not observe any interference from the endogenous compounds in the biological matrix for all standards.

For the optimization of FIA, different compositions of solvent mobile phases, including acetonitrile, methanol and water mixed with varying concentrations of formic acid, were tested. Acetonitrile was found to be superior to methanol in terms of obtaining better peak shape and reducing carry over, as gemini surfactants are amphiphilic compounds that tend to stick to the injection loop and tubing (Figure 2.2). In addition, aqueous solvent and acid condition are required to achieve high ionization efficiency of gemini surfactant compounds for better detection sensitivity. As a result, acetonitrile-water (98:2, v/v) with 0.1% formic acid was the best mobile phase system that can result in high ionization efficiency, minimize peak tailing for all analytes and internal standards, and reduce carry over (Figure 2.S2 in supporting information).

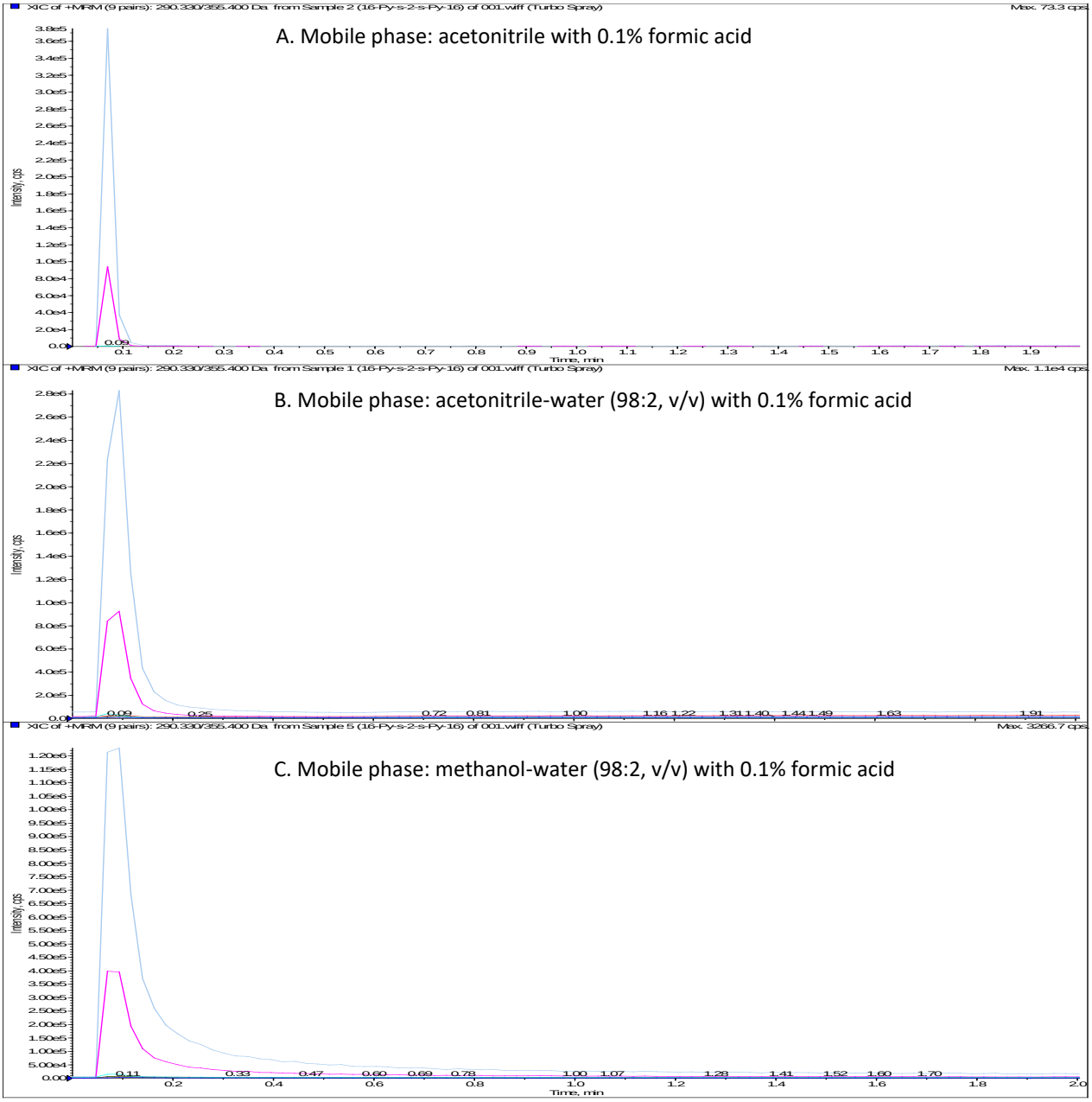

Figure 2.2. FIA-MS/MS chromatogram of 16(Py)-S-2-S-16(Py) using various mobile phases: (a) acetonitrile with 0.1% formic acid, (b) acetonitrile-water (98:2, v/v) with 0.1% formic acid, and (c) methanol-water (98:2, v/v) with 0.1% formic acid.

The Bligh/Dyer extraction method was adapted in this study as it was reported previously to be highly efficient at extracting lipids, including gemini surfactants, from biological matrices [26, 41]. In this method, methanol-chloroform (2:1, v/v) was used as the binary extraction solvent, because

it is highly compatible with the amphiphilic nature of gemini surfactants and thus results in high extraction efficiency. To minimize variation in extraction efficiency across samples, internal standards were spiked into samples at appropriate concentrations prior to extraction.

2.4.2 Selectivity and matrix effects

Selectivity was assessed with the analysis of six different blank cell matrices. These blank cell samples did not contain either the analytes or the internal standards, and a typical chromatogram for the blank cell sample is shown in Figure 2.S3 in supporting information. No interference peak from endogenous compound was observed in the analyte and the internal standard channels from the cell matrix. Furthermore, no cross-talk was observed between the analytes and the internal standards as they have large mass differences due to the presence of multiple (n=4, 10, and 66) deuterated atoms in the structures of internal standards. The peaks of analytes and internal standards eluted at 0.11 min within the data acquisition time of 2 min (Figure 2.3).

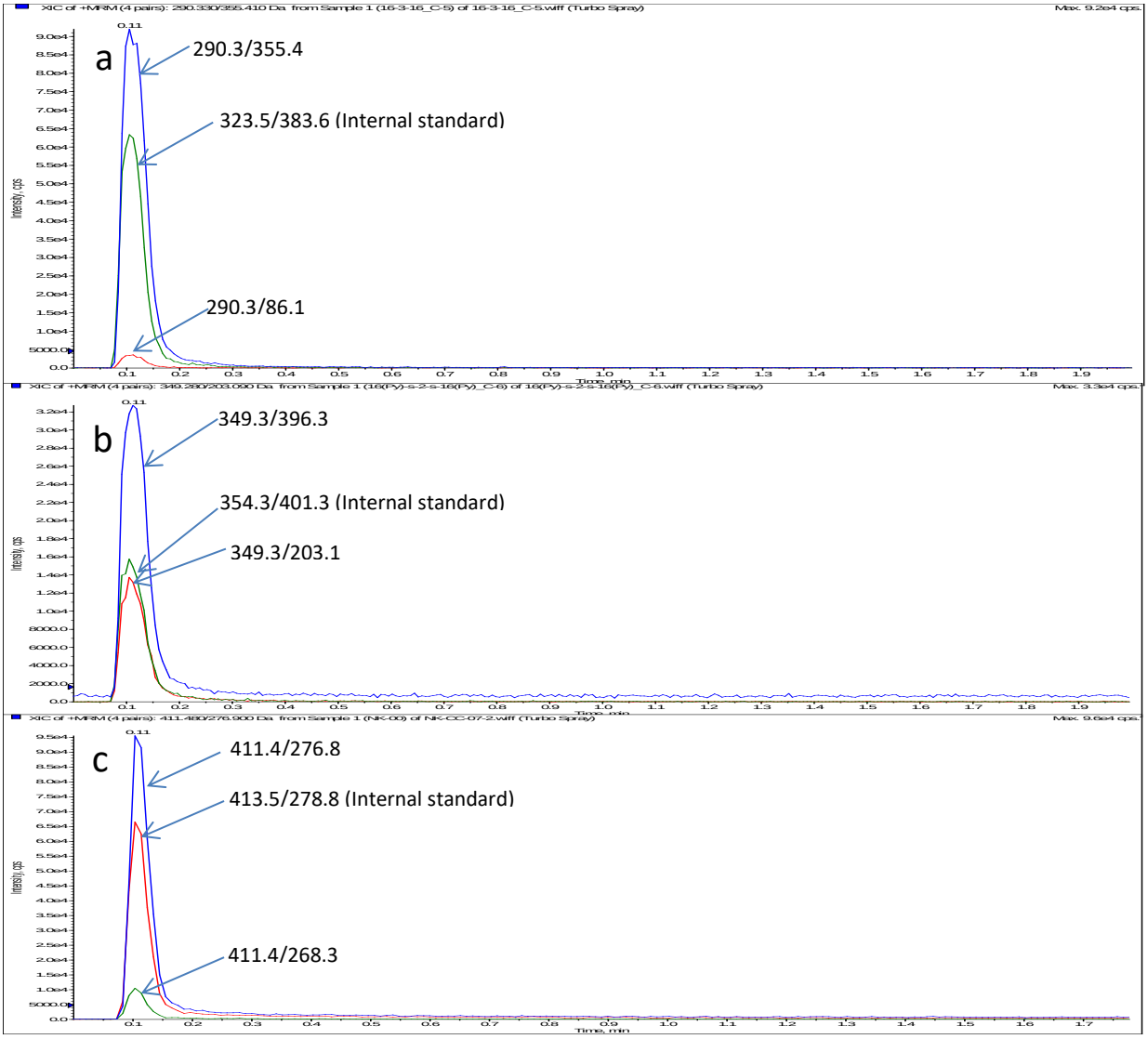

Figure 2.3. FIA-MS/MS chromatograms in the cellular extract. (a) 16-3-16 (0.25 uM) and internal standard (0.2 uM), (b) 16(Py)-S-2-S-16(Py) (0.5 uM) and internal standard (0.2 uM), and (c) 16-7N(GK)-16 (0.5 uM) and internal standard (0.2 uM).

Matrix effects were evaluated by comparing the analyte response in the post-extracted spiked sample with non-extracted neat sample. Three different concentrations for each analyte in three replicates were used for the evaluation. The matrix effects across all concentration levels were calculated, on average, to be 41.5% ± 7.2% for 16-3-16, 40.2% ± 7.8% for 16(Py)-S-2-S-16(Py), and 35.7% ± 4.4% for 16-7N(GK)-16 (Table 2.S1 in supporting information), which were most likely caused by ion suppression. Although a column or additional preparative steps may help

reduce the matrix effect, the observed ion suppression does not undermine the quantification of gemini surfactants as the sensitivity of the method was sufficient for the detection and quantification of target gemini surfactants. In addition, internal standards are used, which are considered to be the gold standard approach for correcting any matrix effects.

2.4.3 Linearity and Sensitivity

Each standard curve was established with a wide range sufficient to cover the expected concentrations of analytes. The standard curves were linear at a concentration range of 10 nM-1,000 nM for 16-3-16 and 16(Py)-S-2-S-(Py)16, and 20 nM-2,000 nM for 16-7N(GK)-16, with r^2 ≥0.998. The LLOD was 4 nM for both 16-3-16 and 16(Py)-S-2-S-16(Py) and 8 nM for 16-7N(GK)-16, whereas the LLOQ was 10 nM for 16-3-16 and 16(Py)-S-2-S-(Py)16, and 20 nM for 16-7N(GK)-16. Compared with the recent HILIC-MS/MS method [26], which reported an LLOQ of 67.5 nM and 58.2 nM for the gemini surfactants 16-3-16 and 16(Py)-S-2-S-16(Py), respectively [26], the current FIA-MS/MS method has a lower LLOQ and thus higher sensitivity. The increase in sensitivity could be attributable to the optimized mobile phase containing appropriate composition of organic and aqueous solvents, which resulted in narrower and more symmetrical analyte peaks compared to those obtained with the HILIC-MS/MS method [26]. In addition, the sample loss during chromatographic separation could also be a contributing factor to the reduced sensitivity of the HILIC-MS/MS method, as gemini surfactants are amphiphilic compounds, prone to sticking to a guard-column and a column. In fact, Buse et al. [24] observed a 10 fold higher sensitivity for the quantification of 16-3-16 using an FC-MS/MS method (LLOQ=37 nM) compared with an LC-MS/MS method (LLOQ =406 nM). Such sensitivity is needed to detect the target analytes in the subcellular matrix.

2.4.4 Intra- and inter-day precision and accuracy

Intra- and inter-day precision and accuracy were evaluated by analyzing samples at four different concentrations LLOQ, LQC, MQC, and HQC as per the USFDA guidelines [42]. Tables 2.2 and 2.3 show the precision and accuracy obtained for gemini surfactants 16-3-16 and 16(Py)-S-2-S-16(Py) at various concentrations. The precision and accuracy of 16-7N(GK)-16 are listed in Tables 2.4 and 2.5. The precision is reported as CV% among all measurements and accuracy is expressed as a percentage of the mean of all measurements relative to their theoretical values. The intra-day precision did not exceed 7.7% for any of the gemini surfactants at the four concentration levels, while accuracy ranged between 94.4% and 108.8%. The inter-day assessment yielded a precision less than 3.3% and accuracy between from 97.2% to 108.4%.

Table 2.2. Intra-day precision and accuracy of the gemini surfactants 16-3-16 and 16(Py)-S-2-S-16(Py)

Samples	Day	Measured concentration (Mean± SD, nM)		Precision		Accuracy	
		16-3-16	16(Py)-S-2-S-16(Py)	16-3-16	16(Py)-S-2-S-16(Py)	16-3-16	16(Py)-S-2-S-16(Py)
LLOQ (10 nM)	1	10.6±0.4	10.3±0.6	3.7%	5.5%	105.8%	102.7%
	2	10.2±0.3	10.8±0.8	3.1%	7.7%	101.9%	108.3%
	3	10.1±0.2	10.2±0.5	2.0%	5.1%	100.6%	102.0%
LQC (30 nM)	1	29.7±0.5	29.0±1.8	1.6%	6.0%	98.9%	96.5%
	2	29.2±0.4	30.2±1.2	1.5%	3.9%	97.4%	100.7%
	3	28.9±0.6	28.3±1.5	1.9%	5.4%	96.3%	94.4%
MQC (150 nM)	1	150.7±1.2	143.3±7.3	0.8%	5.1%	100.4%	95.6%
	2	150.2±1.5	149.8±7.2	1.0%	4.8%	100.1%	99.9%
	3	150.7±1.8	149.0±3.9	1.2%	2.6%	100.4%	99.3%
HQC (800 nM)	1	805.8±8.6	761.7±17.0	1.1%	2.2%	100.7%	95.2%
	2	814.0±6.6	804.0±24.7	0.8%	3.1%	101.8%	100.5%
	3	809.5±7.9	775.7±20.2	1.0%	2.6%	101.2%	97.0%

Table 2.3. Inter-day precision and accuracy of the gemini surfactants 16-3-16 and 16(Py)-S-2-S-16(Py)

Samples	Replicates	Measured concentration (Mean± SD, nM)		Precision		Accuracy	
		16-3-16	16(Py)-S-2-S-16(Py)	16-3-16	16(Py)-S-2-S-16(Py)	16-3-16	16(Py)-S-2-S-16(Py)
LLOQ (10 nM)	18	10.3±0.3	10.4±0.4	2.6%	3.3%	102.8%	104.3%
LQC (30 nM)	18	29.3±0.4	29.2±1.0	1.3%	3.3%	97.6%	97.2%
MQC (150 nM)	18	150.5±0.3	147.4±3.5	0.2%	2.4%	100.3%	98.3%
HQC (800 nM)	18	809.8±4.1	780.4±21.6	0.5%	2.8%	101.2%	97.6%

Table 2.4. Intra-day precision and accuracy of the gemini surfactant 16-7N(GK)-16

Samples	Day	Measured concentration (Mean± SD, nM)	Precision	Accuracy
LLOQ (20 nM)	1	21.7±0.8	3.5%	108.7%
	2	21.5±1.1	5.3%	107.7%
	3	21.8±1.0	4.5%	108.8%
LQC (60 nM)	1	60.3±1.4	2.4%	100.5%
	2	60.1±0.8	1.4%	100.1%
	3	62.8±1.8	2.9%	104.6%
MQC (400 nM)	1	401.2±8.4	2.1%	100.3%
	2	397.0±15.2	3.8%	99.3%
	3	389.0±10.8	2.8%	97.3%
HQC (1600 nM)	1	1613.3±35.6	2.2%	100.8%
	2	1575.0±50.9	3.2%	98.4%
	3	1536.7±57.5	3.7%	96.0%

Table 2.5. Inter-day precision and accuracy of the gemini surfactant 16-7N(GK)-16

Samples	Replicates	Measured concentration (Mean± SD, nM)	Precision	Accuracy
LLOQ (20 nM)	18	21.7±0.1	0.6%	108.4%
LQC (60 nM)	18	61.0±1.5	2.5%	101.7%
MQC (400 nM)	18	395.7±6.2	1.6%	98.9%
HQC (1600 nM)	18	1575.0±38.3	2.4%	98.4%

2.4.5 Recovery

Recovery was determined as the ratio of analyte peak area of the pre-spiked sample before extraction versus that of the post-spiked sample after extraction, expressed as a percentage. Three concentrations for each analyte were evaluated in this study. On average, the recovery was 104.9 ± 10.5% at 30 nM, 111.3 ± 9.7% at 150 nM, and 94.3 ± 6.2% at 800 nM for 16-3-16, 104.0 ± 9.9% at 30 nM, 95.7 ± 8.6% at 150 nM, and 102.9 ± 11.2% at 800 nM for 16(Py)-S-2-S-(Py)16; and 42.9 ± 7.5% at 60 nM, 33.1 ± 3.8% at 400 nM, and 34.4 ± 5.8% at 1,600 nM for 16-7N(GK)-16. Similar to previously published results [26], the Bligh/Dyer method efficiently extracted the gemini surfactants 16-3-16 and 16(Py)-S-2-S-(Py)16 from the cellular matrix. In contrast, the extraction efficiency for the gemini surfactant 16-7N(GK)-16 was significantly reduced. This finding was expected as 16-7N(GK)-16 is a more hydrophilic compound due to the presence of a di-peptide in the spacer region compared with the other two compounds, which decreases its partition to the organic solvent (methanol-chloroform), thereby reducing the extraction efficiency. However, with the use of deuterated internal standards spiked prior to sample extraction, the recovery of analyte was corrected with internal standard. Therefore, the determination of 16-7N(GK)-16 is not

compromised. Such low recovery explains the slightly higher LLOQ for 16-7N(GK)-16 in comparison with the other two analytes (Tables 2.2 and 2.4).

2.4.6 Stability

Freeze-thaw stability, bench top stability, auto-sampler stability, and long-term stability were assessed with the analysis of samples at three different concentrations as shown in Tables 2.S2 and 2.S3 in supporting information. Freeze-thaw stability was determined to be with a precision of less than 6.7% and a accuracy between 94.7% and 104.4%. For the bench top stability, the precision and accuracy varied from 2.6% to 7.3% and from 96.7% to 100.3%, respectively. The stability of these samples in the auto-sampler resulted in a precision range of 2.8% - 5.7% and accuracy range of 96.9% - 102.5%. These results confirmed that the samples were stable during sample preparation and data acquisition. Also, the stability of these samples was not compromised by long-term storage at -80 ^{o}C, with the values of precision ranging from 2.0% to 7.0% and accuracy ranging from 89.1% to 101.1%.

2.5 Application

The uptake and subcellular distribution profiles of the gemini surfactants 16-3-16, 16(Py)-S-2-S-(Py)16, and 16-7N(GK)-16 in PAM 212 cells were studied using the validated FIA-MS/MS method. In this work, we show proof-of-principle application of the method to analyze these compounds in the nuclear fraction. The complete analysis of various subcellular fractions including the nucleus, mitochondria, plasma membrane and cytosol, along with other biological assessments, will be reported upon completion of the analyses. Although the standard curves and QC samples were prepared in the blank cell lysate matrix, no matrix difference was observed among the various

subcellular fractions and the whole cell lysate, which ensured the accurate quantification of the gemini surfactants in each cellular fraction.

The uptake rate of the gemini surfactants in the nuclear fraction increased rapidly over the course of 5 h treatment, reaching a peak concentration of approximately 800 nM for 16(Py)-S-2-S-(Py)16 and 16-7N(GK)-16 and 300 nM for 16-3-16, followed by a gradual decrease after the removal of the dosed culture media (Figure 2.4). The observations are consistent with the reported progressive nanoparticle uptake, which reaches a maximum before a depletion of the intracellular analytes [26]. As expected, the rate of uptake and the biodistribution in the nuclear fraction is different among the three gemini surfactants. Such differences could explain their variable efficiency and toxicity. However, a definitive conclusion may only be drawn upon the completion of the analysis of all four subcellular compartments, which will be conducted in the near future.

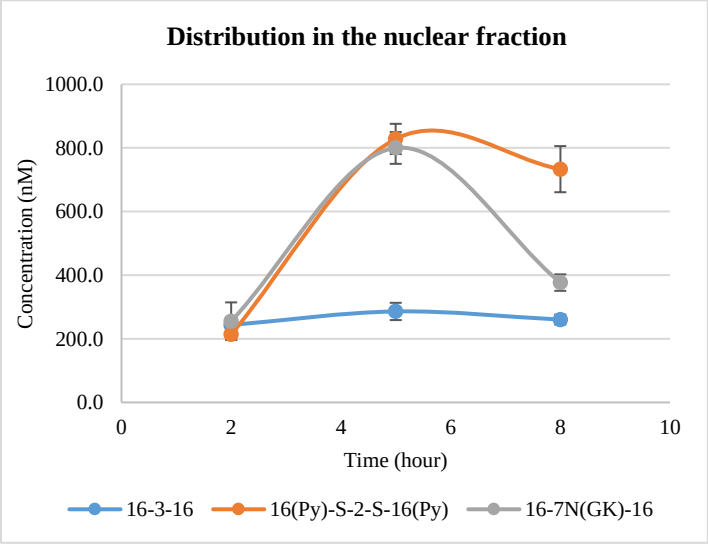

Figure 2.4. Distribution of gemini surfactants: 16-3-16, 16(Py)-S-2-S-16(Py), and 16-7N(GK)-16 in the nuclear fraction of PAM 212 cells treated with gemini surfactant nanoparticles.

2.6 Conclusion

A simple and reliable FIA-MS/MS method was successfully developed and validated for the quantification of the gemini surfactants 16-3-16, 16(Py)-S-2-S-(Py)16, and 16-7N(GK)-16 as gene delivery agents in PAM 212 cells. The sensitivity of the FIA-MS/MS method is superior to the reported HILIC-MS/MS method for the determination of these gemini surfactants at the subcellular level. The specificity, precision, accuracy, recovery, and stability are sufficient to quantify these gemini surfactants in the cellular matrix. Furthermore, the use of chromatographic separation, gradient elution, and an ion pairing reagent is eliminated in the reported approach, thus substantially simplifying the analytical method and reducing sample run time. The method was successfully applied to quantify the three gemini surfactants in the nuclear fraction of PAM 212 cells treated with nanoparticles, which varied significantly and may explain differences in the observed efficiency and toxicity of these gemini surfactants in gene delivery.

2.7 Acknowledgements

The project was supported by a NSERC discovery grant. We would like to thank Ms. Deborah Michael for her technical assistance on the operation of 4000 QTRAP® system and Drs. Jackson M. Chitanda and McDonald Donkuru for the synthesis of gemini surfactants. We also thank Dr. Mays A. Al-Dulaymi for her help in the method development and Dr. Waleed Mohammed-Saeid for the training in transfection experiment. Dr. Randy Purves is acknowledged for the valuable analytical discussion. Postgraduate scholarship for Wei Jin is provided by Natural Sciences and Engineering Research Council of Canada. Funding to purchase the 4000 QTRAP® instrument was obtained through a Canada Foundation for Innovation -Leaders Opportunity Fund.

2.8 References

1. Rosenberg, C.D., et al., *Interspecific DNA-mediated transfer and amplification of a gene specifying a Mr 100,000 human melanoma-associated cell surface glycoprotein.* Cancer Res, 1990. **50**(5): p. 1559-1565.
2. Schiza, A., et al., *Adenovirus-mediated CD40L gene transfer increases Teffector/Tregulatory cell ratio and upregulates death receptors in metastatic melanoma patients.* J Transl Med, 2017. **15**(79): p. 1-12.
3. Slack, R.S., et al., *Adenovirus-mediated gene transfer of the tumor suppressor, p53, induces apoptosis in postmitotic neurons.* J Cell Biol, 1996. **135**(4): p. 1085-1096.
4. Peng, P.D., et al., *Efficient nonviral Sleeping Beauty transposon-based TCR gene transfer to peripheral blood lymphocytes confers antigen-specific antitumor reactivity.* Gene Ther, 2009. **16**(8): p. 1042-1049.
5. Ginn SL, A.A., Alexander IE, Edelstein M, Abedi MR, *Gene therapy clinical trials worldwide to 2017: An update.* J Gene Med., 2018 Mar 25.
6. Cusack Jr, J.C. and K.K. Tanabe, *Introduction to cancer gene therapy.* Surgical oncology clinics of North America, 2002. **11**(3): p. 497-519.
7. Howarth, J.L., Y.B. Lee, and J.B. Uney, *Using viral vectors as gene transfer tools (Cell Biology and Toxicology Special Issue: ETCS-UK 1 day meeting on genetic manipulation of cells).* Cell biology and toxicology, 2010. **26**(1): p. 1-20.
8. Walter, W. and U. Stein, *Viral vectors for gene transfer a review of their use in the treatment of human disease.* Drugs, 2000. **60**: p. 249-271.
9. Hacein-Bey-Abina, S., et al., *A serious adverse event after successful gene therapy for X-linked severe combined immunodeficiency.* N Engl J Med, 2003. **348**(3): p. 255-256.
10. Thomas, C.E., A. Ehrhardt, and M.A. Kay, *Progress and problems with the use of viral vectors for gene therapy.* Nat Rev Genet, 2003. **4**(5): p. 346-358.
11. Fisicaro, E., et al., *Nonviral gene delivery: gemini bispyridinium surfactant-based DNA nanoparticles.* J Phys Chem B, 2014. **118**(46): p. 13183-13191.
12. Ramamoorth, M. and A. Narvekar, *Non viral vectors in gene therapy-an overview.* Journal of clinical and diagnostic research, 2015. **9**(1): p. GE01-06.
13. Nayerossadat, N., T. Maedeh, and P.A. Ali, *Viral and nonviral delivery systems for gene delivery.* Advanced biomedical research, 2012. **1**: p. 27-27.

14. Badea, I., et al., *In vivo cutaneous interferon-gamma gene delivery using novel dicationic (gemini) surfactant-plasmid complexes.* J Gene Med, 2005. **7**(9): p. 1200-1214.
15. Kirby, A.J., et al., *Gemini surfactants: new synthetic vectors for gene transfection.* Angewandte Chemie International Edition, 2003. **42**(13): p. 1448-1457.
16. Menger, F.M. and J.S. Keiper, *Gemini surfactants.* Angewandte Chemie International Edition, 2000. **39**(11): p. 1906-1920.
17. Hait, S. and S. Moulik, *Gemini surfactants: a distinct class of self-assembling molecules.* CURRENT SCIENCE-BANGALORE-, 2002. **82**(9): p. 1101-1111.
18. Karlsson, L., M.C. van Eijk, and O. Söderman, *Compaction of DNA by gemini surfactants: effects of surfactant architecture.* Journal of colloid and interface science, 2002. **252**(2): p. 290-296.
19. Bombelli, C., et al., *Role of the spacer of cationic gemini amphiphiles in the condensation of DNA.* Langmuir, 2005. **21**(23): p. 10271-10274.
20. Cardoso, A.M., et al., *Gemini surfactants mediate efficient mitochondrial gene delivery and expression.* Molecular pharmaceutics, 2015. **12**(3): p. 716-730.
21. Bhadani, A. and S. Singh, *Novel gemini pyridinium surfactants: synthesis and study of their surface activity, DNA binding, and cytotoxicity.* Langmuir, 2009. **25**(19): p. 11703-11712.
22. Yang, P., et al., *Enhanced gene expression in epithelial cells transfected with amino acid-substituted gemini nanoparticles.* European Journal of Pharmaceutics and Biopharmaceutics, 2010. **75**(3): p. 311-320.
23. Al-Dulaymi, M.A., et al., *Di-Peptide-Modified Gemini Surfactants as Gene Delivery Vectors: Exploring the Role of the Alkyl Tail in Their Physicochemical Behavior and Biological Activity.* The AAPS journal, 2016. **18**(5): p. 1168-1181.
24. Buse, J., et al., *The development and assessment of high-throughput mass spectrometry-based methods for the quantification of a nanoparticle drug delivery agent in cellular lysate.* J Mass Spectrom, 2014. **49**(11): p. 1171-1180.
25. Buse, J., et al., *A general liquid chromatography tandem mass spectrometry method for the quantitative determination of diquaternary ammonium gemini surfactant drug delivery agents in mouse keratinocytes' cellular lysate.* Journal of Chromatography A, 2013. **1294**: p. 98-105.

26. Donkuru, M., et al., *Hydrophilic interaction liquid chromatography–tandem mass spectrometry quantitative method for the cellular analysis of varying structures of gemini surfactants designed as nanomaterial drug carriers.* Journal of Chromatography A, 2016. **1446**: p. 114-124.
27. Donkuru, M., et al., *Multi-stage tandem mass spectrometric analysis of novel β-cyclodextrin-substituted and novel bis-pyridinium gemini surfactants designed as nanomedical drug delivery agents.* Rapid Communications in Mass Spectrometry, 2014. **28**(7): p. 757-772.
28. Buse, J., et al., *Tandem mass spectrometric analysis of novel diquaternary ammonium gemini surfactants and their bromide adducts in electrospray-positive ion mode ionization.* Journal of Mass Spectrometry, 2011. **46**(10): p. 1060-1070.
29. Buse, J., et al., *Tandem mass spectrometric analysis of the novel gemini surfactant nanoparticle families G12-s and G18: 1-s.* Spectroscopy Letters, 2010. **43**(6): p. 447-457.
30. Mohammed-Saeid, W., et al., *Mass spectrometric analysis of amino acid/di-peptide modified gemini surfactants used as gene delivery agents: Establishment of a universal mass spectrometric fingerprint.* International Journal of Mass Spectrometry, 2012. **309**: p. 182-191.
31. Al-Dulaymi, M. and A. El-Aneed, *Tandem mass spectrometric analysis of novel peptide-modified gemini surfactants used as gene delivery vectors.* Journal of Mass Spectrometry, 2017. **52**(6): p. 353-366.
32. Boscaro, F., et al., *Rapid quantitation of globotriaosylceramide in human plasma and urine: a potential application for monitoring enzyme replacement therapy in Anderson-Fabry disease.* Rapid communications in mass spectrometry, 2002. **16**(16): p. 1507-1514.
33. Nanita, S.C. and L.G. Kaldon, *Emerging flow injection mass spectrometry methods for high-throughput quantitative analysis.* Analytical and bioanalytical chemistry, 2016. **408**(1): p. 23-33.
34. Niesser, M., B. Koletzko, and W. Peissner, *Determination of creatinine in human urine with flow injection tandem mass spectrometry.* Annals of Nutrition and Metabolism, 2012. **61**(4): p. 314-321.
35. Johnson, D.W., *An acid hydrolysis method for quantification of plasma free and total carnitine by flow injection tandem mass spectrometry.* Clinical biochemistry, 2010. **43**(16-17): p. 1362-1367.

36. Nanita, S.C. and N.L. Padivitage, *Ammonium chloride salting out extraction/cleanup for trace-level quantitative analysis in food and biological matrices by flow injection tandem mass spectrometry.* Analytica chimica acta, 2013. **768**: p. 1-11.
37. Dankers, J., et al., *Determination of nifedipine in human plasma by flow-injection tandem mass spectrometry.* Journal of Chromatography B: Biomedical Sciences and Applications, 1998. **710**(1-2): p. 115-120.
38. Michel, D., et al., *Development and validation of fast and simple flow injection analysis–tandem mass spectrometry (FIA–MS/MS) for the determination of metformin in dog serum.* Journal of pharmaceutical and biomedical analysis, 2015. **107**: p. 229-235.
39. Al-Dulaymi, M., et al., *The development of simple flow injection analysis tandem mass spectrometric methods for the cutaneous determination of peptide-modified cationic gemini surfactants used as gene delivery vectors.* Journal of pharmaceutical and biomedical analysis, 2018. **159**: p. 536-547.
40. Rangel, R., et al., *Targeting mammalian organelles with internalizing phage (iPhage) libraries.* Nature protocols, 2013. **8**(10): p. 1916-1939.
41. Bligh, E.G. and W.J. Dyer, *A rapid method of total lipid extraction and purification.* Canadian journal of biochemistry and physiology, 1959. **37**(8): p. 911-917.
42. FDA, *Guidance for Industry: Bioanalytical Method Validation*. US, Department of Health and Human Services, Food and Drug Administration, Center for Drug Evaluation and Research (CDER), Center for Veterinary Medicine (CVM). 2013.
43. Gosetti, F., et al., *Signal suppression/enhancement in high-performance liquid chromatography tandem mass spectrometry.* Journal of Chromatography A, 2010. **1217**(25): p. 3929-3937.

2.9 Supporting Information

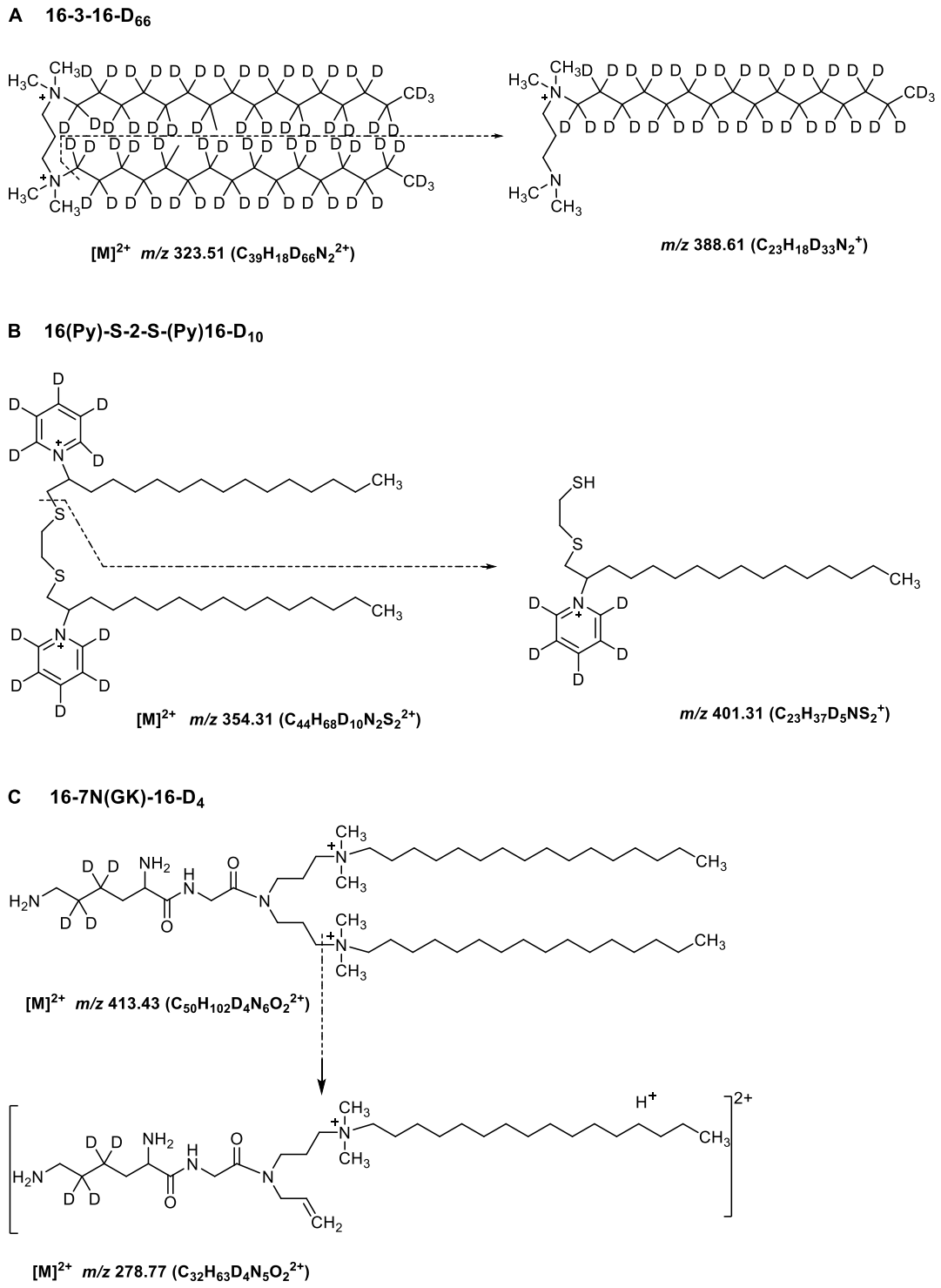

Figure 2.S1. (A) Structures of 16-3-16-D_{66} and the monitored product ion, (B) structures of 16(Py)-S-2-S-16(Py)-D_{10} and the monitored product ion, and (C) structures of 16-7N(GK)-16-D_4 and the monitored product ion.

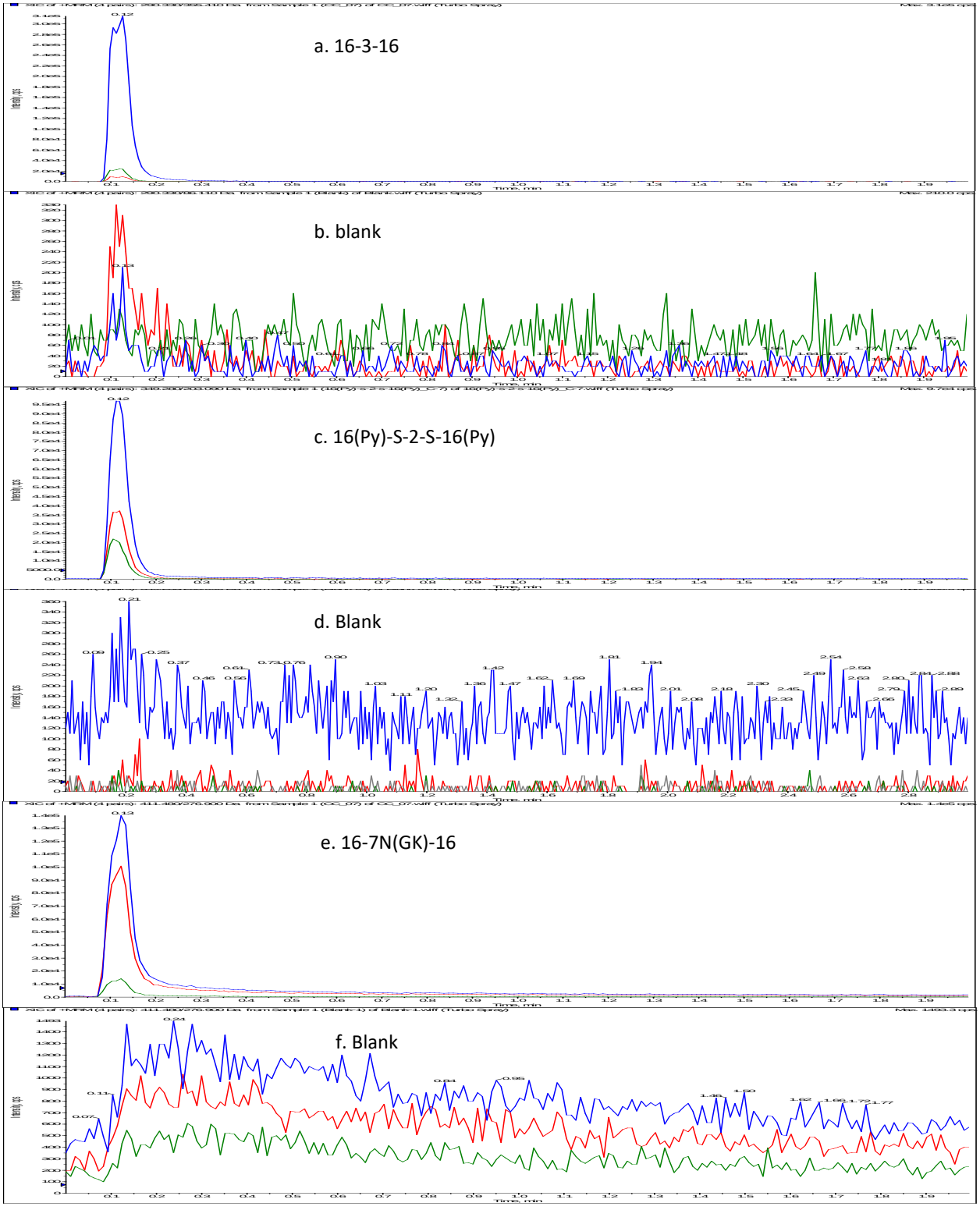

Figure 2.S2. Illustration of no carry over. FIA-MS/MS chromatograms of the highest curve point of (a) 16-3-16, (c)16(Py)-S-2-S-16(Py), and (e) 16-7N(GK)-16, and the following blank samples of (b) 16-3-16, (d)16(Py)-S-2-S-16(Py), and (f) 16-7N(GK)-16.

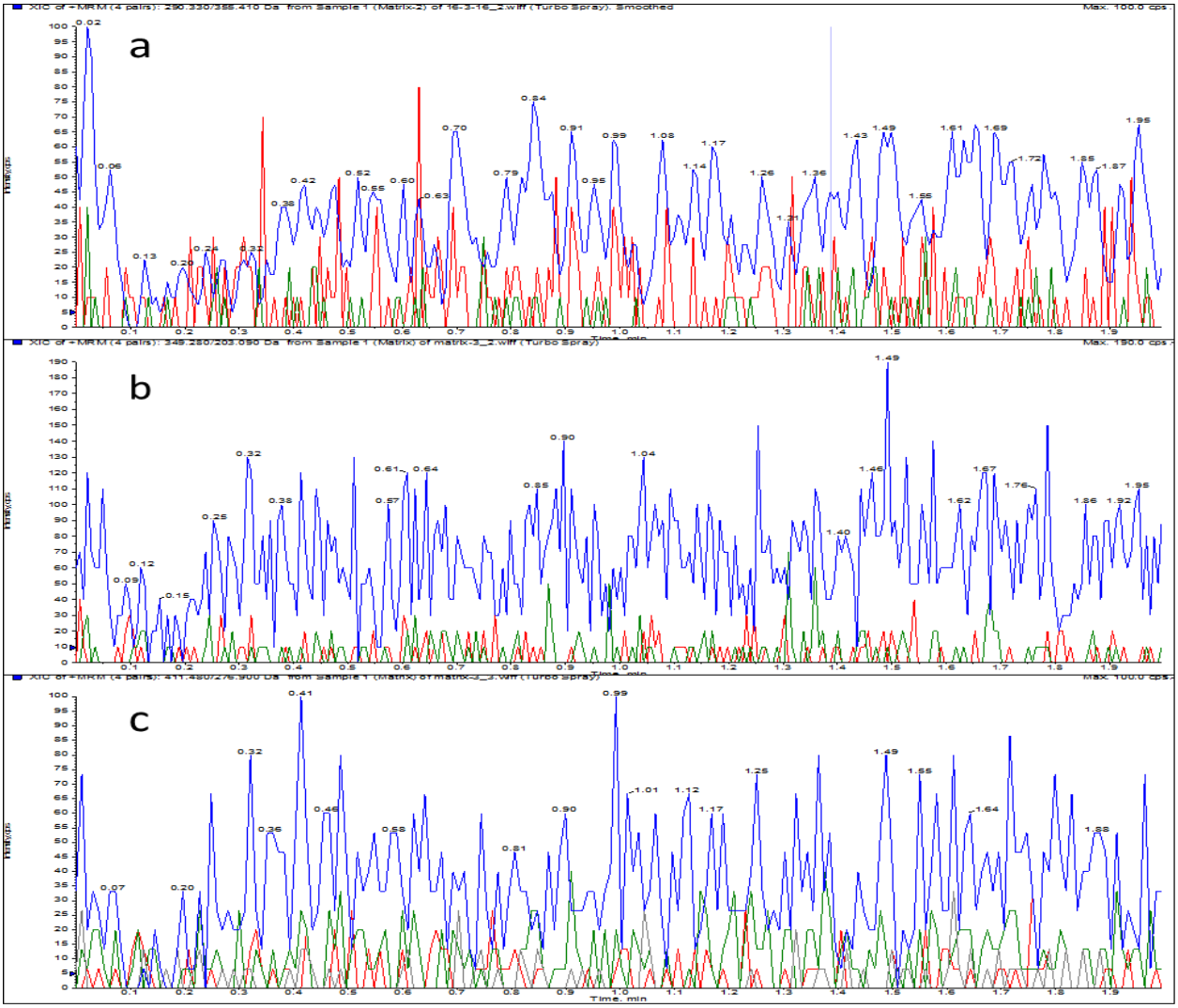

Figure 2.S3. The FIA-MS/MS chromatogram of blank cell matrix for MRM transitions: (a) 16-3-16, (b) 16(Py)-S-2-S-16(Py), and (c) 16-7N(GK)-16.

Table 2.S1. Matrix effect of the gemini surfactants 16-3-16, 16(Py)-S-2-S-16(Py) and 16-7N(GK)-16

Sample	Replicates	Matrix effect (Mean± SD)		
		16-3-16	16(Py)-S-2-S-16(Py)	16-7N(GK)-16
LQC	3	47.1%±1.5%	42.9%±4.9%	31.9%±1.5%
MQC	3	33.4%±5.8%	35.4%±6.0%	40.5%±1.5%
HQC	3	44.0%±5.2%	36.1%±2.4%	34.6%±2.5%
Mean	3	41.5%±7.2%	40.2%±7.8%	35.7%±4.4%

Table 2.S2. Stability of the gemini surfactants 16-3-16 and 16(Py)-S-2-S-16(Py) in cellular matrix

Samples	Stability	Measured concentration (Mean ± SD, nM)		Precision		Accuracy	
		16-3-16	16(Py)-S-2-S-16(Py)	16-3-16	16(Py)-S-2-S-16(Py)	16-3-16	16(Py)-S-2-S-16(Py)
LQC (30 nM)	0 h	32.1±1.1	29.0±0.3	3.4%	1.1%	106.9%	96.8%
	6 freeze-thaw	32.7±0.9	29.5±1.5	2.8%	5.1%	109.1%	98.4%
	8 h (bench top)	33.2±0.3	32.2±0.9	0.8%	2.9%	110.8%	107.4%
	20 h (autosampler)	33.6±0.5	32.1±1.3	1.5%	4.1%	111.8%	107.1%
	90 days at -80℃	28.0±0.9	28.2±1.3	3.2%	4.6%	93.4%	93.9%
MQC (150 nM)	0h	152.7±3.9	144.0±2.8	2.5%	2.0%	101.8%	96.0%
	6 freeze-thaw	162.7±3.8	139.2±5.5	2.3%	4.0%	108.4%	92.8%
	8 h (bench top)	155.3±2.7	153.7±2.3	1.7%	1.5%	103.6%	102.4%
	20 h (autosampler)	156.0±2.2	155.3±3.5	1.4%	2.3%	104.0%	103.6%
	90 days at -80℃	138.8±3.4	138.2±2.8	2.5%	2.0%	92.6%	92.1%
HQC (800 nM)	0 h	823.7±8.0	804.5±16.3	1.0%	2.0%	103.0%	100.6%
	6 freeze-thaw	860.5±24.3	790.3±15.4	2.8%	1.9%	107.6%	98.8%
	8 h (bench top)	824.8±14.7	792.7±11.4	1.8%	1.4%	103.1%	99.1%
	20 h (autosampler)	821.8±10.3	818.7±17.6	1.2%	2.2%	102.7%	102.3%
	90 days at -80℃	748.0±15.6	712.5±43.7	2.1%	6.1%	93.5%	89.1%

Table 2.S3. Stability of the gemini surfactant 16-7N(GK)-16 in cellular matrix

Samples	Stability	Measured concentration (Mean± SD, nM)	Precision	Accuracy
LQC (60 nM)	0 h	56.9±2.5	4.5%	94.9%
	6 freeze-thaw	62.7±4.2	6.7%	104.4%
	8 h (bench top)	58.0±4.2	7.3%	96.7%
	20 h (autosampler)	58.2±2.5	4.4%	96.9%
	90 days at -80 ℃	55.2±2.0	3.6%	91.9%
MQC (400 nM)	0 h	388.8±11.8	3.0%	97.2%
	6 freeze-thaw	394.2±23.9	6.1%	98.5%
	8 h (bench top)	399.8±10.5	2.6%	100.0%
	20 h (autosampler)	410.2±11.5	2.8%	102.5%
	90 days at -80 ℃	386.7±27.1	7.0%	96.7%
HQC (1600 nM)	0 h	1600.0±87.2	5.4%	100.0%
	6 freeze-thaw	1515.0±53.6	3.5%	94.7%
	8 h (bench top)	1605.0±50.9	3.2%	100.3%
	20 h (autosampler)	1618.3±91.7	5.7%	101.1%
	90 days at -80 ℃	1518.3±52.3	3.4%	94.9%

3 Chapter 3 - Cellular Uptake and Distribution of Gemini Surfactant Nanoparticles Used as Gene Delivery Agents

This chapter has been published as a research article, cited from "*The American Association of Pharamaceutical Scientist (AAPS) Journal, (2019) 21:98*"

Cellular uptake and distribution of gemini surfactant nanoparticles used as gene delivery agents

Wei Jin[1], Mays Al-Dulaymi[1], Ildiko Badea[1], Scot C. Leary[2], Jeveria Rehman[3], and Anas El-Aneed[1]*

[1]Drug Design & Discovery Group, College of Pharmacy and Nutrition, University of Saskatchewan, 107 Wiggins Road, Saskatoon, SK, S7N 5E5, Canada.

[2]Department of Biochemistry, Microbiology and Immunology, University of Saskatchewan, 107 Wiggins Road, Saskatoon, SK, S7N 5E5, Canada.

[3]Department of Chemistry, University of Saskatchewan, 110 Science Place, Saskatoon, SK, S7N 5C9, Canada.

*Corresponding author. E-mail address: anas.el-aneed@usask.ca (A. El-Aneed).

Authors' contribution: Wei Jin played a key role in the design of the research question, conducted the experiments, analyzed the data, and drafted the manuscript. Dr. Al-Dulaymin contributed to the experimental design, data analysis and provided input to the writing. Dr. Badea helped with the nanoparticle formulation, experimental design, and data interpretation. Dr. Leary helped with the isolation of the subcellular organelles. Ms. Rehamn helped with data collection and analysis for Langmuir studies. Dr. El-Aneed is the PI; he conceptualized the research question, obtained funding, supervised the work, and revised the manuscript.

Transitioning Rationale:

Once the FIA-MS/MS method was developed and validated in Chapter 2, it was applied for the quantification of three gemini surfactants 16-3-16, 16(Py)-S-2-S-(Py)16, and 16-7N(GK)-16 in four subcellular fractions, namely nucleus, mitochrondria, plasma membrane, and cytosol, to determine their cellular uptake and subcellular distributions in PAM 212 cells, as described in this Chapter. In addition, DNA binding capability and the shape of aggregates were measured to explain the behavior of the three gemini surfactants in biological systems.

3.1 Abstract

Gemini surfactants are promising molecules utilized as non-viral gene delivery vectors. However, little is known about their cellular uptake and distribution after they release their therapeutic cargo. Therefore, we quantitatively evaluated the cellular uptake and distribution of three gemini surfactants, unsubstituted (16-3-16), with pyridinium head groups (16(Py)-S-2-S-16(Py)) and substituted with a glycyl-lysine di-peptide (16-7N(GK)-16). We also assessed the relationship between the cellular uptake and distribution of each gemini surfactant and its overall efficiency and toxicity. Epidermal keratinocytes PAM 212 cells were treated with gemini surfactant nanoparticles formulated with plasmid DNA and harvested at various time points to collect the enriched nuclear, mitochondrial, plasma membrane, and cytosolic fractions. Gemini surfactants were then extracted from each subcellular fraction and quantified using a validated flow injection analysis-tandem mass spectrometry (FIA-MS/MS) method. Mass spectrometry is superior to the use of fluorescent tags that alters the physicochemical properties and pharmacokinetics of the nanoparticles and can be cleaved from gemini surfactant molecules within biological systems. Overall, a significantly higher cellular uptake was observed for 16-7N(GK)-16 (17.0%) compared with 16-3-6 (3.6%) and 16(Py)-S-2-S-16(Py) (1.4%), which explained the relatively higher transfection efficiency of 16-7N(GK)-16. The gemini surfactants 16-3-16 and 16(Py)-S-2-S-16(Py) displayed similar subcellular distribution patterns, with major accumulation in the nucleus, followed by the mitochondrion, cytosol, and plasma membrane. In contrast, the gemini surfactant 16-7N(GK)-16 was relatively evenly distributed across all four subcellular fractions. However, accumulation within the nucleus after 5 h treatment was the highest for 16(Py)-S-2-S-16(Py) (50.3%), followed by 16-3-16 (41.8%) and then 16-7N(GK)-16 (33.4%), possibly leading to the relatively higher toxicity of 16(Py)-S-2-S-16(Py). Ethidium bromide dye exclusion essay indicated that 16-7N(GK)-16 has a relatively

weaker DNA binding property, which has the ability to not only protect DNA but also facilitate its intracellular release, contributing to its high efficiency in gene transfection. In addition, Langmuir studies showed that 16-7N(GK)-16 has a flexible bilayer structure that tends to form the inverted hexagonal phase in combination with DOPE, promoting the cytoplasmic release of DNA from endosome and thus enhancing its gene delivery efficiency.

Key words: Gemini surfactants; Gene delivery; Subcellular distribution; FIA-MS/MS; Toxicity; Transfection.

3.2 Introduction

Gemini surfactants are a versatile family of lipids that have a general structure of two surfactant monomers chemically linked by a spacer [1]. In particular, cationic gemini surfactants possess dual positively charged hydrophilic head groups, a spacer region, and two hydrophobic tails (Figure 4.1) [2]. They are promising vectors for non-viral gene delivery [3-5] as their structures enable them to bind and compact DNA, facilitating its cellular entry for gene transfection [6, 7]. Extensive research has been conducted to design and synthesize novel gemini surfactant compounds with the aim of enhancing transfection efficiency while reducing toxicity. For example, the positively charged head groups were altered using various cationic moieties, such as di-quaternary amines and di-pyridines, to attain effective compaction of DNA [2, 8]. Furthermore, amino acid moieties have been incorporated into the spacer region to enhance the biocompatibility of gemini surfactants and thus increase their transfection efficiency [9]. In addition, the formulation of gemini surfactant-based lipoplexes and their cellular uptake mechanisms have been well studied [10, 11], and it has been found that endocytosis is the main pathway by which gemini surfactant nanoparticles are internalized by the cell [11].

Despite their promise, gemini surfactants are still limited in their gene transfection efficiency [12, 13], hindering their advancement from the experimental stage to clinical application. In addition, there are no clear explanations for the varying toxicities among different gemini surfactant structures. Therefore, a greater understanding of the mechanism of transfection and toxicity is required and will ultimately contribute to the development of more efficient and less toxic gemini surfactants. One factor that may be related to the overall efficiency and toxicity of gemini surfactants is their intracellular biological fate post transfection; that is, how they are distributed at the subcellular and tissue levels. However, as of yet, their biological fate is poorly understood, and little is known about their cellular uptake, distribution, and metabolite formation upon transfection. Garnering such knowledge will contribute to the design and development of more effective gemini surfactants. In addition, an understanding of the cellular distribution of the delivery agents is crucial to achieve targeted delivery at the subcellular level [14]. Our research hypothesis is that the structure of a gemini surfactant significantly influences its cellular uptake and subsequent partitioning which in turn has profound consequences with respect to efficiency and toxicity. In fact, we have recently demonstrated the role of the molecular structure of gemini surfactants in determining their skin penetration efficiency [15].

Gemini surfactants designated as 16-3-16, 16(Py)-S-2-S-16(Py), and 16-7N(GK)-16) have been studied as non-viral gene delivery agents [16-18]. Structurally, 16-3-16 is a conventional *m-s-m* type gemini surfactant bearing two quaternary amines, linked by a 3-carbon spacer region (*m* is the number of carbon atoms in the tail and *s* is the number of carbon atoms in the spacer); while 16(Py)-S-2-S-(Py)16 is a pyrdinium-derived gemini surfactant containing two pyridines in the head groups, and 16-7N(GK)-16 bears a glycyl-lysine di-peptide within the spacer region (Figure 3.1), allowing for a better biocompatibility. In fact, these gemini surfactants have been successfully used for *in*

vitro and *in vivo* gene delivery [16-20]. For instance, the 16-3-16 nanoparticles have shown great promise in the treatment of localized scleroderma, as transgene expression in animal models was significantly increased with treatment of the nanoparticles compared with naked DNA, showing the effectiveness of gemini surfactant-based gene delivery systems [6, 20].

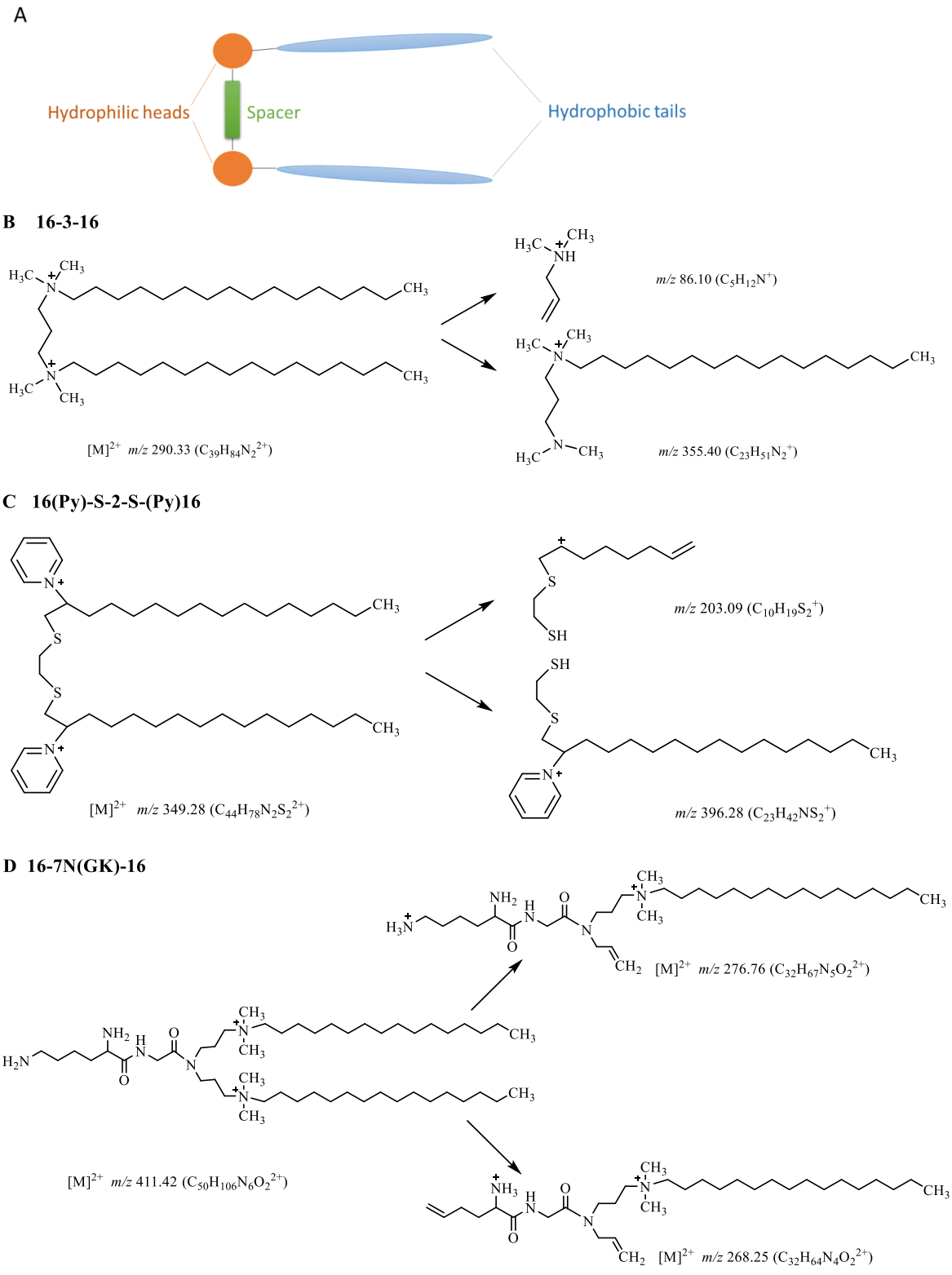

Figure 3.1 Schematic representation of the general structure of a gemini surfactant (A). The structures of gemini surfactants 16-3-16 (B), 16(Py)-S-2-S-16(Py) (C), and 16-7N(GK)-16 (D), showing their m/z values as well as the ions monitored during the FIA-MS/MS analysis.

The selection of the three gemini surfactants (Figure 3.1) was based on the variations in their molecular structures, transfection efficiency, and toxicity profiles [6, 8, 21]. Although these gemini surfactants belong to three different structural families that possess different head groups and spacer regions, they have the same number of carbon atoms in the tails (Figure 3.1). We are currently conducting a wide assessment of the gemini surfactants in various families with respect to the relationship between cellular uptake, subcellular distribution, efficiency, and toxicity. As such, we chose these three structures as model compounds. Previously, we determined that the trend of cellular uptake and clearance of 16-3-16 and 16(Py)-S-2-S-(Py)16 nanoparticles were similar in PAM 212 epidermal keratinocytes cells, which provides no explanation of the differential toxicities between the two compounds [22]. We, therefore, are testing the hypothesis that the relative efficiency and toxicity of these compounds is explained by a difference in their cellular uptake and subcellular distribution.

To assess the cellular uptake and distribution of lipid-based nanoparticles, fluorescent tags have been incorporated into their structures [14, 23]. However, the use of fluorescent tags suffers from two main drawbacks. First, the addition of such structure-modified moieties alters the physicochemical properties and pharmacokinetics of the nanoparticles [24, 25]. Second, the fluorescent tags can be cleaved from the gemini surfactant molecules within biological systems, confounding subsequent data interpretation. Such limitations motivated us to develop mass spectrometry (MS)-based methods to monitor the fate of gemini surfactant nanoparticles in cells [22, 26]. The main advantage of MS is its capability to measure the original intact molecule with high selectivity and sensitivity [27]. Most recently, we developed and validated a simple flow injection analysis-tandem mass spectrometry (FIA-MS/MS) method that allows for the tracking of gemini surfactants at the subcellular level [28].

In the present study, the validated FIA-MS/MS method is applied to provide for the first time a quantitative assessment of the cellular uptake and subcellular distribution of three gemini surfactants gene delivery nanoparticles (Figure 3.1) within PAM 212 cells. We found that variable cellular uptake of the three gemini surfactants explained the differences in transfection efficiency, and that accumulation of gemini surfactant in the nucleus may provide insights into the observed increased toxicity.

3.3 Materials and Methods

3.3.1 Materials

Gemini surfactants 16-3-16, 16(Py)-S-2-S-16(Py), and 16-7N(GK)-16 (Figure 3.1) and their deuterated internal standards 16-3-16-D_{66}, 16(Py)-S-2-S-16(Py)-D_{10}, and 16-7N(GK)-16-D_4 (Figure 3.S1 in supporting information) were synthesized according to established protocols [16, 19, 29]. The neutral lipid 1, 2-dioleoyl-sn-glycero-3-phosphoethanolamine (DOPE) was purchased from Avanti Polar Lipids Inc. (Alabaster, AL, USA). Chloroform, methanol, acetonitrile, formic acid, tissue culture flasks (75 cm^2, 150 cm^2) and petri dishes (150 cm^2) were purchased from Fisher Scientific (Ottawa, ON, Canada). 96-well tissue culture plates were obtained from Falcon (BD Mississauga, ON, Canada). PAM 212 keratinocyte cells were kindly provided by Dr. S. Yuspa, National Cancer Institute, Bethesda, MD, USA. Fetal bovine serum albumin (FBS), antibiotic-antimycotic solution and minimum essential media (MEM) were obtained from Sigma-Aldrich (Oakville, ON, Canada). The protease inhibitor cocktail was purchased from Invitrogen (Burlington, ON, Canada). The plasmid DNA (pGTmCMV.IFN-GFP) was constructed in-house as previously described [6]. The motorized homogenizer was purchased from Fisher Scientific (Toronto, ON, Canada).

3.3.2 Formulation

Gemini surfactants and internal standards were prepared at a concentration of 3 mM in aqueous solutions and stored at -80℃ under darkness. DOPE vesicles were prepared freshly at a concentration of 1 mM in isotonic sucrose solution (9.25% w/v, pH=9) based on an established protocol [5]. The plasmid DNA solution was prepared at 200 µg/mL in ultra-pure water and stored at -80 ℃.

The nano-lipoplex formulation (P/G/L) was prepared with plasmid DNA, gemini surfactant, and lipid DOPE as previously described [6] with a nitrogen (cationic) to phosphate (anionic) charge ratio (N/P) at 10 for 16-3-16 and 16(Py)-S-2-S-16(Py) and at 2.5 for 16-7N(GK)-16. Briefly, to prepare 1 mL of the P/G/L for 16-3-16 and 16(Py)-S-2-S-16(Py), 38 µL of 3 mM gemini surfactants was added to 38 µL of 200 µg/mL plasmid DNA, gently mixed by pipetting up and down several times, and incubated for 15 min at room temperature. Subsequently, 924 µL of 1 mM DOPE solution was added to the binary mixture, gently mixed with a pipette and incubated for 15 min at room temperature to produce the ternary P/G/L system (nanoparticles). To prepare 1 mL of the P/G/L for 16-7N(GK)-16, 9.5 µL of 3 mM gemini surfactant was added to 38 µL of 200 µg/mL plasmid DNA, mixed and incubated for 15 min at room temperature, 952.5 µL of 1 mM DOPE solution was then added, mixed, and incubated to generate the nanoparticles.

3.3.3 *In vitro* transfection

PAM 212 cells were cultured in MEM media supplemented with 10% (v/v) FBS and 1% (v/v) antibiotic-antimycotic solution in 75 cm^2 tissue culture flasks in a humidified incubator at 37 ℃ at an atmosphere of 5% CO_2. Upon reaching 80% confluence, cells were washed with phosphate buffered saline (PBS, 8 mL), dissociated with a 5 min incubation in a versene (10x, 3 mL) and

trypsin (10x, 0.3 mL) mixture, and collected by centrifugation (250 *x g*, 5 min, 4 ℃). Twenty-four hours prior to transfection, three 96-well tissue culture plates were seeded with PAM 212 cells at a density of 2×10^4 cells/well. MEM was replaced with serum-free media 1 h prior to transfection. Cells were treated with 20 µL of the P/G/L nanoparticles per well and incubated for 5 h. The cells were then returned to the supplemented MEM for further incubation and the culture media was collected at 48 h for interferon-gamma (IFN-γ) measurement.

An enzyme-linked immunosorbent assay (ELISA) was carried out to measure secreted IFN-γ using flat bottom 96-well plates (Immulon 2, Greiner Labortechnik, Germany) as per the BD Pharmingen protocol. An IFN-γ standard curve was established using recombinant mouse IFN-γ (BD Biosciences, Missisauga, ON, Canada) to allow for the concentration of secreted IFN-γ in the cell media to be quantified. The experiments were conducted in three plates of quadruplicate wells.

3.3.4 3-(4, 5-dimethylthiazol-2-yl)-2, 5-diphenyltetrazolium bromide assay

A 3-(4, 5-dimethylthiazol-2-yl)-2, 5-diphenyltetrazolium bromide (MTT) assay was performed to determine the cytotoxicity of the gemini surfactants. PAM 212 cells were seeded in three 96-well cell culture plates at a density of 2×10^4 cells/well and treated with the P/G/L nanoparticles. Plates were incubated for 5 h at 37 °C with 5% CO_2 in a humidified incubator and then the cell media was switched to supplemented MEM media. After 48 h of incubation, the cell media was removed, and cell toxicity was evaluated by the determination of cell viability. Briefly, 100 µL of 0.5 mg/mL sterile MTT (Invitrogen, USA) in the supplemented media was added to each well and the plates were incubated for 3 h at 37 °C. The media was then removed and 200 µL of dimethyl sulfoxide (DMSO) (spectroscopy grade, Sigma-Aldrich, ON, Canada) was added to each well to dissolve the formed purple formazan crystal. Subsequently, the plates were incubated at 37 °C for 10 min.

Absorbance was measured at 550 nm using a microplate reader (Bio-Tek® Microplate Synergy, HT, VT, USA). The experiments were conducted in three plates of quadruplicate wells, and the cytotoxicity of gemini surfactants reflects cell viability, expressed as a percentage of non-transfected cells (control).

3.3.5 Size and zeta-potential measurements

Size and zeta-potential of the gemini surfactants-based nanoparticles were measured using a Zeta-sizer Nano ZS instrument (Malvern Instruments, Worcestershire, UK). The nanoparticles were prepared as described in section 3.3.2. Three measurements were conducted for each sample. The reported results are the mean of triplicate measurements ± standard deviation.

3.3.6 Cell treatment and sample collection

PAM 212 cells were cultured in 150 cm^2 flasks until they reached 80% confluence. Cells were then washed with PBS (25 mL), dissociated with versene (10x, 5 mL) and trypsin (10x, 0.5 mL), and collected by centrifugation (250 *x g*, 5 min, 4 ℃). Twenty-four hours prior to treatment, 8×10^6 cells were seeded in each petri dish (150 cm^2). Cells were switched to serum-free media 1 h prior to transfection. 500 µL of freshly prepared P/G/L nanoparticles were added to each dish in a drop-wise manner. Following a 5 h of incubation, the cells were returned to supplemented MEM media for subsequent incubation steps. Triplicates of treated cell samples and one control (untreated cell) were trypsinized and collected at 2 h, 5 h and 8 h. As the treatment duration for PAM 212 cells is 5 h, the collecting schedule was intended to include three time points, one prior to the completion of treatment (2 h), one at the completion of treatment (5 h) and one post the treatment (8 h). The collected cells were pelleted by centrifugation (250 *x g*, 5 min, 4 ℃), rinsed with PBS three times, re-suspended in 500 µL of ice-cold hypotonic homogenization buffer (10 mM NaCl, 1.5 mM

$MgCl_2$, 10 mM Tris-HCl [PH 7.5], and cOmplete™ protease inhibitor), and incubated on ice for 10 min.

3.3.7 Subcellular fractionation using differential centrifugation

Cells were gently homogenized using a motorized homogenizer on ice to break the plasma membrane and release subcellular organelles. The cell homogenates were then diluted with ice-cold hypertonic buffer (420 mM mannitol, 140 mM sucrose, 10 mM Tris-HCl [pH 7.5], and 2 mM EDTA [pH 7.5]) to a final volume of 1 mL and enriched nuclear, mitochondrial, plasma membrane, and cytosolic fractions were isolated by differential centrifugation using an established protocol [30], with slight modifications (Figure 3.2). Briefly, homogenates were first centrifuged at 1,000 *x g* for 10 min at 4 ˚C, and the S_1 supernatant was transferred to a clean ice-cooled microcentrifuge tube while the P_1 pellet was collected as the nuclear fraction (nuclei, unbroken cells, and cell debris). The S_1 supernatant was then subjected to further centrifugation at 15,000 *x g* for 15 min at 4 ˚C, yielding the S_2 supernatant and the P_2 pellet which contained the mitochondrial fraction. The S_2 supernatant was then centrifuged at 100,000 *x g* for 60 min at 4 ˚C. The resultant S_3 supernatant contained the cytosol and the P_3 pellet (the plasma membrane along with microsome, ER and Golgi). All collected fractions were kept on ice prior to being diluted to equal 950 µL volume with PBS and stored at -80 ℃. To verify the successful isolation and relative purity of enriched fractions, western blot analysis was performed. Relevant experimental details and results are shown in the supporting information (see 3.9 Appendix B).

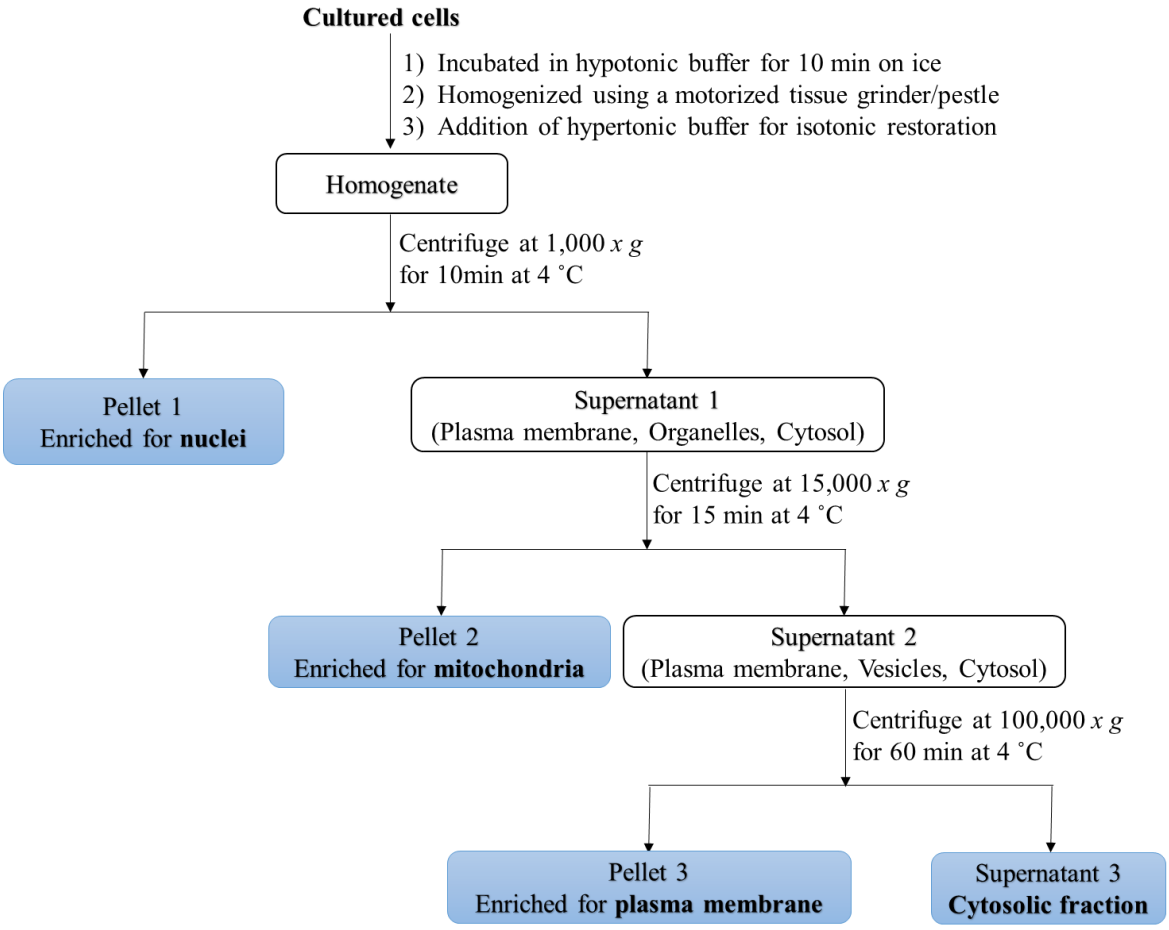

Figure 3.2. Schematic illustration of the homogenization and subcellular fractionation protocol. Differential centrifugation was used to isolate several subcellular fractions, including those enriched for nuclei, mitochondria, plasma membrane and cytosolic fractions.

3.3.8 Sample preparation

As we previously described [28], subcellular fractions (950 µL) were lysed and spiked with 50 µL of internal standard and sample extractions were conducted using the Bligh/Dyer method [31]. Briefly, 3.75 mL of methanol-chloroform (2:1, v/v) was added per 1 mL of sample, followed by the addition of 1.25 mL of chloroform and 1.25 mL of water. At each step, samples and the extraction solvent were vortexed thoroughly. The final mixture was centrifuged at 2,800 *x g* for 10 min at room temperature to separate the aqueous and organic phases. The bottom organic phase (80% portion) was collected and dried under a nitrogen gas stream, followed by reconstitution in 200 µL of methanol. Finally, 150 µL of methanol solution was transferred into an HPLC vial for analysis.

3.3.9 FIA-MS/MS analysis

The FIA-MS/MS analysis was performed on a quadrupole-linear ion trap (4000 QTRAP®) mass spectrometer with an electrospray ionization (ESI) source (AB Sciex, Concord, ON, Canada), coupled with an Agilent 1200 series HPLC (a quaternary pump, degasser, and auto sampler) (Agilent Technologies, Mississauga, ON, Canada). As recently described [28], 3 µL of sample was injected into the ESI source at a flow rate of 0.5 mL/min with an acetonitrile-water mixture (98:2, v/v) containing 0.1% formic acid as the mobile phase. The instrument source temperature was set at 600 ℃ and the ion spray voltage was at 5,500 V. Nitrogen gas was used for curtain gas at 30, nebulizer gas at 55, and heater gas at 50. Multiple reaction monitoring (MRM) in positive ion mode was used to monitor all analytes and internal standards. The monitored MRM transitions were as follows: 16-3-16 $[M]^{2+}$ *m/z* 290.3→355.4, 86.1; 16-3-16-D_{66} $[M]^{2+}$ *m/z* 323.5→388.6; 16(Py)-S-2-S-(Py)16 $[M]^{2+}$ *m/z* 349.3→396.3, 203.1; 16(Py)-S-2-S-(Py)16-D_{10} $[M]^{2+}$ *m/z* 354.3→401.3; and 16-7N(GK)-16 $[M]^{2+}$ *m/z* 411.4→276.8, 268.3; 16-7N(GK)-16-D_4 $[M]^{2+}$ *m/z* 413.4→278.8

(Figures 3.1 and 3.S1). The compound-dependent parameters for analytes and internal standards were optimized as previously described [28]. A stable isotope dilution standard curve and three quality control samples (low, medium, and high) were run along with the samples in each batch. The data acquisition time per sample was 2 min. Data acquisition and analysis was performed using AB Sciex Analyst software (version 1.6.0).

3.3.10 Ethidium bromide dye exclusion assay

The plasmid DNA (200 µg/mL) was complexed with the three gemini surfactants at various charge ratios in the presence or absence of DOPE on 96-well plates. Ethidium bromide was added to all samples at a final concentration of 1 µg/mL. The samples were then incubated for 10 min at room temperature. After that, fluorescence excitation was carried out at 530 nm and emission was measured at 590 nm using a microplate reader (Biotek Microplate Synergy HT, VT, USA). The relative fluorescence of the P/G/L and P/G complexes was expressed as a percentage of fluorescence of the pure plasmid DNA solution. Measurements were conducted in triplicate.

3.3.11 Langmuir studies

Langmuir trough was used to measure the monolayer surface area of the gemini surfactant head group. Surface pressure-mean molecular area isotherms were obtained using a KSV 2,000 Langmuir trough instrument (KSV Instruments Ltd, Helsinki, Finland). A stock solution of each gemini surfactant was prepared at 1 mM in chloroform and 40 µL of each stock solution was added dropwise on the sub-phase using a Hamilton syringe. The monolayer was left for a minimum of 10 min to allow chloroform to evaporate, a constant rate compression of 20 mm/min was then applied on the monolayer molecules until collapse of the monolayer lipid. The ultra-pure water (Millipore, resistivity 18 MΩ· cm) was used as a sub-phase in the trough and the sub-phase temperature was

set at 22 °C. Triplicate measurements were collected for each gemini surfactant and data collection was performed using the KSV software (KSV Instruments Ltd, Helsinki, Finland).

3.3.12 Statistical analysis

Statistical analyses were performed by one-way analysis of variance (ANOVA) and Tukey's multiple comparison tests using SPSS 25 software. Significant difference was established at the $p < 0.05$ level of significance. Results are expressed as the mean of triplicates ± standard deviation.

3.4 Results and Discussion

3.4.1 *In vitro* transfection activity

Since these gemini surfactant nanoparticles have shown great promise in treating the localized scleroderma, a rare skin disease [6, 20], we are currently tuning the gemini surfactant nanoparticles to develop an effective, non-invasive topical gene delivery system for the treatment of the fibrotic skin conditions. As such, the epidermal keratinocyte cells, PAM 212, was used as the cell model in this study. To evaluate the efficiency of the gemini surfactants to mediate transfection in PAM 212 cells, the amount of secreted IFN-γ was quantified 48 h post-transfection. As determined in previous work [6, 16], the optimal N/P to obtain the best transfection efficiency for 16-3-16 is 10 and for 16-7N(GK)-16 is 2.5. We also determined that the optimal N/P for 16(Py)-S-2-S-16(Py) is 10 based on the assessment of various N/P ratios at 0.5, 1, 2.5, 5, 10, and 20 for transfection (data not shown). For the best comparison of transfection capability as well as for proper toxicity assessment, the *in vitro* transfection study was conducted at the optimal N/P of each gemini surfactant, as it reflects the real conditions in which these compounds are used for *in vitro* gene delivery. At the optimal N/P of 10, the P/G/L of 16(Py)-S-2-S-(Py)16 resulted in a significantly

lower level of IFN-γ (1.19 ± 0.08 ng/2x10^4 cells) compared with that of 16-3-16 (2.77 ± 0.13 ng/2x10^4 cells) (p <0.05) (Figure 3.3). In comparison, the P/G/L of 16-7N(GK)-16 at its optimal N/P of 2.5 yielded a IFN-γ level (3.76 ± 0.27 ng/2x10^4 cells) [21] that is significantly higher than that of 16-3-16 (p<0.05). In summary, the relative transfection efficiency of the three gemini surfactant nanoparticles was determined, with 16-7N(GK)-16 being the most effective and 16(Py)-S-2-S-(Py)16 the least effective.

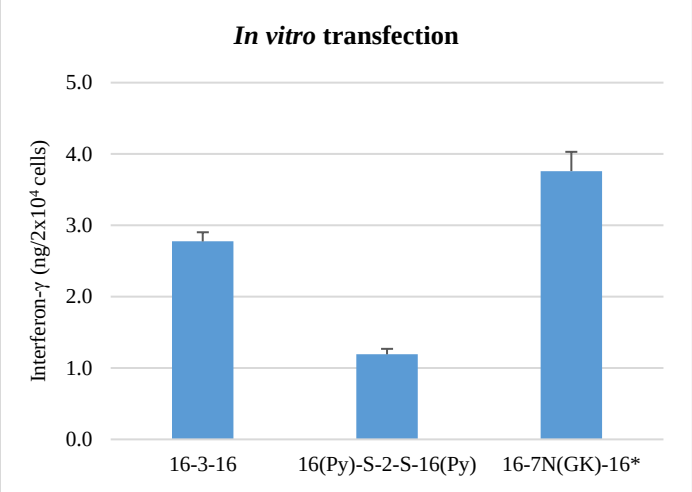

Figure 3.3. Transfection efficiencies of the P/G/Ls of 16-3-16, 16(Py)-S-2-S-(Py)16, and 16-7N(GK)-16 in PAM 212 cells. *16-7N(GK)-16 transfection was recently reported by our group, extracted from ref. [21].

3.4.2 Cytotoxicity

In the present study, the cytotoxicity of the gemini surfactants 16-3-16 and 16(Py)-S-2-S-(Py)16 was evaluated in PAM 212 cells. It was observed that cell viability was significantly higher upon treatment with the P/G/L of 16-3-16 (76%) compared with that of 16(Py)-S-2-S-(Py)16 (61%, p <0.05) (Figure 3.4), indicating that the former has significantly lower cytotoxicity than the latter for the tested PAM 212 cell line. However, 16-7N(GK)-16 was previously reported to have an even

lower toxicity (89% cell viability) than 16-3-16 [21]. Hence, 16-7N(GK)-16 possesses the lowest cytotoxicity and 16(Py)-S-2-S-(Py)16 has the highest cytotoxicity among the three gemini surfactants.

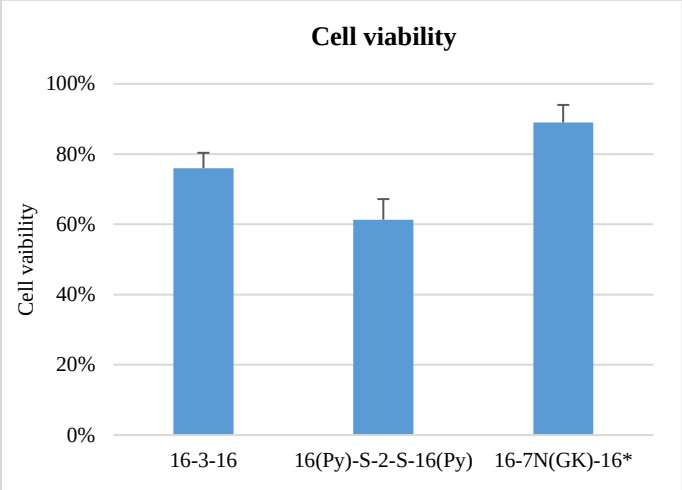

Figure 3.4. Cytotoxicity of the P/G/L of 16-3-16, 16(Py)-S-2-S-(Py)16, and 16-7N(GK)-16 in PAM 212 cells. *16-7N(GK)-16 cytotoxicity was recently reported by our group, extracted from ref. [16, 21].

3.4.3 Determination of size and zeta-potential

Size and zeta potential of the P/G/L nanoparticles were measured as they are important characteristics of the delivery systems, which can have an influence on their stability, cellular uptake, and cytotoxicity [32, 33]. At the optimal N/P of 10, the P/G/L of 16-3-16 displayed a size of 131.9 ± 1.48 nm and positive zeta potential at 17.3 ± 1.38 mV, and the P/G/L of 16(Py)-S-2-S-16 (Py)) showed a comparable size of 123.1 ± 0.76 nm and zeta potential at 23.3 ± 0.32 mV. Compared with the P/G/Ls of 16-3-16 and 16(Py)-S-2-S-16(Py), the P/G/L of 16-7N(GK)-16 at its optimal N/P of 2.5 showed a similar zeta potential at 24 ± 2.00 mV but a bit smaller size of 80 ± 1.00 nm as reported in previous work [21]. Endocytosis has shown to be the main mechanism for the internalization of gemini surfactant-based nanoparticles [34, 35]. In particular, clathrin and

caeolae-mediated endocytosis are most common pathways for the cellular uptake of gemini surfactant nanoparticles. In fact, the internalization of amino acid-substituted gemini surfactant nanoparticles involves equally both clathrin and caeolae-mediated endocytosis [11]. While particles with smaller sizes of 60-80 nm typically undergo caveolae-mediated endocytosis for their internalization, particles with relatively larger size in the range of 120-200 nm often enter the cells via clathrin-mediated endocytosis [36, 37]. As such, all three gemini surfactant nanoparticles have the particle sizes that are appropriate for their cellular uptake. However, the smaller size of the P/G/L of 16-7N(GK)-16 could be a contributing factor for its high efficiency in gene transfection, as nanoparticles with small size at 70 nm have been reported to display significantly higher transfection efficiency than large-sized nanoparticles at 200 nm [32].

3.4.4 Cellular uptake and distribution of gemini surfactants

To determine the cellular uptake and distribution of the gemini surfactants in PAM 212 cells, fractions enriched for nuclei, mitochondria, plasma membrane, and cytosol were isolated by differential centrifugation, extracted, and analyzed by the validated FIA-MS/MS method [28]. Differential centrifugation is an isolation technique that uses stepwise increases in centrifugal force to precipitate subcellular components based on their distinct density, size, and shape [38]. During the FIA-MS/MS analysis, the standard curve achieved a less than 15% deviation of the nominal value for each standard point other than the lower limit of quantification (LLOQ), which was 20%, and the quality control (QC) samples were accepted with a less than 15% deviation of the nominal values, as per FDA guidelines [39].

Cellular uptake of the three gemini surfactants, expressed as percentage of dose, was observed to increase rapidly over the course of a 5 h treatment in PAM 212 cells, reaching a maximum of 17.0%

for 16-7N(GK)-16, 1.4% for 16-3-6, and 3.6% for 16(Py)-S-2-S-16(Py), followed by a gradual depletion after the removal of the nanoparticles from the media (Figure 3.5a). A significantly higher cellular uptake was observed for 16-7N(GK)-16 compared with 16-3-16 and 16(Py)-S-2-S-16(Py) (Figure 3.5a) (p <0.05). It should be noted that the optimal N/P for 16-3-16 and 16(Py)-S-2-S-16(Py) is 10, whereas for the 16-7N(GK)-16 is 2.5 as previously determined in our lab [6, 16], and all transfections were conducted with equal amounts of plasmid DNA in the P/G/L nanoparticles. Therefore, the higher cellular uptake of 16-7N(GK)-16 implies that there is a higher transfection efficiency with this gemini surfactant relative to 16-3-16 and 16(Py)-S-2-S-16(Py) and offers a mechanistic explanation as to why PAM 212 cells exposed to 16-7N(GK)-16 secrete greater amounts of IFN-γ (Figure 3.3).

While the gemini surfactant 16(Py)-S-2-S-16(Py) accumulated more significantly than 16-3-16 in PAM 212 after a 5 h treatment (p <0.05), less IFN-γ was produced, arguing that transfection efficiency is lower with 16(Py)-S-2-S-16(Py) than 16-3-16. The relatively higher toxicity of 16 (Py)-S-2-S-16(Py) (Figure 3.4) might have contributed to its reduced gene transfection efficiency as it caused greater cell death, resulting in a smaller number of live cells available for gene transfection.

In terms of subcellular distribution, normalized for each surfactant to total cellular uptake, the gemini surfactants 16-3-16 and 16(Py)-S-2-S-16(Py) exhibited comparable partitioning with significant accumulation in the nucleus, followed by mitochondria, cytosol, and plasma membrane (Figures 3.5b and c) (p <0.05). In contrast, the distribution of 16-7N(GK)-16 was relatively even across the four subcellular compartments (Figure 3.5d). No significant difference was observed among the three gemini surfactants with respect to their relative distribution in the mitochondrial and cytosolic fractions. However, accumulation in the nucleus was the highest for 16(Py)-S-2-S-

16(Py) (50.3%), followed by 16-3-16 (41.8%) and then 16-7N(GK)-16 (33.4%) (p<0.05) at the 5 h duration of treatment (Figure 3.5e), which correlates with the relative toxicity observed for the three gemini surfactants (Pearson's correlation r = 0.9993). Even at the 2 h and 8 h time points post treatment, 16-7N(GK)-16 still displayed significantly lower accumulation in the nucleus relative to 16(Py)-S-2-S-16(Py) and 16-3-16 (p <0.05). Although there is a difference in the accumulation among the three gemini surfactants at 2 h time point, this accumulation might not be informative as the cellular uptake are still in rapid progress at this stage. Surprisingly, 16(Py)-S-2-S-16(Py) showed a similar distribution percentage in the nucleus as 16-3-16 at the 8 h time point; however, the distribution quantity (in terms of absolute amount) of 16-3-16 is significantly less compared with that of 16(Py)-S-2-S-16(Py) (Table 3.S1 in supporting information) as 16-3-16 has much lower cellular uptake in comparison with 16(Py)-S-2-S-16(Py) (Figure 3.5a), resulting in less toxicity of 16-3-16.

Nuclear accumulation may result from either the entry of the gemini surfactants into the compartment or their association with the nuclear envelope, as it has been reported that lipoplexes can fuse with the membrane and release their DNA cargo into the nucleus [40]. However, it is currently not known that the entry of gemini surfactants into the nucleus is in the form of lipid molecules or lipoplexes. Although the entry of lipoplexes is unlikely due to the small pore size of nuclear membrane, it can take place during cell mitosis. As such, it could be in either form or both.

The nucleus has crucial functions within a cell, ensuring the faithful storage and expression of genetic material essential to regulating cellular metabolism and growth [41]. Therefore, nuclear association or accumulation of gemini surfactants could impact outer membrane integrity and normal organelle function. As such, the higher cellular uptake and preferential accumulation of 16(Py)-S-2-S-16(Py) within the nucleus could provide a basis for its higher toxicity relative to 16-

3-16 and 16-7N(GK)-16. Thus, to date, our findings provide the only quantitative distinction in the subcellular profiles of these three gemini surfactants, without the use of a florescent tag. The results may offer the first mechanistic insight into the various efficiencies and toxicities observed for the three promising gene delivery agents.

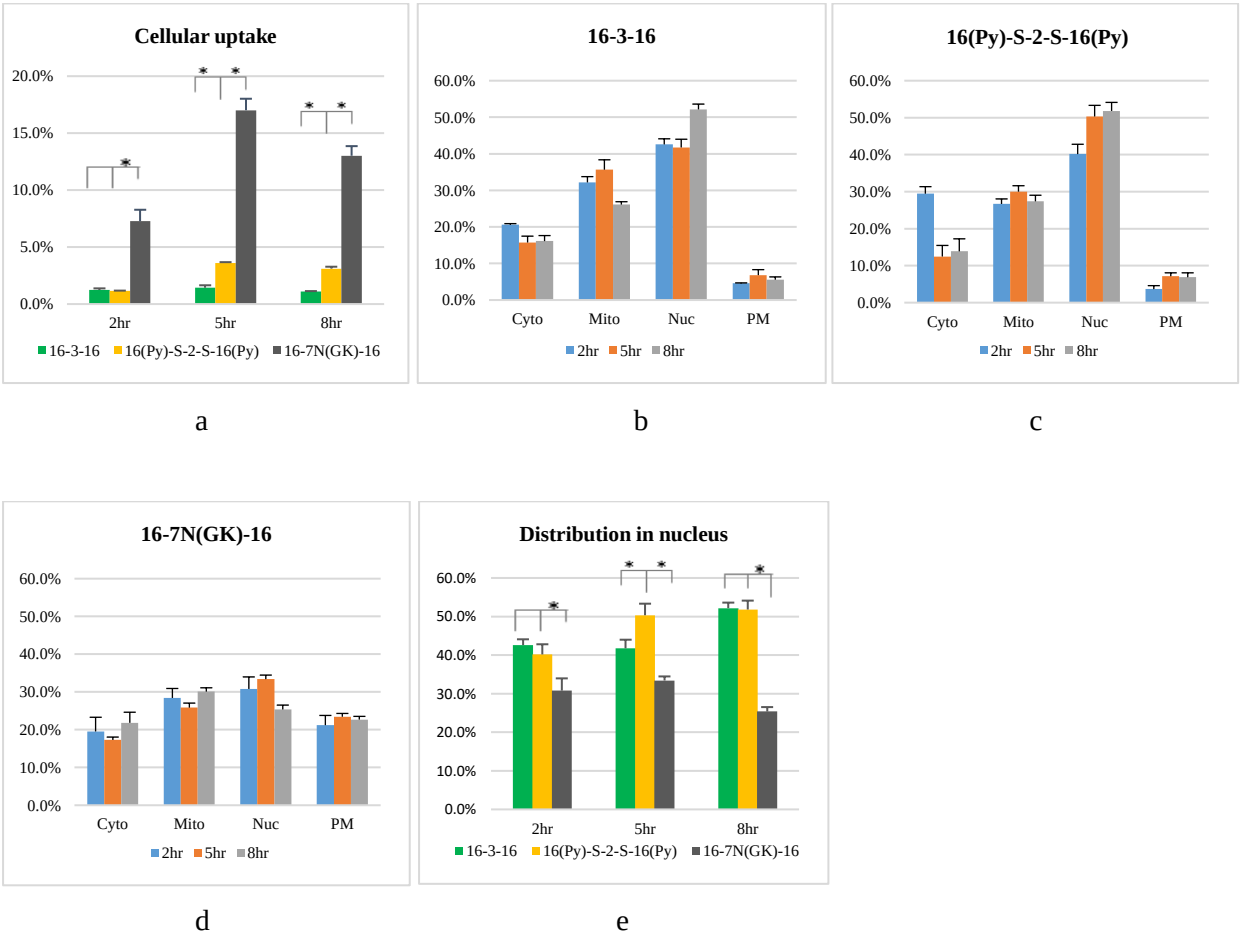

Figure 3.5. The cellular uptake and distribution of gemini surfactants in PAM 212 cells. a) Cellular uptake, normalized based on the dose, of three gemini surfactants; b-d) Subcellular distribution, normalized based on the total cellular uptake, of 16-3-16, 16(Py)-S-2-S-(Py)16, and 16-7N(GK)-16; and e) Distribution percentage in nucleus. (Cyto-cytosol, Mito-mitochondria, Nuc-nucleus and PM-plasma membrane). * indicates p <0.05

In addition, it was observed that 16-7N(GK)-16 has a significantly higher distribution within the plasma membrane compared with 16(Py)-S-2-S-16(Py) and 16-3-16 (Figures 3.5b-d) (p <0.05).

However, this did not result in higher toxicity, as evidenced by the viability of PAM 212 cells treated with the 16-7N(GK)-16 nanoparticles (Figure 3.4). In fact, 16-7N(GK)-16 displayed the lowest cytotoxicity among the three gemini surfactants in gene transfection. Stefanutti *et al.* [42] reported that the internalization of lipoplexes of DMPC and a cationic gemini surfactant traversing cell membrane did not cause a significant biological damage to the cells. In addition, Marjan *et al*. [43] reported that although nanoparticle treatment disturbed membrane integrity, the cells were still alive and metabolically active during the transfection process. Therefore, accumulation in the plasma membrane does not appear to cause toxicity.

3.4.5 Ethidium bromide dye exclusion assay

To explore why unique gemini surfactants differentially accumulate within distinct subcellular compartments, an ethidium bromide dye exclusion assay was conducted to investigate their DNA binding and compaction capabilities. Gemini surfactants bind and compact plasmid DNA via electrostatic interactions to form nanosized particles, which hinder the penetration of ethidium bromide into the complexes. As a result, fluorescence is quenched due to the lack of intercalation between ethidium bromide and the base-pairs of DNA. The stronger the compaction of DNA by gemini surfactants, the more intense the fluorescence quenching in the complex. As shown in Figure 3.6, the lowest fluorescence emission was observed at the N/P of 5, with 13.0% for 16-7N(GK)-16, 8.1% for 16-3-16, and 8.9% for 16(Py)-S-2-S-16(Py) in the absence of the helper lipid DOPE. The data indicate that 16-7N(GK)-16 has a significantly lower DNA compaction capability compared with the other two compounds (p <0.05). In the presence of a helper lipid, the fluorescence values were increased to 45.7% for 16-7N(GK)-16, 23.6% for 16-3-16, and 28.3% for 16(Py)-S-2-S-16(Py), again showing 16-7N(GK)-16 is significantly less efficient at binding and compacting DNA relative to 16-3-16 and 16 (Py)-S-2-S-16(Py) (p <0.05).

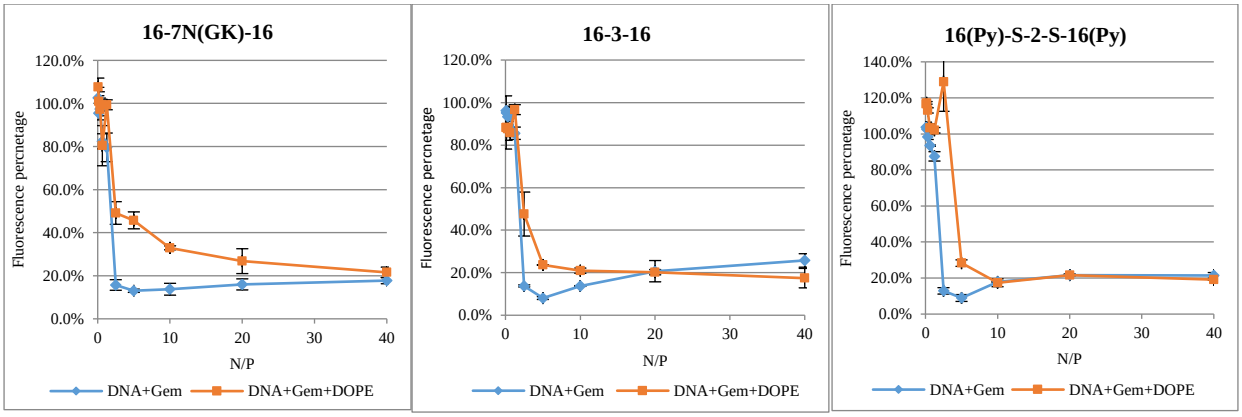

Figure 3.6. Ethidium bromide dye exclusion assay to evaluate the DNA binding and compaction capability of the gemini surfactants. A lower fluorescence indicates stronger DNA binding and compaction.

However, the relatively lower DNA binding capability of 16-7N(GK)-16 does not undermine its gene transfection capability, as evidenced in the transfection study, since gene transfection requires not only effective compaction of DNA for their protection and cellular entry, but also efficient release from the complex into the nucleus for transgene expression . It is believed that the presence of glycyl-lysine moiety in the spacer offers conformational flexibility of the structure, which bestows 16-7N(GK)-16 with softened DNA binding properties [9, 44]. Although 16-7N(GK)-16 has a relatively weaker DNA binding ability than the other two compounds as indicated by its higher fluorescence emission of 13% compared with 8.1% for 16-3-16 and 8.9% for 16(Py)-S-2-S-16(Py), such binding provides the DNA with much needed protection against enzymatic degradation while also facilitating its intracellular release, thereby enhancing overall transfection efficiency [9, 44]. This special binding capability may be caused by the overall interaction of multiple bonding forces, including hydrogen bonding and electrostatic interactions [45]. In addition, the various amine groups in the amino acids can allow for additional buffering capacity, which helps in the disruption of the endosomal membrane for the intracellular release of DNA and their nuclear transport [9].

Due to the weaker DNA binding of 16-7N(GK)-16, the encapsulated DNA could be released more efficiently from the lipoplexes into the cytoplasm to translocate into the nucleus for gene expression. As such, this led to a lesser accumulation of 16-7N(GK)-16 in the nucleus. Conversely, the lipoplexes formed with 16-3-16 and 16(Py)-S-2-S-16(Py) release the DNA less efficiently and potentially at a later stage due to their stronger association with DNA (Figure 3.6), which could be one of the reasons for their lower transfection efficiency relative to 16-7N(GK)-16, as it has been reported that slow vector unpacking is linked to a decreased transfection efficiency [46, 47]. In this case, the lipoplexes rather than free DNAs are more likely to be translocated into the nucleus. Consistent with this idea, we observed elevated accumulation of both 16-3-16 and 16(Py)-S-2-S-16(Py) in the nucleus (Figures 3.5b and c).

3.4.6 Molecular packing parameter

In addition to their DNA compaction and binding property, the molecular shape of gemini surfactants also has a great impact on the performance of the gene delivery system [16, 48]. Therefore, to further understand the behavioral differences among the three gemini surfactants, the structural differences in the formed aggregates were evaluated using the molecular packing parameter (*P*) [48]. The *P* was estimated based on the structures of gemini surfactants and the behavior of gemini surfactants at the air-water interface [49], and is defined as:

$$P = v/a_o l$$

Where v is the volume of the hydrophobic tails, l is the length of the hydrocarbon tails, and a_o is the head group area per molecule in aqueous solution. The v and l are the geometrical properties of gemini surfactants, which can be calculated from their chemical structures [50, 51]. The a_o is an

equilibrium parameter dependent upon both the attractive forces of the hydrophobic chains and the repulsive forces of the head groups, which can be determined by the Langmuir studies. A specific *P* value can be linked to a particular geometrical shape [49]. Spherical micelles typically have a *P* value of less than 0.33, cylindrical micelles possess a *P* value between 0.33 and 0.50, and flexible bilayers (vesicles) usually have a *P* value between 0.5 and 1.0 [49].

As the three gemini surfactants have the same *l* and *v* of hydrophobic tails, the a_o is the main determinant of the *P* value. The *l* was calculated to be 21.74 Å using the Avogadro software [52], and the *v* was calculated to be 918 $Å^3$ with the Gaussian 09 software (revision B. 01) [53] (Table 3.1). Based on the Langmuir studies, the gemini surfactant 16-7N(GK)-16 showed the smallest a_0 of 84 $Å^2$ and thus the largest *P* of 0.51, indicating the aggregates formed by 16-7N(GK)-16 are typically flexible bilayers. The gemini surfactant 16-3-16 displayed an a_0 of 116 $Å^2$ and a *P* value of 0.36, which suggested the formation of aggregates shaped as cylindrical micelles (Table 3.1). This is in agreement with the literature [51, 54] reporting that aggregates formed by *m-3-m* gemini surfactants tend to form cylindrical micelles. Similarly, the gemini surfactant 16(Py)-S-2-S-16(Py) had an a_0 of 110 $Å^2$ and a *P* value of 0.38, which argues it too forms cylindrical micelles in aqueous solution.

Table 3.1. The molecular packing parameter (*p*) and the shapes of aggregates of the gemini surfactants.

Gemini surfactant	a_0($Å^2$)	*l*(Å)	*v*($Å^3$)	*P*	Shape of aggregate
16-3-16	116	21.74	918	0.36	Cylindrical micelle
16(Py)-S-2-S-16(Py)	110	21.74	918	0.38	Cylindrical micelle
16-7N(GK)-16	84	21.74	918	0.51	Flexible bilayer, vesicle

Although 16-3-16 and 16(Py)-S-2-S-16(Py) have unique structural head groups, their areas are comparable and enable them to have similar packing parameters and a preference towards forming cylindrical micelle aggregates (Table 3.1). The same aggregates would allow for a similar internalization process of the two gemini surfactant nanoparticles for gene delivery, which explained the similar trends observed for their uptake and subcellular distribution (Figures 3.5b and c). Conversely, the substitution of a di-peptide in the spacer region provides 16-7N(GK)-16 with conformational flexibility [9]. It has a much smaller head group area and thus a flexible bilayer structure (Table 3.1), which allows for the formation of the inverted hexagonal phase of the lipoplex [48]. Such a conformation facilitates not only the destabilization of endosomal membrane to promote the cytoplasmic release of DNA but also the dissociation of DNA from the lipoplexes, thus resulting in enhanced efficiency in gene transfection [55].

3.5 Conclusions

The cellular uptake and distribution of the gemini surfactants 16-3-16, 16(Py)-S-2-S-16(Py), and 16-7N(GK)-16 as gene delivery agents in PAM 212 cells were evaluated by analyzing subcellular fractions using a validated FIA-MS/MS method. The three gemini surfactants varied with respect to their uptake and subcellular distribution profiles, with 16-7N(GK)-16 exhibiting a greater uptake and a higher transfection efficiency. Preferential nuclear accumulation of 16(Py)-S-2-S-16(Py) may explain its relatively higher toxicity. DNA binding properties and molecular packing parameters provided explanations to the different cellular behaviors of the gemini surfactants. Overall, the results presented herein demonstrate the general applicability of the combined differential centrifugation and MS approach for assessing the uptake and subcellular distribution of gemini surfactants and emphasize that it is superior to a fluorescence-labelling method as it does

not require any structural modifications. We are currently investigating the metabolite formation of the three structures, which may provide additional insight into their relative efficiencies and toxicities. In the future, it may be worthwhile isolating more cellular organelles, such as the endosomes and lysosomes to better understand the cellular trafficking of lipid-based gene delivery agents.

3.6 Acknowledgements

The authors would like to thank Drs. Jackson M. Chitanda and McDonald Donkuru for the synthesis of gemini surfactants and standards, and Ms. Deborah Michael for her technical assistance on the operation of 4000 QTRAP® mass spectrometry system. We also thank Dr. Waleed Mohammed-Saeid for the training in the cell transfection and purification of plasmid DNA. Drs. George Katselis and David Schneberger are greatly appreciated for the training in western blotting assay. We acknowledge Dr. Matthew F. Paige's lab for collecting the data on the Langmuir trough system. Dr. McDonald Donkuru is acknowledged for his initial help and discussion regarding the subcellular fractionation. A postgraduate scholarship for Wei Jin is provided by the Natural Sciences and Engineering Research Council of Canada (NSERC). Funding to purchase the 4000 QTRAP® instrument was obtained through the Canada Foundation for Innovation-Leaders Opportunity Fund. The research was supported by a NSERC discovery grant.

3.7 References

1. Menger, F.M. and J.S. Keiper, *Gemini surfactants.* Angewandte Chemie International Edition, 2000. **39**(11): p. 1906-1920.
2. Wettig, S.D., R.E. Verrall, and M. Foldvari, *Gemini surfactants: a new family of building blocks for non-viral gene delivery systems.* Current gene therapy, 2008. **8**(1): p. 9-23.
3. Donkuru, M., et al., *Advancing nonviral gene delivery: lipid-and surfactant-based nanoparticle design strategies.* Nanomedicine, 2010. **5**(7): p. 1103-1127.
4. Bombelli, C., et al., *Gemini surfactant based carriers in gene and drug delivery.* Current medicinal chemistry, 2009. **16**(2): p. 171-183.
5. Makhlouf, A., I. Hajdu, and I. Badea, *Gemini surfactant-based systems for drug and gene delivery*, in *Organic Materials as Smart Nanocarriers for Drug Delivery*. 2018, Elsevier. p. 561-600.
6. Badea, I., et al., *In vivo cutaneous interferon-gamma gene delivery using novel dicationic (gemini) surfactant-plasmid complexes.* J Gene Med, 2005. **7**(9): p. 1200-1214.
7. Grueso, E., et al., *DNA conformational changes induced by cationic gemini surfactants: the key to switching DNA compact structures into elongated forms.* RSC Advances, 2015. **5**(37): p. 29433-29446.
8. Van Der Woude, I., et al., *Novel pyridinium surfactants for efficient, nontoxic in vitro gene delivery.* Proceedings of the National Academy of Sciences, 1997. **94**(4): p. 1160-1165.
9. Singh, J., et al., *Amino acid-substituted gemini surfactant-based nanoparticles as safe and versatile gene delivery agents.* Current drug delivery, 2011. **8**(3): p. 299-306.
10. Mohammed-Saeid, W., et al., *Development of lyophilized gemini surfactant-based gene delivery systems: influence of lyophilization on the structure, activity and stability of the lipoplexes.* Journal of Pharmacy & Pharmaceutical Sciences, 2012. **15**(4): p. 548-567.
11. Singh, J., et al., *Evaluation of cellular uptake and intracellular trafficking as determining factors of gene expression for amino acid-substituted gemini surfactant-based DNA nanoparticles.* J Nanobiotechnology, 2012. **10**(7): p. 1-14.
12. Ramamoorth, M. and A. Narvekar, *Non viral vectors in gene therapy-an overview.* Journal of clinical and diagnostic research, 2015. **9**(1): p. GE01-06.
13. Al-Dosari, M.S. and X. Gao, *Nonviral gene delivery: principle, limitations, and recent progress.* The AAPS journal, 2009. **11**(4): p. 671-681.

14. Savić, R., et al., *Micellar nanocontainers distribute to defined cytoplasmic organelles.* Science, 2003. **300**(5619): p. 615-618.
15. Al-Dulaymi, M., et al., *The development of simple flow injection analysis tandem mass spectrometric methods for the cutaneous determination of peptide-modified cationic gemini surfactants used as gene delivery vectors.* Journal of pharmaceutical and biomedical analysis, 2018. **159**: p. 536-547.
16. Al-Dulaymi, M.A., et al., *Di-Peptide-Modified Gemini Surfactants as Gene Delivery Vectors: Exploring the Role of the Alkyl Tail in Their Physicochemical Behavior and Biological Activity.* The AAPS journal, 2016. **18**(5): p. 1168-1181.
17. Singh, J., et al., *Development of amino acid substituted gemini surfactant-based mucoadhesive gene delivery systems for potential use as noninvasive vaginal genetic vaccination.* Nanomedicine, 2015. **10**(3): p. 405-417.
18. Badea, I., et al., *Effect of topical interferon-γ gene therapy using gemini nanoparticles on pathophysiological markers of cutaneous scleroderma in Tsk/+ mice.* Gene therapy, 2012. **19**(10): p. 978-987.
19. Bhadani, A. and S. Singh, *Novel gemini pyridinium surfactants: synthesis and study of their surface activity, DNA binding, and cytotoxicity.* Langmuir, 2009. **25**(19): p. 11703-11712.
20. Badea, I., et al., *Topical non-invasive gene delivery using gemini nanoparticles in interferon-gamma-deficient mice.* Eur J Pharm Biopharm, 2007. **65**(3): p. 414-422.
21. Al-Dulaymi, M., et al., *Molecular Engineering as an Approach To Modulate Gene Delivery Efficiency of Peptide-Modified Gemini Surfactants.* Bioconjugate chemistry, 2018. **29**(10): p. 3293-3308.
22. Donkuru, M., et al., *Hydrophilic interaction liquid chromatography-tandem mass spectrometry quantitative method for the cellular analysis of varying structures of gemini surfactants designed as nanomaterial drug carriers.* Journal of Chromatography A, 2016. **1446**: p. 114-124.
23. Wang, C., et al., *Investigation of complexes formed by interaction of cationic gemini surfactants with deoxyribonucleic acid.* Physical Chemistry Chemical Physics, 2007. **9**(13): p. 1616-1628.

24. Wettig, S.D., et al., *Thermodynamic investigation of the binding of dissymmetric pyrenyl-gemini surfactants to DNA.* Physical Chemistry Chemical Physics, 2010. **12**(18): p. 4821-4826.
25. Gemeinhart, R.A., D. Luo, and W.M. Saltzman, *Cellular fate of a modular DNA delivery system mediated by silica nanoparticles.* Biotechnology progress, 2005. **21**(2): p. 532-537.
26. Buse, J., et al., *A general liquid chromatography tandem mass spectrometry method for the quantitative determination of diquaternary ammonium gemini surfactant drug delivery agents in mouse keratinocytes' cellular lysate.* Journal of Chromatography A, 2013. **1294**: p. 98-105.
27. Donkuru, M., et al., *Hydrophilic interaction liquid chromatography–tandem mass spectrometry quantitative method for the cellular analysis of varying structures of gemini surfactants designed as nanomaterial drug carriers.* Journal of Chromatography A, 2016. **1446**: p. 114-124.
28. Jin, W., et al., *The determination of gemini surfactants used as gene delivery agents in cellular matrix using validated tandem mass spectrometric method.* Journal of pharmaceutical and biomedical analysis, 2019. **164**: p. 164-172.
29. Donkuru, M., et al., *Designing pH-sensitive gemini nanoparticles for non-viral gene delivery into keratinocytes.* Journal of Materials Chemistry, 2012. **22**(13): p. 6232-6244.
30. Rangel, R., et al., *Targeting mammalian organelles with internalizing phage (iPhage) libraries.* Nature protocols, 2013. **8**(10): p. 1916-1939.
31. Bligh, E.G. and W.J. Dyer, *A rapid method of total lipid extraction and purification.* Canadian journal of biochemistry and physiology, 1959. **37**(8): p. 911-917.
32. Prabha, S., et al., *Size-dependency of nanoparticle-mediated gene transfection: studies with fractionated nanoparticles.* International journal of pharmaceutics, 2002. **244**(1): p. 105-115.
33. Fröhlich, E., *The role of surface charge in cellular uptake and cytotoxicity of medical nanoparticles.* International journal of nanomedicine, 2012. **7**: p. 5577-5591.
34. Cardoso, A.M., et al., *Gemini surfactants mediate efficient mitochondrial gene delivery and expression.* Molecular pharmaceutics, 2015. **12**(3): p. 716-730.
35. Michel, D., et al., *Design and evaluation of cyclodextrin-based delivery systems to incorporate poorly soluble curcumin analogs for the treatment of melanoma.* European Journal of Pharmaceutics and Biopharmaceutics, 2012. **81**(3): p. 548-556.

36. El-Sayed, A. and H. Harashima, *Endocytosis of gene delivery vectors: from clathrin-dependent to lipid raft-mediated endocytosis.* Molecular Therapy, 2013. **21**(6): p. 1118-1130.
37. Conner, S.D. and S.L. Schmid, *Regulated portals of entry into the cell.* Nature, 2003. **422**(6927): p. 37-44.
38. Graham, J.M. and D. Rickwood, *Subcellular fractionation: a practical approach*. Vol. 173. 1997, New York, United States: Oxford University Press Inc.
39. FDA, *Guidance for Industry: Bioanalytical Method Validation*. US, Department of Health and Human Services, Food and Drug Administration, Center for Drug Evaluation and Research (CDER), Center for Veterinary Medicine (CVM). 2013.
40. Kamiya, H., et al., *Visualization of intracellular trafficking of exogenous DNA delivered by cationic liposomes.* Biochemical and biophysical research communications, 2002. **298**(4): p. 591-597.
41. Alberts, B., et al., *Essential cell biology*. 2013: Garland Science.
42. Stefanutti, E., et al., *Cationic liposomes formulated with DMPC and a gemini surfactant traverse the cell membrane without causing a significant bio-damage.* Biochimica et Biophysica Acta (BBA)-Biomembranes, 2014. **1838**(10): p. 2646-2655.
43. Gharagozloo, M., et al., *A flow cytometric approach to study the mechanism of gene delivery to cells by gemini-lipid nanoparticles: an implication for cell membrane nanoporation.* Journal of nanobiotechnology, 2015. **13**(62): p. 1-13.
44. Yang, P., et al., *Enhanced gene expression in epithelial cells transfected with amino acid-substituted gemini nanoparticles.* European Journal of Pharmaceutics and Biopharmaceutics, 2010. **75**(3): p. 311-320.
45. Colombo, G., P. Soto, and E. Gazit, *Peptide self-assembly at the nanoscale: a challenging target for computational and experimental biotechnology.* TRENDS in Biotechnology, 2007. **25**(5): p. 211-218.
46. Lin, A.J., et al., *Three-dimensional imaging of lipid gene-carriers: membrane charge density controls universal transfection behavior in lamellar cationic liposome-DNA complexes.* Biophysical journal, 2003. **84**(5): p. 3307-3316.
47. Schaffer, D.V., et al., *Vector unpacking as a potential barrier for receptor-mediated polyplex gene delivery.* Biotechnology and bioengineering, 2000. **67**(5): p. 598-606.

48. Smisterová, J., et al., *Molecular shape of the cationic lipid controls the structure of cationic lipid/dioleylphosphatidylethanolamine-DNA complexes and the efficiency of gene delivery.* Journal of Biological Chemistry, 2001. **276**(50): p. 47615-47622.
49. Israelachvili, J.N., D.J. Mitchell, and B.W. Ninham, *Theory of self-assembly of hydrocarbon amphiphiles into micelles and bilayers.* Journal of the Chemical Society, Faraday Transactions 2: Molecular and Chemical Physics, 1976. **72**: p. 1525-1568.
50. Koenig, B.W. and K. Gawrisch, *Specific volumes of unsaturated phosphatidylcholines in the liquid crystalline lamellar phase.* Biochimica et Biophysica Acta (BBA)-Biomembranes, 2005. **1715**(1): p. 65-70.
51. Wang, H. and S.D. Wettig, *Synthesis and aggregation properties of dissymmetric phytanyl-gemini surfactants for use as improved DNA transfection vectors.* Physical Chemistry Chemical Physics, 2011. **13**(2): p. 637-642.
52. Hanwell, M.D., et al., *Avogadro: an advanced semantic chemical editor, visualization, and analysis platform.* Journal of cheminformatics, 2012. **4**(17): p. 1-17.
53. Frisch, M., et al., *Gaussian 09, Revision D. 01*. Wallingford: Gaussian, Inc., 2013.
54. Wettig, S. and R. Verrall, *Thermodynamic studies of aqueous m-s-m gemini surfactant systems.* Journal of colloid and interface science, 2001. **235**(2): p. 310-316.
55. Zuhorn, I.S., et al., *Nonbilayer phase of lipoplex-membrane mixture determines endosomal escape of genetic cargo and transfection efficiency.* Molecular therapy, 2005. **11**(5): p. 801-810.

3.8 Appendix A- Supplementary Figure and Table

A 16-3-16-D_{66}

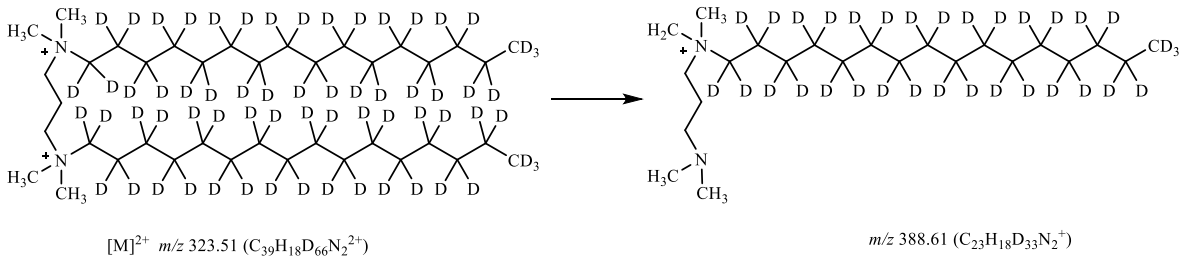

$[M]^{2+}$ *m/z* 323.51 ($C_{39}H_{18}D_{66}N_2^{2+}$)

m/z 388.61 ($C_{23}H_{18}D_{33}N_2^{+}$)

B 16(Py)-S-2-S-(Py)16-D_{10}

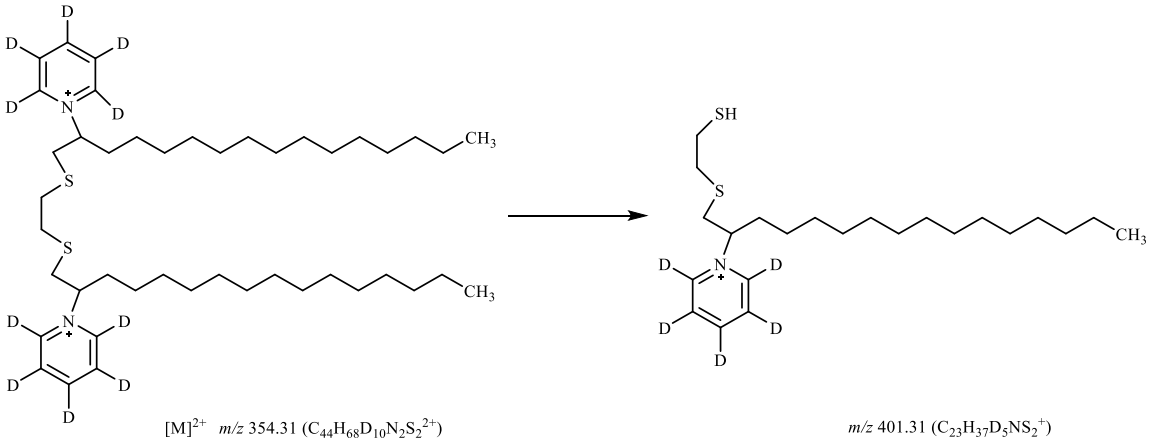

$[M]^{2+}$ *m/z* 354.31 ($C_{44}H_{68}D_{10}N_2S_2^{2+}$)

m/z 401.31 ($C_{23}H_{37}D_5NS_2^{+}$)

C 16-7N(GK)-16-D_4

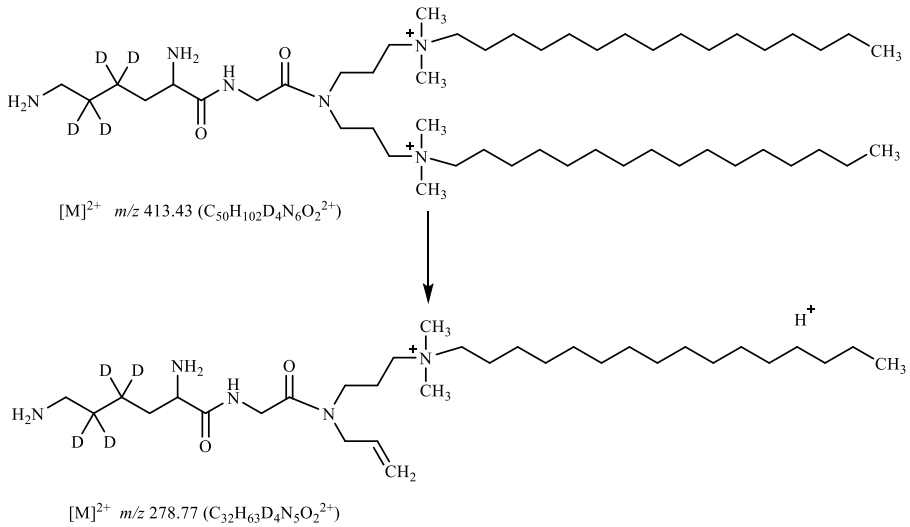

$[M]^{2+}$ *m/z* 413.43 ($C_{50}H_{102}D_4N_6O_2^{2+}$)

$[M]^{2+}$ *m/z* 278.77 ($C_{32}H_{63}D_4N_5O_2^{2+}$)

Figure 3.S1. Structures of (A) 16-3-16-D_{66} and the monitored product ion, (B) 16(Py)-S-2-S-16(Py)-D_{10} and the monitored product ion, and (C) 16-7N(GK)-16-D_4 and the monitored product ion.

Table 3.S1. Cellular uptake and distribution of the three gemini surfactants in PAM 212 cells, expressed as an absolute amount.

Subcellular fraction	2 h			5 h			8 h		
	16-3-16	16(Py)-S-2-S-16(Py)	16-7N (GK)-16	16-3-16	16(Py)-S-2-S-16(Py)	16-7N (GK)-16	16-3-16	16(Py)-S-2-S-16(Py)	16-7N (GK)-16
Cyto (nmoL)	0.15	0.20	0.20	0.13	0.26	0.42	0.10	0.25	0.40
Mito (nmoL)	0.23	0.18	0.29	0.29	0.62	0.63	0.16	0.49	0.56
Nuc (nmoL)	0.30	0.27	0.32	0.34	1.04	0.81	0.33	0.92	0.47
PM (nmoL)	0.03	0.02	0.22	0.06	0.15	0.57	0.03	0.12	0.42
Total uptake (nmoL)	0.72	0.67	1.04	0.82	2.06	2.42	0.63	1.77	1.86
Uptake (%)	1.3%	1.2%	7.3%	1.4%	3.6%	17.0%	1.1%	3.1%	13.0%

(Dose amount: 57 nmoL for 16-3-16 and 16(Py)-S-2-S-16(Py), and 14.25 nmoL for 16-7N(GK)-16. Cyto-cytosol, Mito-mitochondria, Nuc-nucleus, and PM-plasma membrane)

3.9 Appendix B - Supplementary Methods and Results

3.9.1 Western blotting procedure

To solubilize membrane proteins, the freshly collected nuclear, mitochondrial, and plasma membrane fractions were re-suspended in 150 µL of ice-cold RIPA buffer (10 mM Tris-HCl [pH 8], 150 mM NaCl, 5 mM EDTA, 1% Triton X-100, 0.5% sodium deoxycholate, 0.1% SDS, and 1x protease inhibitor cocktail) for 30 min on ice. The clarified extracts were collected after centrifugation (15,000 *x g*, 20 min, 4 ˚C). No protein recovery was needed for the cytosolic fraction.

An appropriate volume of 4x Laemmli sample buffer containing 600 mM dithiothreitol was added to each fraction, which was then incubated for 10 min in a 37 ˚C water bath. Approximately 20 µg of proteins from each fraction was loaded on 4-15% SDS-PAGE gradient gel and electrophoresed for 1.5 h at 120 V. Proteins were then transferred to nitrocellulose membrane at 400 mA for 1.75 h. After a 2 h room temperature incubation in TBST buffer (20 mM Tris [pH 7.5], 150 mM NaCl, and 0.05% Tween-20) containing 5% non-fat dried milk, the membrane was incubated overnight at 4 ˚C with a primary antibody specific to each subcellular fraction. The following day, the membrane was washed 6 times with TBST and incubated in secondary antibody for 2 h at room temperature. Finally, the membrane was washed 6 times with TBST and developed with an enhanced chemiluminescence assay kit (Bio-Rad, Canada). Immunoreactive bands were visualized using a VersaDoc^{TM} Image System (Bio-Rad Laboratory, Hercules, CA, USA).

3.9.2 Western blotting analysis of subcellular fractions

Western blotting was conducted with organelle or compartment-specific markers to verify the relative purify of each subcellular fraction. As showed in Figure 3.S2, each marker was most abundant in the expected fraction. The modest amount of SDH70 shown in the nuclear fraction

likely reflects a small number of residuals and unbroken cells in the preparation. The results indicated that differential centrifugation of homogenates allowed for the successful isolation of enriched nuclear, mitochondrial, plasma membrane and cytosolic fractions from PAM 212 cells.

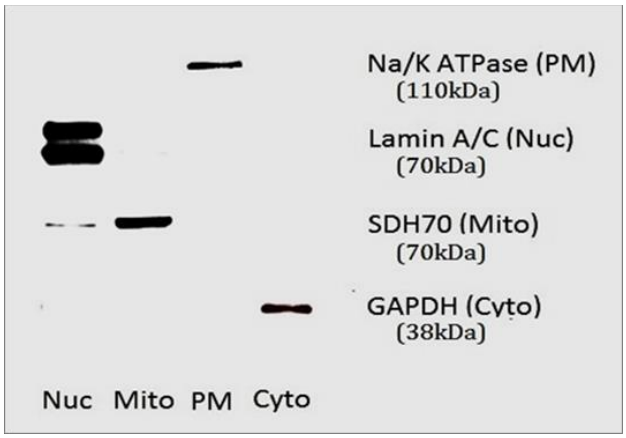

Figure 3.S2. Western blot analysis of the subcellular fractions. Samples were probed with antibodies for organelle-specific markers. The bands correspond to their relevant molecular weights, showing the identities of the proteins and thus the isolation of subcellular fractions. The protein band sizes are Na^+/K^+ ATPase (110 kDa) for plasma membrane (PM), Lamin A/C (70 kDa) for nucleus (Nuc). SDH70 (70 kDa) for mitochondria (Mito), and GAPDH (38 kDa) for cytosol (Cyto).

4 Chapter 4 - Mass Spectrometric Detection and Characterization of Metabolites of Gemini Surfactants Used as Gene Delivery Vectors

The chapter has been submitted to the Journal of the American Society for Mass Spectrometry

Mass Spectrometric Detection and Characterization of Metabolites of Gemini Surfactants Used as Gene Delivery Vectors

Wei Jin[1], Randy Purves[1, 2], Ed Krol[1], Ildiko Badea[1] and Anas El-Aneed[1]*

[1]Drug Design & Discovery Group, College of Pharmacy and Nutrition, University of Saskatchewan, 107 Wiggins Road, Saskatoon, SK, Canada, S7N 5E5.

[2]Centre for Veterinary Drug Residues, Canadian Food Inspection Agency, 116 Veterinary Rd, Saskatoon, SK, Canada, S7N 2R3.

*Corresponding author. E-mail address: anas.el-aneed@usask.ca (A. El-Aneed).

Authors' contribution: Wei Jin played a key role in designing the experiments, conducted the experiments, analyzed the data, and drafted the manuscript. Dr. Purves helped with conducting the experiments using the high-resolution Q-Exactive instrument and provided input in data analysis and interpretation; he also provided signficant feedback to the writing. Dr. Krol helped with data interpretation, particularly the rationalization of the observed metabolites; he also suggested key control experiments. Dr. Badea helped with the nanoparticle formulation and biological relevance of the work. Dr. El-Aneed is the PI; he conceptualized the research question, obtained funding, supervised the work, and revised the manuscript.

Transitioning Rationale:

In addition to the assessment of cellular uptake and subcellular distribution conducted in Chapters 2 and 3, the metabolism of the gemini surfactants 16-3-16, 16(Py)-S-2-S-(Py)16, and 16-7N(GK)-16 was investigated in this Chapter using high-resolution mass spectrometry, which contributes to the comprehensive understanding of the behavior of gemini surfactants in biological systems.

4.1 Abstract

Gemini surfactants are a class of lipid molecules that have been successfully used *in vitro* and *in vivo* as non-viral gene delivery vectors. However, the biological fate of gemini surfactants has not been well investigated. In particular, the metabolism of gemini surfactants after they enter cells as gene delivery vehicles is unknown. In this work, we used a high-resolution quadrupole-Orbitrap mass spectrometry (Q-Exactive®) instrument to detect the metabolites of three model gemini surfactants, namely a) unsubstituted (16-3-16), b) with pyridinium head groups (16(Py)-S-2-S-16(Py)), and c) substituted with a glycyl-lysine di-peptide (16-7N(GK)-16). The metabolites were also characterized, and structures proposed, based on accurate masses and characteristic product ions. Metabolic behaviors of the three gemini surfactants were very different as 16-3-16 was not metabolized in PAM 212 cells, whereas 16(Py)-S-2-S-16(Py) was metabolized primarily *via* phase I reactions, including oxidation and de-alkylation, producing metabolites that could be linked to its observed high toxicity. The third gemini surfactant 16-7N(GK)-16 was metabolized mainly *via* phase II reactions, including methylation, acetylation, glucose conjugation, palmityl conjugation, and stearyl conjugation. The metabolism of gemini surfactants provides insight for future directions in the design and development of more effective gemini surfactants with lower toxicity. The reported approach can also be applied to study the metabolism of other structurally related gemini surfactants.

Key words: Gemini surfactants; Gene delivery; Metabolites; High-resolution mass spectrometry; Efficiency and toxicity; Q-Exactive.

4.2 Introduction

Gemini surfactants are a class of self-assembled lipid molecules that have a general structure of two hydrophilic head groups, a spacer region, and two hydrophobic tails (Figure 4.1a) [1]. Gemini surfactants have been extensively studied as non-viral gene delivery vectors [2-4], as they have the ability to compact DNA to form nanosized particles, facilitating their cellular entry [5, 6]. Numerous studies evaluated gemini surfactants to increase their transfection efficiency and reduce toxicity. First, a wide range of gemini surfactants were designed and synthesized by varying the head groups, the spacer region, and the length and saturation of the hydrophobic tails [7, 8]. Second, the formulation strategy for gemini surfactant-based lipoplexes has been studied, such as the application of lyophilization [9]. Lastly, the internalization mechanism of gemini surfactants was determined to be endocytosis, with the aim in increasing cellular uptake and thereby enhancing transfection efficiency [10]. These efforts have greatly contributed to the development of novel gemini surfactants used as gene delivery agents.

Despite the substantial improvements, gemini surfactants as non-viral vectors are still limited in gene transfection abilities, particularly for *in vivo* applications [11, 12]. In addition, the differences in cellular toxicities among different structures are not fully understood. Currently, studies are primarily focused on the development of efficient delivery systems by modifications of the structures of gemini surfactants, optimization of the formulation methods, and facilitation of endosomal escape [9, 10, 13]. However, the biological fate of gemini surfactants has not been fully explored and little is known about their cellular uptake, distribution, and metabolite formation upon entry into biological systems, which can be an important contributing factor for their observed efficiencies and toxicities. High-resolution mass spectrometry (MS) instruments, such as a quadrupole-time of flight (Q-TOF) and a quadrupole-Orbitrap (Q-Exactive®), have been

extensively used for the identification and characterization of a wide range of molecules as they can provide high sensitivity, accurate mass measurement, and a wide dynamic range [14, 15]. Typically, these instruments can achieve a mass accuracy of less than 5 ppm, allowing for the determination of molecular formula to assist in the identification of unknown compounds [16, 17]. In addition, tandem mass spectrometric (MS/MS) analysis can aid in the characterization of the target metabolites. For example, the gemini surfactants G12-s and G18:1-s have been characterized with mass accuracy less than 5 ppm for their structural elucidation using a Q-TOF instrument with internal calibration [18]. Similarly, a Q-Exactive instrument was used for the identification and characterization of phase II pharmaceutical metabolites in reclaimed water [19].

To assess the biological fate of gemini surfactants, we have evaluated three gemini surfactants, designated as 16-3-16, 16(Py)-S-2-S-16(Py), and 16-7N(GK)-16) (Figures 4.1b-d) to understand their biological fate and explore the relationship between the cellular uptake, distribution, and metabolism in relation to their overall efficiencies and toxicities. The three gemini surfactants belong to different structural families; 16-3-16 is a conventional gemini surfactant with two quaternary amines in the head groups, whereas 16(Py)-S-2-S-(Py)16 contains two pyridine moieties in the head groups and 16-7N(GK)-16 is a glycyl-lysine di-peptide substituted gemini surfactant (Figures 4.1b-d). These gemini surfactants have been successfully used *in vitro* and *in vivo* as non-viral gene delivery agents [20-22]; however, they vary among each other in terms of gene transfer efficiencies and toxicities [23, 24].

As our main therapeutic use for gemini surfactants is topical application, particularly for the treatment of localized scleroderma, a connective tissue disease, the epidermal keratinocytes PAM 212 cells were selected for the evaluation of the biological fate of these three gemini surfactants. In fact, we have shown recently in an ex-vivo experiment that gemini surfactants localized mainly

in the skin with minimal penetration of skin tissues to enter the compartment representing the circulation [25]. As such, it is of great importance to evaluate their metabolism within a cell line that represents the target organ, i.e., the skin. Our group previously evaluated the cellular uptake and distribution of these three gemini surfactants within murine keratinocytes PAM 212 cells using mass spectrometric (MS) methods [26]. Typically, high cellular uptake of the gemini surfactants resulted in high gene transfection, whereas unfavorable accumulation in the nucleus was likely a major contributing factor to their toxicity [26]. However, the metabolism of the gemini surfactants remains unclear and there is no report describing the metabolite profiles of the gemini surfactants when used as gene delivery agents. An investigation of metabolite formation will help determine how the gemini surfactants interact within biological systems to generate different metabolic products, such as phase I and phase II metabolites. Such information will ultimately contribute to the design and development of novel gemini surfactants with better therapeutic profiles. Therefore, we utilized a high-resolution mass spectrometry instrument to detect and characterize the metabolites of the three lead gemini surfactants within PAM 212 cell line.

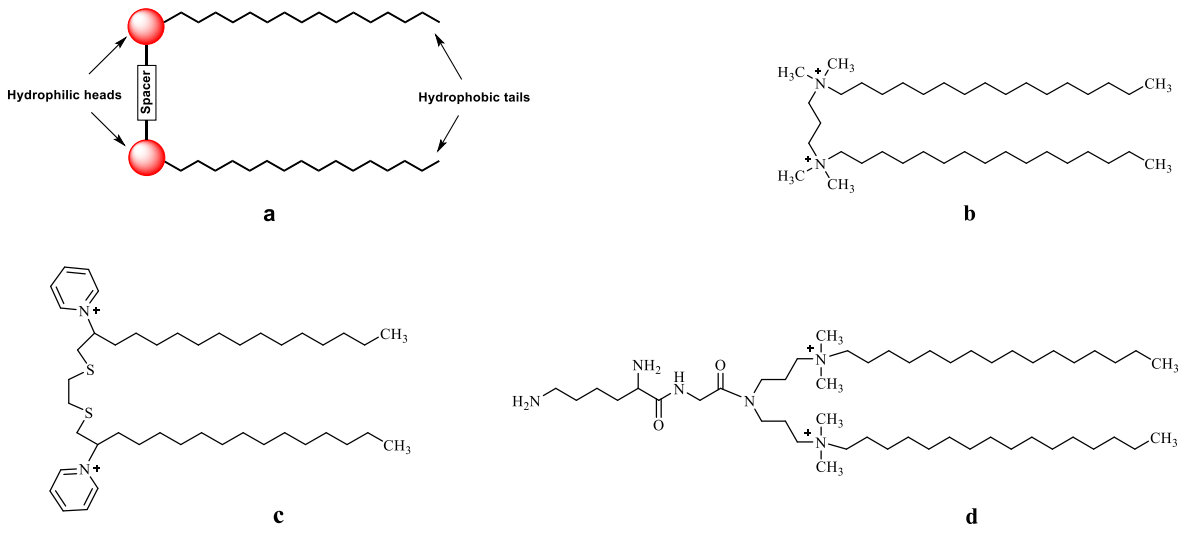

Figure 4.1. The structures of gemini surfactants. a) The general structure of gemini surfactants, b) 16-3-16, c) 16(Py)-S-2-S-16(Py), and d) 16-7N(GK)-16.

4.3 Materials and Methods

4.3.1 Materials

All gemini surfactants 16-3-16, 16(Py)-S-2-S-16(Py), and 16-7N(GK)-16 (Figures 4.1b-d) and their deuterium-labelled counterparts 16-3-16-D_{66}, 16(Py)-S-2-S-16(Py)-D_{10}, and 16-7N(GK)-16-D_4 (Figure 4.S1 in supporting information) were synthesized based on established protocols [21, 22, 23]. The neutral lipid, 1, 2-dioleoyl-sn-glycero-3-phosphoethanolamine (DOPE), was obtained from Avanti Polar Lipids Inc. (Alabaster, AL, USA). Chloroform, methanol, formic acid, cell culture flasks (75 cm^2), and petri dishes (60 cm^2) were purchased from Fisher Scientific (Ottawa, ON, Canada). Murine keratinocyte PAM 212 cells were obtained from Dr. S. Yuspa, National Cancer Institute, Bethesda, MD, USA. Minimum essential media (MEM), fetal bovine serum (FBS) albumin, and antibiotic-antimycotic solution were purchased from Sigma-Aldrich (Oakville, ON, Canada).

4.3.2 Formulation

All gemini surfactants were prepared as 3 mM aqueous solution and stored at -80 ℃ under darkness. The DOPE vesicles were prepared freshly in isotonic sucrose solution (9.25%, w/v, pH=9) at a concentration of 1 mM as per an established protocol [22]. The plasmid DNA solution was prepared in ultra-pure water at 200 µg/mL and stored at -80 ℃, and was allowed to thaw at room temperature prior to use.

Lipoplexes were prepared with plasmid DNA, gemini surfactant (labeled or non-labeled), and helper lipid DOPE (P/G/L) as previously described [22], with a nitrogen (cationic) to phosphate (anionic) charge ratio (N/P) of 10 for 16-3-16, 16-3-16-D_{66}, 16(Py)-S-2-S-16(Py), 16(Py)-S-2-S-16(Py)-D_{10}, and N/P of 2.5 for 16-7N(GK)-16 and 16-7N(GK)-16-D_4. Briefly, an appropriate

amount of 3 mM aqueous solution of labeled or non-labeled gemini surfactants was added to the 200 μg/mL plasmid DNA and gently mixed with a pipette, followed by a 15 min incubation at room temperature. A 1 mM DOPE solution was then added to the binary mixture, gently mixed, and subsequently incubated at room temperature for 15 min to produce the ternary P/G/L system (i.e., nanoparticles).

4.3.3 Cell treatment and sample collection

PAM 212 cells were cultured in 75 cm^2 cell culture flasks inside a humidified incubator at 37 ℃ in an atmosphere of 5% CO_2. When the cells reached 80% confluence, they were washed with phosphate buffered saline (PBS, 6 mL), dissociated with a 5 min incubation in a mixture of versene (10x, 3 mL) and trypsin (10x, 0.3 mL) and collected by centrifugation (250 *x g*, 5 min, 4 ℃). At 24 h prior to treatment, the cells were seeded at 2×10^6 cells per petri dish (60 cm^2), and at 1 h prior to transfection the cell media was switched to a serum-free media. Freshly prepared nanoparticle formulations (100 μL) were added to each dish drop by drop, followed by an incubation for 5 h based on previously established protocol [22]; upon completion, the cells were returned to the supplemented media for all subsequent incubation steps. During the incubation period, duplicates of treated cell samples and one control (untreated cells) were trypsinized and collected at 5 h. At 10 h, two additional treated cell samples and one control were also collected. The collected cells were pelleted (250 *x g*, 5 min, 4 ℃), rinsed with PBS twice, reconstituted in 250 μL of PBS solution, and stored at -80 ℃ for subsequent sample preparation. In addition, each gemini surfactant was incubated in the media for 10 h as a control experiment

4.3.4 Sample preparation

The 250 µL collected cell samples were thawed and lysed by undergoing six freeze/thaw cycles plus 1 h sonication at 25 kHz in a water bath at room temperature. Liquid-liquid extraction of the gemini surfactants from cellular matrix was carried out using the Bligh/Dyer method [27]. Briefly, each 250 µL of sample was mixed with 937.5 µL of methanol-chloroform (2:1, v/v), followed by mixing with 312.5 µL of chloroform and finally 312.5 µL of water. At each step, samples were vortexed thoroughly. The final combined mixture was then centrifuged at 2,800 *x g* for 10 min at room temperature to separate the aqueous and organic phases. The bottom organic phase was retrieved and dried under a nitrogen gas stream, followed by reconstitution in 250 µL of methanol. Methanol solution (200 µL) was transferred into an HPLC vial for analysis.

4.3.5 Flow-injection mass spectrometric analysis

Flow injection was performed using a Thermo UltiMate 3000 HPLC system equipped with a well plate autosampler. Twenty microlitres of sample at 6 ℃ was directly injected (i.e., no column) into the source with an isocratic mobile phase consisting of methanol-water containing 0.000625% formic acid (90:10, v/v) at a flow rate of 0.2 mL/min. The data acquisition time was 2 min.

All samples were analyzed using a quadrupole-Orbitrap mass spectrometer (Q-Exactive®, Thermo Scientific, Waltham, MA, USA) equipped with a heated electrospray ionization (HESI) source operated in positive ion mode. The HESI source voltage was optimized at 3 kV. The vaporizer and capillary temperatures were set to 350 °C and 300 °C, respectively. Ultra-high purity nitrogen was used as the ion source and collision gas. Mass spectrometric parameters were set as follows: Sheath gas, 40; Aux gas, 20; and Sweep gas, 5. MS full scans with a range of *m/z* 80-1200 at a resolving power of 140,000 (at *m/z* 200) and data dependent MS/MS scans with a product ion resolving

power of 17,500 (at *m/z* 200) were employed. A mass accuracy was obtained with less than 2 ppm for metabolite ions and less than 10 ppm for their product ions. The *m/z* values for ions of interest were entered in an inclusion list to trigger MS/MS scans. The isolation window for MS/MS scans was set at *m/z* 0.7 and dynamic exclusion was 15 s. For MS/MS analysis, normalized collision energy (NCE) was stepped between 20, 30, and 40. Data acquisition and analysis was performed with Xcalibur™ software (Thermo Scientific, Waltham, MA, USA).

4.4 Results and Discussion

4.4.1 Detection of gemini surfactant metabolites

The metabolic profiles of gemini surfactants were established by comparing control cells (i.e., no treatment) to cells treated with gemini surfactant nanoparticles (deuterium labeled or non-labeled). Possible metabolites were initially detected based on high-resolution full scan mass spectra as their molecular formulae were determined according to accurate mass measurements. Since gemini surfactants contain two positive charges in their structures, positive ion mode was used to identify potential metabolites. In fact, a preliminary analysis of treated cell extracts with a Q-TOF instrument (QSTAR® Elite, Concord, ON, Canada) indicated the absence of potential metabolites of the gemini surfactants in the negative ion mode. In addition to non-labeled gemini surfactants, deuterium-labeled gemini surfactants were also used to formulate nanoparticles and treat cells to confirm the presence of potential metabolites.

No difference was observed in the full scan MS analysis between controls and cells treated with 16-3-16 nanoparticles at 5 h and 10 h, indicating that the gemini surfactant 16-3-16 was not metabolized in PAM 212 cells. This result was confirmed by the metabolic profile of cells treated

with 16-3-16-D_{66} nanoparticles in which no metabolites were observed. Therefore, the gemini surfactant 16-3-16 is a non-biodegradable compound within PAM 212 cells.

Conversely, cells treated with 16(Py)-S-2-S-16(Py) nanoparticles revealed the presence of three possible metabolites observed as doubly charged ions at *m/z* 357.2770 (M-1), 365.2748 (M-2), and 373.2720 (M-3), and two metabolites as singly charged ions observed at *m/z* 396.2756 (M-4) and 412.2703 (M-5), which were not present in the control (Table 4.1 and Figure 4.S2 in supporting information). The accurate masses of these metabolites are all within 1.0 ppm mass error compared with the proposed molecular formula (Table 4.1). The doubly charged ion at *m/z* 357.2770 suggests that metabolite M-1 is an oxidization product of 16(Py)-S-2-S-16(Py), with one oxygen atom (15.9949 Da) added to the original structure (Table 4.1). The presence of a doubly charged ion at *m/z* 362.3084 (M-1') in cells treated with the deuterium version of this compound (i.e., 16(Py)-S-2-S-16(Py)-D_{10}; the *m/z* shift of 5.0314 corresponds to the addition of 10 deuteriums) supports the existence of such a metabolite (Figure 4.S2 and Table 4.S1 in supporting information). Similarly, metabolites M-2 (*m/z* 365.2748) and M-3 (*m/z* 373.2720) were also determined based on their accurate mass measurements, showing two and three oxygen atoms added to the structures of 16(Py)-S-2-S-16(Py) (Table 4.1). The deuterium-labeled compound gave corresponding metabolites M-2' and M-3' (Table 4.S1 in supporting information).

The metabolites of 16(Py)-S-2-S-16(Py) observed at *m/z* 396.2756 (M-4) and 412.2703 (M-5) are singly charged ions, which are consistent with a dealkylation product and its oxidized form, respectively (Table 4.1). As expected, the deuterated gemini surfactant 16(Py)-S-2-S-16(Py)-D_{10} metabolites at *m/z* 401.3070 (M-4') and 417.3017 (M-5') were also observed (Figure 4.S2 and Table 4.S1 in supporting information), which confirmed the presence of the two metabolites of 16(Py)-S-2-S-16(Py). It should be noted that 16(Py)-S-2-S-16(Py) was also oxidized by incubation

in the media alone, generating the products of M-1 and M-2. However, the ion intensity of M-1 and M-2 is significantly lower compared with those obtained in the media with PAM 212 cells and the production of M-3 was not observed in the media as shown in Figure 4.S3 in supporting information). In addition, the production of the oxidation metabolite M-3 was not observed in the media, confirming that oxidation was a process mediated by cellular enzyme and not merely due to natural oxidation within the aqueous media. As indicated in Table 4.1, the gemini surfactant 16(Py)-S-2-S-16(Py) was mainly metabolized *via* phase I reactions, including oxidation and dealkylation. Although authentic reference standards are needed for the unambiguous authentication of the proposed structures, additional MS/MS analyses were performed to confirm the proposed metabolic reactions and the analysis is discussed in section 4.4.2.

Likewise, possible metabolites of gemini surfactant 16-7N(GK)-16 were also initially detected based on the comparison of the metabolic profiles of treated cells versus controls. Unlike 16(Py)-S-2-S-16(Py), the gemini surfactant 16-7N(GK)-16 was metabolized primarily *via* phase II reactions, including methylation, acetylation, glucose conjugation, palmitoyl conjugation, and stearyl conjugation (Table 4.1). This is probably due to the presence of a reactive functional group of an amino acid within its structure, prone to phase II reactions [27].

Six metabolites showing doubly charged ions at *m/z* 432.4238, 439.4317, 447.4291, 492.4448, 530.5334, and 544.5491 were observed (Figure 4.S4 in supporting information) and their chemical formulae were determined according to their accurate masses (mass accuracy <1.0 ppm, Table 4.1). Metabolite M-a at *m/z* 432.4238 is a possible phase II product from an acetylation reaction, whereas metabolites M-b and M-c at *m/z* at 439.4317 and 447.4291 are the result of acetylation with methylation, and acetylation with methylation and hydroxylation, respectively (Table 4.1). In addition, metabolites M-d, M-e, and M-f observed at *m/z* 492.4448, 530.5334, and 544.5491 were

also determined as possible phase II reaction products corresponding to the addition of glucose, palmitoyl, and stearyl groups to the original structure, respectively (Table 4.1). The presence of these metabolites is confirmed by the metabolism of 16-7N(GK)-16-D_4, showing six similar metabolites with the expected mass shift of 2.0136 Da at *m/z* 434.4362, 441.4438, 449.4413, 494.4569, 532.5454, and 546.5611 (Figure 4.S4 and Table 4.S1 in supporting information). MS/MS analyses discussed below (section 4.4.3) are used to confirm the proposed metabolic reactions.

Table 4.1 Potential metabolites based on accurate mass measurements for the gemini surfactants 16(Py)-S-2-S-16(Py) and 16-7N(GK)-16.

Name	Molecular Formula	Exact Mass (*m/z*)	Observed Mass (*m/z*)	Mass Accuracy (ppm)	Metabolic Reactions
16(Py)-S-2-S-16(Py)	$C_{44}H_{78}N_2S_2^{2+}$	349.2798	349.2805	2.0	
M-1	$C_{44}H_{78}N_2OS_2^{2+}$	357.2772	357.2770	0.6	Oxidation
M-2	$C_{44}H_{78}N_2O_2S_2^{2+}$	365.2747	365.2748	0.3	Oxidation
M-3	$C_{44}H_{78}N_2O_3S_2^{2+}$	373.2722	373.2720	0.5	Oxidation
M-4	$C_{23}H_{42}NS_2^{+}$	396.2753	396.2756	0.8	Dealkylation
M-5	$C_{23}H_{42}NOS_2^{+}$	412.2702	412.2703	0.2	Dealkylation, Oxidation
16-7N(GK)-16	$C_{50}H_{106}N_6O_2^{2+}$	411.4183	411.4186	0.7	
M-a	$C_{52}H_{108}N_6O_3^{2+}$	432.4236	432.4238	0.5	Acetylation
M-b	$C_{53}H_{110}N_6O_3^{2+}$	439.4314	439.4317	0.7	Acetylation, Methylation
M-c	$C_{53}H_{110}N_6O_4^{2+}$	447.4289	447.4291	0.4	Acetylation, Methylation, Hydroxylation
M-d	$C_{56}H_{116}N_6O_7^{2+}$	492.4447	492.4448	0.2	Glucose conjugation
M-e	$C_{66}H_{136}N_6O_3^{2+}$	530.5331	530.5334	0.6	Palmitoyl conjugation
M-f	$C_{68}H_{140}N_6O_3^{2+}$	544.5488	544.5491	0.6	Stearyl conjugation

4.4.2 MS/MS analysis of 16(Py)-S-2-S-16(Py) and its metabolites

An MS/MS analysis was performed in an effort to determine the proposed metabolic pathways of each gemini surfactant and thereby support the structural assignments of the proposed metabolites. Specifically, the metabolites detected based on accurate mass measurements were subjected to MS/MS analysis. The observed product ions were then compared with those of their respective parent compounds to explore structural similarities and determine structural changes within the metabolites. Thus, the combination of high-resolution accurate mass measurements and MS/MS data resulted in high confidence in the proposed metabolite assignments.

Figure 4.2 shows the MS/MS spectra of 16(Py)-S-2-S-16(Py) and its metabolites. The gemini surfactant 16(Py)-S-2-S-16(Py) displayed four major characteristic product ions at *m/z* 396.2749, 317.2326, 309.7588, and 257.2294, along with other product ions (Figure 4.2a). These observed product ions are the same as those obtained on a triple quadrupole linear ion trap (Q-LIT) instrument in our previous work in which the structures of all product ions were determined [28]. The product ion at *m/z* 309.7588 was formed through the loss of one pyridine moiety from the parent molecule that further underwent S-dealkylation to generate the product ion at *m/z* 257.2294. The product ion at *m/z* 396.2749 was produced *via* loss of the pyrdinium group along with the alkyl chain through S-dealkylation. The ion further lost one pyridine moiety to generate the product ion at *m/z* 317.2326, followed by S-dealkylation to also yield the product ion at *m/z* 257.2294 (Figure 4.3a). As expected, the deuterated gemini surfactant 16(Py)-S-2-S-16(Py)-D_{10} displayed similar characteristic product ions observed at *m/z* 401.3065, 317.2332, 312.2740, and 257.2295 (Figure 4.S5a in supporting information).

The metabolite M-1 was determined as an oxidized species of 16(Py)-S-2-S-16(Py) with an *m/z* value of 357.2770. MS/MS analysis of M-1 yielded characteristic product ions at *m/z* 412.2701,

352.2671, 333.2279, 302.2841, and 257.2296 (Figure 4.2b). Similar to the formation of the product ions at *m/z* 396.2749, 317.2326, and 257.2294 of 16(Py)-S-2-S-16(Py), the product ions at *m/z* 412.2701, 333.2279, and 257.2296 of M-1 were formed *via* S-dealkylation, N-dealkylation resulting in loss of one pyridine moiety, and subsequent S-dealkylation (Figure 4.3b). By comparing with the product ions at *m/z* 396.2749 and 317.2326 of 16(Py)-S-2-S-16(Py), the product ions at *m/z* 412.2701 and 333.2279 of M-1 suggested that an oxygen atom was added to one of the two sulfur atoms in the original structure (Figure 4.3b). The product ion at *m/z* 352.2671 was formed through S-dealkylation, which further yielded the product ion at *m/z* 302.2841, also confirming the oxidation reaction (Figure 4.3b). This conclusion is supported by the corresponding metabolite M-1' at *m/z* 362.3084 of 16(Py)-S-2-S-16(Py)-D_{10} (Figure 4.S2 in supporting information), which displayed characteristic product ions at *m/z* 417.3004, 357.2973, 333.2277, 307.3152, and 257.2296 (Figure 4.S5b in supporting information).

Similarly, metabolites M-2 and M-3 were also determined to be oxidation products of 16(Py)-S-2-S-16(Py) with accurate masses at *m/z* 365.2748 and 373.2720, respectively. Like the metabolite M-1, the metabolite M-2 was characterized with its unique product ions at *m/z* 428.2627, 352.2639, 349.2233, 302.2830, and 273.2266, indicating two oxygens were added to the sulfur atoms (Figures 4.2c and 4.3c). In particular, the product ion at *m/z* 352.2639 indicated the presence of one oxygen on each sulfur atom, as it was formed through S-dealkylation with the loss of one oxygen-containing alkyl group (Figure 4.3c). The product ions at *m/z* 428.2627, 349.2233, and 273.2266 also support the attachment of an oxygen to each of the two sulfur atoms (Figure 4.3c). In addition, the deuterated gemini surfactant 16(Py)-S-2-S-16(Py)-D_{10} displayed a similar metabolite M-2' with an accurate mass at *m/z* 370.3064 (Figure 4.S2 in supporting information), which showed

corresponding product ions at *m/z* 433.2959, 357.2975, 307.3151, and 273.2238 (Figure 4.S5c in supporting information).

Due to low ion abundance, the MS/MS spectra of metabolite M-3 was not obtained; its structure was proposed to contain three oxygen atoms based on accurate mass measurement (Table 4.1 and Figure 4.S2 in supporting information). On the contrary, the MS/MS spectra of metabolite M-3' of 16(Py)-S-2-S-16(Py)-D_{10} was obtained and showed characteristic product ions at *m/z* 449.2918, 399.3087, 357.2977, 307.3153, and 273.2244 (Figure 4.S5d in supporting information), suggesting three oxygens were added to the sulfur atoms in the original structure. This dissociation behavior mimics what was observed for metabolite M-2, supporting the proposed structure (Figure 4.S6 in supporting information).

The metabolite M-4, a singly charged ion at *m/z* 396.2756, is an S-dealkylation product of 16(Py)-S-2-S-16(Py) (Figure 4.3d), whereas the metabolite M-5, with an accurate mass at *m/z* 412.2703, is proposed to be an oxidized form of M-4 (Figure 4.3e). An MS/MS analysis of metabolite M-4 showed two major product ions at *m/z* 317.2336 and 257.2297 (Figure 4.2d); whereas metabolite M-5 displayed two major product ions at *m/z* 333.2272 and 257.2294 (Figure 4.2e), indicating it is an oxidized version of M-4. Likewise, the deuterated gemini surfactant 16(Py)-S-2-S-16(Py)-D_{10} also showed two singly charged metabolites M-4' and M-5' with accurate masses at *m/z* 401.3070 and 417.3017, which displayed similar fragmentation patterns as metabolites M-4 and M-5, supporting the proposed structures of the two metabolites (Figures 4.S5e and f in supporting information).

Based on the proposed structures of the metabolites, a suggested metabolic pathway for the gemini surfactant 16(Py)-S-2-S-16(Py) is presented in Figure 4.4, indicating that this compound is mainly

metabolized *via* phase I metabolic reactions. In particular, it can either go through a series of oxidations to generate S-oxidized products, or a second pathway involving S-dealkylation and subsequent S-oxidation to produce dealkylation and sulfoxide oxidation metabolites. Metabolites of the deuterated gemini surfactant 16(Py)-S-2-S-16(Py)-D_{10} (Figure 4.S7 in supporting information) support this metabolic pathway.

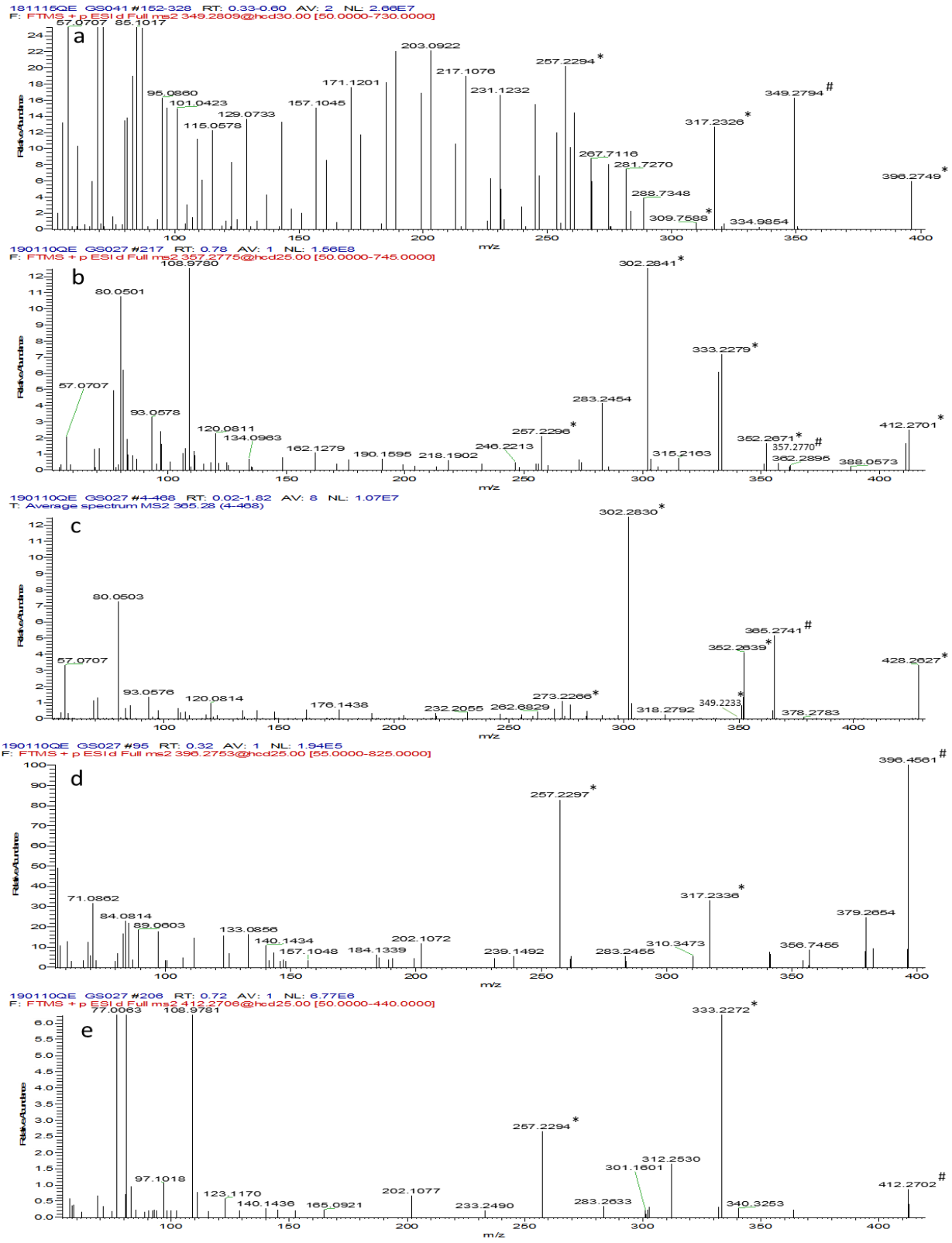

Figure 4.2. The MS/MS spectra of 16(Py)-S-2-S-16(Py) and its metabolites: a) 16(Py)-S-2-S-16(Py), b) M-1, c) M-2, d) M-4, and e) M-5. (# denotes the parent ion and * denotes the diagnostic product ion). The MS/MS spectra of M-3 was not available due to low ion abundance.

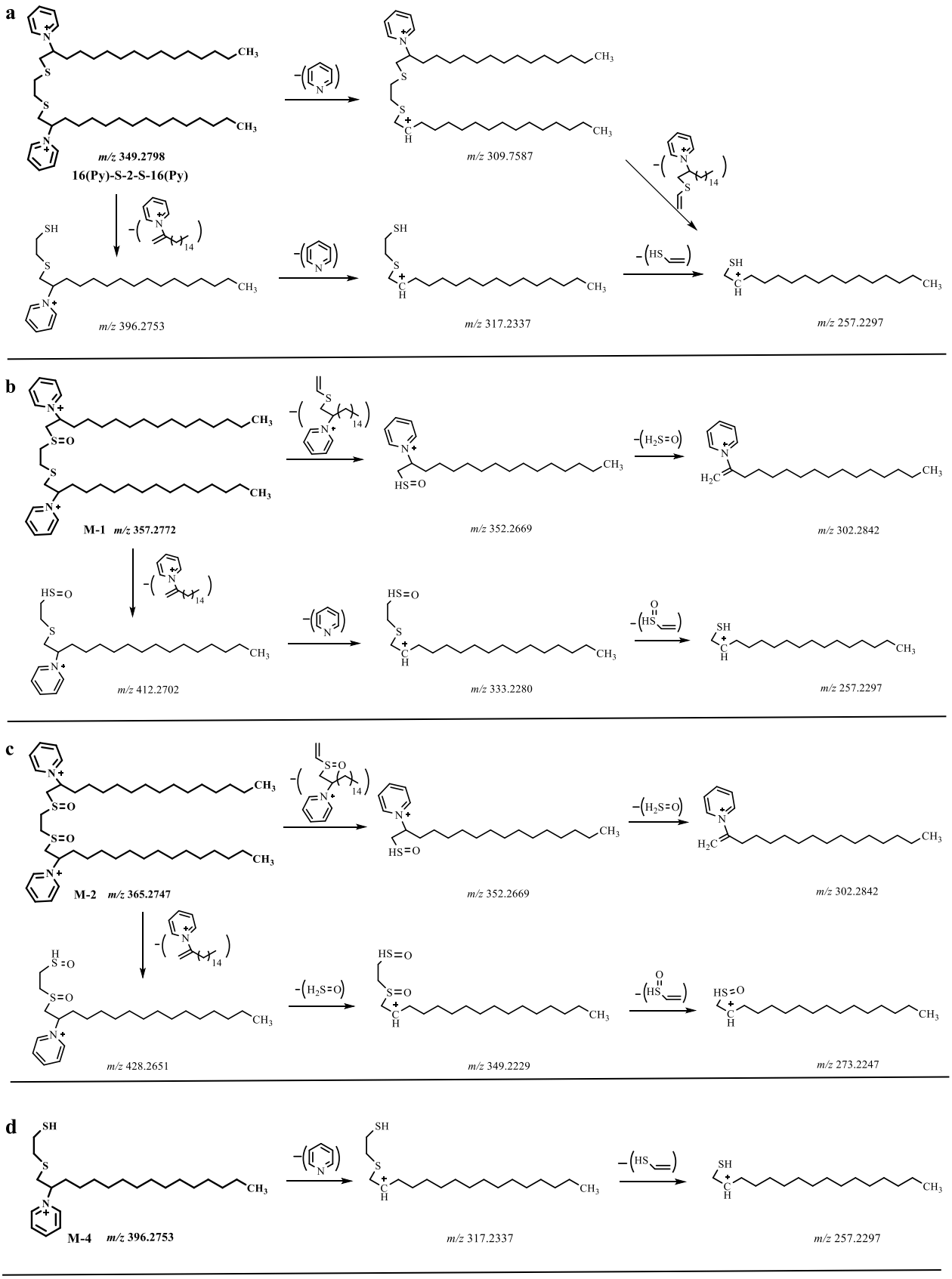
a
m/z 349.2798
16(Py)-S-2-S-16(Py)
m/z 309.7587
m/z 396.2753
m/z 317.2337
m/z 257.2297
b
M-1 m/z 357.2772
m/z 352.2669
m/z 302.2842
m/z 412.2702
m/z 333.2280
m/z 257.2297
c
M-2 m/z 365.2747
m/z 352.2669
m/z 302.2842
m/z 428.2651
m/z 349.2229
m/z 273.2247
d
M-4 m/z 396.2753
m/z 317.2337
m/z 257.2297

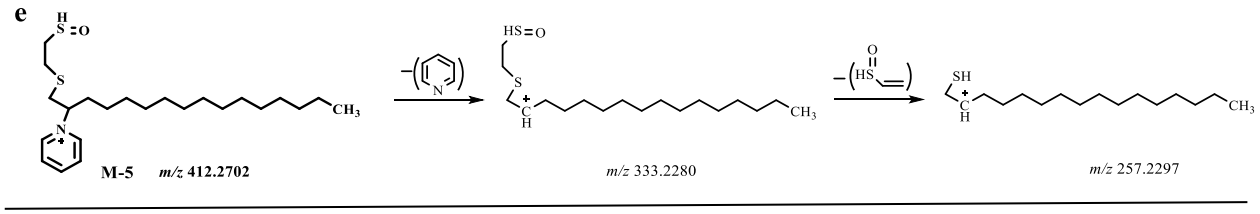

Figure 4.3. The proposed structures of major product ions of 16(Py)-S-2-S-16(Py) and its metabolites. a) 16(Py)-S-2-S-16(Py), b) M-1, c) M-2, d) M-4, and e) M-5.

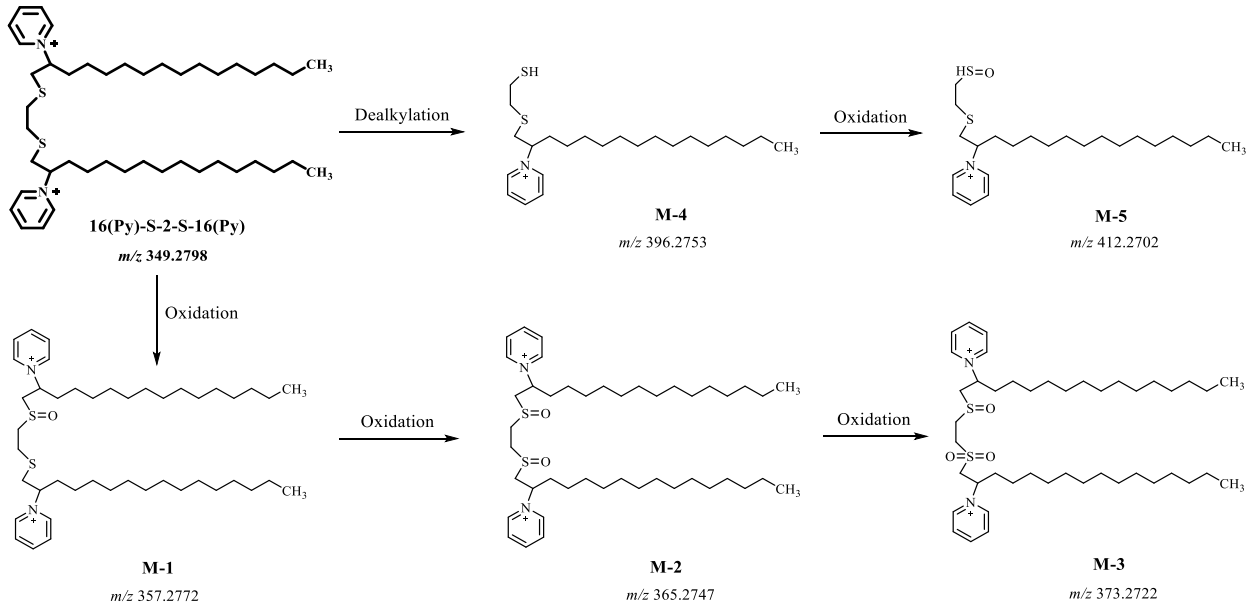

Figure 4.4. The metabolites of 16(Py)-S-2-S-16(Py) and its proposed metabolic pathway.

4.4.3 MS/MS analysis of 16-7N(GK)-16 and its metabolites

MS/MS analysis of 16-7N(GK)-16 showed characteristic product ions at *m/z* 283.2132, 276.7643, 270.3153, and 268.2510 (Figure 4.5a). The doubly charged product ion at *m/z* 276.7643 was formed *via* deamination of the tail region and subsequent deamination of the second tail region resulted in the singly charged product ion at *m/z* 283.2132. Conversely, the product ion at *m/z* 276.7643 could instead lose an ammonia moiety to form a doubly charged ion containing a 6-membered ring observed at *m/z* 268.2510. Subsequent dealkylation of this ion, by losing the spacer group with its

attached amino acid, results in the formation of the product ion at *m/z* 270.3153 (Figure 4.6a). This fragmentation pattern is consistent with what was previously obtained *via* collision induced dissociation (CID) on a Q-LIT instrument [29]. In a similar manner, the deuterated gemini surfactant 16-7N(GK)-16-D_4 produced characteristic product ions with the expected mass shift of 2.0136 Da at *m/z* 287.2389, 278.7767, 270.3151, and 270.2637 (Figure 4.S8a in supporting information).

The metabolite M-a was proposed to be an acetylation product of 16-7N(GK)-16, with an accurate mass at *m/z* 432.4238, corresponding to N-acetylation (42.0106 Da) of the original structure. However, the precise location of substitution on the lysine could not be determined (shown for illustration on the lysine side chain), as the acetylation products with both primary amines generate the same characteristic product ions. MS/MS analysis showed that M-a has the expected characteristic product ions at *m/z* 297.7698, 276.7638, 270.3154, and 268.2511 (Figure 4.5b). The product ion at *m/z* 297.7698 is a deamination product containing an acetyl moiety (Figure 4.6b); whereas the product ions at *m/z* 276.7638, 268.2511, and 270.3154 were formed through sequential deacetylation, loss of ammonia, and eventual N-dealkylation (Figure 4.6b), similar to the formation of the same product ions observed for 16-7N(GK)-16 (Figure 4.6a). As expected, the deuterated gemini surfactant 16-7N(GK)-16-D_4 also showed corresponding metabolite, M-a', with an accurate mass at *m/z* 434.4362 (Figure 4.S3 in supporting information), which displayed characteristic product ions at *m/z* 299.7821, 278.7776, and 270.3162 (Figure 4.S8b in supporting information), supporting the proposed acetylation reaction.

Similar to metabolite M-a, metabolites M-b and M-c were also determined to be the acetylation-related products of 16-7N(GK)-16, with accurate masses at *m/z* 439.4317 and 447.4291, respectively. These two metabolites were formed *via* acetylation, followed by methylation in case

of M-b and methylation along with hydroxylation for M-c. Acetylation is shown on the terminal amine on the lysine side chain, and methylation on the backbone amine for illustrative purposes as the precise location of N-acetylation and N-methylation on lysine could not be determined. M-b has characteristic product ions at *m/z* 304.7587, 276.7651, 270.3150, and 268.2498 (Figure 4.5c), which were formed *via* deamination, loss of acetyl and methyl groups, loss of an ammonia, and N-dealkylation, respectively (Figure 4.6c); whereas M-c showed characteristic product ions at *m/z* 312.7746, 296.7601, 289.7542, and 270.3150 (Figure 4.5d), which were generated through deamination, loss of a methanol, loss of an ammonia, loss of a methyl group, and N-dealklyation (Figure 4.6d). The formation of these product ions is similar to that of the product ions observed for metabolite M-a (Figure 4.5a). The deuterated gemini surfactant 16-7N(GK)-16-D_4 also exhibited corresponding metabolites M-b' (*m/z* 441.4438) and M-c' (*m/z* 449.4413), which displayed similar fragmentation patterns (Figures 4.S8c and d in supporting information) as those of metabolites M-b and M-c, supporting the proposed metabolite pathway .

In addition, metabolites M-d, M-e and M-f were observed with accurate masses at *m/z* 492.4448, 530.5334, and 544.5491, which were determined to be phase II metabolites of 16-7N(GK)-16 with the addition of glucose, palmitoyl, and stearyl groups, respectively (Figures 4.6e and f, substitution shown on the terminal amine of lysine). Due to low ion abundance, the MS/MS spectra of metabolite M-d was not obtained; the structure of M-d was proposed based on accurate mass measurement (Table 4.1 and Figure 4.S4 in supporting information). In contrast, the MS/MS spectrum for metabolite M-d' of 16-7N(GK)-16-D_4 was obtained (Figure 4.S8e in supporting information), which displayed characteristic product ions at m/z 359.8058, 287.2389, 278.7776, and 270.3152, suggesting a glucose moiety attached to the structure (Figure S9 in supporting information).

Similarly, metabolite M-e showed characteristic product ions at *m/z* 395.8799, 283.2132, 276.7643, 270.3158, and 268.2517 (Figure 4.5e). The doubly charged product ion at *m/z* 395.8799 was formed *via* deamination, which further underwent the loss of one palmitoyl group to produce the ion at *m/z* 276.7643. Subsequent loss of ammonia, deamination of the tail region, and dealkylation of the spacer resulted in the formation of the ions at *m/z* 268.2517, 283.2132, and 270.3158 (Figure 4.6e), similar to the formation of the same product ions of 16-7N(GK)-16 (Figure 4.6a). The metabolite M-f displayed characteristic product ions at *m/z* 409.8953, 283.2123, 276.7648, 270.3166, and 268.2505 (Figure 4.5f); these ions were formed in a manner similar to the generation of the characteristic product ions of M-e (Figure 4.6f). As anticipated, the deuterated gemini surfactant 16-7N(GK)-16-D_4 showed corresponding metabolites M-e' and M-f', with the expected mass shift of 2.0136 Da at *m/z* 532.5454 and 546.5611 (Figure 4.S3 and table 4.S1 in supporting information), which displayed similar product ions as those of metabolites M-e and M-f (Figures 4.S8f and g in supporting information), suggesting the accuracy of the proposed metabolic reactions.

According to the suggested structures of the metabolites, a metabolic pathway of the gemini surfactant 16-7N(GK)-16 is described (Figure 4.7), showing that phase II metabolic reactions mainly occur for this compound. Specifically, the gemini surfactant 16-7N(GK)-16 can be metabolized *via* acetylation, acetylation with methylation, and acetylation with methylation and hydroxylation to generate a variety of acetylation-related products. In addition, it also can be metabolized through various conjugation processes, such as glucose conjugation, palmitoyl conjugation, and stearyl conjugation, to produce conjugated metabolites. Such a metabolic pathway is supported by the metabolites of the deuterated gemini surfactant 16-7N(GK)-16-D_4 (Figure 4.S10 in supporting information).

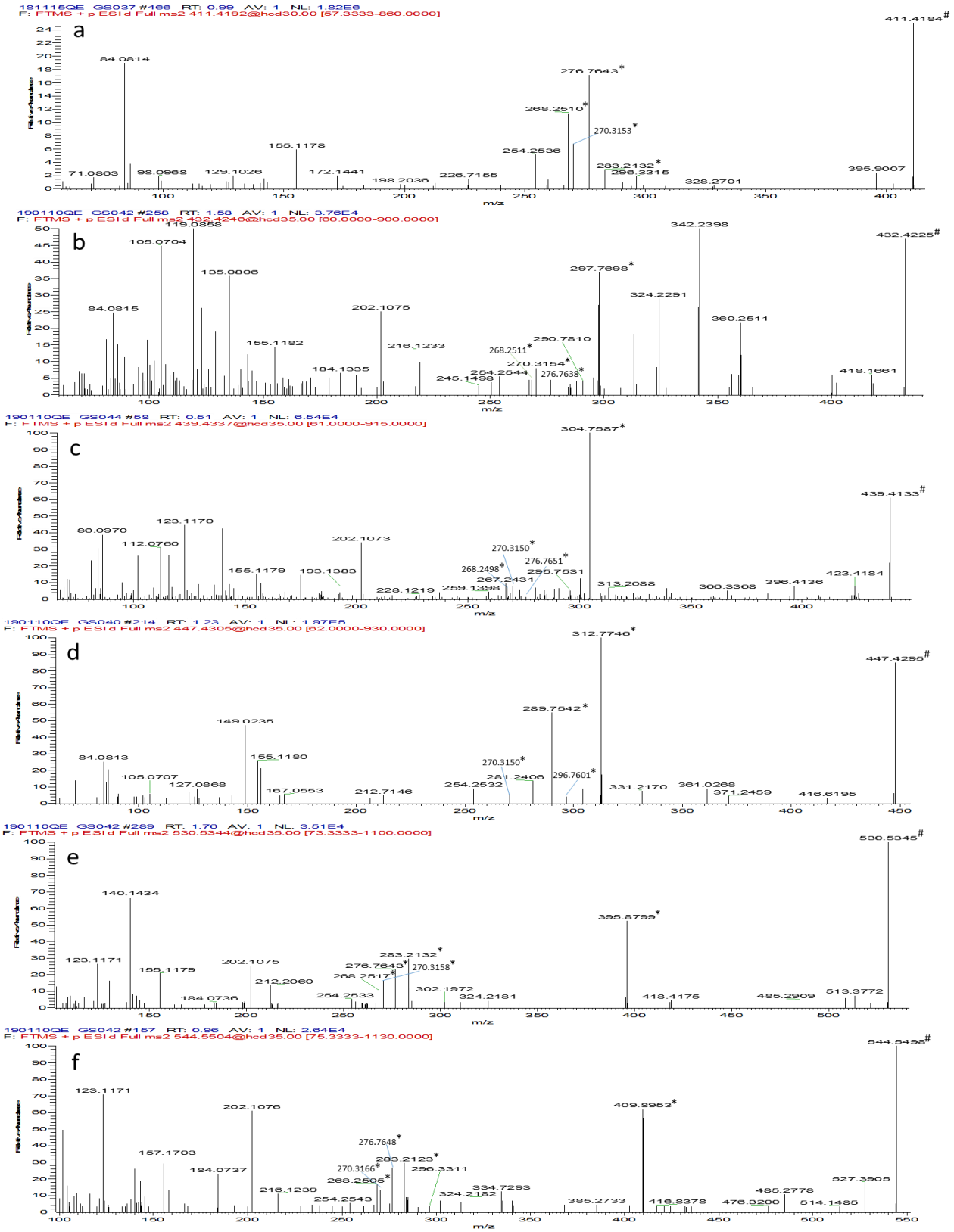

Figure 4.5. The MS/MS spectra of 16-7N(GK)-16 and its metabolites: a) 16-7N(GK)-16, b) M-a, c) M-b, d) M-c, e) M-e, and f) M-f. ($^{\#}$ denotes the parent ion and * denotes the diagnostic product ion). The MS/MS spectra of M-d is not available due to low ion abundance.

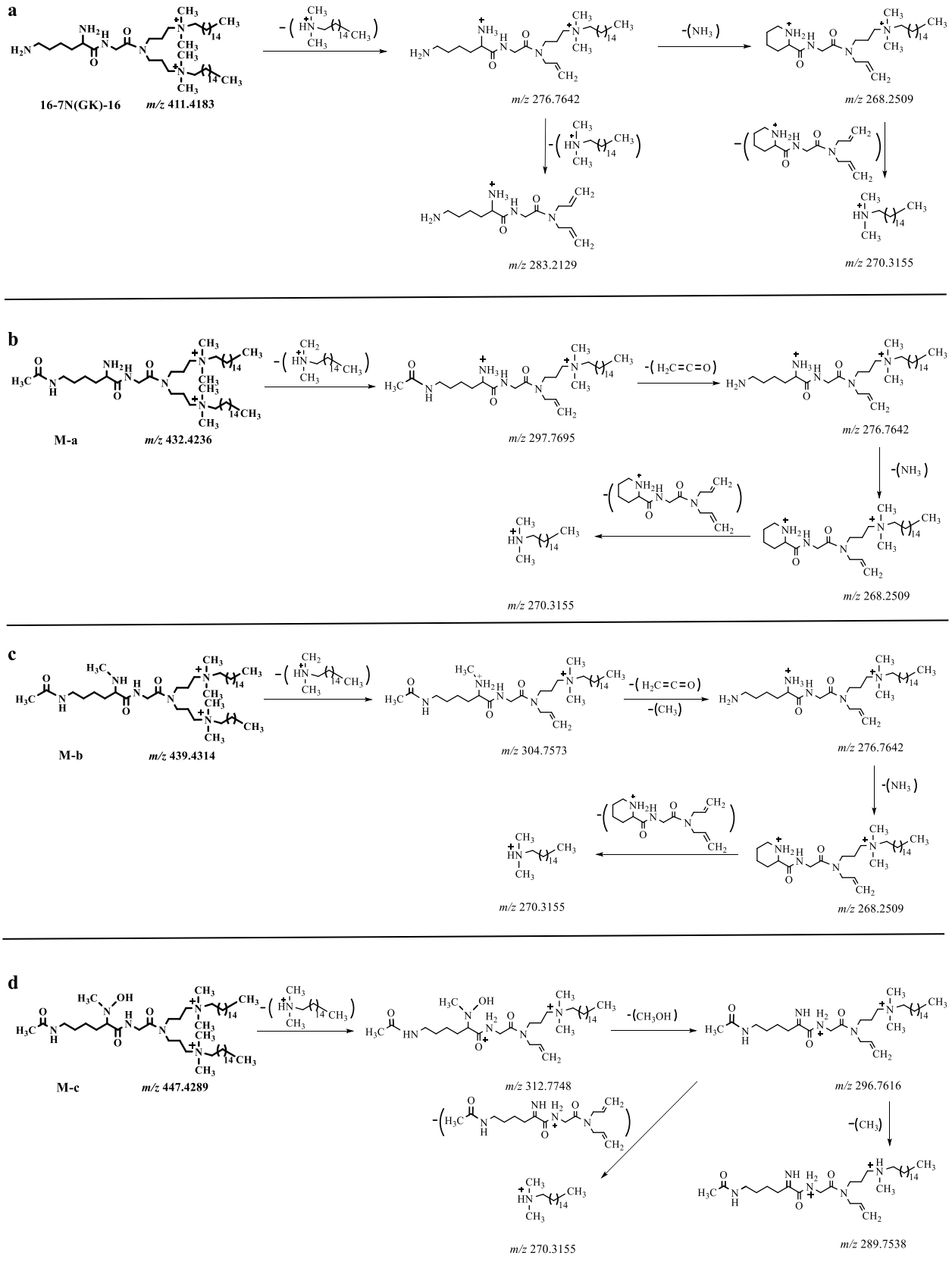
a
16-7N(GK)-16
m/z 411.4183
m/z 276.7642
m/z 268.2509
m/z 283.2129
m/z 270.3155
b
M-a
m/z 432.4236
m/z 297.7695
m/z 276.7642
m/z 268.2509
m/z 270.3155
c
M-b
m/z 439.4314
m/z 304.7573
m/z 276.7642
m/z 268.2509
m/z 270.3155
d
M-c
m/z 447.4289
m/z 312.7748
m/z 296.7616
m/z 289.7538
m/z 270.3155

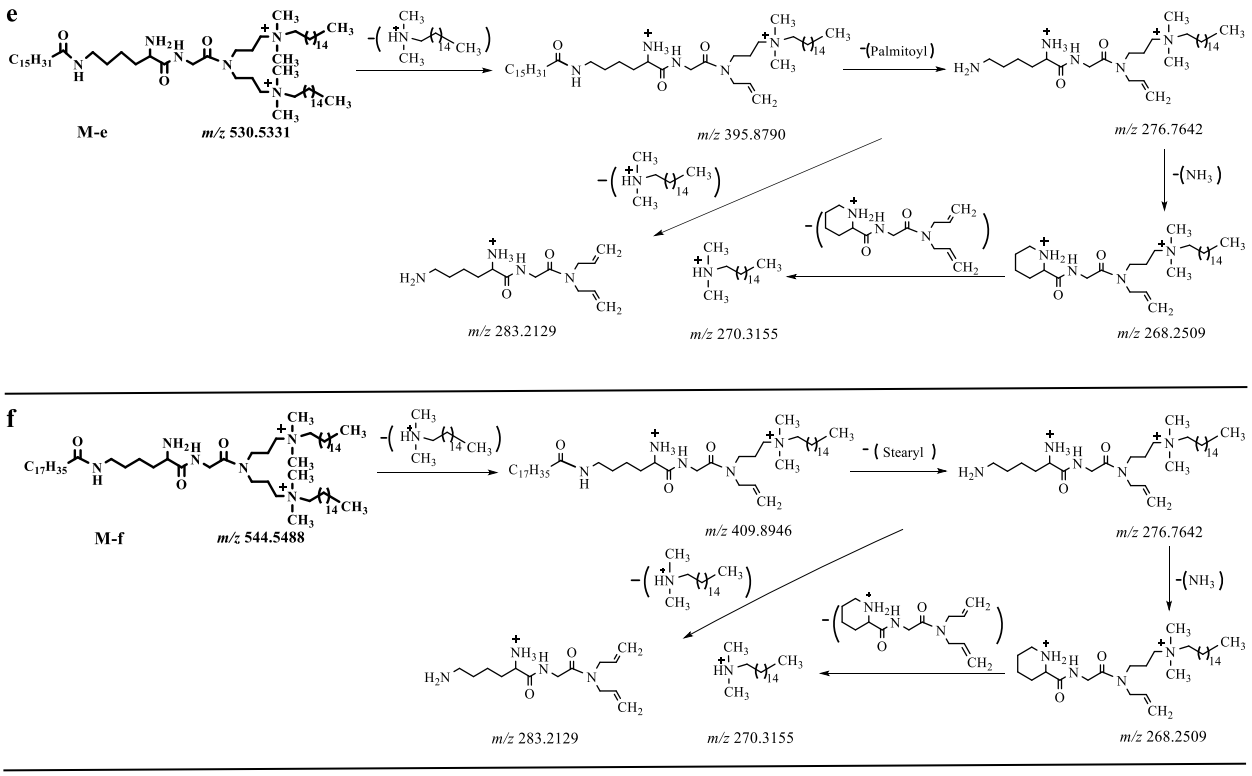

Figure 4.6. The proposed structures of major product ions of 16-7N(GK)-16 and its metabolites: a) 16-7N(GK)-16, b) M-a, c) M-b, d) M-c, e) M-e, and f) M-f.

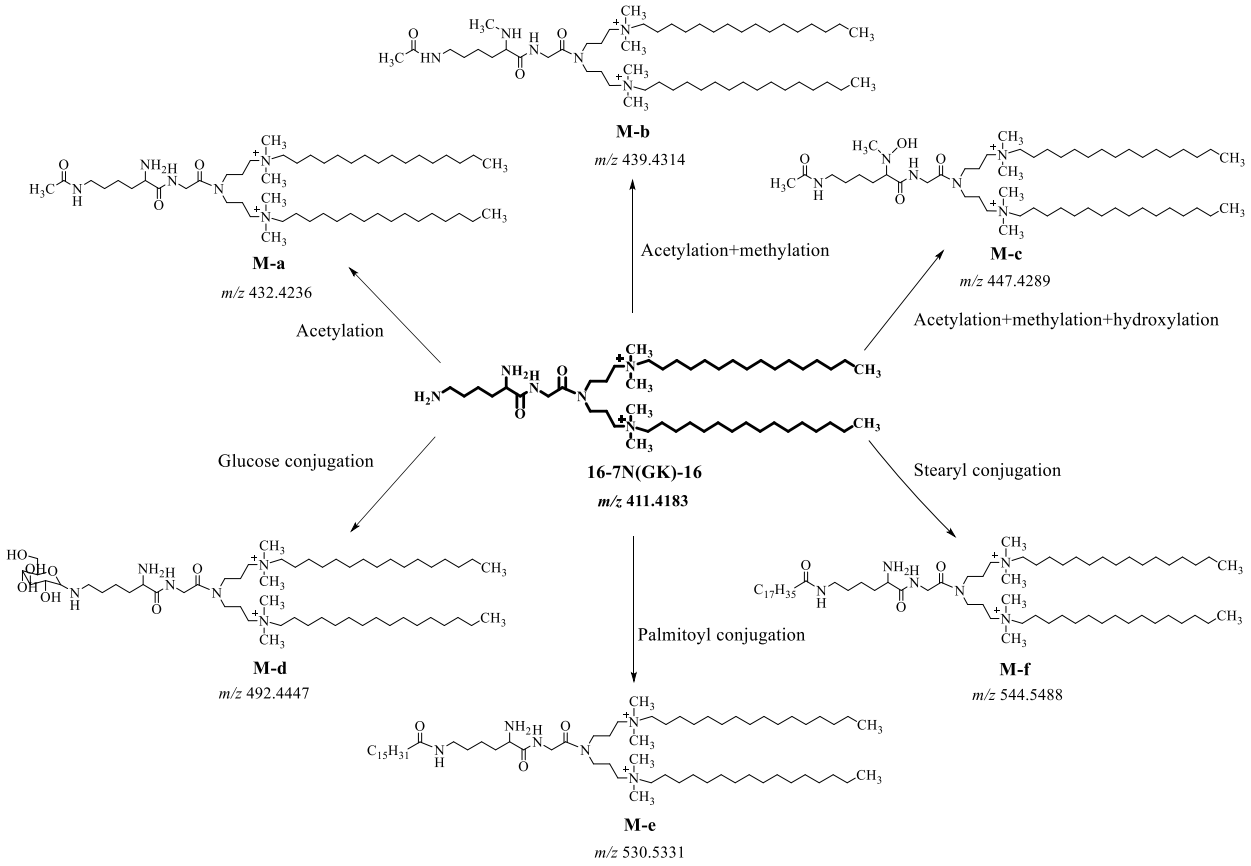

Figure 4.7. The metabolites of 16-7N(GK)-16 and its proposed metabolic pathway.

4.4.4 Significance of gemini surfactant cellular metabolism

Ideally, lipid-based nanoparticles should deliver their therapeutic materials to the desired site(s), followed by degradation and excretion, to achieve optimal efficiency and minimal toxicity. However, the release of therapeutic agents and degradation of nanoparticles may take place at any time during the delivery process, which can result in reduced efficiency and increased toxicity. Furthermore, the longer the nanoparticles remain inside the biological systems, the higher toxicity they may cause [30]. In addition, the cellular metabolism of the building blocks of the nanoparticles might be harmful to host cells, contributing to the overall toxicity of the delivery systems [7].

Phase I and II biotransformations are common pathways for drugs and other foreign substances to be detoxified and eliminated [31, 32]. Although liver is the principal organ of drug metabolism, other tissues, such as the gastrointestinal tract, the lungs, the skin, the kidneys, and the brain, also display considerable enzymatic activities [33-35]. In particular, both phase I and phase II drug metabolizing enzymes, such as cytochrome P450 and UDP-glucuronosyltransferase, have been reported in the mammalian skin [36, 37]. The gemini surfactant 16-3-16 was found to be a non-biodegradable in PAM 212 cells as there was not metabolite determined for this compound. This suggests that 16-3-16 will likely remain intact during detoxification and cellular elimination. It is also possible that metabolism was minimum and the current instrument was not sufficiently sensitive to detect minor metabolite formation for 16-3-16.

Although the gemini surfactants 16(Py)-S-2-S-16(Py) and 16-7N(GK)-16 were metabolized in PAM 212 cells, they underwent different biotransformation pathways. Phase I reactions, including oxidation and dealkylation, mainly occurred for 16(Py)-S-2-S-16(Py), resulting in oxidized and dealkylated products. In contrast, 16-7N(GK)-16 was primarily metabolized *via* phase II reactions, such as methylation, acetylation, glucose conjugation, palmityl conjugation, and stearyl conjugation, which generated a variety of metabolized products. However, the roles of these metabolites regarding gene delivery efficiency and cellular toxicity remain unclear and more research needs to be conducted to better understand their metabolic pathways. In general, hydrophilic phase II metabolites are more rapidly excreted and less toxic compared to phase I metabolites in biological systems [38]. As the gemini surfactant 16-7N(GK)-16 has been shown to be less toxic than 16(Py)-S-2-S-16(Py) [24, 26], this could be the result of the formation of phase II metabolites of 16-7N(GK)-16, leading to more rapid clearance than the phase I metabolites of 16(Py)-S-2-S-16(Py). In addition, phase I metabolites, such as M-4, could be involved in reactions

with thiol groups in proteins, potentially contributing to toxicity. During the data analysis, we observed additional peaks associated with chloride and formic acid adducts, as well as possible amino acid and peptide adducts/conjugates, which will be further confirmed to evaluate their biological impact. Furthermore, the Bligh-Dyer extraction method might not be efficient in extracting relatively polar metabolites of gemini surfactants, possibly resulting in not identifying them. Future studies will be conducted using various sample extraction methods to improve the coverage of possible gemini surfactant metabolites. For example, Al-Dulaymi et al [25] has reported a modified Folch method that provides high extraction recovery for gemini surfactants with more hydrophilic nature. In addition, the amount of the metabolites of tested gemini surfactants have not been determined in this study, future studies should also include the quantification of these metabolites using LC-MS/MS to further investigate their roles in biological systems.

The current work provides a foundation study describing the various metabolic pathways. To further understand the role of these metabolites, we will confirm their structures with synthesized standards and assess the rate of metabolite formation, which will allow their roles with respect to efficiency and toxicity to be determined.

4.5 Conclusions

The metabolism of the three gemini surfactants 16-3-16, 16(Py)-S-2-S-16(Py), and 16-7N(GK)-16 were investigated using a high-resolution quadrupole-Orbitrap mass spectrometer instrument, and the structures of their metabolites were characterized based on accurate mass measurements and their corresponding MS/MS analysis. The gemini surfactant 16-3-16 was found not to be metabolized in PAM 212 cells. The gemini surfactant 16(Py)-S-2-S-16(Py) was metabolized

primarily *via* phase I reactions, generating metabolized products that could contribute to its high toxicity; while 16-7N(GK)-16 was metabolized mainly *via* phase II reactions, resulting in metabolites that could lead to its low toxicity in gene transfection. The metabolism of 16-7N(GK)-16 indicates that a phase II reaction-prone moiety, such as an amino acid, in the structure could play an important role for degradation and elimination of gemini surfactants, thus reducing its potential toxicity. In the future, we will be identifying the structures of the metabolites and evaluating the rate of metabolism. Finally, the reported approach can be applied to study metabolite formation of other gemini surfactants in various families for better understanding of their toxicities.

4.6 Acknowledgements

We would like to thank Drs. Jackson M. Chitanda and McDonald Donkuru for the synthesis of all gemini surfactants. We also thank Dr. Waleed Mohammed-Saeid for the training in cell transfection and purification of plasmid DNA. Centre for Veterinary Drug Residues, Canadian Food Inspection Agency is acknowledged for access to the Q-Exactive system. A postgraduate scholarship for Wei Jin is provided by the Natural Sciences and Engineering Research Council of Canada (NSERC). The research is supported by a NSERC Discovery Grant.

4.7 References

1. Wettig, S.D., R.E. Verrall, and M. Foldvari, *Gemini surfactants: a new family of building blocks for non-viral gene delivery systems.* Current gene therapy, 2008. **8**(1): p. 9-23.
2. Donkuru, M., et al., *Advancing nonviral gene delivery: lipid-and surfactant-based nanoparticle design strategies.* Nanomedicine, 2010. **5**(7): p. 1103-1127.
3. Bombelli, C., et al., *Gemini surfactant based carriers in gene and drug delivery.* Current medicinal chemistry, 2009. **16**(2): p. 171-183.
4. Makhlouf, A., I. Hajdu, and I. Badea, *Gemini surfactant-based systems for drug and gene delivery*, in *Organic Materials as Smart Nanocarriers for Drug Delivery*. 2018, Elsevier. p. 561-600.
5. Karlsson, L., M.C. van Eijk, and O. Söderman, *Compaction of DNA by gemini surfactants: effects of surfactant architecture.* Journal of colloid and interface science, 2002. **252**(2): p. 290-296.
6. Bombelli, C., et al., *Efficient transfection of DNA by liposomes formulated with cationic gemini amphiphiles.* Journal of medicinal chemistry, 2005. **48**(16): p. 5378-5382.
7. Singh, J., et al., *Amino acid-substituted gemini surfactant-based nanoparticles as safe and versatile gene delivery agents.* Curr Drug Deliv, 2011. **8**(3): p. 299-306.
8. Van Der Woude, I., et al., *Novel pyridinium surfactants for efficient, nontoxic in vitro gene delivery.* Proceedings of the National Academy of Sciences, 1997. **94**(4): p. 1160-1165.
9. Mohammed-Saeid, W., et al., *Development of lyophilized gemini surfactant-based gene delivery systems: influence of lyophilization on the structure, activity and stability of the lipoplexes.* Journal of Pharmacy & Pharmaceutical Sciences, 2012. **15**(4): p. 548-567.
10. Singh, J., et al., *Evaluation of cellular uptake and intracellular trafficking as determining factors of gene expression for amino acid-substituted gemini surfactant-based DNA nanoparticles.* J Nanobiotechnology, 2012. **10**(7): p. 1-14.
11. Ramamoorth, M. and A. Narvekar, *Non viral vectors in gene therapy-an overview.* Journal of clinical and diagnostic research, 2015. **9**(1): p. GE01-06.
12. Al-Dosari, M.S. and X. Gao, *Nonviral gene delivery: principle, limitations, and recent progress.* The AAPS journal, 2009. **11**(4): p. 671-681.
13. Singh, J., et al., *Amino acid-substituted gemini surfactant-based nanoparticles as safe and versatile gene delivery agents.* Current drug delivery, 2011. **8**(3): p. 299-306.

14. Rose, R.J., et al., *High-sensitivity Orbitrap mass analysis of intact macromolecular assemblies.* Nature methods, 2012. **9**(11): p. 1084-1086.
15. Michalski, A., et al., *Mass spectrometry-based proteomics using Q Exactive, a high-performance benchtop quadrupole Orbitrap mass spectrometer*. Molecular & Cellular Proteomics, 2011. **10**(9): p. 1-10.
16. Jiwan, J.-L.H., P. Wallemacq, and M.-F. Hérent, *HPLC-high resolution mass spectrometry in clinical laboratory?* Clinical biochemistry, 2011. **44**(1): p. 136-147.
17. Solliec, M., A. Roy-Lachapelle, and S. Sauvé, *Quantitative performance of liquid chromatography coupled to Q-Exactive high resolution mass spectrometry (HRMS) for the analysis of tetracyclines in a complex matrix.* Analytica chimica acta, 2015. **853**: p. 415-424.
18. Buse, J., et al., *Tandem mass spectrometric analysis of the novel gemini surfactant nanoparticle families G12-s and G18: 1-s.* Spectroscopy Letters, 2010. **43**(6): p. 447-457.
19. Wang, J. and P.R. Gardinali, *Identification of phase II pharmaceutical metabolites in reclaimed water using high resolution benchtop Orbitrap mass spectrometry.* Chemosphere, 2014. **107**: p. 65-73.
20. Bhadani, A. and S. Singh, *Novel gemini pyridinium surfactants: synthesis and study of their surface activity, DNA binding, and cytotoxicity.* Langmuir, 2009. **25**(19): p. 11703-11712.
21. Al-Dulaymi, M.A., et al., *Di-Peptide-Modified Gemini Surfactants as Gene Delivery Vectors: Exploring the Role of the Alkyl Tail in Their Physicochemical Behavior and Biological Activity.* The AAPS journal, 2016. **18**(5): p. 1168-1181.
22. Badea, I., et al., *In vivo cutaneous interferon-gamma gene delivery using novel dicationic (gemini) surfactant-plasmid complexes.* J Gene Med, 2005. **7**(9): p. 1200-1214.
23. Donkuru, M., et al., *Designing pH-sensitive gemini nanoparticles for non-viral gene delivery into keratinocytes.* Journal of Materials Chemistry, 2012. **22**(13): p. 6232-6244.
24. Al-Dulaymi, M., et al., *Molecular Engineering as an Approach To Modulate Gene Delivery Efficiency of Peptide-Modified Gemini Surfactants.* Bioconjugate chemistry, 2018. **29**(10): p. 3293-3308.
25. Al-Dulaymi, M., et al., *The development of simple flow injection analysis tandem mass spectrometric methods for the cutaneous determination of peptide-modified cationic gemini surfactants used as gene delivery vectors.* Journal of pharmaceutical and biomedical analysis, 2018. **159**: p. 536-547.

26. Jin, W., et al., *Cellular Uptake and Distribution of Gemini Surfactant Nanoparticles Used as Gene Delivery Agents.* The AAPS journal, 2019. **21**(5): p. 98.
27. Bligh, E.G. and W.J. Dyer, *A rapid method of total lipid extraction and purification.* Canadian journal of biochemistry and physiology, 1959. **37**(8): p. 911-917.
28. Donkuru, M., et al., *Multi-stage tandem mass spectrometric analysis of novel β-cyclodextrin-substituted and novel bis-pyridinium gemini surfactants designed as nanomedical drug delivery agents.* Rapid Communications in Mass Spectrometry, 2014. **28**(7): p. 757-772.
29. Al-Dulaymi, M. and A. El-Aneed, *Tandem mass spectrometric analysis of novel peptide-modified gemini surfactants used as gene delivery vectors.* Journal of Mass Spectrometry, 2017. **52**(6): p. 353-366.
30. Vega-Villa, K.R., et al., *Clinical toxicities of nanocarrier systems.* Advanced drug delivery reviews, 2008. **60**(8): p. 929-938.
31. Brodie, B.B., J.R. Gillette, and B.N. La Du, *Enzymatic metabolism of drugs and other foreign compounds.* Annual review of biochemistry, 1958. **27**(1): p. 427-454.
32. Omiecinski, C.J., et al., *Xenobiotic metabolism, disposition, and regulation by receptors: from biochemical phenomenon to predictors of major toxicities.* Toxicological Sciences, 2010. **120**(suppl_1): p. S49-S75.
33. Gonzalez, F.J. and R.H. Tukey, *Drug metabolism.* Goodman & Gilman's. The Pharmacological Basis of Therapeutics. 11th ed. New York: McGraw-Hill, 2006: p. 71-91.
34. Pannatier, A., et al., *The skin as a drug-metabolizing organ.* Drug metabolism reviews, 1978. **8**(2): p. 319-343.
35. Lohr, J.W., G.R. Willsky, and M.A. Acara, *Renal drug metabolism.* Pharmacological reviews, 1998. **50**(1): p. 107-142.
36. Oesch, F., et al., *Drug-metabolizing enzymes in the skin of man, rat, and pig.* Drug metabolism reviews, 2007. **39**(4): p. 659-698.
37. Sharma, A.M. and J. Uetrecht, *Bioactivation of drugs in the skin: relationship to cutaneous adverse drug reactions.* Drug metabolism reviews, 2014. **46**(1): p. 1-18.
38. Klaassen, C.D. and M.O. Amdur, *Casarett and Doull's toxicology: the basic science of poisons*. 8th ed. Vol. 1236. 2013: McGraw-Hill New York. 189

4.8 Supporting information

a **16-3-16-D_{66}**

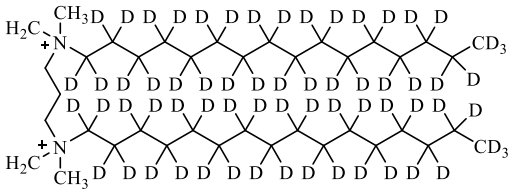

$[M]^{2+}$ *m/z* 323.51 ($C_{39}H_{18}D_{66}N_2^{2+}$)

b **16(Py)-S-2-S-16(Py)-D_{10}**

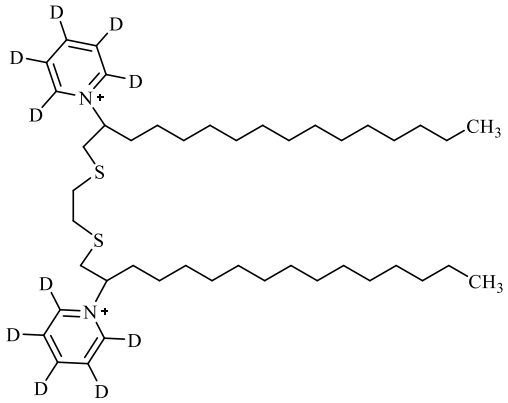

$[M]^{2+}$ *m/z* 354.31 ($C_{44}H_{68}D_{10}N_2S_2^{2+}$)

c **16-7N(GK)-16-D_4**

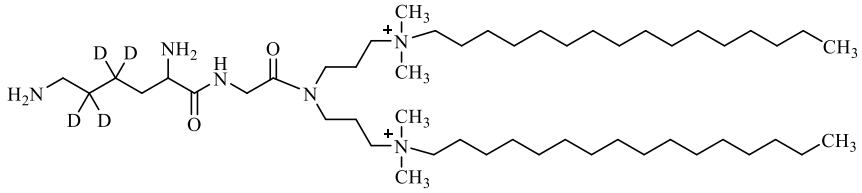

$[M]^{2+}$ *m/z* 413.43 ($C_{50}H_{102}D_4N_6O_2^{2+}$)

Figure 4.S1. The structures of deuterated gemini surfactants, a) 16-3-16-D_{66}, b) 16(Py)-S-2-S-16(Py)-D_{10}, and c) 16-7N(GK)-16-D_4.

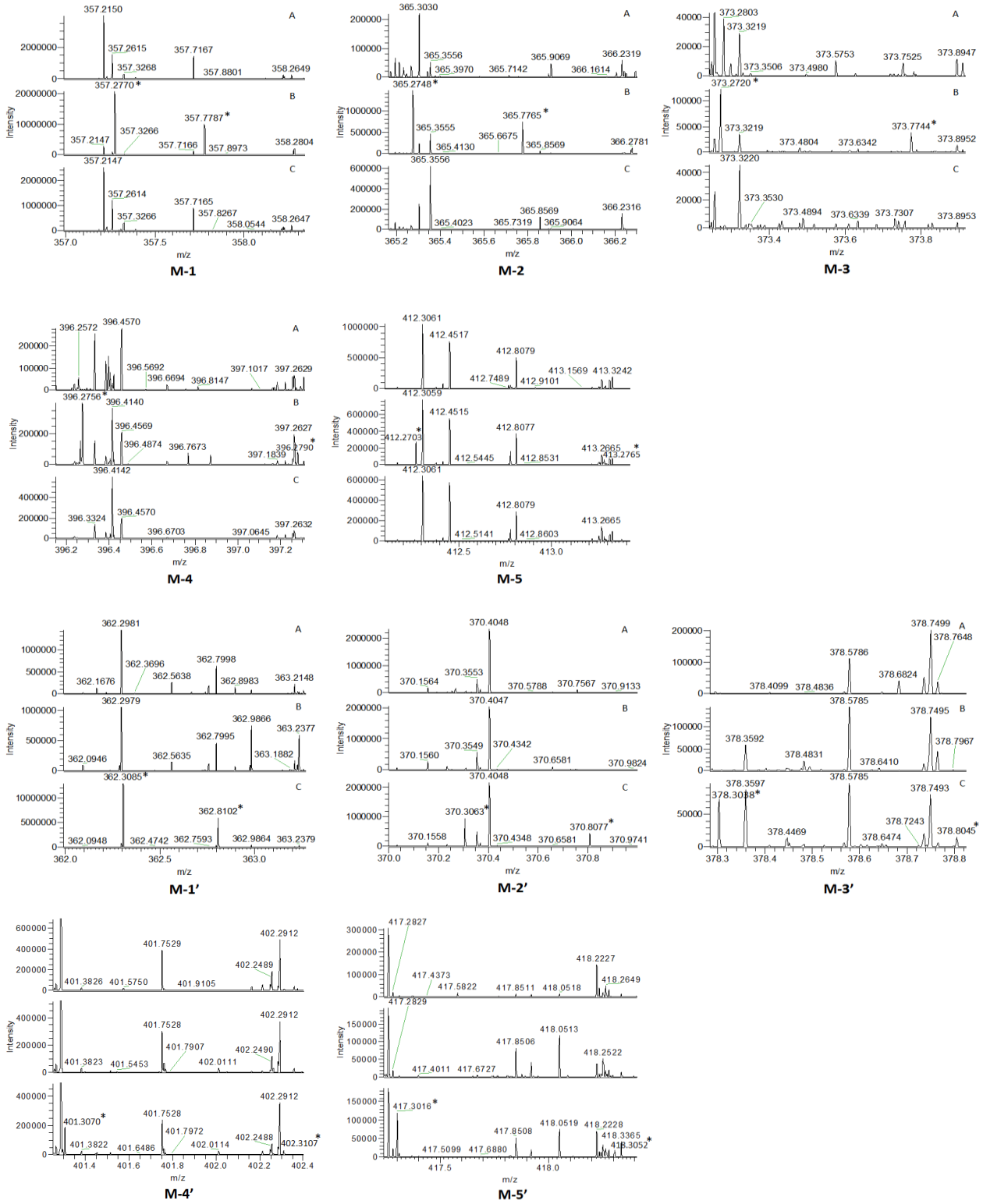

Figure 4.S2. MS spectra of the metabolites of 16(Py)-S-2-S-16(Py) and 16(Py)-S-2-S-16(Py)-D_{10} based on accurate mass measurement at 5 h of treatment. (* denotes the peak of the metabolite. panel A-control, panel B-cells treated with 16(Py)-S-2-S-16(Py) nanoparticles, and panel C-cells treated with 16(Py)-S-2-S-16(Py)-D_{10} nanoparticles. Zoomed in all three panels to show the peaks of the metabolites).

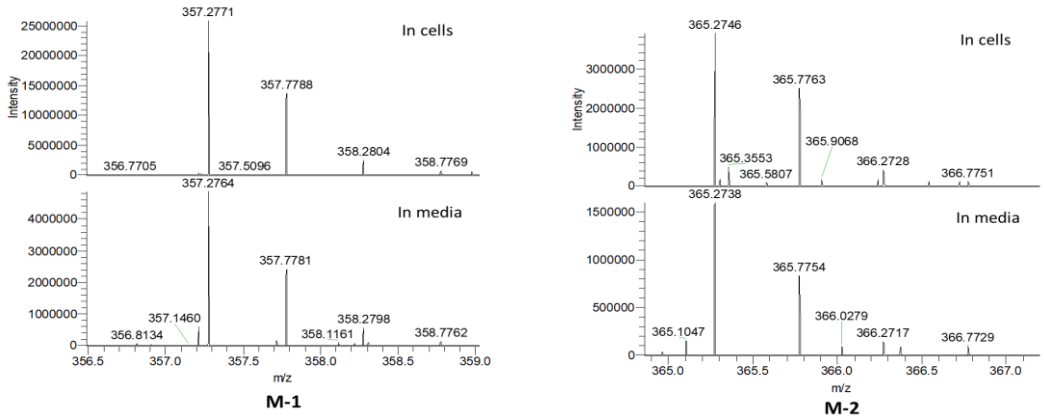

Figure 4.S3. MS spectra of metabolite M-1 and M-2 of 16(Py)-S-2-S-16(Py) produced in PAM 212 cells and media at 10 h of treatment. The ion intensity of M-1 and M-2 generated by natural oxidation of 16(Py)-S-2-S-16(Py) in media is significantly lower compared with that in cells, indicating the oxidation metabolism in cells

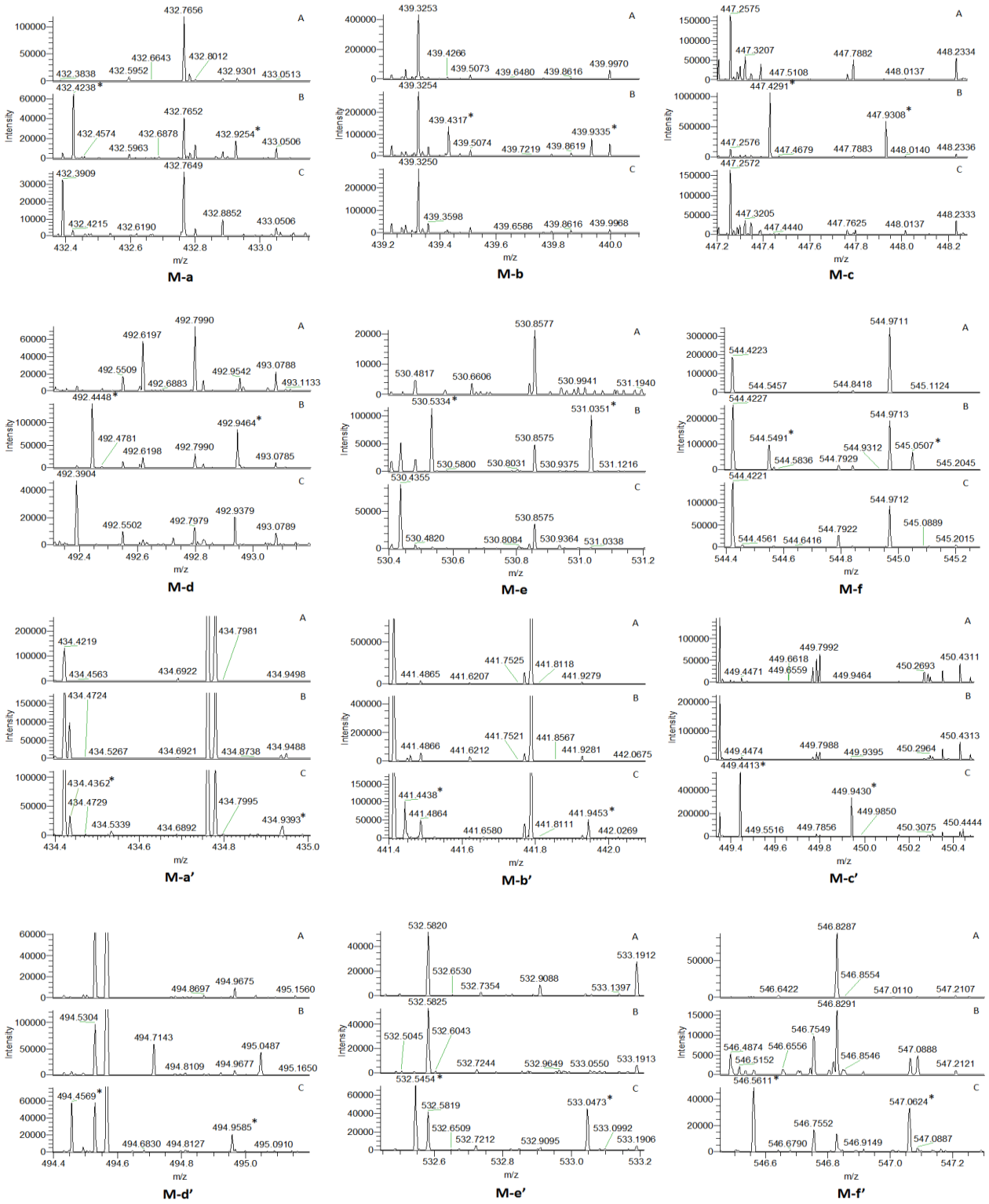

Figure 4.S4. MS spectra of the metabolites of 16-7N(GK)-16 and 16-7N(GK)-16-D_4 based on accurate mass measurement at 5 h treatment. (* denotes the peaks of the identified metabolites. panel A-control, panel B-cells treated with 16-7N(GK)-16 nanoparticles, and panel C-cells treated with 16-7N(GK)-16-D_4 nanoparticles. Zoomed in all panels to show the peaks of the metabolites).

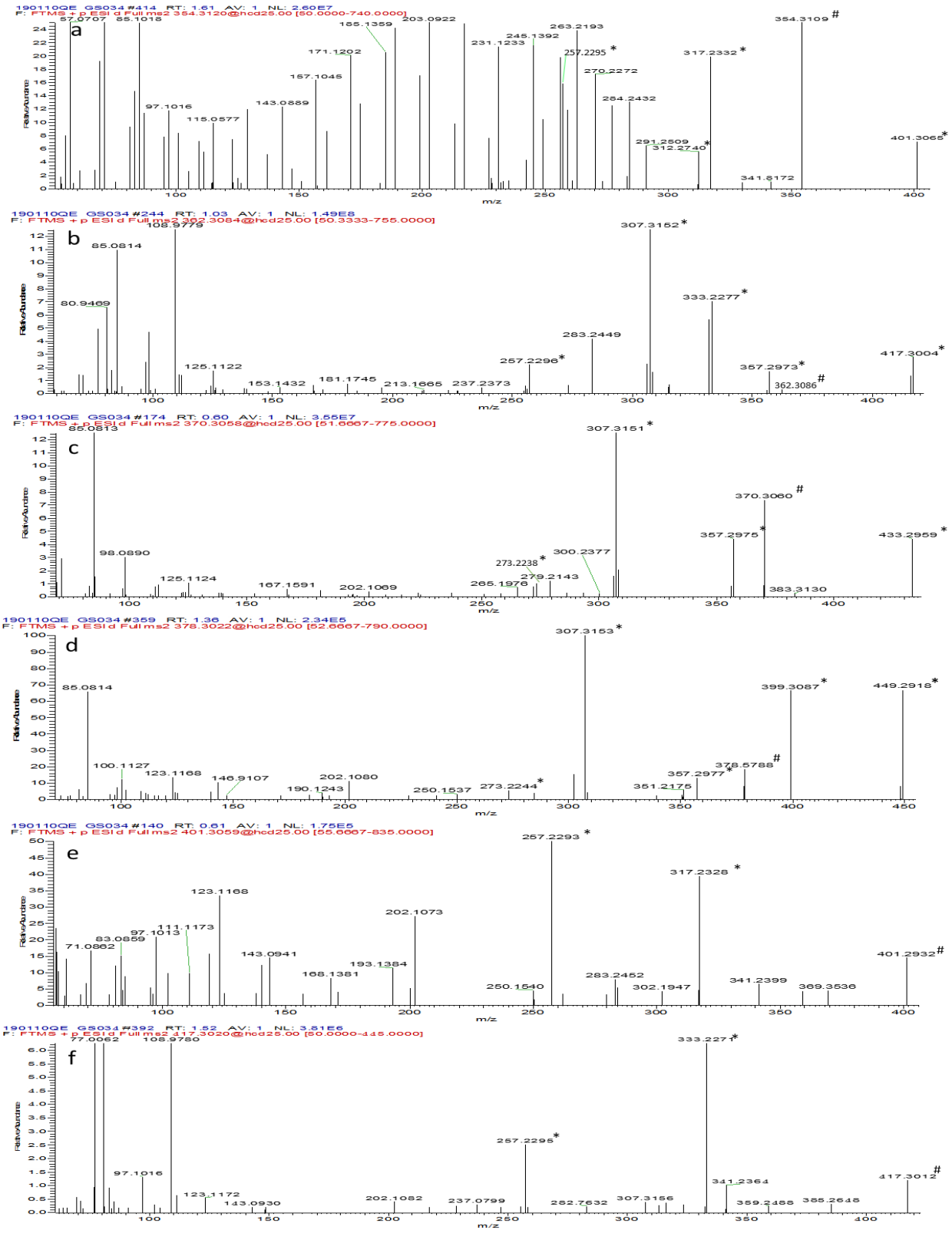

Figure 4.S5. The MS/MS spectra of 16(Py)-S-2-S-16(Py)-D_{10} and its metabolites: a) 16(Py)-S-2-S-16(Py)-D_{10}, b) M-1', c) M-2', d) M-3', e) M-4', and f) M-5' ($^{\#}$ denotes the parent ion and * denotes the diagnostic product ion).

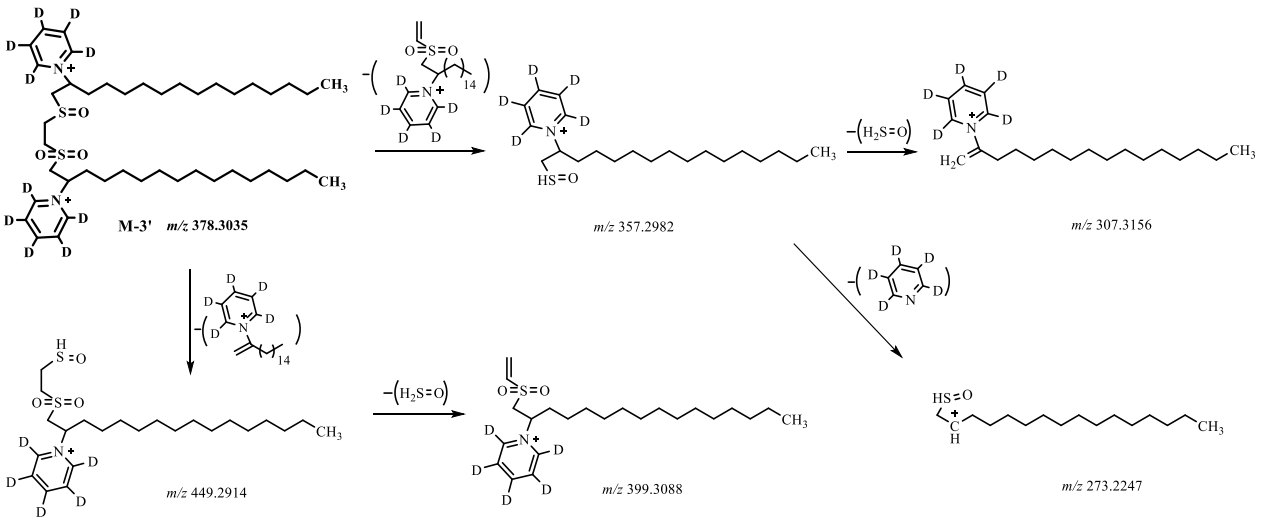

Figure 4.S6. The proposed structures of major product ions of metabolite M-3' of 16(Py)-S-2-S-16(Py)-D_{10}.

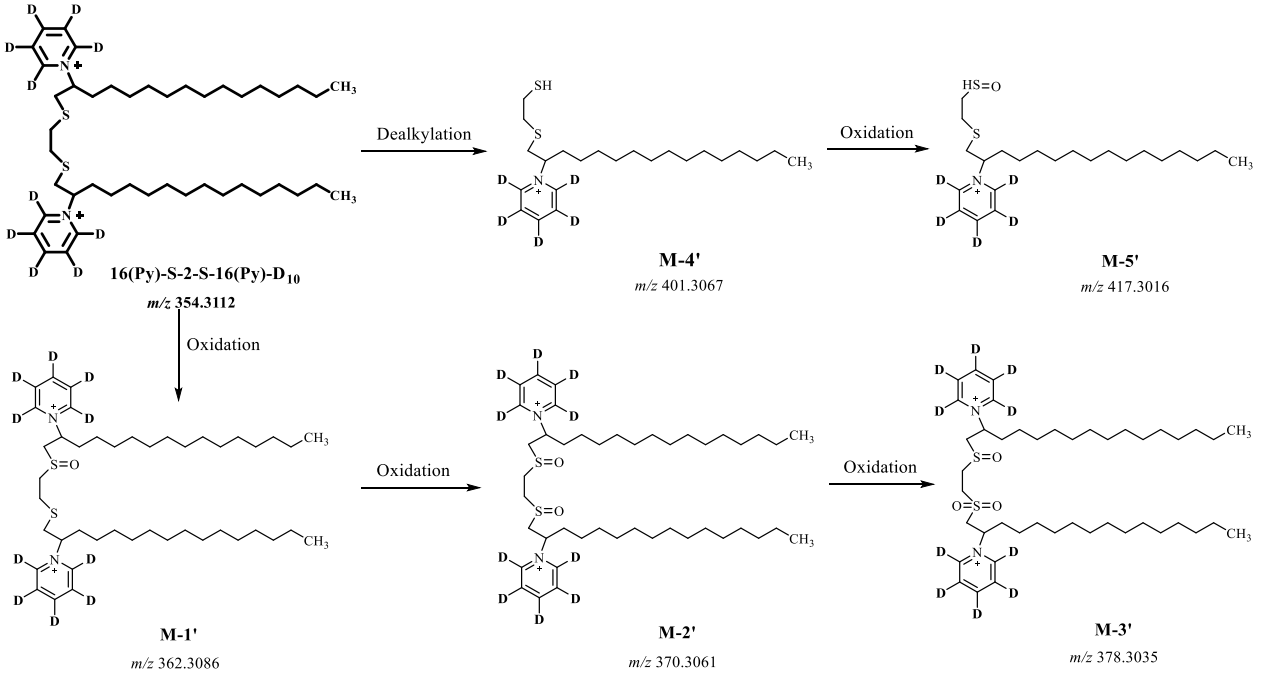

Figure 4.S7. The metabolites of 16(Py)-S-2-S-16(Py)-D_{10} and its proposed metabolic pathway.

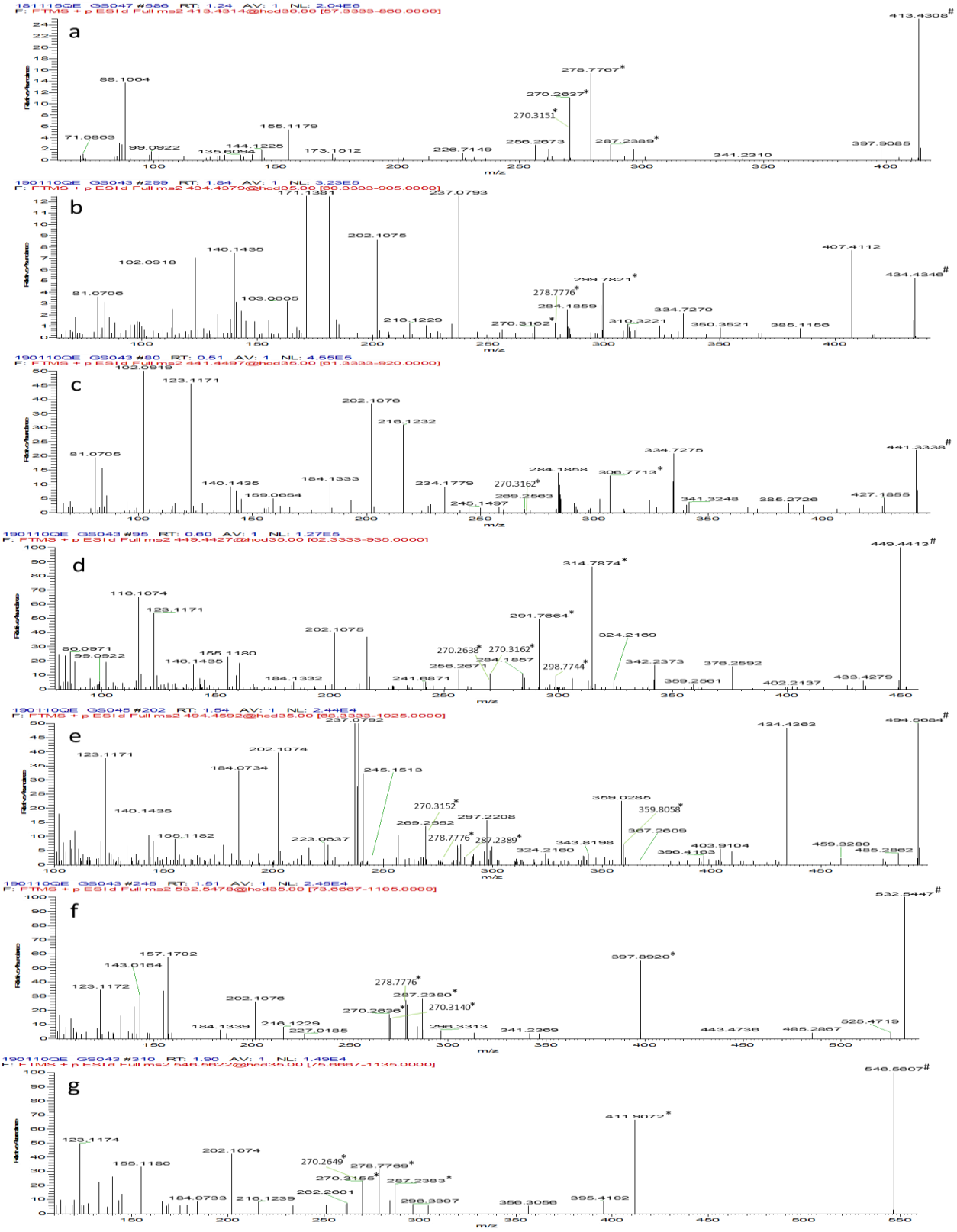

Figure 4.S8. The MS/MS spectra of 16-7N(GK)-16-D_4 and its metabolites: a) 16-7N(GK)-16-D_4, b) M-a', c) M-b', d) M-c', e) M-d', f) M-e', and g) M-f'. ($^{\#}$ denotes the parent ions and * denotes the diagnostic product ions).

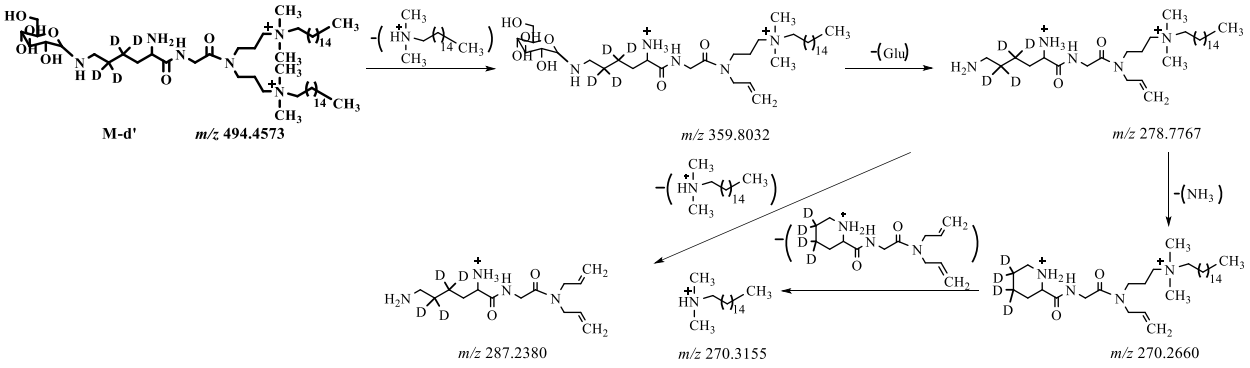

Figure 4.S9. The proposed structures of major product ions of the metabolite M-d' of 16-7N(GK)-16-D_4.

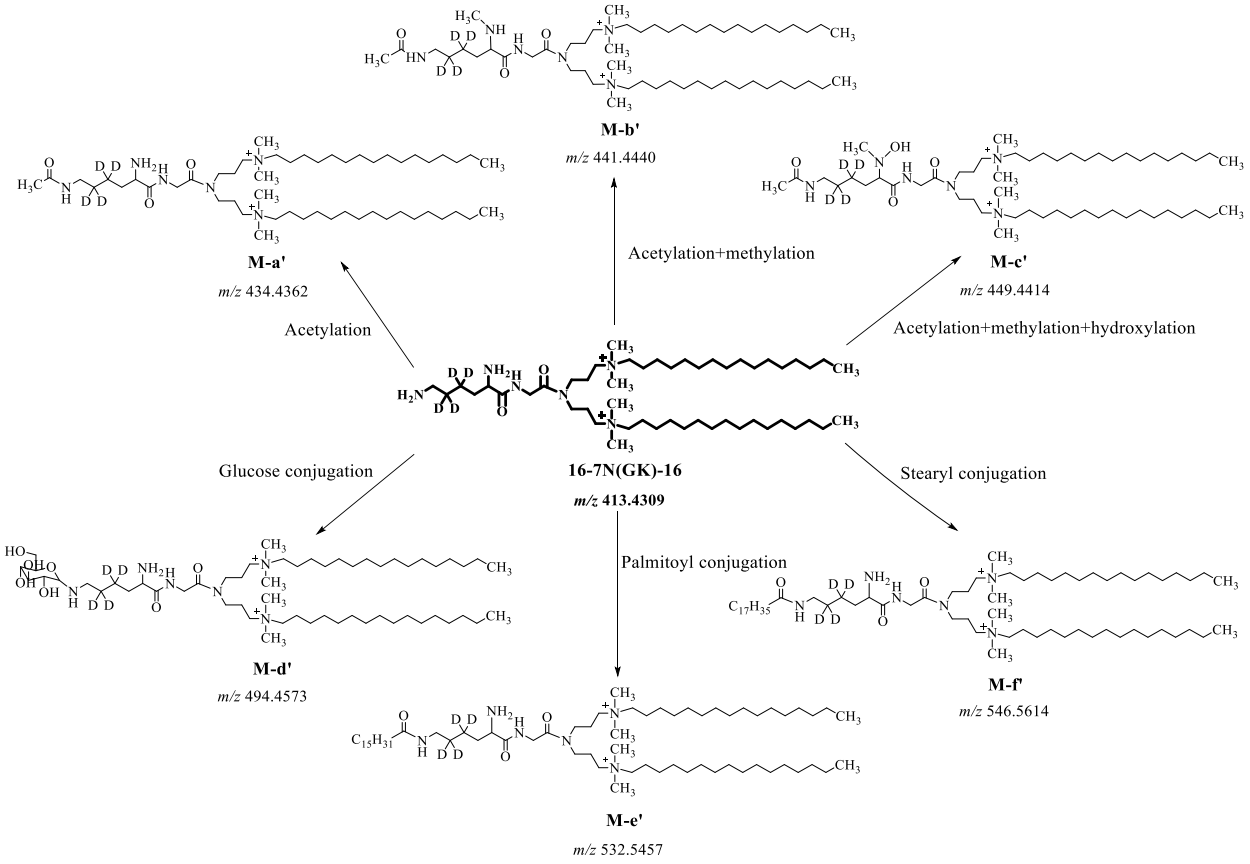

Figure 4.S10. The metabolites of 16-7N(GK)-16-D_4 and its proposed metabolic pathway.

Table 4.S1. Potential metabolites based on accurate mass measurements for the gemini surfactants 16(Py)-S-2-S-16(Py)-D_{10} and 16-7N(GK)-16-D_4.

Name	Molecular Formula	Exact Mass (*m/z*)	Observed Mass (*m/z*)	Mass Accuracy (ppm)	Metabolic Reactions
16(Py)-S-2-S-16(Py)-D_{10}	$C_{44}H_{68}D_{10}N_2S_2^{2+}$	354.3112	354.3115	0.8	
M-1’	$C_{44}H_{68}D_{10}N_2OS_2^{2+}$	362.3086	362.3084	0.6	Oxidation
M-2’	$C_{44}H_{68}D_{10}N_2O_2S_2^{2+}$	370.3061	370.3063	0.5	Oxidation
M-3’	$C_{44}H_{68}D_{10}N_2O_3S_2^{2+}$	378.3035	378.3038	0.8	Oxidation
M-4’	$C_{23}H_{37}D_5NS_2^{+}$	401.3067	401.3070	0.7	Dealkylation
M-5’	$C_{23}H_{37}D_5NOS_2^{+}$	417.3016	417.3016	0.0	Dealkylation, Oxidation
16-7N(GK)-16-D_4	$C_{50}H_{102}D_4N_6O_2^{2+}$	413.4309	413.4307	0.5	
M-a’	$C_{52}H_{104}D_4N_6O_3^{2+}$	434.4362	434.4362	0.0	Acetylation
M-b’	$C_{53}H_{106}D_4N_6O_3^{2+}$	441.4440	441.4438	0.5	Acetylation, Methylation
M-c’	$C_{53}H_{106}D_4N_6O_4^{2+}$	449.4414	449.4413	0.2	Acetylation, Methylation, Hydroxylation
M-d’	$C_{56}H_{112}D_4N_6O_7^{2+}$	494.4573	494.4569	0.8	Glucoside conjugation
M-e’	$C_{66}H_{132}D_4N_6O_3^{2+}$	532.5457	532.5454	0.6	Palmitoyl conjugation
M-f’	$C_{68}H_{136}D_4N_6O_3^{2+}$	546.5614	546.5611	0.5	Stearyl conjugation

5 Chapter 5 - Discussion, Future Perspectives, and Conclusions

5.1 Discussion

Cationic lipids have been increasingly used as non-viral vectors for gene delivery in recent years [1-3]. In particular, cationic gemini surfactants are promising gene delivery agents as they have the ability to compact nucleic acids into nanoparticles, facilitate their cellular entry, and prevent them from cytoplasmic enzymatic degradation [4-6]. In addition, gemini surfactants displayed significantly better transfection activity and biocompatibility than other cationic lipids in gene delivery [7, 8]. To date, a large number of gemini surfactants have been successfully used *in vitro* and *in vivo* for gene delivery, showing their great potential for clinical applications [9-12]. Towards this goal, extensive investigations and development have been performed to increase efficiency and decrease toxicity of gemini surfactants, which include the development of novel gemini surfactant compounds [13-16], optimization of the formulation strategy of gemini surfactant-based lipoplexes [17], and investigation of the mechanism of their cellular uptake [18]. As a result, significant progress has been achieved in improving the efficiency and toxicity profiles of gemini surfactants used as non-viral gene delivery agents.

While gemini surfactant nanoparticle-based gene delivery are taking strides towards clinical applications, their biological fate has not been investigated. In particular, the cellular uptake, distribution, and metabolite formation of gemini surfactant nanoparticles upon entering a biological system are not well understood, which could be linked to their efficiencies and toxicities. An understanding of the relationship between cellular uptake, subcellular distribution, metabolite formation, efficiency, and toxicity will aid in the development of less toxic and more effective

gemini surfactant compounds. Therefore, the focus of my Ph.D. research is the assessment of the biological behavior of gemini surfactant nanoparticles using mass spectrometry, with an emphasis on the qualitative and quantitative analysis of gemini surfactant nanoparticles in the cellular matrix.

5.1.1 Determination of gemini surfactants in cellular matrix using a validated FIA-MS/MS method

To investigate the cellular uptake and distribution of gemini surfactants, an effective analytical method is needed. In light of the complexity of the cellular matrix, an analytical method with high sensitivity and specificity is preferred for the analysis of gemini surfactant nanoparticles in treated cells. As gemini surfactants lack a chromophore or fluorophore and contain permanent positive charges in their structures [19], MS is ideal for their detection and quantification. In particular, MRM scan provides high sensitivity and specificity [20], allowing for the determination of gemini surfactants in complex biological matrices. Therefore, an FIA-MS/MS method that is simple and sensitive was developed for the quantification of three gemini surfactants 16-3-16, 16(Py)-S-2-S-(Py)16, and 16-7N(GK)-16 in my Ph.D. research.

The FIA-MS/MS method was developed and validated as per the USFDA guidelines [21]. It is the first FIA-MS/MS method that was developed for the quantification of gemini surfactants within different structural families. Compared with previous analytical methods employing cyano and HILIC columns for the quantification of 16-3-16 and 16(Py)-S-2-S-16(Py) in treated cells [22, 23], the FIA-MS/MS method eliminated the use of chromatographic separation, gradient elution, and an ion pairing reagent, which substantially simplified the method, shortened the time needed for method development, and reduced sample analysis time [24]. Furthermore, the sensitivity of the method is superior to the previous methods [22, 23], which could be attributable to the narrower and more symmetrical analyte peaks obtained with the optimized solvent mobile phases. In fact,

Buse et al. [25] conducted a comparison of various MS-based methods for the quantification of 16-3-16, and a 10 fold higher sensitivity was achieved in the FC-Qtrap-MS/MS method compared with the LC-Qtrap-MS/MS method. To avoid potential matrix effect, deuterium-labelled gemini surfactants were used as internal standards that were added into samples prior to sample extraction and analysis. In addition, an efficient liquid-liquid extraction was achieved for 16-3-16 (104.2 ± 9.5%) and 16(Py)-S-2-S-16(Py) (100.6 ± 4.3%) with the use of the Bligh/Dyer lipid extraction method [26], contributing to their determination in the cellular matrix. However, the extraction recovery of 16-7N(GK)-16 (36.2 ± 5.1%) is relatively low due to its highly hydrophilic nature, which is a limitation to this method. Although the use of internal standards allows for the correction for different extraction recoveries, various extraction methods including different extraction solvents and techniques should be explored to increase the recovery of 16-7N(GK)-16 as articulated in the future directions.

Overall, the FIA-MS/MS method is effective for the determination of the three studied gemini surfactants at the subcellular level. As demonstrated in the application, the determined concentrations of the three gemini surfactants showed that there are significant variations in their accumulation in the nuclear fraction of treated PAM 212 cells (Figure 2.4), which may explain the observed differences in their toxicity.

5.1.2 Cellular uptake and distribution of gemini surfactant nanoparticles

The cellular uptake and distribution of gemini surfactants nanoparticles provides information on how they behave in biological systems, thus offering a better understanding of their observed efficiency and toxicity. To determine the cellular uptake and subcellular distribution of the three gemini surfactant nanoparticles in treated PAM 212 cells, four subcellular fractions (namely nuclei,

mitochondria, plasma membrane, and cytosol) were collected by differential centrifugation and subsequently extracted and analyzed by the FIA-MS/MS method (Chapter 2). The determination of gemini surfactants in subcellular fractions allowed for evaluating the relationship between cellular uptake, subcellular distribution, efficiency, and toxicity.

The cellular uptake data revealed that the three gemini surfactants were rapidly taken up by PAM 212 cells during a course of 5 h treatment, followed by subsequent depletion after removal of the nanoparticles from the media (Figure 3.5a). These observations are consistent with previously obtained results for 16-3-16 and 16(Py)-S-2-S-16(Py), which showed a maximal uptake prior to a decrease in their cellular concentrations [22]. The rapid cellular uptake of gemini surfactants corresponds to the quick internalization of the gemini surfactants-based DNA nanoparticles for gene transfection, whereas subsequent depletion reflects their cellular degradation and elimination. In fact, it was observed that 16(Py)-S-2-S-16(Py) and 16-7N(GK)-16 were metabolized in PAM 212 cells post treatment (Chapter 4), which could contribute to their depletion. Overall, a significantly higher cellular uptake was observed for 16-7N(GK)-16 relative to the other two compounds (Figure 3.5a), which explained its relatively high efficiency in gene transfection (Figure 3.3).

In addition to cellular uptake, the subcellular distribution of the three gemini surfactants was also determined in an effort to explain their varying efficiencies and toxicities. The subcellular data showed different distribution profiles among the three gemini surfactants in PAM 212 cells. In general, the gemini surfactants 16-3-16 and 16(Py)-S-2-S-16(Py) displayed a similar subcellular distribution pattern that showed significant variations in different subcellular compartments (Figures 3.5b and c), whereas 16-7N(GK)-16 showed a relatively even distribution within the four compartments (Figure 3.5d). The difference in subcellular distribution might be due to their distinct

physicochemical properties, as 16-7N(GK)-16 possesses a di-peptide in its structure, providing greater biocompatibility and flexibility compared to the other two compounds [13]. While there is no significant difference among the three compounds in terms of their distributions in the mitochondria, plasma membrane and cytosol, the distribution in the nucleus is the highest for 16(Py)-S-2-S-16(Py), followed by 16-3-16 and then 16-7N(GK)-16 (Figure 3.5e), which is in agreement with the observed toxicity of the three gemini surfactant nanoparticles (Figure 3.4). This differential nuclear distribution may provide an explanation for the toxicity of the three gemini surfactants, as non-preferable accumulation in the nucleus may pose harmful effects to the biological integrity and function of the cells.

To further explain the difference of the three gemini surfactant nanoparticles in terms of their cellular uptake and subcellular distribution, ethidium bromide dye exclusion assays were carried out to determine their DNA binding capabilities. The results indicated that 16-7N(GK)-16 has a relatively weaker DNA binding property compared with the other two compounds (Figure 3.6). As gene transfection involves not only proper compaction and cellular delivery of DNA but also efficient endosomal escape and dissociation of DNA from lipoplexes [13, 18], neither a weak binding nor a strong binding will allow for an efficient gene transfection. A weak binding cannot provide sufficient compaction and protection of DNA for efficient delivery, whereas a strong binding will not enable efficient release of DNA for transgene expression [27]. Due to the presence of amino acid moieties in the structure, providing structural flexibility [27], the gemini surfactant 16-7N(GK)-16 has the ability to provide sufficient protection for DNA while at the same time facilitate its intracellular release, thereby resulting in enhanced transfection efficiency. The similar results have also been previously obtained with other amino acid-substituted gemini surfactants due to their improved biocompatibility and structural flexibility [13].

Additionally, Langmuir studies were conducted to measure the molecular packing parameters of the three gemini surfactants for determining their aggregate shapes. Similar to the previous results determined for peptide-modified gemini surfactants [28], we observed that the shape of aggregates of gemini surfactants has a great impact on their performance as gene delivery agents. Specifically, the gemini surfactant 16-7N(GK)-16 forms a flexible bilayer structure in aqueous solution (Table 3.1), which tends to generate an inverted hexagonal phase with DOPE to facilitate the cytoplasmic release of DNA from the endosomes [29], thus resulting in enhanced gene transfection and less accumulation in the nucleus. In contrast, the gemini surfactants 16-3-16 and 16(Py)-S-2-S-16(Py) are prone to form cylindrical micelle structures that restricted their endosomal scape (Table 3.1), leading to reduced efficiency in transfection. Together, the DNA binding capability and the shape of the aggregates of the gemini surfactants explained the different behaviors of the three gemini surfactant nanoparticles in biological systems.

In this study, the isolation of subcellular fractions, namely nuclei, mitochondria, plasma membrane, and cytosol, was confirmed by western blotting assay, showing the identity of each cellular compartment. However, coomassie reagent was not used to stain the gel to thoroughly visualize all protein bands, which is a limitation in this study. The coomassie staining can provide a further evaluation of the relative purity of each fraction. As such, future studies should consider this as a complementary approach to confirm the isolated subcellular fractions.

5.1.3 Detection and characterization of gemini surfactant metabolites using high-resolution mass spectrometry

Despite the substantial advancement with gemini surfactants as gene delivery agents, their metabolism is still not well understood. Investigation of the metabolite formation is of great importance as it provides information to understand how gemini surfactants interact with biological

components. Such information will aid in the design and development of novel gemini surfactants that are more efficient and less toxic. Therefore, we studied the metabolism of the three gemini surfactants 16-3-16, 16(Py)-S-2-S-16(Py), and 16-7N(GK)-16 in PAM 212 cells, as they belong to three structural families with different functional groups. We attempted to assess the impact of various functional groups on the metabolism of gemini surfactants in relation to their efficiencies and toxicities.

As we are developing gemini surfactant-based gene delivery systems mainly for topical applications, particularly for the treatment of localized scleroderma, the keratinocyte PAM 212 cells were used in this study. In light of the relatively low quantity of the metabolites in the cellular matrix, MS is an ideal technique for their detection and analysis, especially high-resolution mass spectrometry that provides accurate mass measurement, high sensitivity, and high selectivity for the analysis of chemical compounds [30, 31]. Furthermore, MS/MS analysis offers characteristic product ions that can aid in the characterization and structural elucidation of a compound [32]. As such, we employed a high-resolution quadrupole-Orbitrap (Q-Exactive®) mass spectrometer to detect and characterize the metabolites of the three gemini surfactants in biological systems.

While there is no metabolite found for 16-3-16 in PAM212 cells, suggesting it most likely remained as an intact molecule during the elimination process in biological systems; the gemini surfactant 16(Py)-S-2-S-16(Py) was metabolized primarily *via* phase I reactions, including oxidation and dealkylation. Oxidation is mainly due to the presence of sulfur atoms in the structure, which enables the formation of a series of oxidation products [33]. In addition, the covalent carbon-sulfur bond tends to break in biological systems to form the dealkylation metabolic products. Conversely, the gemini surfactant 16-7N(GK)-16 was metabolized mainly *via* phase II reactions, including methylation, acetylation, and various conjugations as shown in Figure 4.7. This is largely due to

the existence of reactive amino acid moieties in the structure [33], which are prone to conjugations with various endogenous compounds, such as glucose, palmitic acid, and stearic acid. Although conjugations with fatty acids are not common phase II reactions for drug metabolites, a number of such conjugation reactions, particularly with palmitic acid and stearic acid, have been reported [34, 35]. For example, it has been reported that 11-hydroxy-Δ^9-tetrahydrocannabinol was metabolized *via* a conjugation reaction with palmitic acid to form the product 11-palmitoyloxy-Δ^9-tetrahydrocannabinol in rat tissue and the metabolite 11-palmitoyloxy-Δ^9-tetrahydrocannabinol showed a less pronounced pharmacological activity compared to the original compound [36]. As phase II metabolites are generally less toxic compared to phase I metabolites in biological systems [37], phase II reactions of 16-7N(GK)-16 might have contributed to reducing its toxicity. Thus, the metabolic pathways of gemini surfactants provide an insight for future directions in the design and development of more effective and less toxic compounds.

In light of the complexity of cellular matrix and the variability of the abundance of metabolites, the dynamic exclusion was used in the MS method in order to detect the metabolites with low ion intensity [38]. This technique enables the detection of ions with low intensity by excluding high intense ions in previous scans [39], thus resulting in the discovery of more metabolites. However, although a number of metabolites have been determined for tested gemini surfactants, the detection of their metabolites may have not been complete. This is in part due to the Bligh/Dye method used in this study that probably does not effectively extract relatively polar compounds. This is particularly concerning for the metabolites of relatively hydrophilic 16-7N(GK)-16. To increase the metabolite coverage, future studies should seek more efficient extraction methods to increase the extraction recovery of polar compounds. A modified Folch method has been reported with relatively high recovery for hydrophilic gemini surfactants [40], which might be suitable for the

extraction of polar metabolites. Another limitation is the use of FIA-MS that could possibly reduce the number of determined metabolites in the sample as the metabolites in low abundance may not be properly detected and characterized due to matrix effects and potential interferences. As such, it will be important to employ LC-MS to investigate the metabolism of gemini surfactants, which can provide additional insights into metabolite formation for gemini surfactants within biological systems. In addition, it will also be worthwhile to investigate the metabolite formation of these gemini surfactants in other cell lines as described in the future directions to confirm the detected metabolites by ruling out any degradation products and possibly discovery new metabolites, providing a better understanding of their metabolic pathways.

While the metabolites of 16(Py)-S-2-S-16(Py) and 16-7N(GK)-16 were determined and characterized based on accurate mass measurements and characteristic product ions, their structures have not been unambiguously identified. To identify the structures of these metabolites, two approaches can be applied. One approach is to compare the accurate masses and characteristic product ions of potential metabolites with those of authentic reference standards [41]. In addition, the retention time of metabolites and reference standards can be compared for authentication if LC separation is used [41]. Such an approach provides a high confidence for the identification of the metabolites. For example, phase II pharmaceutical metabolites in reclaimed water have been identified and characterized based on accurate mass measurements, characteristic product ions, and retention time in comparison with reference standards [42]. However, this approach requires the use of reference standards for all metabolites, which are typically difficult to obtain if they are unknown compounds and not commercially available. Alternatively, the metabolites of gemini surfactants can be isolated and purified, and then subjected to nuclear magnetic resonance (NMR) analysis for structural elucidation [41]. For instance, nine phase I metabolites of phillyrin, a

bioactive component of the fruit of *Frosythia suspens*a, have been isolated in rats and structurally identified using MS and NMR analyses [43]. Similarly, eight phase II metabolites of echinacoside, an antioxidant, have been isolated from rat's bile after intravenous administration and their structures were elucidated using ^{1}H and ^{13}C-NMR spectroscopies [44]. However, NMR analysis typically requires a relatively large quantity of purified compounds, which is often not achievable in *in vitro* studies due to the limited capacity of cells.

In summary, this work provided an example for investigating the metabolism of gemini surfactants in biological systems. We demonstrated the feasibility of using a high-resolution mass spectrometry instrument to detect and characterize the metabolites of gemini surfactants based on accurate mass measurements and characteristic product ions. This approach can also be applied to study the metabolite formation of other gemini surfactants in various families for better understanding of their toxicities.

5.2 Future Perspectives

The work in my Ph.D. research lays the foundation to investigate the behavior of gemini surfactant nanoparticles in biological systems. As a powerful analytical technique, mass spectrometric platform can still play a key role in future studies of gemini surfactants as non-viral gene delivery vectors in two main directions, as outlined below.

5.2.1 Evaluation of the *in vivo* fate of gemini surfactants in animals

The determination of the cellular uptake and distribution of the three gemini surfactants 16-3-16, 16(Py)-S-2-S-16(Py), and 16-7N(GK)-16 using an FIA-MS/MS analysis sets the foundation to study their *in vivo* fate in biological systems. Such an investigation will help gain information about

the absorption, distribution, and excretion of the gemini surfactants within the host body in relation to their efficiency and toxicity. The three gemini surfactant nanoparticles have demonstrated *in vitro* transfection capabilities within PAM 212 cells, suggesting their potentials for an *in vivo* application. In fact, the gemini surfactant 16-3-16 nanoparticles have demonstrated great promise as topical gene delivery system in treating localized scleroderma [10, 45], as they were able to deliver a significantly higher level of transgenic materials than naked DNA in animal models of scleroderma [45]. As such, future studies should be conducted to evaluate the efficiency and toxicity of these three gemini surfactants in delivering therapeutic genes to animals. In particular, the gemini surfactant 16-7N(GK)-16 should be thoroughly investigated *in vivo* as it displayed the highest *in vitro* gene transfection efficiency with lowest toxicity among the three compounds, showing the greatest potential for topical applications. As such, an evaluation of the *in vivo* fate, including the absorption, distribution, and excretion, of these gemini surfactants in skin tissue upon application would be of great importance to understand their efficiency and toxicity profiles for *in vivo* gene delivery.

To quantify gemini surfactants in skin tissue and systemic circulation, an FIA-MS/MS method can be developed in the tissue matrix for simple and fast analysis. Alternatively, an LC-MS/MS can also be developed to minimize potential matrix effect and interferences for quantitative analysis. Our group has recently developed an FIA-MS/MS relative quanitification method for the *ex-vivo* cutaneous determination of peptide-modified gemini surfactants and found that the relative amount of gemini surfactants accumulated in skin tissue correlated with their transfection efficiencies [40]. In addition, a minimal escape of gemini surfactants into the circulation compartment was observed, showing their potential low toxicity for topical applications [40]. As the Bligh/Dyer extraction method used in this study has a low extraction efficiency for polar compounds, it is important to

explore various extraction methods and develop a method that can effectively extract relatively polar compounds, especially for hydrophilic gemini surfactant 16-7N(GK)-16 and its metabolites, from the skin tissue. The modified Folch method in combination with solid phase extraction was previously used for the extraction of peptide-substituted gemini surfactants and relatively high extraction recovery was achieved in the *ex vivo* cutaneous experiment [35]. As such, it will be valuable to employ these methods to extract gemini surfactants and their metabolites in the skin tissue for MS analysis. Together, these studies on *in vitro* and *in vivo* fate of gemini surfactants will assist in the comprehensive understanding of the relationship between their structures, biological fate, efficiency, and toxicity.

5.2.2 Investigation of the metabolite formation of other gemini surfactants

The investigation on the metabolism of the three gemini surfactants conducted in my Ph.D. research offered effective approaches to study the metabolite formation of gemini surfactants in general. Future research can be conducted using similar approaches to evaluate the metabolite formation of other gemini surfactants from various structural families, as their metabolic pathways remain unclear. The metabolite formation of gemini surfactants provides information on their metabolic pathways, which will aid in understanding their efficiency and toxicity in relation to their structures.

In addition to the epidermal keratinocyte cell, PAM 212, used in this work, other epithelial cell lines, such as cottontail rabbit epithelial cell, Sf 1Ep, and African green monkey kidney fibroblast cell, COS-7, can also be used. Sf 1Ep and COS-7 cells have been widely used *in vitro* to evaluate the transfection efficiency and toxicity of gemini surfactants for the treatment of atopic dermatitis and for wound healing as these cells represent the intended organ, eg., skin, for applications [27, 46]. They may contain different enzymes than PAM 212 cells that can metabolize gemini

surfactants in various ways, contributing to the extensive understanding of their metabolite profiles. Thus, it is crucial to investigate the metabolism of gemini surfactants within various cell lines. In the long term, knowledges on the metabolism will benefit the development of novel gemini surfactants that are more efficient and less toxic.

5.3 Conclusions

The biological fate, including cellular uptake, distribution, and metabolite formation, of three gemini surfactants 16-3-16, 16(Py)-S-2-S-16(Py), and 16-7N(GK)-16 was investigated for the first time to explain their various efficiencies and toxicities in gene transfection. Specifically, high cellular uptake of gemini surfactants corresponds to high efficiency in gene transfection and high accumulation in the nucleus may contribute to the observed high toxicity. In addition, different metabolic pathways were determined for the three gemini surfactants, suggesting that phase II metabolites could contribute to reduced toxicity. Among the three gemini surfactants, 16-7N(GK)-16 has been shown to be most promising gene delivery agent with high efficiency and low toxicity, which should be further studied as the next generation of gemini surfactants in the future.

Overall, my work on assessing the biological behavior of gemini surfactants will feed into the rationale for designing novel and better gene delivery systems, which also provides a new paradigm for future investigation and development of gemini surfactants. Ultimately, the results will contribute to the development of novel gene delivery systems with increased efficiency and reduced toxicity.

5.4 References

1. del Pozo-Rodríguez, A., M.Á. Solinís, and A. Rodríguez-Gascón, *Applications of lipid nanoparticles in gene therapy.* European Journal of Pharmaceutics and Biopharmaceutics, 2016. **109**: p. 184-193.
2. Zhao, Y. and L. Huang, *Lipid nanoparticles for gene delivery,* in *Advances in genetics*. 2014, Elsevier. p. 13-36.
3. Ramamoorth, M. and A. Narvekar, *Non viral vectors in gene therapy-an overview.* Journal of clinical and diagnostic research, 2015. **9**(1): p. GE01-06.
4. Ahmed, T., A.O. Kamel, and S.D. Wettig, *Interactions between DNA and Gemini surfactant: impact on gene therapy: part I.* Nanomedicine, 2016. **11**(3): p. 289-306.
5. Karlsson, L., M.C. van Eijk, and O. Söderman, *Compaction of DNA by gemini surfactants: effects of surfactant architecture.* Journal of colloid and interface science, 2002. **252**(2): p. 290-296.
6. Mislick, K.A. and J.D. Baldeschwieler, *Evidence for the role of proteoglycans in cation-mediated gene transfer.* Proceedings of the National Academy of Sciences, 1996. **93**(22): p. 12349-12354.
7. Bombelli, C., et al., *Gemini surfactant based carriers in gene and drug delivery.* Current medicinal chemistry, 2009. **16**(2): p. 171-183.
8. Wettig, S.D., R.E. Verrall, and M. Foldvari, *Gemini surfactants: a new family of building blocks for non-viral gene delivery systems.* Current gene therapy, 2008. **8**(1): p. 9-23.
9. Mohammed-Saeid, W., et al., *Design and Evaluation of RGD-Modified Gemini Surfactant-Based Lipoplexes for Targeted Gene Therapy in Melanoma Model.* Pharmaceutical Research, 2017. **34**(9): p. 1886-1896.
10. Badea, I., et al., *In vivo cutaneous interferon-gamma gene delivery using novel dicationic (gemini) surfactant-plasmid complexes.* J Gene Med, 2005. **7**(9): p. 1200-1214.
11. Singh, J., et al., *Development of amino acid substituted gemini surfactant-based mucoadhesive gene delivery systems for potential use as noninvasive vaginal genetic vaccination.* Nanomedicine, 2015. **10**(3): p. 405-417.
12. Cardoso, A.M., et al., *Gemini surfactants mediate efficient mitochondrial gene delivery and expression.* Molecular pharmaceutics, 2015. **12**(3): p. 716-730.

13. Singh, J., et al., *Amino acid-substituted gemini surfactant-based nanoparticles as safe and versatile gene delivery agents.* Current drug delivery, 2011. **8**(3): p. 299-306.
14. Bhadani, A. and S. Singh, *Novel gemini pyridinium surfactants: synthesis and study of their surface activity, DNA binding, and cytotoxicity.* Langmuir, 2009. **25**(19): p. 11703-11712.
15. Donkuru, M., et al., *Designing pH-sensitive gemini nanoparticles for non-viral gene delivery into keratinocytes.* Journal of Materials Chemistry, 2012. **22**(13): p. 6232-6244.
16. Alvarez Alcalde, M., et al., *Synthesis and characterization of a new gemini surfactant derived from 3α, 12α-dihydroxy-5β-cholan-24-amine (steroid residue) and ethylenediamintetra acetic acid (spacer).* Langmuir, 2008. **24**(12): p. 6060-6066.
17. Mohammed-Saeid, W., et al., *Development of lyophilized gemini surfactant-based gene delivery systems: influence of lyophilization on the structure, activity and stability of the lipoplexes.* Journal of Pharmacy & Pharmaceutical Sciences, 2012. **15**(4): p. 548-567.
18. Singh, J., et al., *Evaluation of cellular uptake and intracellular trafficking as determining factors of gene expression for amino acid-substituted gemini surfactant-based DNA nanoparticles.* J Nanobiotechnology, 2012. **10**(7): p. 1-14.
19. Menger, F.M. and C. Littau, *Gemini-surfactants: synthesis and properties.* Journal of the American chemical society, 1991. **113**(4): p. 1451-1452.
20. Jain, D.S., et al., *Rapid and sensitive method for the determination of sertraline in human plasma using liquid chromatography–tandem mass spectrometry (LC–MS/MS).* Journal of Chromatography B, 2005. **829**(1-2): p. 69-74.
21. FDA, *Guidance for Industry: Bioanalytical Method Validation*. US, Department of Health and Human Services, Food and Drug Administration, Center for Drug Evaluation and Research (CDER), Center for Veterinary Medicine (CVM). 2013.
22. Donkuru, M., et al., *Hydrophilic interaction liquid chromatography-tandem mass spectrometry quantitative method for the cellular analysis of varying structures of gemini surfactants designed as nanomaterial drug carriers.* Journal of Chromatography A, 2016. **1446**: p. 114-124.
23. Buse, J., et al., *A general liquid chromatography tandem mass spectrometry method for the quantitative determination of diquaternary ammonium gemini surfactant drug delivery agents in mouse keratinocytes' cellular lysate.* Journal of Chromatography A, 2013. **1294**: p. 98-105.

24. Jin, W., et al., *The determination of gemini surfactants used as gene delivery agents in cellular matrix using validated tandem mass spectrometric method.* Journal of pharmaceutical and biomedical analysis, 2019. **164**: p. 164-172.
25. Buse, J., et al., *The development and assessment of high-throughput mass spectrometry-based methods for the quantification of a nanoparticle drug delivery agent in cellular lysate.* J Mass Spectrom, 2014. **49**(11): p. 1171-1180.
26. Bligh, E.G. and W.J. Dyer, *A rapid method of total lipid extraction and purification.* Canadian journal of biochemistry and physiology, 1959. **37**(8): p. 911-917.
27. Yang, P., et al., *Enhanced gene expression in epithelial cells transfected with amino acid-substituted gemini nanoparticles.* European Journal of Pharmaceutics and Biopharmaceutics, 2010. **75**(3): p. 311-320.
28. Al-Dulaymi, M., et al., *Molecular Engineering as an Approach To Modulate Gene Delivery Efficiency of Peptide-Modified Gemini Surfactants.* Bioconjugate chemistry, 2018. **29**(10): p. 3293-3308.
29. Zuhorn, I.S., et al., *Nonbilayer phase of lipoplex-membrane mixture determines endosomal escape of genetic cargo and transfection efficiency.* Molecular therapy, 2005. **11**(5): p. 801-810.
30. Rose, R.J., et al., *High-sensitivity Orbitrap mass analysis of intact macromolecular assemblies.* Nature methods, 2012. **9**(11): p. 1084-1086.
31. Michalski, A., et al., *Mass spectrometry-based proteomics using Q Exactive, a high-performance benchtop quadrupole Orbitrap mass spectrometer.* Molecular & Cellular Proteomics, 2011. **10**(9): p. 1-10.
32. Wu, X. and R.L. Prior, *Systematic identification and characterization of anthocyanins by HPLC-ESI-MS/MS in common foods in the United States: fruits and berries.* Journal of agricultural and food chemistry, 2005. **53**(7): p. 2589-2599.
33. Jakoby, W.B., *Metabolic basis of detoxication: metabolism of functional groups*. 2012: Elsevier.
34. Leighty, E.G., A.F. Fentiman Jr, and R.M. Thompson, *Conjugation of fatty acids to DDT in the rat: possible mechanism for retention.* Toxicology, 1980. **15**(2): p. 77-82.

35. Leighty, E.G. and A.F. Fentiman, *Conjugation of pentachlorophenol to palmitic acid by liver microsomes.* Bulletin of environmental contamination and toxicology, 1982. **28**(3): p. 329-333.
36. Haggerty, G.C., et al., *The pharmacological activity of the fatty acid conjugate 11-palmitoyloxy-Δ9-tetrahydrocannabinol.* Toxicology and applied pharmacology, 1986. **84**(3): p. 599-606.
37. Klaassen, C.D. and M.O. Amdur, *Casarett and Doull's toxicology: the basic science of poisons*. 8th ed. Vol. 1236. 2013: McGraw-Hill New York. 189.
38. Zhang, J.-Y., et al., *Rapid screening and identification of target constituents using full scan-parent ions list-dynamic exclusion acquisition coupled to diagnostic product ions analysis on a hybrid LTQ-Orbitrap mass spectrometer*. Talanta, 2014. **124**: p. 111-122.
39. Prakash, A., S.M. Peterman, and D. Sarracino, *Variable data-dependent acquisition and dynamic exclusion method for mass spectrometry*. 2018, Google Patents.
40. Al-Dulaymi, M., et al., *The development of simple flow injection analysis tandem mass spectrometric methods for the cutaneous determination of peptide-modified cationic gemini surfactants used as gene delivery vectors.* Journal of pharmaceutical and biomedical analysis, 2018. **159**: p. 536-547.
41. Sumner, L.W., et al., *Proposed minimum reporting standards for chemical analysis.* Metabolomics, 2007. **3**(3): p. 211-221.
42. Wang, J. and P.R. Gardinali, *Identification of phase II pharmaceutical metabolites in reclaimed water using high resolution benchtop Orbitrap mass spectrometry*. Chemosphere, 2014. **107**: p. 65-73.
43. Li, C., et al., *Isolation and identification of phase I metabolites of phillyrin in rats.* Fitoterapia, 2014. **97**: p. 92-97.
44. Jia, C., et al., *Metabolism of echinacoside, a good antioxidant, in rats: isolation and identification of its biliary metabolites.* Drug Metabolism and Disposition, 2009. **37**(2): p. 431-438.
45. Badea, I., et al., *Topical non-invasive gene delivery using gemini nanoparticles in interferon-gamma-deficient mice.* Eur J Pharm Biopharm, 2007. **65**(3): p. 414-422.
46. Wettig, S.D., et al., *Structural and transfection properties of amine‐substituted gemini surfactant‐based nanoparticles.* The journal of gene medicine, 2007. **9**(8): p. 649-658.

6 Appendix - Metabolic Profiles of Treated Cells and Control

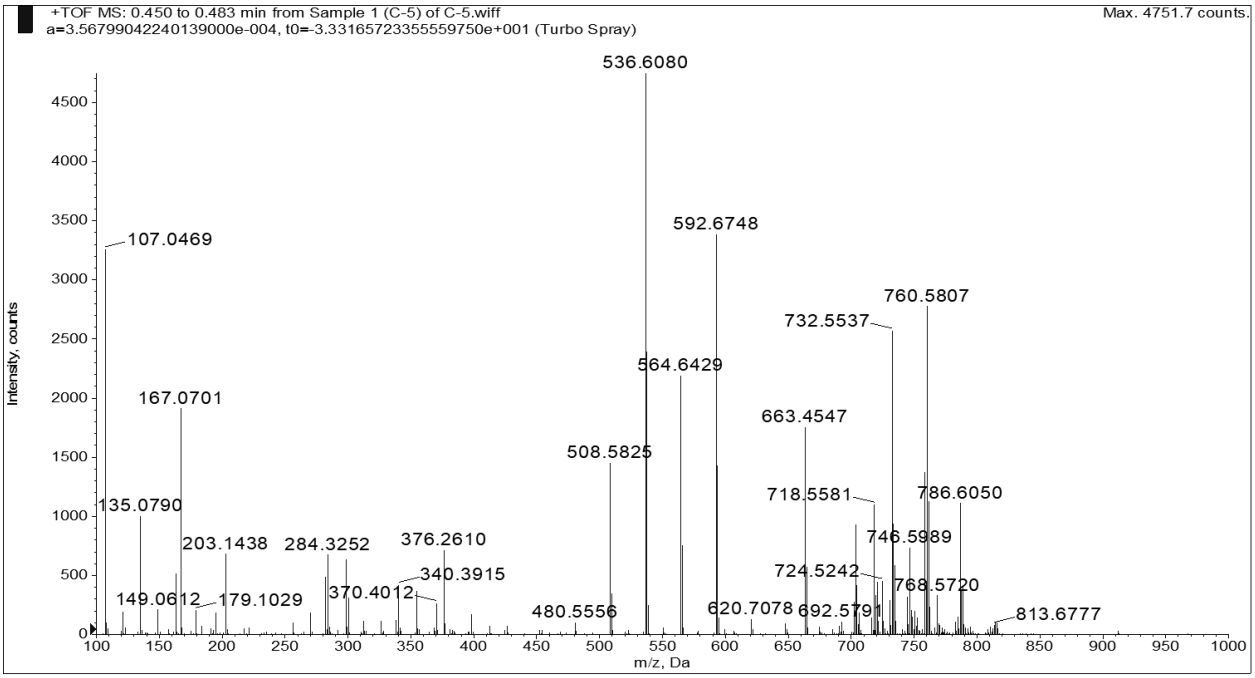

Figure 6.1. The metabolic profile of control (untreated PAM 212 cells) established in positive ESI mode on a Q-TOF instrument.

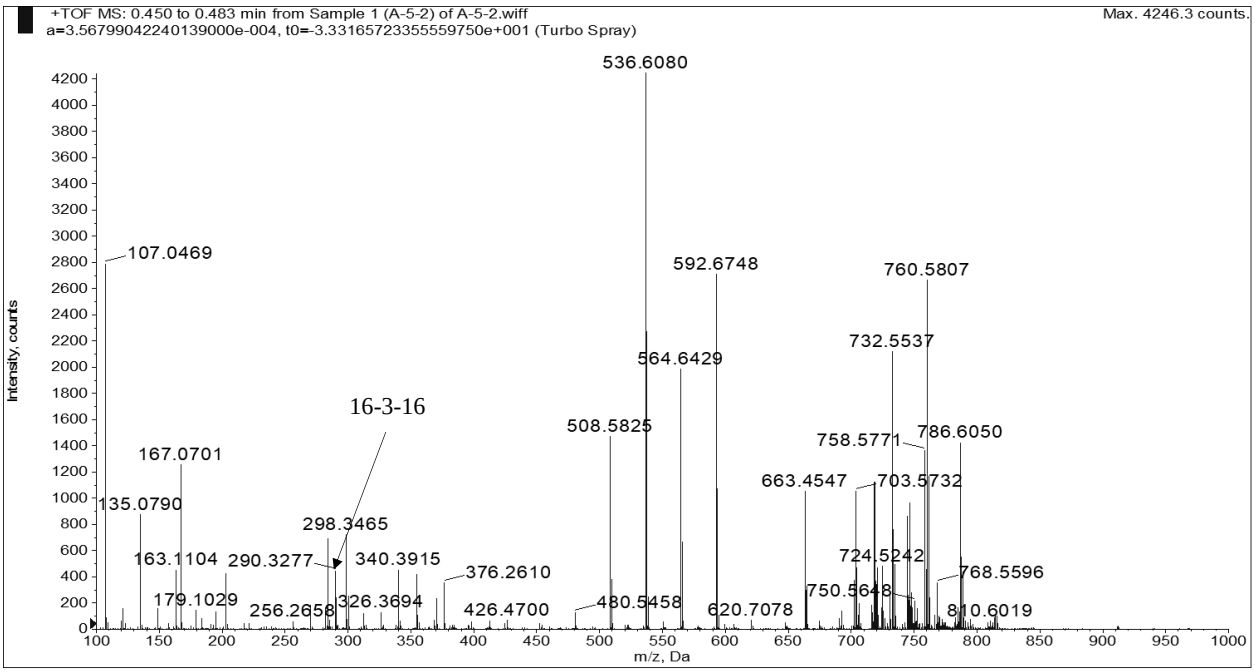

Figure 6.2. The metabolic profile of PAM 212 cells treated with 16-3-16 nanoparticles established in positive ESI mode on a Q-TOF instrument. No peak was detected as potential metabolite of 16-3-16.

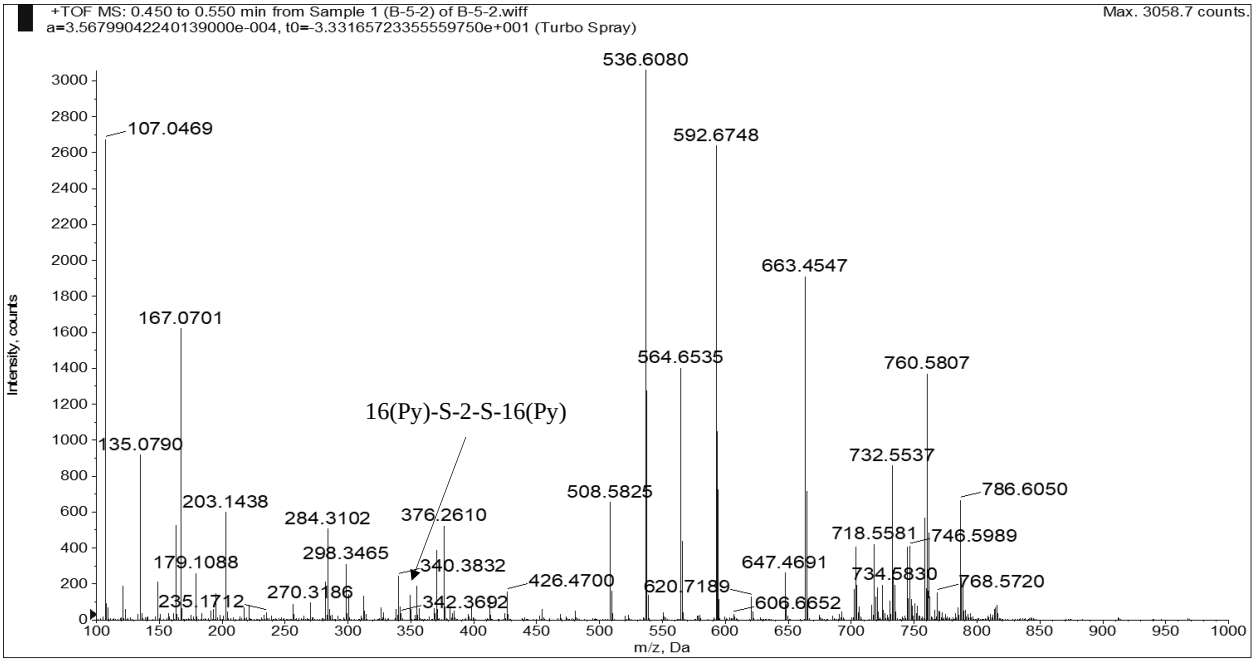

Figure 6.3. The metabolic profile of PAM 212 cells treated with 16(Py)-S-2-S-16(Py) nanoparticles established in positive ESI mode on a Q-TOF instrument. Several peaks were detected as potential metabolites of 16(Py)-S-2-S-16(Py).

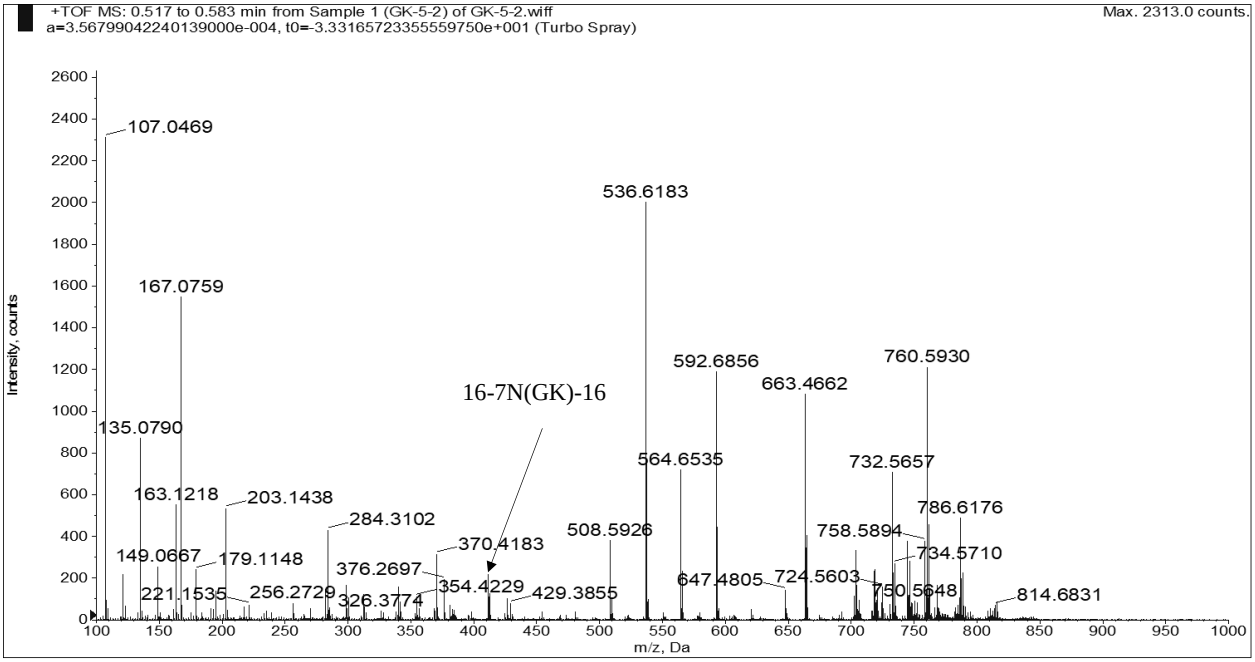

Figure 6.4. The metabolic profile of PAM 212 cells treated with 16-7N(GK)-16 nanoparticles established in positive ESI mode on a Q-TOF instrument. Several peaks were detected as potential metabolites of 16-7N(GK)-16.

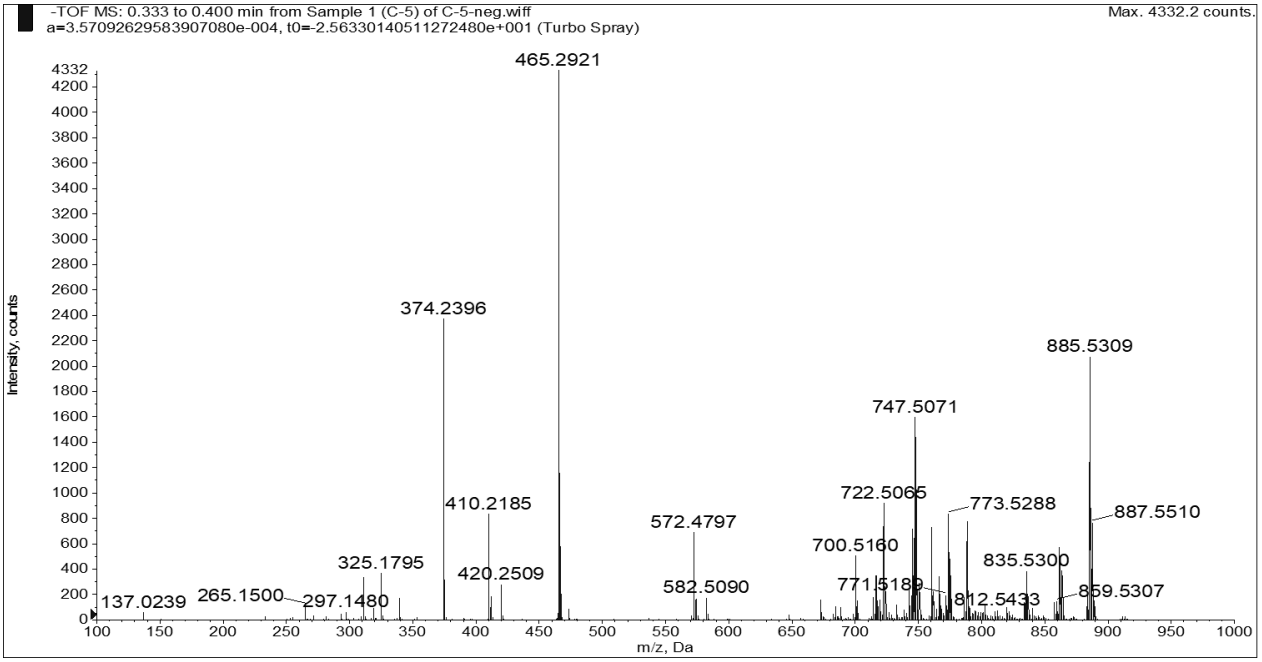

Figure 6.5 The metabolic profile of control (untreated PAM 212 cells) established in negative ESI mode on a Q-TOF instrument.

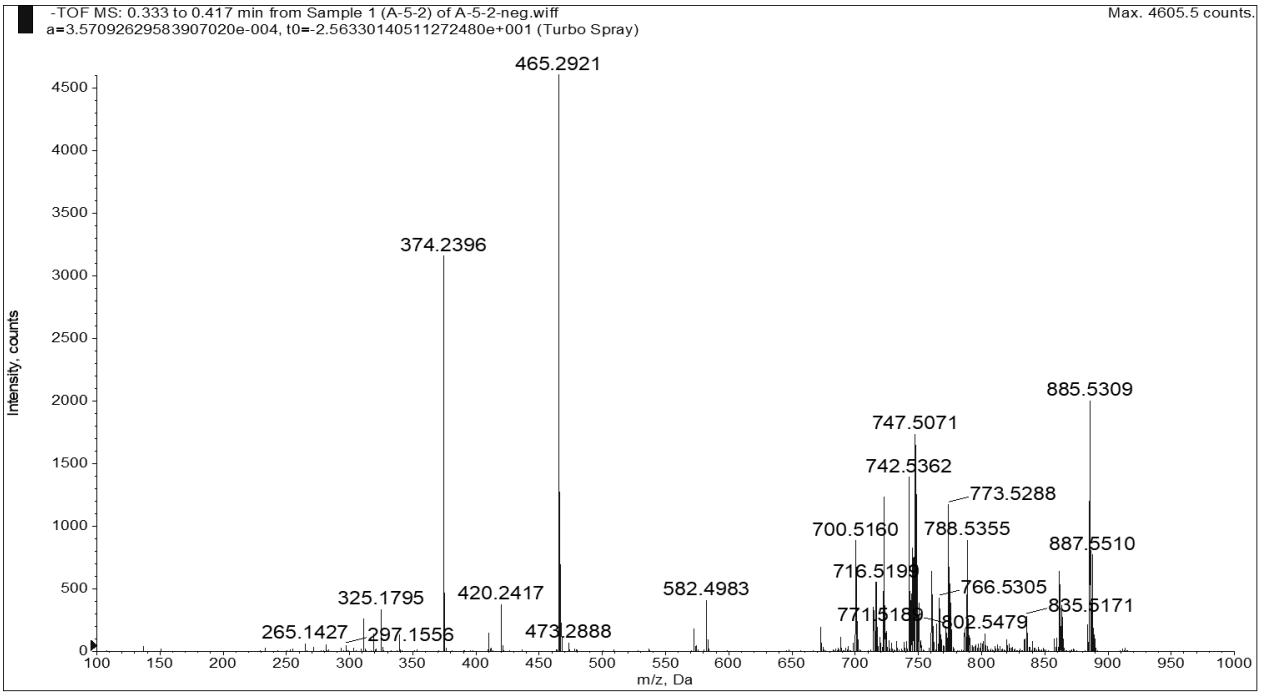

Figure 6.6. The metabolic profile of PAM 212 cells treated with 16-3-16 nanoparticles established in negative ESI mode on a Q-TOF instrument. The gemini surfactant 16-3-16 and its potential metabolites were not detected.

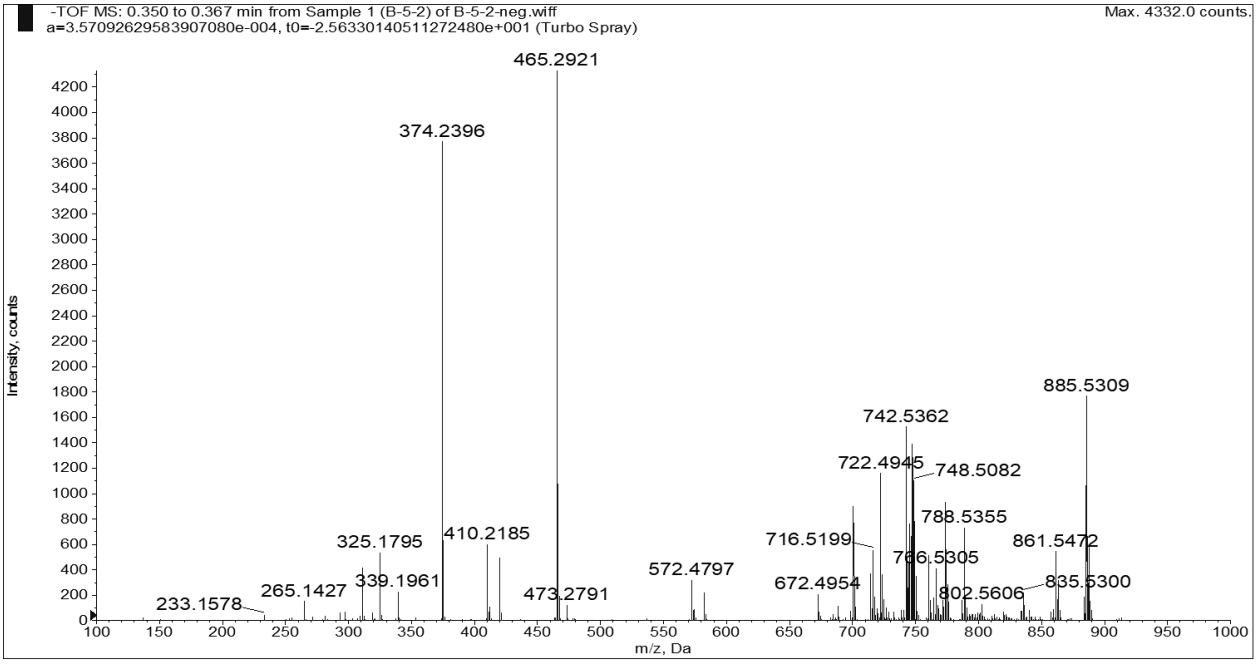

Figure 6.7. The metabolic profile of PAM 12 cells treated with 16(Py)-S-2-S-16(Py) nanoparticles established in negative ESI mode on a Q-TOF instrument. The gemini surfactant 16(Py)-S-2-S-16(Py) and its potential metabolites were not detected.

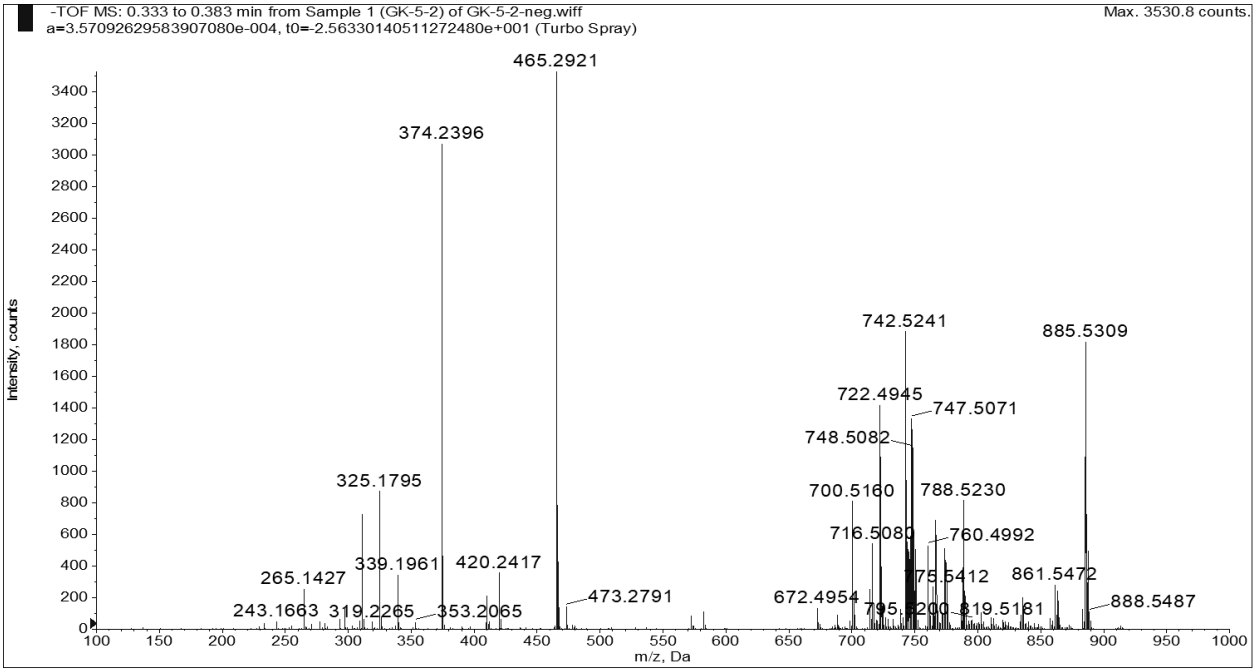

Figure 6.8. The metabolic profile of PAM212 cells treated with 16-7N(GK)-16 nanoparticles established in negative ESI mode on a Q-TOF instrument. The gemini surfactant 16-7N(GK)-16 and its potential metabolites were not detected.

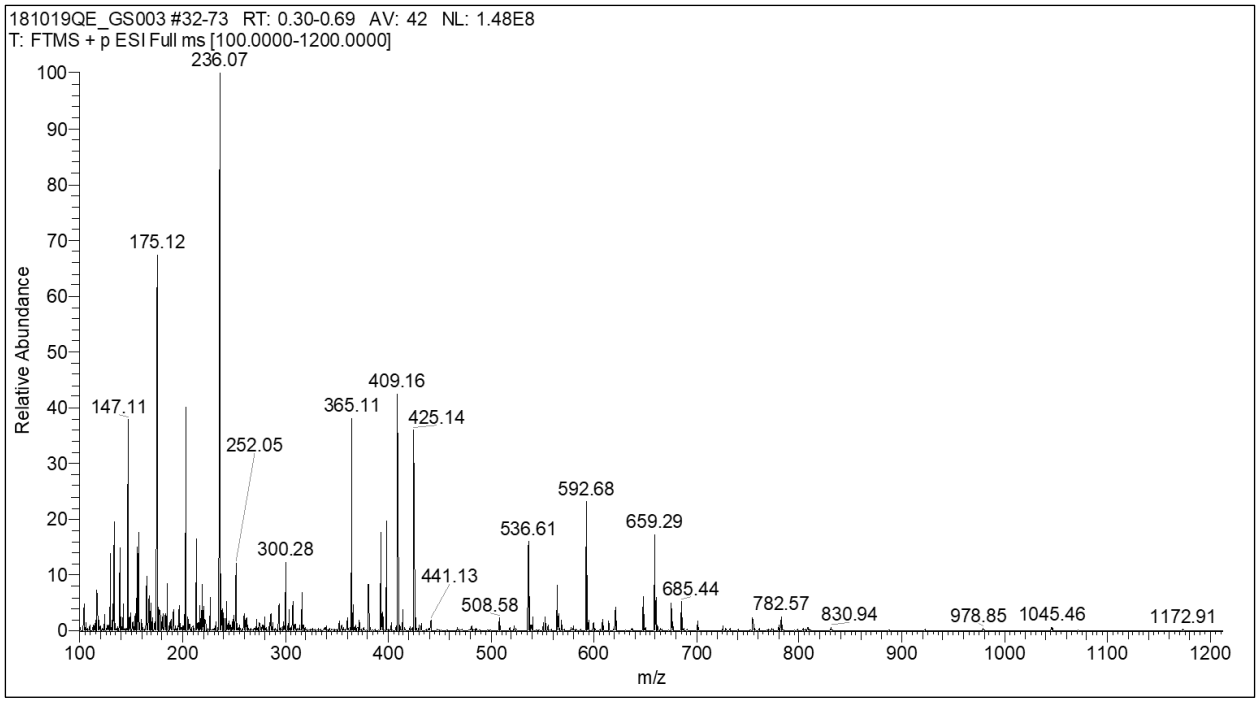

Figure 6.9. The metabolic profile of control (untreated PAM 212 cells) established in positive ESI mode on a Q-exactive instrument.

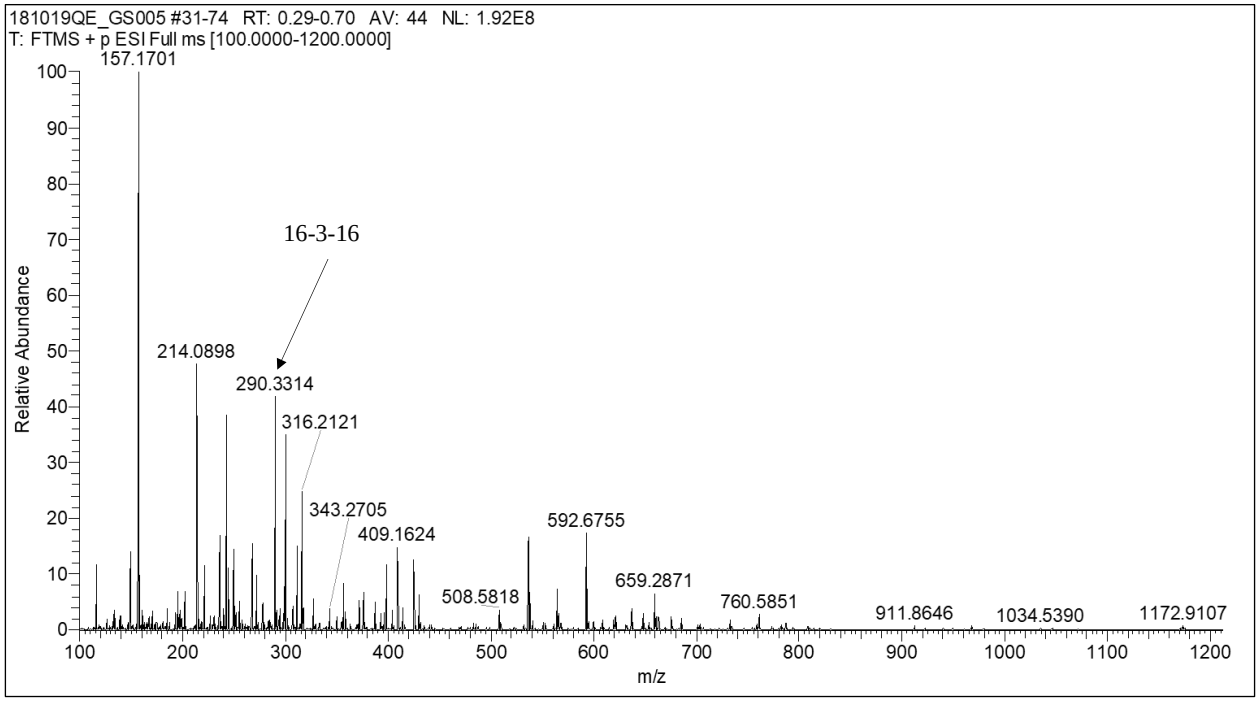

Figure 6.10. The metabolic profile of PAM 212 cells treated with 16-3-16 nanoparticles established in positive ESI mode on a Q-exactive instrument. No metabolite was determined for 16-3-16.

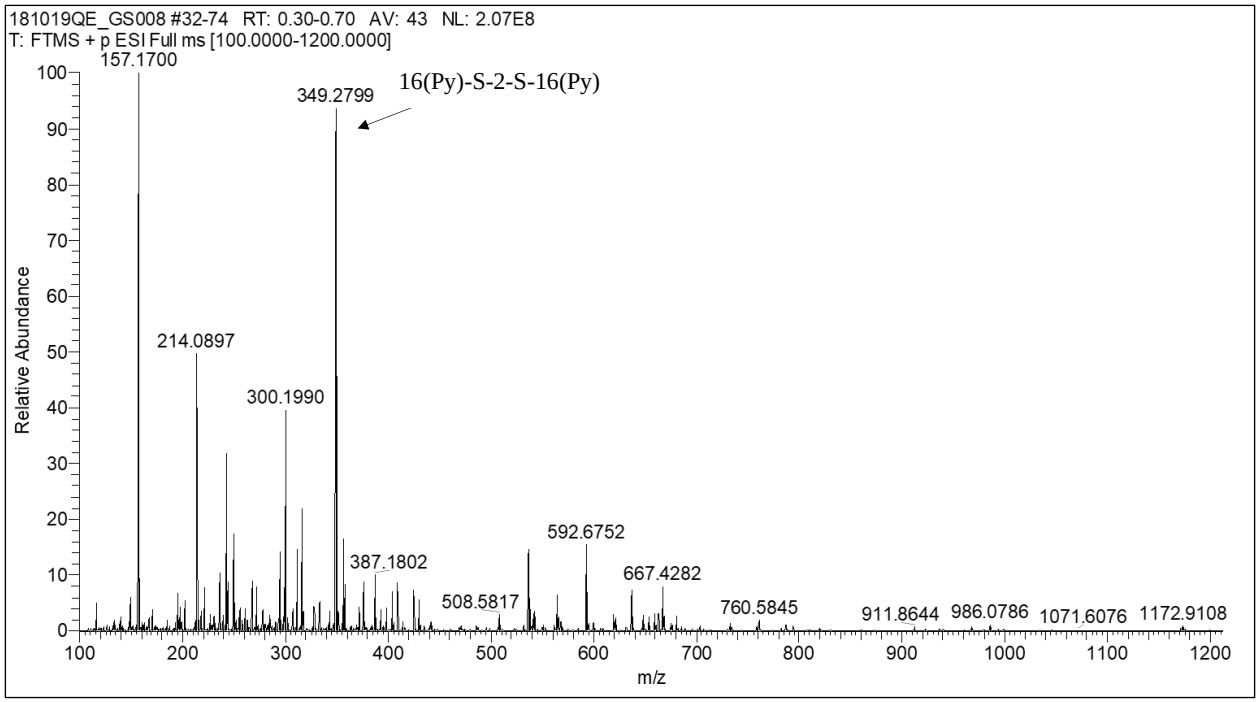

Figure 6.11. The metabolic profile of PAM 212 cells treated with 16(Py)-S-2-S-16(Py) nanoparticles established in positive ESI mode on a Q-exactive instrument. The metabolites M-1, M-2, M-3, M-4, and M-5 were determined for 16(Py)-S-2-S-16(Py).

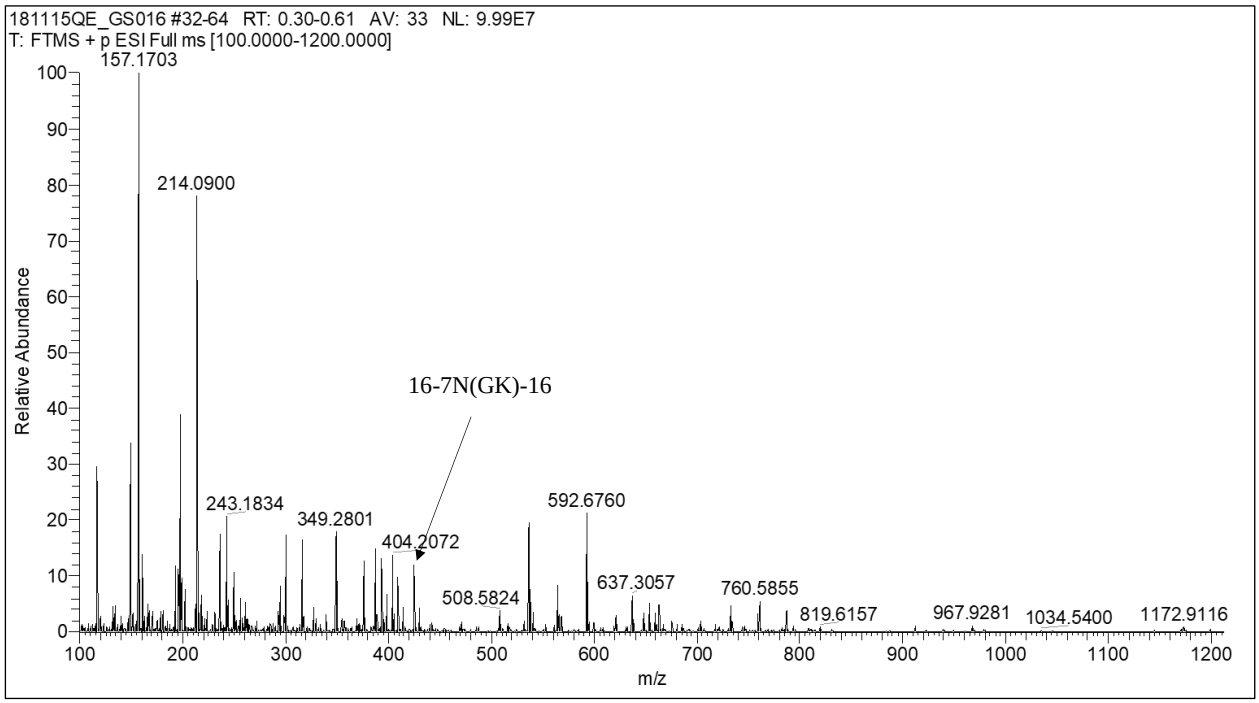

Figure 6.12. The metabolic profile of PAM 212 cells treated with 16-7N(GK)-16 nanoparticles established in positive ESI mode on a Q-exactive instrument. The metabolites M-a, M-b, M-c, M-d, M-e, and M-f were determined for 16-7N(GK)-16.

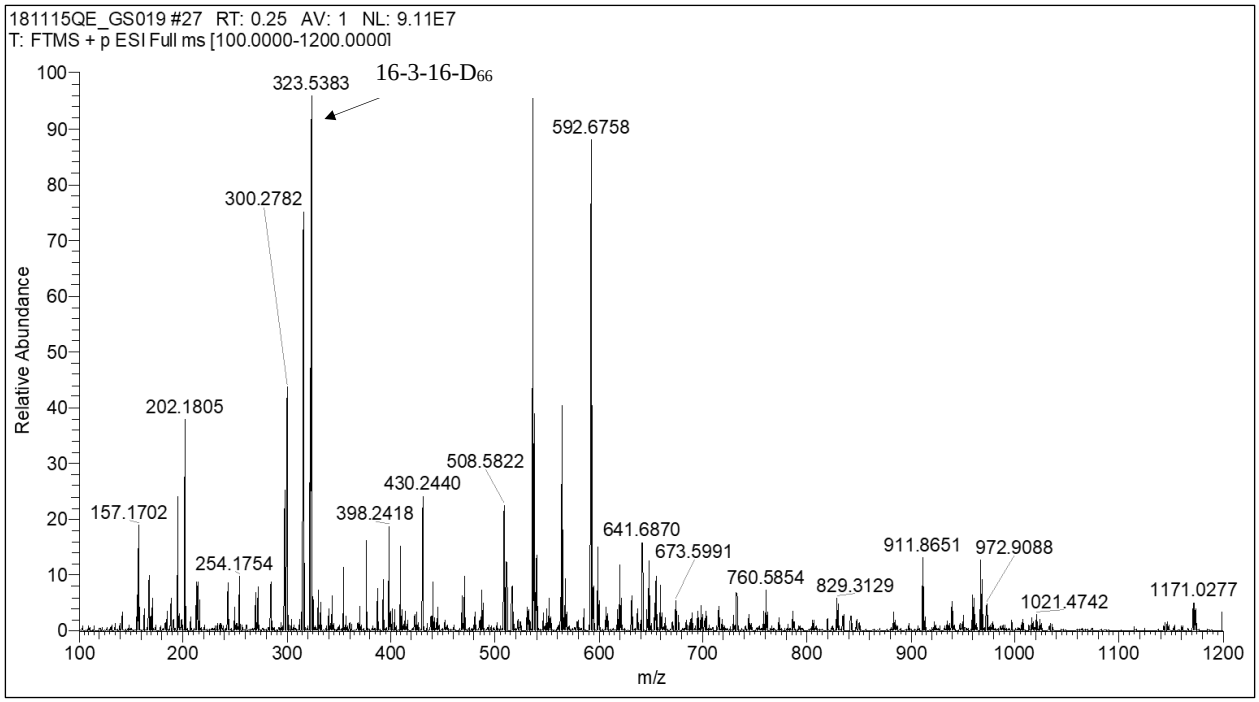

Figure 6.13. The metabolic profile of PAM 212 cells treated with 16-3-16-D_{66} nanoparticles established in positive ESI mode on a Q-exactive instrument. No metabolite was determined for 16-3-16-D_{66}.

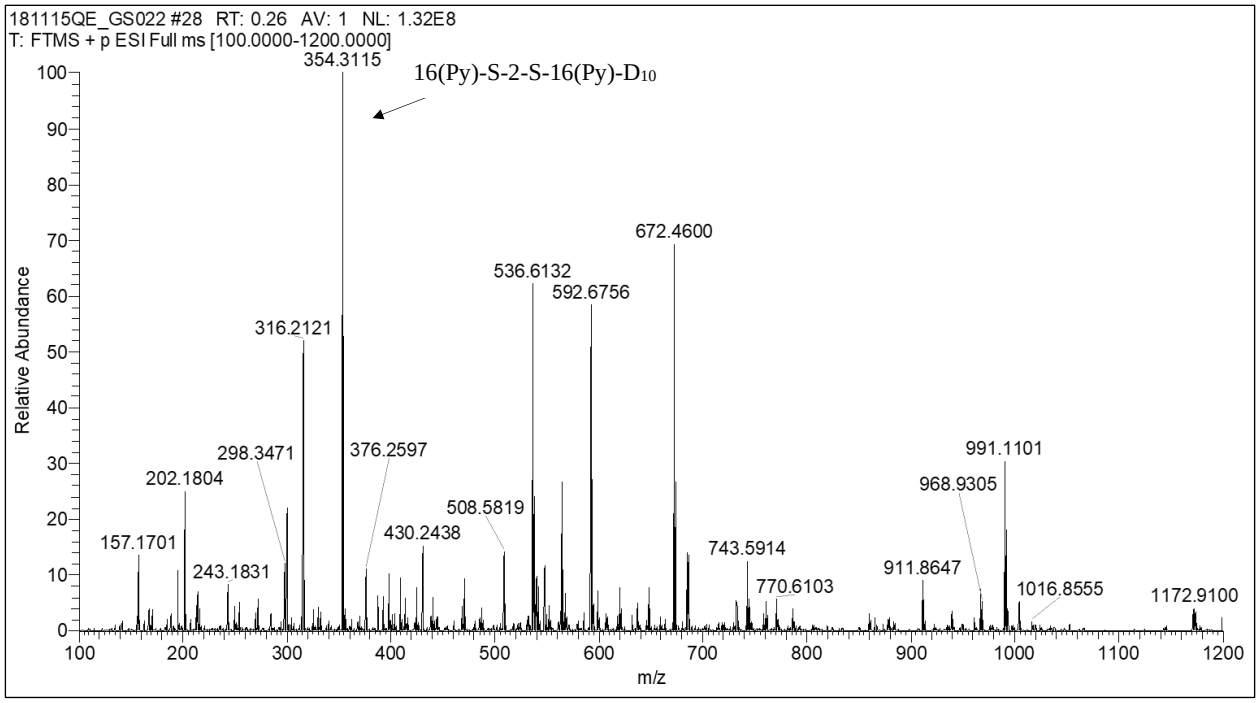

Figure 6.14.The metabolic profile of PAM 212 cells treated with 16(Py)-S-2-S-16(Py)-D_{10} nanoparticles established in positive ESI mode on a Q-exactive instrument. The metabolites M-1', M-2', M-3', M-4', and M-5' were determined for 16(Py)-S-2-S-16(Py)-D_{10}.

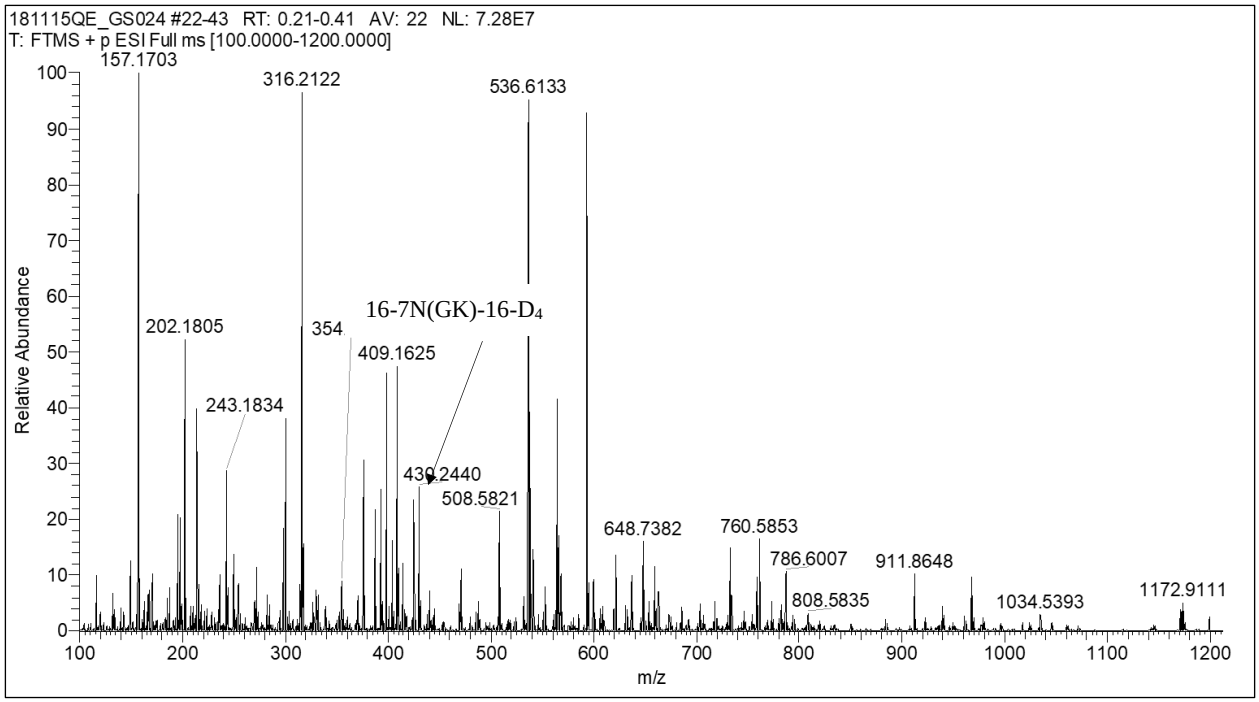

Figure 6.15. The metabolic profile of PAM 212 cells treated with 16-7N(GK)-16-D_4 nanoparticles established in positive ESI mode on a Q-exactive instrument. The metabolites M-a', M-b', M-c', M-d', M-e', and M-f' were determined for 16-7N(GK)-16-D_4.